JAERI 1303

JAERI 1303

Benchmark Calculations by the Nuclear Criticality Safety Analysis Code System JACS(MGCL, KENO-IV)

November 1986

日 本 原 子 力 研 究 所

Japan Atomic Energy Research Institute

JAERIレポートは，日本原子力研究所が研究成果編集委員会の審査を経て不定期に公刊している研究報告書です。

入手の問合わせは，日本原子力研究所技術情報部情報資料課（〒319-11茨城県那珂郡東海村）あて，お申しこしください。なお，このほかに財団法人原子力弘済会資料センター（〒319-11 茨城県那珂郡東海村日本原子力研究所内）で複写による実費頒布をおこなっております。

JAERI reports are reviewed by the Board of Editors and issued irregularly.

Inquiries about availability of the reports should be addressed to Information Division Department of Technical Information, Japan Atomic Energy Research Institute, Tokai-mura, Naka-gun, Ibaraki-ken 319-11, Japan.

編集兼発行　日本原子力研究所
印　　刷　いばらき印刷㈱

Benchmark Calculations by the Nuclear Criticality Safety Analysis Code System JACS(MGCL, KENO-IV)

Yasushi NOMURA, Jun-ichi KATAKURA, Yoshitaka NAITO,
Yuichi KOMURO and Hiroshi OKUNO

Department of Fuel Safety Research
Tokai Research Establishment
Japan Atomic Energy Research Institute
Tokai-mura, Naka-gun, Ibaraki-ken

(Received July 3, 1986)

Abstract

Since 1980, as many as 1394 cases of benchmark calculations on criticality problems have been performed by the KENO-IV Monte Carlo calculation code with the MGCL cross section data library. The code system is a part of the criticality safety evaluation code system JACS developed at JAERI. The code validation results have been published in a series of JAERI-M reports and others. This report summarizes these results and the reliability of the code system systematically.

The number of the calculated cases briefly described in this report together with their experimental systems and data are 502 for 17 kinds of homogeneous single-unit systems, 331 for 8 kinds of homogeneous multi-unit systems and 561 for 16 kinds of heterogeneous systems.

Discussions and interpretations are made on the calculated k_{eff}'s (neutron multiplication factors) with their bias errors. The factors related to the bias errors are confirmed together with their causes and trends.

Keywords: Criticality Safety, Analysis Code System, Benchmark Calculation, Monte Carlo Code, Data Library, Code Validation, Homogeneous System, Heterogeneous System, Single Unit, Multi Unit, Bias Error, Neutron Multiplication Factor

臨界安全解析コードシステムJACS(MGCL, KENO-IV)によるベンチマーク計算

日本原子力研究所東海研究所燃料安全工学部

野村　靖・片倉　純一・内藤　俶孝

小室　雄一・奥野　浩

（1986年7月3日受理）

要　旨

原研で開発された臨界安全解析コードシステムJACSのうち，KENO－Ⅳモンテカルロ・コードとMGCLデータ・ライブラリーの組合せによる計算の精度を検証するため，1980年以来多種多様な核燃料施設を模擬した臨界実験のデータを用いてベンチマーク計算が実施されてきた．これらの結果は，その都度JAERI－Mレポートその他に発表されてきた．本報告は，これらの計算精度検証に関する成果について，既発表のものを含め，他の結果を追加し，総合的に評価し，まとめたものである．

記載した実験体系及び計算ケースは，均質単一ユニット体系の17種類502ケース，均質複数ユニット体系8種類331ケース及び非均質体系16種類561ケースに上り，それぞれ実験体系，実験データ及び計算結果について簡明に記述してある．また，k_{eff}計算値にバイアス誤差を生ずる各因子を摘出し，その原因，影響について考察した．

CONTENTS

目　　次

List of Tables and Figures

List of Tables

List of Figures

1. Introduction

A computer code system named JACS[1] has been developed at JAERI to evaluate criticality safety of nuclear fuel cycle facilities such as fuel fabrication plants, reprocessing plants, transportation casks, storage pools and so on.

Since physical and chemical properties of fissile material appearing in nuclear facilities cover so many varieties that calculated values of k_{eff} are supposed to have a wide range of bias errors according to the properties of fissile material:

$$\Delta k_{eff} = k_{eff}\ (\text{calculated neutron multiplication factor}) - k_{eff.\,true}\ (\text{true neutron multiplication factor})$$

with their particular trends and uncertainties. In order to obtain the bias error mentioned above, in other words, the bias correction to the calculated k_{eff} for any kind of nuclear facility, it is considered appropriate to assess the accuracy of the code system with experimental data of as many variety as possible. The bias corrections are determined by:

$$\Delta k_{eff.\,exp} = k_{eff.\,exp}\ (\text{calculated neutron multiplication factor for an experimental system}) - 1.0\ (\text{true neutron multiplication factor for the experiment}).$$

Δk_{eff} for any system is, then, derived from analysing $\Delta k_{eff.\,exp}$ through some mathematical treatment.

At JAERI, as a part of the development of the JACS code system, some 1400 cases of benchmark calculations of criticality problems for the suitably devised experimental systems simulating various nuclear facilities have been made with the Monte Carlo code KENO-IV and the multigroup constant library MGCL.

Some results of the benchmark calculations have been already published separately in several JAERI-M reports. The calculated results published in each report, however, are concerned with some restricted area of experimental data. The present report has gathered all the available benchmark calculations including those published up to now, and discusses the reliability of the code system systematically. Referring to these discussions, one can supposedly give a reasonable bias correction to the calculated k_{eff} in his criticality analysis for a nuclear fuel cycle facility.

As for the contents of this report, outline of the JACS code system and calculational method adopted in this report are given in Chapter 2. In Chapter 3, three subchapters are provided. Subchapter A is for homogeneous single-unit systems, Subchapter B for homogeneous multi-unit systems and Subchapter C for heterogeneous systems. Each subchapter is then divided to several sections. Each section deals with experiments and calculations considered to be grouped in the same kind of benchmark calculations. Discussions and interpretations of the calculated results are given in Chapter 4.

2. Calculational Method

2.1 Outline of the Code System

General flow diagram of the JACS code system for nuclear criticality safety evaluation is shown in **Fig. 2.1.1**. The multigroup constant library MGCL[2] has been generated from the evaluated nuclear data file ENDF/B-IV[3] or JENDL (Japanese Evaluated Nuclear Data Library)[4]. The MGCL Library is the same type of library as the ABBN set[5] or the JAERI-FAST set[6], consisting of one- and two-dimensional cross section data with a Bondarenco type shielding table. One-dimensional data such as σ_t, σ_a, σ_f, ν, σ_e, σ_{in}, $\sigma_{n,2n}$ has been tabulated as infinite dilution cross sections and self-shielding factors. Two-dimensional data are matrices of elastic and inelastic scattering kernels and $(n, 2n)$ reaction cross section data. Angular dependent elastic scattering kernels are tabulated as Legendre Expansion coefficients. These scattering matrices are obtained by utilizing the SUPERTOG code[7] and the PIXSE code[8]. In these matrices, up-scattering of thermal neutrons is considered for energies up to 1.855 ev.

General flow diagram of the MGCL library production code system is shown in **Fig. 2.1.2**. Temperature dependent ultra fine cross sections (some 70,000 energy point data) are produced by the RESEND-D code developed at JAERI from the RESEND code[9]. To collapse the energy groups of the ultra fine data points, the following weighting function is provided.

$$\phi(E)=\phi_s/(\sigma_t^i+\sigma_0^i),$$

here, ϕ_s is a standard neutron-energy spectrum consisting of fission spectrum, $1/E$ and Maxwellian functions, and

$$\sigma_0^i=(\mathrm{Sum}_{j\neq i} N^j\sigma_t^j+aG/l)/N^i,$$

N^i : Atomic number density of the nuclide i,
l : Mean cord length of the fuel lump,
G : Dancoff correction factor,
a : Bell factor.

The 137 energy group structure of the MGCL master library is shown in **Table 2.1.1**. The number of the energy groups of the MGCL master library can be collapsed into any fewer number of energy groups by the COLLAPS code using the standard neutron energy spectrum described above. In this way, a sub-master library is generated.

The MGCL master or sub-master library data together with atomic number densities and geometrical data are used in the MAIL code to generate effective macroscopic cross section data as follows:

$$\Sigma_{x,eff}=\mathrm{Sum}_j N^j\sigma_{x,eff}^j$$

$$\sigma_{x,eff}^j=\sigma_{x,\infty}^j f_x(\sigma_0^j)$$

$$\sigma_0^j=(\mathrm{Sum}_{i\neq j} N^i\sigma_t^i-aG/l)/N^j$$

where,

l : Mean cord length of the fuel lump,
G : Dancoff correction factor,
a : Bell factor,
i,j : Nuclide indices,
N^i : Atomic number density of the nuclide i,
$\sigma^j_{x,eff}$: Effective microscopic cross section of the reaction x and the nuclide j,
$\sigma^j_{x,\infty}$: Infinite dilution cross section of the reaction x and the nuclide j,
σ^j_0 : Background cross section of the nuclide j,
σ^i_t : Effective total microscopic cross section of the nuclide i,
$f_x(\sigma^j_0)$: Self-shielding factor of the reaction x,
$\Sigma_{x,eff}$: Effective macroscopic cross section of the reaction x.

The background cross section σ^j_0 is determined by the iteration method. The self-shielding factor $f_x(\sigma^j_0)$ is interpolated over the one-dimensional data table in the MGCL library. The effective microscopic cross section is obtained as the product of the infinite dilution cross section and the self-shielding factor. Macroscopic cross sections are obtained by multiplying thus obtained effective microscopic cross sections with atomic number densities.

An effective neutron multiplication factor k_{eff} for a given problem is calculated by an appropriate transport code such as the KENO-IV code[10], the MULTI-KENO code[11], the ANISN-JR code[12], or the DOT3.5 code[13] with macroscopic cross section data and geometry data. A diffusion code such as CITATION[14] is also available in the code system. The Monte Carlo code KENO-IV, for example, is very useful in analyses of nuclear fuel cycle facilities with three-dimensional complex geometries. If necessary, cell averaged cross section data are obtained by the CELL-CAL code prior to k_{eff} calculations. The reliability of the calculated k_{eff} is evaluated by the YENMA code referring to various benchmark calculations stored in a data file.

2.2 Calculational method

Some 1400 cases of benchmark calculations were performed with Monte Carlo code KENO-IV and multi-group constants library MGCL. In each calculation, the history of neutrons were taken to be 103 batches of 300 neutrons. In this case, about 0.4% of standard deviation is obtained on average. This value of standard deviation is admitted to be adequate for code validation. The first three batches, in each calculation, were skipped and the results of these batches were discarded to obtain reliable calculation results. Number of neutron energy groups is 137, since the MGCL master library has been used in the calculations. Starting neutron distributions were taken to be flat. Most of the geometrical data and existing material were taken into the KENO-IV input as exactly as possible. In tracking a neutron in a reflector, albedo and adjoint biasing techniques were not used.

Table 2.1.1 Energy group structure of MGCL

137 group master library			Ultra fine group	109 G.L.		67 G.L.		26 G.L.	
Group No.	Upper Energy Boundary	Lethargy Width Δu	Lethargy Width Δu	Group No.	Δu	Group No.	Δu	Group No.	Δu
1	16.487 MeV	0.125	0.001 (5000)	1	0.25				
2	14.550					1	0.5		
3	12.840			2					
4	11.331								
5	10.000			3				1	1.25
6	8.825								
7	7.788			4		2	0.75		
8	6.8729								
9	6.0653			5					
10	5.3526								
11	4.7237			6					
12	4.1686								
13	3.6788			7		3	0.75		
14	3.2465								
15	2.8650			8					
16	2.5284							2	1.50
17	2.2313			9					
18	1.9691								
19	1.7377			10		4	0.75		
20	1.5335								
21	1.3533			11					
22	1.1943								
23	1.0540			12					
24	930.14 keV								
25	820.85			13		5	0.75		
26	724.40								
27	639.28			14					
28	564.16								
29	497.87			15				3	1.75
30	439.37								
31	387.74			16					
32	342.18					6	1.00		
33	301.97			17					
34	266.49								
35	235.18			18					
36	207.54								
37	183.16			19					
38	161.63					7	0.50		
39	142.64			20					
40	125.88								
41	111.09		0.00025 (12000)	21				4	1.25
42	98.037								
43	86.517			22		8	0.75		
44	76.351								
45	67.379			23					
46	59.462								

Table 2.1.1 (continued)

137 group master library			Ultra fine group	109 G.L.		67 G.L.		26 G.L.	
Group No.	Upper Energy Boundary	Lethargy Width Δu	Lethargy Width Δu	Group No.	Δu	Group No.	Δu	Group No.	Δu
47	52.475 keV	0.125	0.00025	24	0.25				
48	46.309								
49	40.868			25		9	0.75		
50	36.066								
51	31.828			26				5	1.25
52	28.088								
53	24.788			27					
54	21.875					10	0.50		
55	19.305			28					
56	17.036								
57	15.034	0.25		29					
58	11.709			30		11	1.00	6	1.00
59	9.1188			31					
60	7.1017			32					
61	5.5308		0.000125 (30000)	33					
62	4.3075			34		12	0.75		
63	3.3546			35					
64	2.6126			36					
65	2.0347			37		13	0.75	7	2.25
66	1.5846			38					
67	1.2341			39					
68	961.12 eV			40		14	0.75		
69	748.52			41					
70	582.95			42					
71	454.00			43		15	0.75		
72	353.58			44				8	1.50
73	275.36			45					
74	214.45			46		16	0.75		
75	167.02			47					
76	130.07		0.00025 (17000)	48					
77	101.30			49		17	0.75		
78	78.893			50				9	1.50
79	61.442			51					
80	47.851			52		18	0.75		
81	37.267			53					
82	29.023			54					
83	22.603			55		19	0.75		
84	17.603			56				10	1.50
85	13.710			57					
86	10.677			58		20	0.75		
87	8.3153			59					
88	6.4760			60					
89	5.0435			61		21	0.75		
90	3.9279			62				11	1.25
91	3.0590			63		22	0.50		
92	2.3824			64					

Table 2.1.1 (continued)

137 group master library			Ultra fine group	109 G.L.		67 G.L.		26 G.L.	
Group No.	Upper energy Boundary	Lethargy Width Δu	Lethargy Width Δu	Group No.	Δu	Group No.	Δu	Group No.	Δu
93	1.8554 eV	0.25	0.00025	65	0.125	23	0.125		
94	1.6374			66		24		12	0.375
95	1.4450			67		25			
96	1.2752			68		26		13	0.375
97	1.1254			69		27			
98	0.99312			70		28			
99	0.87642	0.125	0.00025 (6000)	71		29		14	0.25
100	0.77344			72		30			
101	0.68256			73		31			
102	0.60236			74		32		15	0.50
103	0.53158			75		33			
104	0.46912			76		34			
105	0.41399	Δv 270 m/sec		77		35			
106	0.38925			78		36		16	
107	0.36528			79		37			
108	0.34206			80		38		17	
109	0.31961			81		39			
110	0.29792			82		40			
111	0.27699			83		41		18	
112	0.25683			84		42			
113	0.23742			85		43			
114	0.21878			86		44		19	
115	0.20090			87		45			
116	0.18378			88		46			
117	0.16743			89		47		20	
118	0.15183			90		48			
119	0.13700			91		49			
120	0.12293			92		50		21	
121	0.10962			93		51			
122	0.09708			94		52			
123	0.085295			95		53		22	
124	0.074274			96		54			
125	0.064015			97		55			
126	0.054518			98		56		23	
127	0.045783			99		57			
128	0.037811			100		58			
129	0.030600			101		59		24	
130	0.024152			102		60			
131	0.018465			103		61			
132	0.013541			104		62		25	
133	0.009379			105		63			
134	0.005979			106		64			
135	0.003341			107		65		26	
136	0.001466			108		66			
137	0.000352			109		67			
	0.000031								

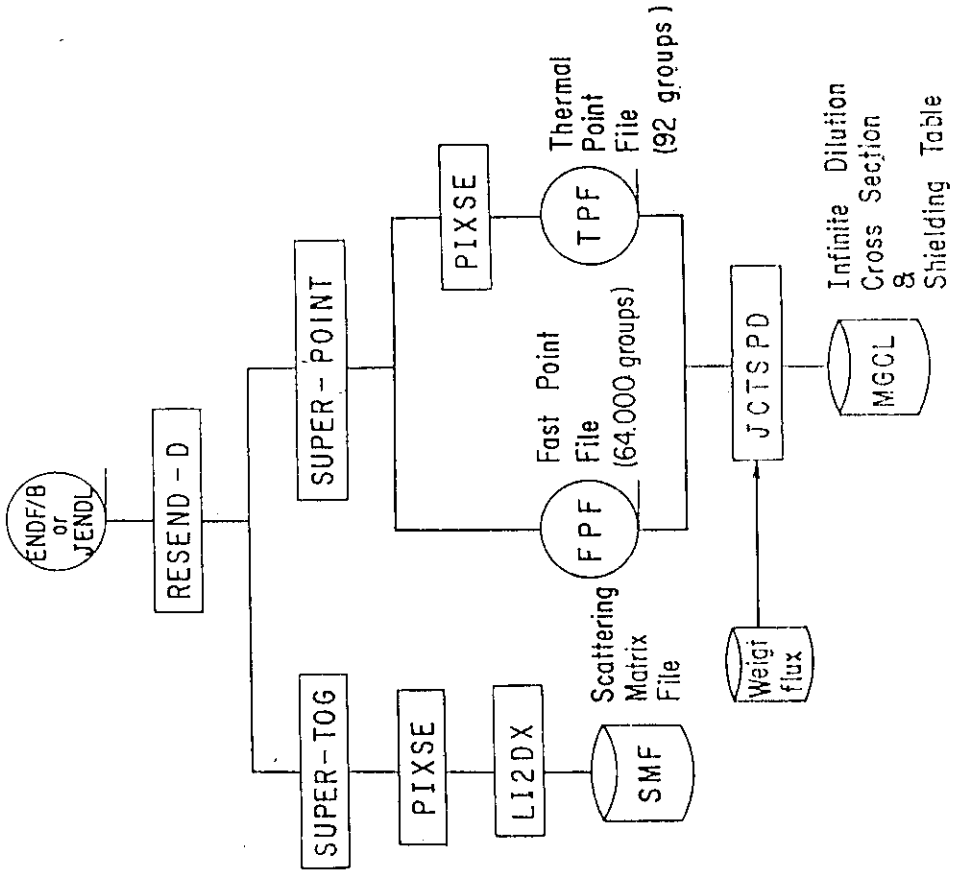

Fig. 2.1.2 General flow diagram of a computer code system MGCL-ACE.

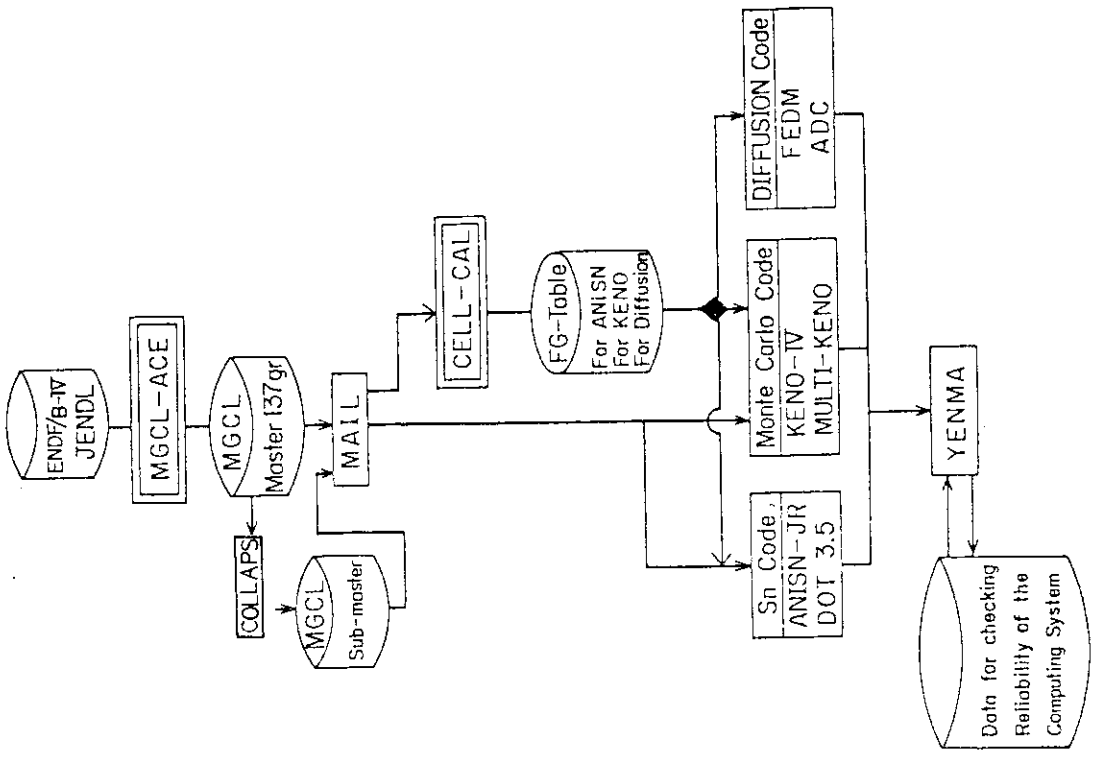

Fig. 2.1.1 General calculation flow of JACS.

3. Experimental Data and Calculated Results

Most of the experimental data has been taken from some 40 reports published by American laboratories. A part of them are from French reports or English reports. They cover a wide range of fuel compositions, moderating conditions, reflecting conditions, fuel shape/dimensions and so on, due to their variety in simulating nuclear fuel facilities.

In this chapter, three subchapters are provided corresponding to the differences of experimental systems. Subchapter A is for homogeneous single-unit systems, Subchapter B for homogeneous multi-unit systems and Subchapter C for heterogeneous systems. Each subchapter is then divided into several sections. Each section deals with experiments and calculations considered to be in the same group of benchmark calculations. In each section, brief descriptions are presented on the experimental system and the calculational model together with the calculated results made easy to grasp by the aid of graphs and tables. More concerned readers should refer to original documents listed at the end of this report.

A. Homogeneous Single-Unit System

3.A.1 Pile of PuO_2-UO_2-Polystyrene Compacts with Various Poison-Plate Materials

Experiments were performed at BNWL, USA, simulating the storage of mixed oxide fuel.[15] Fuel compacts are made of homogeneous mixture of PuO_2-UO_2-Polystyrene. There are two sets of fuels: one for an atomic H/(Pu+U) ratio of 30.6 and a plutonium enrichment of 14.6 wt%, the other for an atomic H/(Pu+U) ratio of 2.8 and a plutonium enrichment of 29.3 wt%. Geometry of a compact is either a 5.09 cm × 5.09 cm × 5.09 cm cube or a 5.09 cm × 5.09 cm × 1.38 cm slab, clad with 0.12 mm thick vinyl tape. These compacts are piled up to form a rectangular parallelepiped assembly of which base consists of 8 × 8 fuel compacts. One of the following poison materials is used as neutron absorber plates in each case.

304L Stainless steel,
304L Stainless steel containing 1.1 wt% natural Boron,
304L Stainless steel containing 1.6 wt% natural Boron,
Uranium depleted to 0.2 wt% ^{235}U,
Boral,
Cadmium,
Lead.

The assembly is fully reflected with at least 15 cm thick Plexiglas (methacrylate plastic : $C_5H_8O_2$). The experimental configuration is shown in **Fig. 3.A.1.1**. Criticality approach was made by adding fuel compacts, one by one, to the top face of the assembly. Critical heights are given in **Tables 3.A.1.1** and **3.A.1.2**.

The KENO-IV calculational models are shown in **Fig. 3.A.1.2** for the two different basic fuel assemblies.[16] Thickness of the reflector is assumed to be 15 cm in all directions. Cladding tape and void existing between fuel compacts are neglected in geometry modelling, but they are taken in calculating atomic number densities of the fuel region.

Calculated results are listed in **Tables 3.A.1.3** and **3.A.1.4**[16]. Histogram of the calculated k_{eff}'s for 51 cases in all is shown in **Fig. 3.A.1.3**. One can see that the averaged k_{eff} values

are 1.023 for the 30.6 H/(Pu+U) fuel system, and 1.026 for the 2.8 H/(Pu+U) fuel (partly with the 30.6 H/(Pu+U) fuel). These calculated k_{eff}'s are about 2–3% higher than unity.

3.A.2 Pile of PuO_2-UO_2-Polystyrene Compacts with Various Plutonium Enrichments

Experiments were performed at BNWL, USA, using compacts of homogeneous PuO_2-UO_2-Polystyrene with various plutonium enrichments.[17),18)] There are six batches of fuels having various plutonium enrichments and atomic H/(Pu+U) ratios as follows:

29.3 wt% Pu and 2.8 H/(Pu+U),
15.0 wt% Pu and 2.86 H/(Pu+U),
8.1 wt% Pu and 7.3 H/(Pu+U),
30.0 wt% Pu and 47.4 H/(Pu+U),
14.62 wt% Pu and 30.6 H/(Pu+U),
7.89 wt% Pu and 51.8 H/(Pu+U).

A compact is a 5.09 cm cube or a slab of 5.09 cm square with 1.3 cm thickness, clad in 0.12 mm thick vinyl tape. These compacts are piled up to form a rectangular parallelepiped assembly with or without Plexiglas reflector of 150 mm thickness at least. Criticality approach was made by adding the compacts, one by one, to the top face of the assembly.

The basic KENO-IV calculational model is shown in **Fig. 3.A.2.1**. Thickness of Plexiglas reflector is assumed to be 15 cm in all directions. Cladding tape and stacking void existing between the compacts are not expressed explicitly in the calculational model. Corrections have been made to the measured critical heights of the assembly to compensate reactivity effects of the cladding tape, the stacking voids and the structural supports.

Calculated results together with critical dimensions and masses for 52 assemblies in all are listed in **Tables 3.A.2.1** through **3.A.2.6**. Histograms of the calculated k_{eff}'s are shown in **Figs. 3.A.2.2** and **3.A.2.3**, respectively, corresponding to the different H/(Pu+U) atomic ratios. The calculated k_{eff}'s for low (2 to 8) H/(Pu+U) systems are seen to be between 0.980 and 1.025 with the average value of 1.005. On the other hand, the calculated k_{eff}'s for high (30 to 50) H/(Pu+U) systems are between 0.980 and 1.030 with the average value of 1.010, about 1% higher than unity.

3.A.3 Pile of PuO_2-UO_2-Polythene Compacts

Experiments were performed in Britain using compacts of homogeneous PuO_2-U(natural)O_2-Polythene fuel.[19)] Plutonium enrichment is 23.1 atomic percent, and H/(Pu+U) atomic ratio is 4.67. A compact is a slab of 4.28 cm square with 2.15, 2.69 or 3.25 cm height, clad with 0.2 mm thick polythene tape. These compacts are piled up to form a rectangular parallelepiped assembly having a base of 5×5 to 8×8 compacts. Criticality approach was made by adding compacts, one by one, to the top face of the assembly.

The basic KENO-IV calculational model is the same as that shown in **Fig. 3.A.2.1** except for the fuel material. Thickness of Polythene reflector is assumed to be 20 cm in all directions. Fuel region is assumed to contain atoms of the cladding tape homogeneously.

Calculated results together with critical dimensions and masses for 4 assemblies in all are listed in **Table 3.A.3.1**. Average value of the four calculated k_{eff}'s is 1.018, about 2% higher than unity.

3.A.4 Pile of PuO_2 (-Polystyrene) Compacts

Experiments were performed at BNWL, USA, using compacts of homogeneous PuO_2 or PuO_2-Polystyrene fuel.[20),21),22)] There are four batches of fuels having various plutonium

isotopic compositions and atomic H/(Pu+U) ratios as follows:

2.2 wt% ^{240}Pu and 15.0 H/Pu,
8.0 wt% ^{240}Pu and 15.0 H/Pu,
11.46 wt% ^{240}Pu and 5.0 H/Pu,
18.35 wt% ^{240}Pu and 0.04 H/Pu.

A compact is a 5.1 cm cube or a slab of 5.1 cm square with 3.8 cm height, clad with 0.3 mm polymer coating. These compacts are piled up to form a rectangular parallelepiped assembly with or without Plexiglas reflector of 150 mm thickness at least. Criticality approach was made by adding the compacts, one by one, to the top face of the assembly.

The basic KENO-IV calculational model is the same as that shown in **Fig. 3.A.2.1** except for the fuel material. Thickness of Plexiglas reflector is assumed to be 15 cm in all directions. Corrections have been made to the measured critical heights of the assemblies to compensate voids existing between compacts and temperature effect.

Calculated results together with critical dimensions and masses are listed in **Tables 3.A.4.1** through **3.A.4.3**. Histogram of the calculated k_{eff}'s for 30 cases in all is shown in **Fig. 3.A.4.1**. As seen from the histogram, the calculated k_{eff}'s are between 0.975 and 1.035 with the average value of 1.015, about 1.5% higher than unity.

3.A.5 Single Tank Containing Uranyl-Nitrate Solution

Experiments were performed at Rockey Flats, USA, using single tank containing 93.17% ^{235}U enriched uranyl-nitrate solution.[23] Uranium concentration is ranged from 54.89 to 357.71 gU/l. Unreflected experiments have been reported, as well as measurements within thick-walled cubical reflector shells composed of concrete or plastics. The single tank is composed of either Type 6061 aluminum or Type 304 stainless steel with inner diameter ranging from 27.88 to 50.69 cm, and has a coaxial tailpipe about 30 cm long, welded to its bottom. Uranyl-nitrate solution was introduced into the single tank through the tailpipe. Critical height inside the single tank was decided by linear interpolation between a slightly supercritical and a slightly subcritical height.

In the calculational model, the tailpipe is neglected, as shown in **Fig. 3.A.5.1**.

Calculated k_{eff}'s are listed in **Tables 3.A.5.1** through **3.A.5.3**[24]. Histogram of the calculated k_{eff}'s for 45 cases in all is shown in **Fig. 3.A.5.2**. As seen from the histogram, the calculated k_{eff}'s are between 0.960 and 0.995 with the average value of 0.973. The average value of 0.970 for minimally reflected systems is about 0.8% lower than the average value of 0.978 for concrete reflected systems.

3.A.6 Plutonium Fuel in Various Shapes

The US NUREG report[25] contains several different experiments concerning homogeneous plutonium fuels having various shapes as listed in **Table 3.A.6.1**. These experiments have been selected to provide data for benchmark calculations to validate the accuracy of the neutron cross sections for the isotopes of plutonium. They cover a wide range of H/Pu ratio (a wide variation of neutron spectrum) and a wide range of ^{240}Pu content in plutonium.

Calculational models for 15 cases selected from these experiments are shown in **Figs. 3.A.6.1** through **3.A.6.10**, respectively.

Calculated results are summarized in **Table 3.A.6.2**[26]. The calculated k_{eff}'s distribute from 0.984 to 1.031 with the average value of 1.008. **Figure 3.A.6.11** shows that the calculated k_{eff} decreases with the increase of H/Pu atomic ratio.

3.A.7 Intersecting Cylinders Containing Uranyl-Fluoride Solution

Experiments were performed at ORNL, USA, simulating intersecting pipes or vessels in fuel manufacturing plants.[27] Aqueous $U(5)O_2F_2$ solution was used as fissile material. Two types of intersections were studied. They are nominally called "30 degrees lateral" and "cross". Critical approach was made by increasing the level of fissile solution.

Experimental arrangement of "30 degrees lateral" is shown in **Fig. 3.A.7.1**. The lateral and the vertical cylinders have the inner diameter of 27.9 cm. A vent tube of 2.2 cm i.d. connects the top of the lateral cylinder with the vertical cylinder. The top of the lateral cylinder is closed by welding a 0.64 cm thick plate, and the top of the vertical cylinder is open. The bottom plate of the vertical cylinder is 1.3 cm thick and penetrated by a 5.1 cm i.d. coaxial tube. Through this tube, the fissile solution was introduced into the vertical cylinder. The bottom plate is located at 22.9 cm above the floor of reflector tank.

Experimental arrangement of "cross" is shown in **Fig. 3.A.7.2**. The cylinders and the supporting plates are made of Plexiglas having density of 1.18 g/cm^3. Four types of cylinders, of which inner diameters are 26.7, 27.3, 27.9 and 28.6 cm, are used depending on the experimental phase. The crossing cylinders are fixed rigidly with the Plexiglas plates so that the centerlines of the cylinders intersect at a central point. The upper and the lower vertical cylinders are held coaxial, but the horizontal cylinders are slightly tilted down by 2 degrees toward the central point to drain the solution. The ends of the horizontal cylinders are cemented closely by 3.17 cm thick Plexiglas discs with vent lines for air escaping. The end of the lower vertical cylinder is cemented by a bottom flange of 1.27 cm thick stainless steel. The top of the upper vertical cylinder is open.

Experimental configurations have been modelled for KENO calculations as shown in **Figs. 3.A.7.3** and **3.A.7.4**[28]. Detailed structures such as vent-lines or lead-tubes are neglected in the models. Surface equations expressed by quadratic functions for KENO general geometry input data are shown in **Fig. 3.A.7.3**. As shown in **Fig. 3.A.7.4**, the Plexiglas plates supporting the cylinders are neglected in the model.

Calculated results for the "30 degrees lateral" systems are listed in **Table 3.A.7.1** and those for "cross" are listed in **Table 3.A.7.2**. For the former, the calculated k_{eff}'s for 18 cases in all are between 0.96 and 0.99 with the average value of 0.978, about 2% lower than unity as shown in the histogram of **Fig. 3.A.7.5**. For the latter, the calculated k_{eff}'s for 27 cases in all distribute from 0.97 and 0.99 with the average value of 0.985, about 1.5% lower than unity as shown in the histogram of **Fig. 3.A.7.6**.

3.A.8 Sphere or Cylinder Containing Uranyl-Fluoride Solution

Critical dimensions of aqueous solutions of UO_2F_2 were measured at ORNL, USA, to provide data useful in criticality calculations.[29] The solution is contained in a cylindrical or spherical vessel made of aluminum or stainless steel, unreflected or reflected with water. Uranium is enriched to 4.9 wt% ^{235}U. High solubility of uranyl fluoride (nearly 890 gU/l) allows experiments with solutions having an $H/^{235}U$ atomic ratio as low as some 500.

Calculational models for typical experimental systems are shown in **Figs. 3.A.8.1** and **3.A.8.2**. One can see that structural materials other than the cylinder vessel are neglected in the calculational models.

Table 3.A.8.1 lists calculated results together with experimental conditions. Histogram of the calculated k_{eff}'s for 23 critical experiments (except for 4 subcritical cases) is shown in **Fig. 3.A.8.3**. As seen from the histogram, the calculated k_{eff}'s are between 0.950 and 1.005 with the average value of 0.981, about 2% lower than unity.

3.A.9 Cylinder Containing Uranyl-Fluoride Solution with Combination of Reflectors

Experiments were performed at ORNL, USA, to study the effect of steel/water composite reflectors on reactivity of a cylinder containing aqueous UO_2F_2 solution.[30] A stainless-steel cylinder having 0.079 cm thick wall with inner diameter of 33.09 cm or 39.09 cm was utilized to contain low ^{235}U enriched (4.98 wt%) uranyl-fluoride solution. A lateral steel reflector adjacent to the solution region ranges up to 5.08 cm in thickness, and is surrounded by an infinitely thick water reflector.

Figure 3.A.9.1 shows the calculational model for a typical experimental system.

Table 3.A.9.1 lists calculated results together with experimental conditions for 24 cases in all. Histogram of the calculated k_{eff}'s is shown in **Fig. 3.A.9.2**. As seen from the histogram, the calculated k_{eff}'s are between 0.970 and 1.000 with the average value of 0.983, about 2% lower than unity.

3.A.10 Pile of UF_4-Paraffin Compacts

Experiments were performed at ORNL, USA, with homogeneous mixtures of finely divided $U(2)F_4$ or $U(3)F_4$ dispersed in paraffin.[31] The mixture was pressed into rectangular parallelepipes with dimensions ranging from 0.63 cm × 2.54 cm × 2.54 cm to 10.16 cm cubes and covered with the 0.02 cm thick aluminum foil. The H/U atomic ratio varies from 4 to 20. The uranium in the fuel mixtures containes either 2 or 3 wt% ^{235}U. The assembly was constructed in rectangular geometry with or without paraffin/Plexiglas reflectors. Critical dimensions of the assembly were measured in the experiment. Measured data are listed in **Table 3.A.10.1**.

Figure 3.A.10.1 shows the calculational model for a typical reflected experimental pile of UF_4-paraffin compacts. The calculational model for a typical unreflected experimental pile is shown in **Fig. 3.A.10.2**.

Calculated results for these experimental systems are listed in **Table 3.A.10.2**. Histogram of the calculated k_{eff}'s for 22 reflected piles is shown in **Fig. 3.A.10.3**, and histogram for 30 unreflected piles is shown in **Fig. 3.A.10.4**. As seen from these histograms, the average value of 1.007 for the reflected piles is slightly higher than 1.004 for the unreflected piles.

3.A.11 Sphere Containing Plutonium-Nitrate Solution with Various Reflectors

Experiments were performed at BNWL, USA, with plutonium (4.6% ^{240}Pu) nitrate solution in stainless steel spheres of 11.5, 14.0, and 15.2 in. diameters.[32] Reflectors are of water, concrete, paraffin, and stainless steel. In some cases, unreflected spheres of 15.2 in. diameter were used in the experiment. The critical conditions of the spheres were obtained at various plutonium concentrations from 24 to 435 g plutonium/liter and various molalities from 0.2 to 7.7. The effect of a 0.030 in. cadmium shell and a 4 in. air gap between the reflector and the vessel was also studied in the experiment. **Table 3.A.11.1** lists experimental conditions for 48 cases in all.

The calculational model is shown in **Fig. 3.A.11.1**. Calculated results for all experimental cases are listed in **Table 3.A.11.2**. Histogram of the calculated k_{eff}'s is shown in **Fig. 3.A.11.2**.

As seen from the histogram, the calculated k_{eff}'s are between 0.980 and 1.025 with the average value of 1.003, about 0.3% higher than unity.

3.A.12 Annular Cylinder Containing Plutonium-Nitrate Solution

Experiments were performed in France using stainless steel annular cylinders containing plutonium-nitrate solution immersed in a larger water-reflector tank.[33] The annular vessel with 3 mm thick wall, 200 mm i.d. and 500 mm o.d., has either an inner void region for some

cases of experiments, or an inner cadmium-paraffin region for other cases of experiments. The ^{240}Pu content in Pu of $PU(NO_3)_4$ is about 19%. The reflecting water level is adjusted to be equal to the solution level in the vessel. Criticality approach was made by increasing the solution height gradually, as well as by varing the plutonium concentration from 28.7 to 165 g/l, and the nitrate concentration from 1.85 to 3.85 mol..

The calculational model for a typical case of these experiments is shown in **Fig. 3.A.12.2**.

Tables 3.A.12.1 and **3.A.12.2** list the calculated results together with the experimental conditions. Histogram of the calculated k_{eff}'s for 17 cases in all is shown in **Fig. 3.A.12.3**. As seen from the histogram, the calculated k_{eff}'s are between 0.980 and 1.005 with the average value of 0.994, about 0.6% lower than unity.

3.A.13 Cylinder or Sphere Containing Plutonium-Uranyl-Nitrate Solution Reflected by Water

Experiments were performed at BNWL, USA, with plutonium-uranyl nitrate solution in a stainless steel cylinder of 61.0 cm i.d. reflected by water.[34] Stainless steel spheres of 35.7 and 38.6 cm diameter were also utilized in the experiment. For the experiment in cylindrical geometry, the ^{240}Pu content in Pu is either 5.6 wt% or 23.0 wt%. For the water reflected spheres, the ^{240}Pu content in Pu is 4.7 wt%. The uranium in the mixture is slightly depleted, containing 0.66 wt% ^{235}U. The plutonium concentration is ranged from 12.4 to 97.3 gPu/l (uranium plus plutonium concentration from 42 to 432 g (U+Pu)/l). Experimental arrangements for cylindrical and spherical geometries are shown in **Figs. 3.A.13.1** and **3.A.13.2**, respectively.

The calculational model for a typical cylindrical geometry is shown in **Fig. 3.A.13.3**.

Calculated results together with experimental conditions for 29 cases in all are listed in **Tables 3.A.13.1** and **3.A.13.2**. Histograms of the calculated k_{eff}'s for the cylindrical geometries are shown in **Figs. 3.A.13.4** and **3.A.13.5**, respectively, corresponding to the ^{240}Pu contents in Pu in the plutonium-uranyl-nitrate solution. As seen from the histograms, the calculated k_{eff}'s are between 0.985 and 1.020. The average value of k_{eff} for the 29 cases in all is almost equal to unity.

3.A.14 Assembly of Low-Enriched Uranium-Oxide (U_3O_8) Compacts

Experiments were performed at Rocky Flats, USA, using low-enriched damp uranium oxide (U_3O_8) systems.[35] The experimental core consists of 152 mm cubical aluminum cans containing low enriched (4.46 wt% ^{235}U) uranium oxide. The uranium oxide was compacted to a density of 4.68 g/cm^3 and moistened to an H/U atomic ratio of 0.77. These aluminum cans were piled up to be a 770 mm cubical assembly. Since the uranium oxide in an assembly of this size could not go critical state by itself, a highly enriched (about 93 wt% ^{235}U) uranium metal or solution "driver" shown in **Fig. 3.A.14.1** was used. As shown in this figure, the experiments were performed on a horizontal split table. Each half of the table supports a portion of the experimental core. Criticality approach was made by decreasing the distance between the two interfaces of the core. Measurements are reported for systems having the minimum reflector and for systems reflected by 254 mm thick concrete or plastic.

Calculated results together with principal critical conditions are listed in **Table 3.A.14.1**[36]. Histogram of the calculated k_{eff}'s for 10 cases in all is shown in **Fig. 3.A.14.2**. The calculated k_{eff}'s are between 0.970 and 1.010 with the average value of 0.991, about 1% lower than unity.

3.A.15 Cylinder Containing Plutonium-Nitrate Solution of High-Fissile Content Poisoned with Gadolinium

Experiments were performed at BNWL, USA, utilizing gadolinium as a soluble neutron absorber in the plutonium-nitrate solution.[37] Plutonium concentration of the solution is either 116 gPu/l with 1.85 mol. of nitric acid, or 363 gPu/l with 4.1 mol. of nitric acid. Gadolinium concentration ranges between 0.00 and 20.25 gGd/l.

Experimental vessel is a stainless steel cylinder of 61.03 cm i.d. and 0.079 cm wall thickness, as shown in **Fig. 3.A.13.1**. The ^{239}Pu content in Pu is 90.7 wt%.

The KENO-IV calculational model is shown in **Fig. 3.A.15.1**. Calculated results together with the critical conditions are listed in **Table 3.A.15.1**.[36] Histogram of the calculated k_{eff}'s for 15 cases in all is shown in **Fig. 3.A.15.2**. As seen from the histogram, the calculated k_{eff}'s are between 0.980 and 1.005 with the average value of 0.988, about 1.2% lower than unity.

3.A.16 Cylinder Containing Plutonium-Uranyl-Nitrate Solution with Soluble Neutron Poison

Experiments were performed at BNWL, USA, simulating dissolution of spent fuel elements in a dissolver vessel.[38] A schema of the experimental system is the same as that shown in **Fig. 3.A.13.1**. Plutonium-(uranyl-)nitrate solution in the stainless steel cylindrical vessel of 61.03 cm i.d. contains gadolinium and/or boron as a soluble neutron absorber. The ^{239}Pu content in Pu is about 93 wt%, and uranium is slightly depleted, containing 0.66 wt% ^{235}U. Experimental conditions are listed in **Table 3.A.16.1**. As listed in this table, plutonium concentration ranges between 75.6 and 363 gPu/l, and uranium concentration between 0.0 and 182.6 gU/l. Gadolinium concentration was varied up to 20.25 gGd/l, and natural boron concentration up to 1.54 gB/l. Criticality approach was made by increasing the solution height incrementally and the critical height was measured.

The calculational model for a typical case is shown in **Fig. 3.A.16.1**.

Calculated results for all 34 cases are listed in **Table 3.A.16.2**. Histogram of the calculated k_{eff}'s is shown in **Fig. 3.A.16.2**. As shown in this figure, the calculated k_{eff}'s are between 0.965 and 1.025 with the average value of 0.987, about 1.3% lower than unity.

3.A.17 Homogeneous Systems with Boron Containing Glass Raschig Rings

Experiments were performed at BNWL, USA, to obtain data for checking calculational models for raschig ring poisoned systems containing mixture of uranium and plutonium in solution.[38] Borosilicate glass rings, 1.5 in. o.d., 1.25 in. i.d., and 1.7 in. long, fill a cylindrical vessel containing the plutonium-uranyl-nitrate solution of the concentration ranging from 79 to 92 gPu/l and from 147 to 182 gU/l. The plutonium contains 5.6 wt% ^{240}Pu. The ^{235}U enrichment is 0.66 wt%. The raschig ring contains about 0.5 wt% natural boron. The experimental vessel is 107 cm in height and 61 cm in i.d., and is reflected with water, as shown in **Fig. 3.A.17.1**.

The calculational model is shown in **Fig. 3.A.17.2**. As shown in the figure, the stack of raschig rings at random disposition is modelled to be an uniformly arranged triangular lattice with zig-zag boundary. The experimental vessel is neglected in the calculational model.

Calculated results together with principal experimental conditions are listed in **Table 3.A.17.1**.[36] The average value of the calculated k_{eff}'s for 8 cases in all is 0.9833, about 2% lower than unity.

B. Homogeneous Multi-Unit (Interacting) System

3.B.1 Array of Cylinders Containing UF_6

Experiments were performed at ORNL, USA, simulating a storage of UF_6 transport container.[39] The 97.7 wt% ^{235}U enriched UF_6 is contained in 20.3 cm i.d./125.0 cm high/0.48 cm thick Monel steel cylinders. The H/U atomic ratio of UF_6 fuel is reported to be less than 0.088. A split table carrying the array of the cylinders was utilized in the experiment. The table top measures 180 cm × 300.0 cm at the closure and is of 2.5 cm thick mild steel. Criticality approach was done by gradually narrowing the spacing between each halves of the table. Unreflected experiments are reported, as well as measurements with concrete and/or polyethylene reflectors. Plexiglas was used as a moderator in some cases.

Figure 3.B.1.1 shows a typical calculational model for the experiment. The split table is not taken into consideration explicitly in the calculational model of the reflected experiments. On the other hand, in the calculational model of the unreflected experiment, the table is taken into consideration to be located beneath UF_6 cylinders. The H/U atomic ratio is assumed to be 0.044, just a half of the measured maximum value.

Calculated results together with critical conditions are listed in **Tables 3.B.1.1** through **3.B.1.15**.[40] Histograms of the calculated k_{eff}'s are shown in **Fig. 3.B.1.2** for the 16 unreflected systems and in **Fig. 3.B.1.3** for the 51 reflected systems. The calculated k_{eff}'s for the unreflected systems are between 0.95 and 0.975 with the average value of 0.963. Those for the reflected systems are between 0.975 and 1.02 with the average value of 0.996.

3.B.2 Slab-Cylinder Configurations of Uranyl-Nitrate Solution

Experiments were performed at Rocky Flats, USA, simulating tanks and pipes containing uranyl-nitrate solution in spent fuel reprocessing plants.[41] A slab tank and several cylindrical vessels containing 93.2 wt% ^{235}U enriched uranyl-nitrate aqueous solution were arranged with or without Plexiglas reflector, as typically shown in **Fig. 3.B.2.1**. Vertical cylinders are arrayed on the bottom of slab tank and supported rigidly by two mild steel grid plates. These plates, 152 cm square and 0.159 cm thick each, are fastened to a framework. The cylinders are uniformly spaced in a square pattern with equal center-to-center distance. The space between the centerline of the outermost cylinders and the inner surface of the side walls of the tank was adjusted to be a half of the center-to-center distance of the cylinders. Inner size of the stainless steel slab tank is 120.7 cm square and 20.3 cm high, and the thickness of the side wall is 0.15 cm and that of the bottom is 0.635 cm. This tank is supported by six mild steel pipes. These pipes stand on a mild steel table, 152 cm square and 1.9 cm thick. This table is elevated to 137 cm above concrete floor. Concrete walls of the experimental room are located more than 3 m away from the side walls of the slab tank. Uranium concentration in the uranyl-nitrate solution increases from 465 to 525 gU/l during the experiments because of the evaporation of water. This uranium concentration was measured at each step of the experiments. The H/^{235}U ratio was measured at both the beginning and the end of the experiments. Criticality approach was made by increasing the solution height in the cylinders and/or in the slab tank.

In the calculational model, the drain hose in the slab tank, the mild steel support-pipes and -plates are not included due to the lack of information of their geometric configuration. A typical calculational model for the KENO-IV code is illustrated in **Fig. 3.B.2.2**.[42] Measured uranium concentrations were used for the calculation. The H/^{235}U ratios for the calculation were estimated by the interpolation principle.

Calculated results together with critical conditions for reflected and unreflected slab

cylinder systems are listed in **Tables 3.B.2.1** through **3.B.2.4**.[42] Histogram of the calculated k_{eff}'s for 96 cases in all is shown in **Fig. 3.B.2.3**. The calculated k_{eff}'s for the unreflected systems are between 0.905 and 0.965 with the average value of 0.929, about 7% lower than unity. Those for the reflected systems are between 0.955 and 1.015 with the average value of 0.989, about 1% lower than unity.

3.B.3 Array of Cylinders Containing Uranyl-Nitrate Solution

Experiments were performed at Rocky Flats, USA, using the array of cylinders containing 93.17% ^{235}U enriched uranyl-nitrate solution.[23] Uranium concentration is ranged from 60.32 to 369.96 gU/l. The cylinders are positioned in a cubical plastic or a concrete reflector. Cylindrical containers used in the experiment are made of aluminum with inner diameters from 16.12 cm to 21.12 cm. Each has a coaxial tail pipe, about 30 cm long, welded to the bottom of the container, through which uranyl-nitrate solution is introduced. Stainless steel sleeves are used to cover the cylinders in some experiments. A critical height inside the cylinders is determined by interpolation between a slightly supercritical height and a slightly subcritical height.

In the calculational model, the tail pipes leading uranyl-nitrate solution into the cylinders are neglected, as shown in **Fig. 3.B.3.1**.

Calculated k_{eff}'s are listed in **Tables 3.B.3.1** and **3.B.3.2**.[24] Histogram of the calculated k_{eff}'s for 31 cases in all is shown in **Fig. 3.B.3.2**. As seen from the histogram, the calculated k_{eff}'s are between 0.965 and 1.000 with the average value of 0.982, about 2% lower than unity.

3.B.4 Two Parallel Cylinders Containing Uranyl-Fluoride Solution

Experiments were performed at ORNL, USA, using two parallel cylinders containing 93.4% ^{235}U enriched uranyl-fluoride solution.[43] Uranium concentration ranges from 78.72 gU/l to 758.84 gU/l. Cylindrical containers used in the experiments are made of aluminum with inner diameters of 8, 10 and 15 in.. An experimental system consists of two parallel such cylinders, with or without a water reflector. Criticality approach was done by increasing the solution height inside the cylinders. The uranyl-fluoride solution was introduced into the inside of cylinder through a feeding pipe attached to the bottom of each cylinder.

In the calculational model, a plastic feeding pipe attached to one of the cylinders is neglected, as shown in **Figs. 3.B.4.1** and **3.B.4.2**, due to the lack of information.

Calculated k_{eff}'s are listed in **Table 3.B.4.1** for 29 cases in all.[44] Histogram of these calculated k_{eff}'s is shown in **Fig. 3.B.4.3**. As seen from this figure, the calculated k_{eff}'s are between 0.945 and 1.01 with the average value of 0.976, about 2% lower than unity.

3.B.5 Three-Dimensional Array of Uranium-Metal Cylinders

Experiments were performed at ORNL, USA, using uranium metal cylindrical units arranged in a three-dimensional array.[45] A unit is a cylinder of 11.5 cm in diameter and 5.40 to 13.47 cm in height. Uranium is enriched to 93.2% ^{235}U. The units are supported, with their axes vertical, by stainless steel rods passing through two holes of 0.51 cm diameter in each cylinder. The holes are parallel to the cylinder axis and are separated 8.55 cm each other on a diameter. Paraffin reflectors of 1.3 cm, 2.5 cm, 3.8 cm, 7.6 cm or 15.2 cm thickness were provided for some experimental systems.

In the calculational model, the supporting rods and holes of uranium cylinders are neglected and filled with uranium fuel. **Figure 3.B.5.1** shows a typical calculational model for this array experiment.

Tables 3.B.5.1 and **3.B.5.2** list calculated k_{eff}'s for 31 cases in all.[44] Histogram of these k_{eff}'s is shown in **Fig. 3.B.5.2**. As seen from this histogram, the calculated k_{eff}'s are between 0.995 and 1.025 with the average value of 1.012, about 1% higher than unity.

3.B.6 Two- and Three-Dimensional Array of Plutonium-Metal Cylinders

Experiments were performed at LRL, USA, using plutonium-metal billets in two- or three-dimensional array.[46] A unit of array is a cylinder of 6.53 cm diameter and 4.63 cm height, weighing 3 kg. The ^{239}Pu content in Pu is 93.6%. Doubled billets (6 kg) are also used as a unit of array. The plutonium billets are placed inside supporting tubes. These tubes are fastened upright and arrayed on the assembly table. Vertical positioning within the tube was accomplished with tubular aluminum spacers. Plastic moderator discs are attached to the supporting tubes in some cases. Polyethylene reflector slabs are arranged along the surface of the fissile array in other cases. The parameter used for criticality approach is the distance between units.

The calculational model for a 3 kg plutonium-metal unit is shown in **Fig. 3.B.6.1**. **Figure 3.B.6.2** shows the calculational model for a 6 kg plutonium-metal unit. Calculational models for typical array dispositions are shown in **Figs. 3.B.6.3** and **3.B.6.4**.

Table 3.B.6.1 lists calculated results for 19 experimental cases in all.[44] Histogram of these k_{eff}'s is shown in **Fig. 3.B.6.5**. As seen from the histogram, the calculated k_{eff}'s are between 0.975 and 1.02 with the average value of 0.999, nearly equal to unity.

3.B.7 Three-Dimensional Array of Cylinders Containing Uranyl-Nitrate Solution

Experiments were performed in USA using Plexiglas cylinders containing 93.2% ^{235}U enriched uranyl-nitrate solution.[47] The 5 liter of uranium solution having concentration of 415 gU/l and specific gravity of 1.555 is contained in each of 0.64 cm thick Plexiglas cylinders of 20.32 cm o.d. and 19.05 cm outside height. These cylinders are arranged to be a cubical array of 2×2×2, 3×3×3, 4×4×4 or 5×5×5 units with or without a Plexiglas or paraffin reflector of various thicknesses. The parameter used for criticality approach is the distance between untis.

The calculational model for a typical experimental arrangement is shown in **Fig. 3.B.7.1**.

Tables 3.B.7.1 and **3.B.7.2** list calculated results for 29 cases in all.[44] Histogram of the calculated k_{eff}'s is shown in **Fig. 3.B.7.2**. As seen from the histogram, the calculated k_{eff}'s are between 0.955 and 1.01 with the average value of 0.989, about 1% lower than unity.

3.B.8 Array of Tin Cans Containing UO_2 or UO_2-Alcohol Slurry

Experiments were performed at ORNL, USA, using highly enriched (93.2 wt% ^{235}U) UO_2 and UO_2-alcohol slurry canned in tin and positioned on a split table.[48] Descriptions of four types of fissile units utilized in the experiment are summarized in **Table 3.B.8.1**. **Table 3.B.8.2** lists experimental conditions for 29 cases in all. As shown in this table, experimental cases, from No.1 to No.4, are related to Type I unit. Experiments No.5 to No.19 are related to Type II, and experiments No.20 to No.29 to Type III and Type IV. Type III and Type IV units contain alcohol, which is intended to simulate such conditions as wet oxide powders in processing, transport or storage.

The KENO-IV calculational models for the fissile units are shown in **Fig. 3.B.8.1**.[36] Canning material, tin, is assumed to be steel, since the MGCL data library does not provide cross section data for tin. A calculational array model is shown in **Fig. 3.B.8.2**. As shown in this figure, the reflector thickness is assumed to be 18.1 cm.

Calculated results together with principal experimental parameters[36] are listed in **Table 3.B.8.3**. As seen from this table, C/E value ranges between 0.976 and 1.015.

C. Heterogeneous System

3.C.1 LWR Critical Assemblies with Various Lattice Pitches and Patterns

Experiments were performed using the Tank-type Critical Assembly (TCA) at the Japan Atomic Energy Research Institute.[49] Critical assemblies of TCA consist essentially of fuel rods, grid plates and a core tank with a water moderator and reflector. The core tank is 1.83 m in diameter and 2.08 m in height as shown in **Fig. 3.C.1.1**. Experimental lattices were built in the core tank, and made critical by raising the water level incrementally. No control-rod operation was needed to attain criticality. Fuel is either of 2.6% ^{235}U enriched UO_2 or of 3.0% PuO_2-U(natural)O_2, as shown in **Fig. 3.C.1.2**. Water-to-fuel volume ratio in a lattice cell ranges from 1.50 to 3.00 for the UO_2 fuel, and from 2.42 to 5.55 for the PuO_2-UO_2 fuel. Fuel rods are held vertical in the core tank by the grid plates. In some experiments, the water gap was formed by removing several rows from a uniform square-pitch lattice array. In some cases, H_3BO_3 soluble poison was added into the water in the core tank. In other cases, poison plates such as Al-Cd sheets were inserted between fuel-rod rows. There are five types of experimental systems as follows:

(1) UO_2-H_2O systems,
(2) PuO_2-UO_2-H_2O systems,
(3) UO_2-Water Gap systems,
(4) UO_2-H_3BO_3-H_2O systems,
(5) UO_2-poison plate-H_2O systems.

The KENO calculational model for UO_2-H_2O systems is shown as a typical case in **Fig. 3.C.1.3**.[50] As shown in this figure, a UO_2 fuel rod is modeled to be a cylinder of 12.50 mm o.d. with 1441.5 mm height, clad with an aluminum cylinder of 14.17 mm o.d. with 0.76 mm thickness. For PuO_2-UO_2-H_2O systems, a fuel rod is modelled to be a cylinder of 10.65 mm o.d. and 706 mm height, clad with a zircaloy-2 cylinder of 12.23 mm o.d. with 0.70 mm thickness. The gap between pellet and cladding is replaced by fuel. Water reflector thickness around submerged lattices is assumed to be more than 40 cm in these calculational models.

Calculated k_{eff}'s for 125 cases in all are listed in **Tables 3.C.1.1** through **3.C.1.5**,[50] respectively, corresponding to five experimental systems. Histograms of the calculated k_{eff}'s are shown in **Figs. 3.C.1.4** through **3.C.1.6**. The average values of these calculated k_{eff}'s are about 0.99 for all systems, in good agreement with experimental values.

3.C.2 UO_2 Rod Clusters Partially Immersed in Water with Various Lattice Pitches and Patterns

Experiments were performed in France, simulating water storage of UO_2 fuel assemblies with variation of lattice pitches and patterns.[51] Uranium is enriched to 4.75 wt% ^{235}U. The lattice pattern is either hexagonal or square as shown in **Figs. 3.C.2.1** and **3.C.2.2**. There are three types of UO_2 rod clusters, i.e., without removal of rods, with systematic removal of rods and with removal of rods in a small zone. The experimental arrangement of fuel rods in water is shown in **Fig. 3.C.2.3**. Criticality approach was made by raising the water level incrementally.

The calculational model consists of a part of fuel assembly submerged in water, bottom

plugs, support plate, lower grid and water.

Calculated k_{eff}'s together with experimental conditions are listed in **Tables 3.C.2.1** through **3.C.2.3**. Histogram of the calculated k_{eff}'s is shown in **Fig. 3.C.2.4**. The average value of these 26 k_{eff}'s is 0.990, about 1% lower than unity.

3.C.3 UO_2 Rod Clusters Fully Immersed in Water at Near-Optimum Neutron Moderation with Various Poison Plates

Experiments were performed at BNWL, USA, simulating a spent fuel storage in water pools or shipping casks with various neutron absorbing materials.[52),53)] Three identical subcritical UO_2 clusters aligned in a row were used in the experiment. Uranium in UO_2 is enriched to either 2.35 wt% ^{235}U or 4.31 wt% ^{235}U. There are two types of UO_2 rod, as are depicted in **Figs. 3.C.3.1** and **3.C.3.2**. The UO_2 rods are arrayed in a water pool in a square pitch of 2.032 cm or 2.450 cm, providing near-optimum neutron moderation. The experimental arrangement is shown in **Fig. 3.C.3.3**. Critical separation Xc, as shown in this figure, was determined with various poison plate materials/thicknesses located between the clusters. The following materials are utilized for the poison plates in the experiment:

Boral,
304L Stainless Steel with 0.0, 1.1 and 1.6 wt% Boron,
Copper with 0.0 and 1.0 wt% Cadmium,
Cadmium,
Aluminum,
Zircaloy-4.

The KENO-IV calculational model for the UO_2 lattice cell is shown in **Fig. 3.C.3.4**.[54)] The calculational model for a typical experimental arrangements is shown in **Fig. 3.C.3.5**. As shown in this figure, the calculational model consists of three UO_2 rod clusters submerged in water and two poison plates. Thickness of the water reflector surrounding the clusters is assumed to be more than 20 cm. Supporting materials such as 12.7 mm thick acrylic plates, aluminum angles, aluminum spacer rods and acrylic grid plates are all substituted by water to simplify the model.

Calculated k_{eff}'s together with critical experimental data are listed in **Tables 3.C.3.1** and **3.C.3.2**.[54)] Histograms of the calculated k_{eff}'s are shown in **Figs. 3.C.3.6** and **3.C.3.7**. The average value of these 75 calculated k_{eff}'s is 0.990, about 1% lower than unity, irrespective of the difference in the uranium enrichment.

3.C.4 UO_2 Rod Clusters Fully Immersed in Water at Near-Optimum Neutron Moderation with Reflecting Walls

Experiments were performed at BNWL, USA, simulating spent fuel storage in water pool or shipping casks with reflecting walls.[55)] Three identical subcritical UO_2 rod clusters aligned in a row were used in the experiment. Uranium in UO_2 is enriched to either 2.35 wt% ^{235}U or 4.31 wt% ^{235}U. The UO_2 rods are the same as depicted in **Figs. 3.C.3.1** and **3.C.3.2**. These UO_2 rods are arrayed in a water pool in a square pitch of 2.032 cm or 2.450 cm to be a rectangular parallelepiped cluster, providing near-optimum neutron moderation. The experimental arrangement of the clusters is shown in **Fig. 3.C.4.1**. As shown in this figure, lead or depleted uranium reflecting walls are set up on both sides of the three aligned clusters. The critical separation (Xc) between the clusters was determined at various distances (Y) between the reflecting walls and the side of the clusters.

The KENO-IV calculational model for two types of UO_2 lattice cell is shown in **Fig.**

3.C.3.4. The calculational model for a typical experimental system is shown in **Fig. 3.C.4.2**. The calculational model consists of three UO_2 rod clusters submerged in water, lead or depleted uranium side reflectors and the water reflector of more than 20 cm thickness around the clusters. Supporting materials such as 12.7 cm thick acrylic plates, aluminum angles, aluminum spacer rods and acrylic grid plates are all substituted by water in the simplified model.

Calculated k_{eff}'s together with critical experimental data are listed in **Table 3.C.4.1**. Histogram of the calculated k_{eff}'s is shown in **Fig. 3.C.4.3**. The average value of these 23 calculated k_{eff}'s is 0.990, about 1% lower than unity, irrespective of the difference in the uranium enrichment and reflecting wall.

3.C.5 UO_2 Rod Clusters Fully Immersed in Water at Under-moderation with Various Poison Plates

Experiments were performed at BNWL, USA, simulating a spent fuel storage in water pool or shipping casks with various neutron absorbing materials.[56] Three subcritical UO_2 rod clusters aligned in a row and four cross arranged subcritical UO_2 rod clusters are used in the experiment. Uranium in UO_2 is enriched to either 2.35 wt% ^{235}U or 4.31 wt% ^{235}U. The UO_2 rods are the same as those depicted in **Figs. 3.C.3.1** and **3.C.3.2**. These UO_2 rods are arrayed in a water pool in a square pitch of 1.684 cm or 1.892 cm to be a rectangular parallelepiped cluster, providing typical LWR fuel moderating conditions at under-moderation. For the experiments of three aligned clusters, the critical separation (Xc), as shown in **Fig. 3.C.3.3**, was measured with various poison plate materials of various thicknesses inserted between each of the three clusters. In the experiments of four cross arranged clusters, the poison plates were attached to the cell boundaries on one side of the clusters, as shown in **Fig. 3.C.5.1**, and fuel rods were added, one by one, in the opposit side of the poison plates to reach criticality. The following materials are used for the poison plates:

Aluminum,
Zircaloy-4,
304L Stainless steel (0.0, 1.1 and 1.6 wt% Boron),
Boral (A, B, C),
Boroflex,
Cadmium,
Copper,
Copper-Cadmium.

The KENO-IV calculational models for the two types of UO_2 lattice cells are shown in **Fig. 3.C.3.4**. The calculational model for a typical four cross arranged clusters is shown in **Fig. 3.C.5.2**. The calculational model for three aligned clusters is the same as that shown in **Fig. 3.C.3.5** except for the lattice pitch. The calculational model consists of three or four rod clusters submerged in water, two poison plates parallel or crossed, and the water reflector of more than 20 cm thickness around the clusters. Supporting materials such as 12.7 cm thick acrylic plates, aluminum angles, aluminum spacer rods and acrylic grid plates are all substituted by water in the simplified model.

Calculated k_{eff}'s together with critical experimental data are listed in **Tables 3.C.5.1** and **3.C.5.2**. Histograms of calculated k_{eff}'s are shown in **Figs. 3.C.5.3** and **3.C.5.4**. The average value of these 110 calculated k_{eff}'s is 0.995, about 0.5% lower than unity, irrespective of the difference in uranium enrichment and the poison plates.

3.C.6 UO_2 Rod Clusters Fully Immersed in Water at Under-moderation with Reflecting Walls

Experiments were performed at BNWL, USA, simulating a spent fuel storage in water pools or shipping casks with reflecting walls.[57] Three identical subcritical UO_2 rod clusters aligned in a row were used in the experiment. Uranium of UO_2 is enriched to either 2.35 wt% or 4.31 wt% ^{235}U. The UO_2 rods are the same as those depicted in **Fig. 3.C.3.1** or **Fig. 3.C.3.2**. These UO_2 rods are arrayed in a water pool in a square pitch of 1.684 cm or 1.892 cm to be a rectangular parallelepiped cluster, providing typical LWR neutron moderation. Lead or depleted uranium reflecting walls are set up on both sides of the three clusters. The critical separation (Xc) is measured at various distances (Y) between the reflecting wall and the side of the cluster, as shown in **Fig. 3.C.4.1**.

The KENO-IV calculational model for two types of UO_2 lattice cells is shown in **Fig. 3.C.3.4**. The calculational model for a typical experimental system is the same as that shown in **Fig. 3.C.4.2** except for the lattice pitch. The calculational model consists of three UO_2 rod clusters submerged in water, lead or depleted uranium side reflectors and the water reflector of more than 20 cm thickness around the clusters. Supporting materials such as 12.7 cm thick acrylic plates, aluminum angles, aluminum spacer rods and acrylic grid plates are all substituted by water in the simplified model.

Calculated k_{eff}'s together with critical experimental data are listed in **Table 3.C.6.1**. Histogram of the calculated k_{eff}'s is shown in **Fig. 3.C.6.1**. The average value of these 22 calculated k_{eff}'s is 0.990, about 1% lower than unity, irrespective of the difference in the uranium enrichment and the reflecting wall.

3.C.7 UO_2 Rod Clusters Fully Immersed in Water at Various Pitches with Poison Plates and Reflecting Walls

Experiments were performed at BNWL, USA, simulating a spent fuel storage in water pools or shipping casks with poison plates and reflecting walls.[58] Three subcritical UO_2 rod clusters aligned in a row were used in the experiment. Uranium in UO_2 is enriched to either 2.35 wt% or 4.31 wt% ^{235}U. The UO_2 rods are the same as those depicted in **Fig. 3.C.3.1** or **Fig. 3.C.3.2**. These UO_2 rods are arrayed in a water pool in a square pitch of 1.684, 1.892, 2.032 and 2.540 cm to be a rectangular parallelepiped cluster. The critical separation Xc, as shown in **Fig. 3.C.7.1**, is measured with various poison plate materials of various thicknesses inserted between each of the three rod clusters and with steel reflecting walls set up on both sides of the three clusters. The following materials are used for the poison plates:

304L Stainless steel (0.0 and 1.1 wt% Boron),
Boral B,
Boroflex,
Cadmium,
Copper,
Copper-Cadmium.

The KENO-IV calculational models for two types of UO_2 lattice cell are shown in **Fig. 3.C.3.4**. Calculational model for a typical experimental system is shown in **Fig. 3.C.7.2**. The calculational model consists of three rod clusters submerged in water, two poison plates, two steel side reflectors and the water reflector of more than 20 cm thickness around the clusters. Supporting materials such as 12.7 cm thick acrylic plates, aluminum angles, aluminum spacer rods and acrylic grid plates are all substituted by water in the simplified model.

Calculated k_{eff}'s together with critical experimental data are listed in **Table 3.C.7.1**.

Histograms of the calculated k_{eff}'s are shown in **Figs. 3.C.7.3** and **3.C.7.4**. The average values of the 49 calculated k_{eff}'s are 0.990 for 2.35 wt% ^{235}U enriched UO_2 systems and 0.992 for 4.31 wt% ^{235}U enriched UO_2 systems.

3.C.8 Triangular Lattice of Plutonium Alloy or Mixed Oxide Fuel Moderated by Borated Water

The US NUREG report[25] contains 20 critical experiments concerning water moderated triangular lattices of plutonium alloy or mixed oxide fuel. These experiments were selected to provide data for benchmark calculations to evaluate the accuracy of neutron cross sections for the plutonium isotopes. They cover a wide range of H/Pu ratio, i.e., a wide variation in neutron spectrum. They also cover a wide range of ^{240}Pu content as listed in **Table 3.C.8.1**. Fuel rods are arrayed in a water pool in a triangular lattice to be a cylindrical assembly. The assembly is surrounded by water of more than 20 cm thickness.

Since the configuration of fuel rods is not precisely given in the report, the fuel assembly is assumed to have a cylindrical periphery as perfect as possible in calculational models. Typical calculational models are shown in **Figs. 3.C.8.1** and **3.C.8.2**.

Calculated results are listed in **Table 3.C.8.2**.[59] Histogram of the calculated k_{eff}'s for 20 cases in all is shown in **Fig. 3.C.8.3**. One can see that the calculation predicts an average value of 1.004, close to unity.

3.C.9 Mixed Oxide Fuel Lattice Moderated by Borated Water

Experiments were performed at EPRI, USA, at the Plutonium Recycle Facility (PRCF) to obtain the critical number of fuel rods in water moderator with various boron concentration.[60] The PRCF is an experimental reactor generating low power (15 kW thermal), designed for studying neutronics phenomina in liquid moderated reactor cores. **Figure 3.C.9.1** shows an example of loading pattern of fuel pins. The fuel is either of 2.35 wt% ^{235}U enriched UO_2 or UO_2 2 wt% PuO_2 (8 wt% ^{240}Pu). Descriptions of these fuel rods are shown in **Figs. 3.C.9.2** and **3.C.9.3**. Lattice pitch is determined to provide under-moderation, near-optimum moderation or over-moderation for each of the fuel types.

In the KENO-IV calculational model, supporting structure is neglected, so that the calculational model consists of the lattice of fuel rods surrounded borated water as moderator or reflector.

Calculated results together with critical experimental data are listed in **Table 3.C.9.1**.[36] The calculated k_{eff}'s for 12 cases in all range from 0.983 to 1.022 with the average value of just 1.000. The calculated k_{eff}'s for the UO_2-PuO_2 fuel systems are about 1% larger on average than those for the UO_2 fuel systems.

3.C.10 Water Storage of Power Reactor Fuel in Close Proximity

Experiments were performed at BAW, USA, supporting close proximity water storage of spent fuel assemblies of power reactor fuel.[61] Uranium of UO_2 is enriched to 2.46 wt% ^{235}U. The UO_2 fuel pins are arrayed in a square pitch of 1.636 cm to be a 14×14 pin assembly. These fuel assemblies are arranged to make a 3×3 square assembly array with assembly-to-assembly gaps of zero to four pin pitches, i.e., 0.0, 3.27, 4.91 and 6.54 cm. The 3×3 array is set up in a water tank of 152.4 cm i.d., 198 cm height, 1.27 cm wall thickness. The following materials are inserted in the gaps between the fuel assemblies, providing various experimental loadings:

B_4C filled pins,

Stainless steel sheets,
Borated aluminum sheets.

An example of core loading patterns is shown in **Fig. 3.C.10.1**.

Typical calculational models are shown in **Figs. 3.C.10.2** and **3.C.10.3**. As shown in these figures, the experimental core loadings patterns are classified into two groups according to the supporting method of fuel pins. Structural materials such as aluminum top grids and aluminum core frames are neglected in the calculational model.

Calculated k_{eff}'s together with measured values for 21 cases in all are listed in **Table 3.C.10.1**.[36] It is seen that the calculated k_{eff}'s range from 0.99 to 1.02 with the average value of 1.003. **Table 3.C.10.2** shows inter-comparison of the measured and calculated k_{eff}'s for the different spacings between the assemblies.

3.C.11 Array of UO_2-BeO Fuel Pins in Uranyl-Nitrate Solution

Experiments were performed at ORNL, USA, simulating a dissolver in spent fuel reprocessing facility.[62] A homogeneous mixture of UO_2-BeO is compacted to ceramic pellets. Uranium is enriched to 62.4 wt% ^{235}U. The pellets are clad with Hastelloy 280 tubings of 0.952 cm o.d. and 196.8 cm length. The effective length of fuel is 143 cm. These fuel pins are arrayed in a square pitch in a moderator/reflector tank, filled with water for one series of experiments and with borated uranyl-nitrate solution for another series of experiments. Fuel pins are fixed by Plexiglas spacers and aluminum struts. The lattice pitch and its pattern are varied from case to case, as shown in **Fig. 3.C.11.1**. Criticality approach was made by increasing the aqueous moderator/reflector height in the tank.

The calculational model for the fuel pin is shown in **Fig. 3.C.11.2**. **Figure 3.C.11.3** shows calculational model for a water reflected system, and **Fig. 3.C.11.4** for a uranyl-nitrate solution system. In these models, the Plexiglas spacers and the aluminum struts are neglected.

Calculated results together with experimental conditions are listed in **Tables 3.C.11.1** and **3.C.11.2**.[36] The average k_{eff} values are 0.965 for the 12 water reflected systems and 0.976 for the 6 uranyl-nitrate solution systems, about 3 to 4% lower than unity.

3.C.12 UO_2 Rod Clusters Fully Immersed in Borated Water

Experiments were performed at BNWL, USA, simulating a close proximity water storage of spent fuel assemblies.[63] Uranium is enriched to 4.31 wt% ^{235}U. The schema of fuel rod is shown in **Fig. 3.C.12.1**. Maximum of 1237 UO_2 fuel rods are arrayed in a square pitch of 1.890 cm or 1.715 cm in a rectangular fashion. This fuel assembly is set up in a Plexiglas box of 79.7 cm width, 83.41 cm length and 116.8 cm height with 1.905 cm wall thickness. Borated water is poured into the box to reach a level of 15.2 cm above the top end of the fuel rods, as shown in **Fig. 3.C.12.2**. With the array width remaining constant as 40 or 44 rods depending on the pitch, the array length is increased symmertically one by one to reach criticality. Critical experimental data such as the number of fuel rods required to attain criticality, are shown in **Table 3.C.12.1**.

The calculational model is shown in **Fig. 3.C.12.3**. Supporting materials such as upper and bottom polypropylene templates are neglected in the model. The KENO-IV calculation was performed by varing the number of neutrons per batch.

Calculated k_{eff}'s for 9 cases in all are listed in **Table 3.C.12.2**. Histograms of the calculated k_{eff}'s are shown in **Figs. 3.C.12.4** and **3.C.12.5**. The average value is 0.98, about 2% lower than unity, irrespective of the difference in the number of neutrons per batch.

3.C.13 UO_2 Rod Clusters in Sodium-Nitrate Solution

Experiments were performed in France, simulating UO_2 fuel assemblies in a dissolver of reprocessing plant.[64] Maximum of 600 fuel rods are laid out in a square pitch lattice by means of a stainless steel basket made up of two spacing grids and a support plate. The square pitch is selected from 1.260 cm, 1.600 cm, 2.100 cm and 2.520 cm. Uranium is enriched to 4.74 wt% ^{235}U. The fuel assembly is put into an experimental tank. Sodium-nitrate solution, acting as a moderator/reflector, is introduced through an inlet into the bottom of the tank. The solution height is the critical approach parameter. The experimental set up is shown in **Fig. 3.C.13.1**.

The calculational model for a fuel rod is shown in **Fig. 3.C.13.2**. **Figure 3.C.13.3** shows the calculational model for a typical experimental set up. Structural materials except for the lower grid and the support plate are neglected, as shown in this figure.

Calculated k_{eff}'s for 6 cases in all are listed in **Table 3.C.13.1**. The average value of the calculated k_{eff}'s is 0.986, about 1% lower than unity.

3.C.14 Triangular Lattice of UO_2 Fuel Moderated by Poisoned Water

Experiments were performed at BNWL, USA, using soluble neutron absorbers (poisons) to determine their effectiveness for criticality prevention of UO_2 fuel lattice assemblies.[65] UO_2 rods enriched to 4.3 wt% ^{235}U are assembled in a triangular pitch in a water tank with soluble neutron absorbers such as boron, cadmium, and gadolinium. The triangular pitch is selected from 2.29, 2.79 and 3.30 cm. Experimental systems are set up as shown in **Fig. 3.C.14.1**. Criticality approach was done by adding fuel rods, one by one, on the cylindrical periphery of the assembly.

The calculational model is shown conceptually in **Fig. 3.C.14.2**. As shown in this figure, structural materials other than the lower lattice plate are neglected.

Table 3.C.14.1 lists calculated results together with experimental conditions for 20 cases in all. Histogram of the calculated k_{eff}'s is shown in **Fig. 3.C.14.3**. The calculated k_{eff}'s distribute between 0.955 and 1.035, with the average value of 0.989, about 1% lower than unity.

3.C.15 UO_2 Rod Clusters Partially Immersed in Uranyl-Nitrate Solution

Experiments were performed at BNWL, USA, to determine the effect of gadolinium as a soluble neutron absorber on the criticality of UO_2 fuel rod assemblies in uranyl-nitrate solution.[66] Uranium in UO_2 is enriched to 4.3 wt% ^{235}U. The UO_2 rods are cylindrically arrayed in an experimental vessel in a triangular pitch selected from 2.29, 2.79 and 3.30 cm. Uranyl-nitrate solution with the same ^{235}U enrichment as that of UO_2 was subsequently added to approach criticality. Outside the experimental vessel is the water provided by a steel tank, as shown in **Fig. 3.C.15.1**.

The calculational model is shown in **Fig. 3.C.15.1**. Structural materials other than the experimental vessel are neglected in the calculational model.

Calculated results together with experimental conditions are listed in **Table 3.C.15.1**. Histogram of the calculated k_{eff}'s for all 12 cases is shown in **Fig. 3.C.15.2**. As seen from the histogram, the calculated k_{eff}'s are distributed between 0.895 and 0.975 with the average value of 0.938, about 6% lower than unity.

3.C.16 UO_2-PuO_2 Rod Clusters Partially Immersed in Uranyl-Plutonium-Nitrate Solution with Soluble Poisons

Experiments were performed at BNWL, USA, simulating spent fuel elements in a

dissolver vessel.[38] Total of 301 UO_2-PuO_2 mixed oxide fuels are assembled to be a triangular lattice array with cylindrical boundary, and positioned in a 55.5 cm i.d. stainless steel vessel. The vessel is, in turn, included in a larger cylindrical tank, providing a water reflector. The lattice pitch is specified to be 3.048 cm. Subsequently, plutonium-uranyl-nitrate solution, containing gadolinium and/or boron at various concentrations as soluble neutron absorbers, is added to the loaded lattice assembly to obtain criticality. **Figure 3.C.16.1** gives schema of the experimental system, showing water reflector, vents, dump lines, etc.

In the calculational model, the stainless steel vessel containing fuel rods and solution together with water reflector is taken into consideration, but other structural materials are neglected, as shown in **Fig. 3.C.16.2**. The vessel diameter is assumed to be 67.16 cm, since the diameter of 55.5 cm specified in the experiment report cannot accomodate 301 fuel rods in the specified pitch. The MULTI-KENO code, a modified version of the KENO-IV code, was utilized, since cylindrical boundary, in which "CUBOID" type fuels are arrayed, cannot be treated easily by the KENO-IV code. The reason is that, in this case, intersection, which is not allowed in KENO-IV, is occured between the cylindrical boundary and the fuel array.

Table 3.C.16.1 lists calculated results together with experimental conditions. Histogram of the calculated k_{eff}'s for 13 cases in all is shown in **Fig. 3.C.16.3**. As seen from the histogram, the calculated k_{eff}'s are between 1.00 and 1.025 with the average value of 1.010, about 1% higher than unity.

Table 3.A.1.1 Experimentally determined critical heights for 30.6 H/(Pu+U) fuel systems

Serial No.	Layers of fuel (50.9mm)	Neutron poison plate: Type	Plate mass (kg)	Plate thickness (mm)	Plate+Void thickness (mm)	Layers of fuel (50.9 mm)	Layers of fuel (13.84mm)	Total layers of fuel (50.9 mm)
001	3	None (g)	0	0	—	1	3.578	4.921±0.006
002	3	Steel (g)	3.902±0.010	3.10±0.05	3.5±0.5	2	0.781	5.201±0.002
003	3	Steel (g)	7.804±0.014	6.20±0.07	6.9±0.8	2	1.655	5.426±0.002
004	3	Steel (g)	19.510±0.022	15.50±0.11	15.9±0.5	2	3.667	5.944±0.505
005	3	Steel (g)	31.216±0.028	24.80±0.14	25.2±0.5	3	1.317	6.339±0.003
006	3	Steel (g)	46.824±0.034	37.20±0.17	38.0±1.0	3	2.770	6.713±0.003
007	3	Steel (g)	62.432±0.040	49.64±0.19	51.2±0.8	4	0.012	7.003±0.004
008	3	1.1WT% B-Steel	3.908±0.028	2.98±0.06	3.8±0.9	3	1.251	6.322±0.004
009	3	1.1WT% B-Steel	7.816±0.040	5.95±0.08	7.0±0.8	3	2.937	6.756±0.006
010	3	1.1WT% B-Steel	15.632±0.056	11.91±0.11	13.2±0.7	4	0.866	7.223±0.006
011	3	1.1WT% B-Steel	23.448±0.069	17.86±0.14	18.9±0.6	4	1.663	7.428±0.002
012	3	1.1WT% B-Steel	42.998±0.094	32.75±0.18	35.1±0.5	4	2.813	7.724±0.006
013	3	1.6WT% B-Steel	3.834±0.008	2.98±0.05	3.4±0.5	3	2.074	6.534±0.004
014	3	1.6WT% B-Steel	3.834±0.008	2.98±0.05	3.4±0.5	3	2.024	6.521±0.005
015	3	1.6WT% B-Steel	15.336±0.017	11.94±0.11	12.8±1.0	4	1.336	7.344±0.003
016	3	1.6WT% B-Steel	30.672±0.024	23.87±0.15	25.6±1.9	4	2.661	7.685±0.005
017	3	Uranium	20.165±0.021	6.58±0.13	6.7±0.2	2	1.445	5.372±0.002
018	3	Uranium	61.370±0.030	19.53±0.18	20.2±0.5	2	3.586	5.923±0.002
019	3	Uranium	141.195±0.042	45.05±0.24	46.5±0.7	3	2.762	6.711±0.003
020	3	Uranium	182.370±0.047	57.99±0.30	60.1±1.5	4	0.109	7.028±0.004
021	3	Boral	1.552±0.002	3.68±0.06	4.2±0.6	4	0.967	7.249±0.005
022	3	Boral	3.142±0.002	7.52±0.08	8.2±0.7	4	2.479	7.638±0.005
023	3	Boral	7.840±0.002	18.71±0.12	19.5±0.8	5	0.047	8.012±0.006
024	3	Boral	10.907±0.002	25.98±0.15	26.8±0.8	5	0.548	8.141±0.006
025	3	Boral	15.393±0.002	36.60±0.18	38.2±0.8	5	3.885	8.246±0.006
026	3	Cadmium	1.442±0.001	1.058±0.005	1.28±0.2	3	1.736	6.447±0.004
027	3	Cadmium	2.847±0.001	2.079±0.005	2.30±0.2	3	2.350	6.605±0.005
028	3	Lead	12.231±0.021	6.44±0.03	6.5±0.1	2	0.190	5.049±0.002
029	3	Lead	30.496±0.030	16.02±0.02	16.1±0.1	2	0.921	5.237±0.002
030	3	Lead	61.386±0.036	32.00±0.02	32.8±0.5	2	1.989	5.512±0.003
031	3	Lead	86.136±0.042	44.86±0.02	45.7±0.8	2	2.984	5.768±0.003
032	3	Lead	110.896±0.047	57.71±0.03	58.0±0.3	3	0.062	6.016±0.002

Table 3.A.1.2 Experimentally determined critical heights for 2.8 H/(Pu+U) fuel (partly replaced with 30.6 H/(Pu+U) fuel) systems

Serial no.	Layers of 2.8H:Pu+U fuel (50.9mm)	Neutron poison plate: Type	Plate mass (kg)	Plate thickness (mm)	Plate+Void thickness (mm)	Layers of fuel: 2.8H:Pu+U fuel (50.9mm)	30.6H:Pu+U fuel (50.9mm)	30.6H:Pu+U fuel (13.84mm)	Total layers of fuel (50.9mm)
033	2	None	0	0	--	2	2	0.233	6.060±0.003
034	2	Steel	19.510±0.022	15.50±0.11	16.4±0.5	2	2	1.309	6.337±0.003
035	2	Steel	42.922±0.033	34.11±0.16	34.8±0.3	2	2	2.292	6.590±0.003
036	2	1.1WT% B-Steel	3.908±0.028	2.98±0.06	3.1±0.3	2	2	0.995	6.256±0.003
037	2	1.1WT% B-Steel	19.540±0.063	14.88±0.12	15.8±0.1	2	2	2.754	6.709±0.003
038	2	1.1WT% B-Steel	42.988±0.094	32.75±0.18	34.7±1.5	2	2	3.966	7.021±0.003
039	2	1.6WT% B-Steel	3.834±0.008	2.98±0.05	3.2±0.3	2	2	1.173	6.302±0.003
040	2	1.6WT% B-Steel	30.672±0.024	23.87±0.15	25.2±1.2	2	2	3.733	6.961±0.003
041	2	Uranium	20.165±0.021	6.58±0.13	7.1±0.7	2	2	0.761	6.196±0.003
042	2	Uranium	61.370±0.030	19.53±0.18	20.1±0.7	2	2	1.472	6.379±0.003
043	2	Uranium	182.370±0.047	57.99±0.30	59.8±0.7	2	2	3.302	6.850±0.003
044	2	Boral	1.552±0.002	3.68±0.06	3.9±0.3	2	2	2.300	6.592±0.003
045	2	Boral	4.747±0.002	11.38±0.10	11.7±0.4	2	2	3.908	7.006±0.004
046	2	Boral	15.393±0.002	36.60±0.18	39.2±1.9	2	2	1.670	7.430±0.004
047	2	Cadmium	2.847±0.001	2.079±0.005	2.30±0.21	2	2	1.049	6.270±0.003
048	2	Lead	18.265±0.021	9.58±0.03	10.9±1.4	2	2	0.719	6.185±0.003
049	2	Lead	49.265±0.030	25.55±0.04	26.3±0.8	2	2	1.395	6.359±0.003
050	2	Lead	79.761±0.042	41.58±0.06	43.2±1.4	2	2	1.872	6.482±0.003
051	2	Aluminum	11.910±0.056	26.78±0.06	27.1±0.4	2	2	1.620	6.419±0.003

Table 3.A.1.3 Calculated k_{eff}'s for 30.6 H/(Pu+U) fuel systems

No.	k_{eff}	σ
None		
001	1.0248	0.0054
Steel		
002	1.0205	0.0047
003	1.0260	0.0046
004	1.0181	0.0044
005	1.0214	0.0047
006	1.0210	0.0043
007	1.0246	0.0047
Average	1.0219	
1.1 wt% boron steel		
008	1.0197	0.0049
009	1.0285	0.0047
010	1.0186	0.0050
011	1.0138	0.0045
012	1.0226	0.0047
Average	1.0206	
1.6 wt% boron steel		
013	1.0213	0.0045
014	1.0251	0.0051
015	1.0152	0.0049
016	1.0139	0.0039
Average	1.0189	

No.	k_{eff}	σ
Uranium		
017	1.0215	0.0046
018	1.0206	0.0049
019	1.0206	0.0050
020	1.0276	0.0044
Average	1.0236	
Boral		
021	1.0276	0.0049
022	1.0285	0.0050
023	1.0266	0.0046
024	1.0332	0.0048
025	1.0189	0.0053
Average	1.0269	
Cadmium		
026	1.0121	0.0051
027	1.0214	0.0048
Average	1.0167	
Lead		
028	1.0316	0.0048
029	1.0287	0.0046
030	1.0294	0.0055
031	1.0274	0.0046
032	1.0184	0.0047
Average	1.0271	

Table 3.A.1.4 Calculated k_{eff}'s for 2.8 H/(Pu+U) fuel (partly replaced with 30.6 H/(Pu+U) fuel) systems

No.	k_{eff}	σ
None		
033	1.0212	0.0047
Steel		
034	1.0224	0.0045
035	1.0239	0.0037
Average	1.0231	
1.1 wt% boron steel		
036	1.0240	0.0043
037	1.0284	0.0043
038	1.0281	0.0044
Average	1.0268	
1.6 wt% boron steel		
039	1.0276	0.0046
040	1.0233	0.0049
Average	1.0254	
Uranium		
041	1.0320	0.0047
042	1.0303	0.0043
043	1.0252	0.0043
Average	1.0292	

No.	k_{eff}	σ
Boral		
044	1.0274	0.0046
045	1.0160	0.0042
046	1.0292	0.0047
Average	1.0242	
Cadmium		
047	1.0329	0.0043
Lead		
048	1.0283	0.0043
049	1.0271	0.0043
050	1.0254	
Average	1.0208	0.0051
Aluminum		
051	1.0284	0.0044

Table 3.A.2.1 Critical assembly configurations and calculated k_{eff}'s for PuO_2-UO_2-Polystyrene fuel compacts of 29.3 wt% Pu and 2.8 H/(Pu+U)

No.	Critical Number of Fuel Compacts						
	Reflector	Length (5.090 cm)	Width (5.083 cm)	Height (5.090 cm)	Height (1.339 cm)	Corrected Height (5.090 cm)	KENO $k_{eff} \pm \sigma$
1	None	10	10	8	3.768 ± 0.008	8.888 ± 0.019	0.9895 ± 0.0036
2	None	10	11	8	1.510 ± 0.002	8.252 ± 0.004	0.9845 ± 0.0045
3	Plexiglas	7	7	7	0.646 ± 0.001	7.060 ± 0.010	1.0085 ± 0.0036
4	Plexiglas	8	8	5	2.548 ± 0.004	5.615 ± 0.008	0.9976 ± 0.0042
5	Plexiglas	9	9	4	4.192 ± 0.011	4.997 ± 0.013	1.0112 ± 0.0045
6	Plexiglas	10	10	4	1.300 ± 0.002	4.316 ± 0.007	1.0021 ± 0.0044
7	Plexiglas	10	10	4	1.297 ± 0.003	4.308 ± 0.009	1.0036 ± 0.0041
8	Plexiglas	12	10	4	0.038 ± 0.001	3.948 ± 0.006	1.0015 ± 0.0041
9	Plexiglas	12	12	3	2.791 ± 0.004	3.668 ± 0.005	1.0024 ± 0.0039
10	Plexiglas	12	13	3	2.407 ± 0.005	3.578 ± 0.006	1.0019 ± 0.0046
11	Plexiglas	14	13	3	2.068 ± 0.007	3.487 ± 0.009	1.0068 ± 0.0036
12	Plexiglas	∞	∞	-	---	2.540 ± 0.028	1.0070 ± 0.0042
						Average	1.0014

Table 3.A.2.2 Critical assembly configurations and calculated k_{eff} for PuO_2-UO_2-Polystyrene fuel compacts of 15.0 wt% Pu and 2.86 H/(Pu+U)

No.	Critical Number of Fuel Compacts						
	Reflector	Length (5.090 cm)	Width (5.090 cm)	Height (5.082 cm)	Height (1.265 cm)	Corrected Height (5.082 cm)	KENO $k_{eff} \pm \sigma$
13	Plexiglas	10	10	9	6.651 ± 0.016	10.749 ± 0.031	0.9955 ± 0.0042

Table 3.A.2.3 Critical assembly configurations and calculated k_{eff}'s for PuO_2-UO_2-Polystyrene fuel compacts of 8.1 wt% Pu and 7.3 H/(Pu+U)

No.	Critical Number of Fuel Compacts						
	Reflector	Length (5.090 cm)	Width (5.090 cm)	Height (5.081 cm)	Height (1.274 cm)	Corrected Height (5.081 cm)	KNEO $k_{eff} \pm \sigma$
14	Plexiglas	10	9	9	1.135 ± 0.001	9.274 ± 0.003	1.0220 ± 0.0046
15	Plexiglas	10	11	7	3.239 ± 0.001	7.780 ± 0.002	1.0197 ± 0.0046
16	Plexiglas	12	12	6	2.526 ± 0.003	6.609 ± 0.007	1.0119 ± 0.0042
17	Plexiglas	14	13	5	3.733 ± 0.005	5.919 ± 0.008	1.0154 ± 0.0041
						Average	1.017

Table 3.A.2.4 Critical assembly configurations and calculated k_{eff}'s for PuO_2-UO_2-Polystyrene fuel compacts of 30.0 wt% Pu and 47.7 H/(Pu+U)

No.	Reflector	Critical Dimensions, cm			Critical Mass		k_{eff}	$\pm\sigma$
		Length	Width	Height	kg of Pu	kg of U		
1	Plexiglas	30.54±0.03	30.54±0.03	30.89±0.02	3.23±0.05	7.53±0.12	1.00370	0.00466
2	Plexiglas	35.63±0.04	35.63±0.04	23.95±0.10	3.40±0.05	7.94±0.12	1.00268	0.00493
3	Plexiglas	40.72±0.04	40.72±0.04	20.22±0.05	3.75±0.05	8.76±0.13	1.01852	0.00496
4	Plexiglas	50.90±0.05	45.81±0.05	17.14±0.07	4.48±0.06	10.44±0.16	1.00809	0.00458
5	Plexiglas	61.08±0.06	50.90±0.05	15.53±0.11	5.44±0.08	12.69±0.20	1.01107	0.00537
6	Plexiglas	61.08±0.06	55.99±0.06	15.16±0.02	5.80±0.09	13.51±0.21	1.01092	0.00550
7	Plexiglas	66.17±0.06	61.08±0.06	14.43±0.10	6.53±0.09	15.24±0.22	1.01265	0.00453
8	Plexiglas	50.90±0.05	50.90±0.05	16.49±0.04	4.78±0.08	11.14±0.18	1.00578	0.00490
9	Plexiglas	30.60±0.02	30.60±0.02	30.60±0.02	3.21±0.05	7.49±0.12	1.00305	0.00517
10	Plexiglas	∞	∞	10.80±0.11	–	–	1.02113	0.00423
11	Bare	45.81±0.05	40.72±0.04	37.98±0.06	7.93±0.12	18.51±0.78	0.98832	0.00651
12	Bare	40.72±0.04	40.72±0.04	42.24±0.03	7.84±0.11	18.30±0.77	0.99719	0.00579
13	Bare	45.81±0.05	50.90±0.05	32.49±0.02	8.48±0.12	19.80±0.84	0.99243	0.00548
14	Bare	41.20±0.05	41.20±0.05	41.20±0.05	7.83±0.11	18.28±0.77	0.98490	0.00572

Table 3.A.2.5 Critical assembly configurations and calculated k_{eff}'s for PuO_2-UO_2-Polystyrene fuel compacts of 14.62 wt% Pu and 30.6 H/(Pu+U)

No.	Reflector	Critical Dimensions, cm			Critical Mass		k_{eff}	$\pm\sigma$
		Length	Width	Height	kg of Pu	kg of U		
15	Plexiglas	30.54±0.03	40.72±0.04	29.81±0.15	3.14±0.04	18.35±0.35	1.01453	0.00558
16	Plexiglas	40.72±0.04	40.72±0.04	23.84±0.10	3.35±0.04	19.57±0.37	1.02512	0.00511
17	Plexiglas	45.81±0.04	50.90±0.05	19.82±0.11	3.92±0.05	22.89±0.44	1.01600	0.00513
18	Plexiglas	50.90±0.05	50.90±0.05	18.92±0.09	4.16±0.05	24.28±0.46	1.01860	0.00484
19	Plexiglas	61.08±0.06	50.90±0.05	17.72±0.09	4.67±0.06	27.28±0.52	1.02585	0.00490
20	Plexiglas	61.08±0.06	61.08±0.06	16.63±0.09	5.26±0.06	30.73±0.59	1.01231	0.00508
21	Plexiglas	33.30±0.17	33.30±0.17	33.30±0.17	3.13±0.05	18.28±0.40	1.01960	0.00501
22	Plexiglas	∞	∞	11.56±0.09	–	–	1.00941	0.00447
23	Bare	40.72±0.04	40.76±0.17	52.39±0.07	7.37±0.09	43.06±0.82	1.01296	0.00475
24	Bare	40.72±0.04	45.86±0.19	45.10±0.06	7.14±0.08	41.70±0.79	1.00897	0.00495
25	Bare	50.90±0.005	45.86±0.19	36.99±0.05	7.32±0.08	42.75±0.81	1.01258	0.00497
26	Bare	43.78±0.07	43.78±0.07	43.78±0.07	7.12±0.08	41.55±0.80	1.01379	0.00484

Table 3.A.2.6 Critical assembly configurations and calculated k_{eff}'s for PuO_2-UO_2-Polystyrene fuel compacts of 7.89 wt% Pu and 51.8 H/(Pu+U)

No.	Reflector	Critical Dimensions, cm			Critical Mass		k_{eff}	$\pm\sigma$
		Length	Width	Height	kg of Pu	kg of U		
27	Plexiglas	40.72±0.04	45.72±0.09	32.89±0.12	1.74±0.01	20.29±0.22	1.02113	0.00429
28	Plexiglas	50.90±0.05	50.80±0.10	26.40±0.10	1.94±0.02	22.63±0.25	1.01579	0.00453
29	Plexiglas	61.08±0.06	60.96±0.12	22.66±0.08	2.39±0.02	27.88±0.31	1.01035	0.00413
30	Plexiglas	61.08±0.06	66.04±0.13	22.09±0.18	2.53±0.03	29.53±0.39	1.01510	0.00442
31	Plexiglas	61.08±0.06	55.88±0.11	23.22±0.08	2.25±0.02	26.26±0.28	1.00651	0.00470
32	Plexiglas	61.08±0.06	50.80±0.10	24.37±0.09	2.15±0.02	25.06±0.28	1.02532	0.00414
33	Plexiglas	40.72±0.05	40.64±0.08	36.42±0.13	1.71±0.01	19.97±0.22	1.01814	0.00455
34	Plexiglas	39.12±0.28	39.12±0.28	39.12±0.28	1.70±0.01	19.84±0.32	1.01560	0.00440
35	Plexiglas	∞	∞	14.83±0.60	–	–	0.98698	0.00438

Table 3.A.3.1 Critical assembly configurations and calculated k_{eff}'s for PuO_2-UO_2-Polystyrene fuel compacts of 23.1 atomic plutonium enrichment percent and 4.67 H/(Pu+U) atomic ratio

No.	Base Side (cm)	Height (cm)	Critical Mass (kg)			Calculatrd $k_{eff} \pm \sigma$
			Oxide	Pu	Pu-239	
1	25.7	32.7	92.4	20.5	19.2	1.0158 ± 0.0042
2	30.0	24.3	94.2	20.9	19.6	1.0169 ± 0.0036
3	34.3	20.7	104.9	23.2	21.7	1.0189 ± 0.0048
4	30.0 × 21.5	37.5	104.1	23.0	21.6	1.0215 ± 0.0044
					Average	1.0183

Table 3.A.4.1 Critical assembly configurations and calculated k_{eff}'s for PuO_2-UO_2-Polystyrene fuel compacts of 2.2 wt% ^{240}Pu and those of 8.0 wt% ^{240}Pu

No.	Reflector	Critical Dimensions, cm			Critical Mass, kg of Pu		Calculated $k_{eff} \pm \sigma$
		Length	Width	Height	Experiment	Corrected	
		2.2 % ^{240}Pu Compacts					
1	Plexiglas	51.69	46.13	9.04 ± 0.06	23.39 ± 0.17	24.14 ± 0.18	1.0273 ± 0.0046
2	Plexiglas	41.35	38.46	10.34 ± 0.05	17.84 ± 0.09	18.42 ± 0.09	1.0201 ± 0.0048
3	Plexiglas	31.01	31.01	13.13 ± 0.02	13.70 ± 0.02	14.14 ± 0.02	1.0280 ± 0.0052
4	Plexiglas	25.86	25.86	16.43 ± 0.06	11.92 ± 0.04	12.30 ± 0.04	1.0218 ± 0.0050
5	Plexiglas	23.27	23.27	19.79 ± 0.05	11.63 ± 0.03	12.01 ± 0.03	1.0203 ± 0.0055
6	Plexiglas	20.68	20.68	24.87 ± 0.06	11.54 ± 0.03	11.91 ± 0.03	1.0193 ± 0.0046
7	Plexiglas	15.52	18.08	50.04 ± 0.13	15.23 ± 0.04	15.72 ± 0.04	1.0205 ± 0.0047
8	Bare	31.01	31.01	31.87 ± 0.06	33.25 ± 0.06		1.0017 ± 0.0052
9	Bare	30.68	30.68	32.84 ± 0.52		34.62 ± 0.55	1.0052 ± 0.0050
		8.0 % ^{240}Pu Compacts					
10	Plexiglas	51.31	68.25	10.36 ± 0.03	37.19 ± 0.11	38.09 ± 0.11	1.0078 ± 0.0045
11	Plexiglas	35.92	35.92	15.42 ± 0.03	20.39 ± 0.04	20.89 ± 0.04	1.0038 ± 0.0053
12	Plexiglas	30.78	30.78	18.56 ± 0.02	18.07 ± 0.02	18.46 ± 0.02	1.0040 ± 0.0045
13	Plexiglas	25.65	25.65	25.03 ± 0.05	16.88 ± 0.03	17.29 ± 0.03	1.0041 ± 0.0051
14	Plexiglas	25.65	25.65	25.13 ± 0.03	16.95 ± 0.02	17.36 ± 0.02	1.0053 ± 0.0044
15	Plexiglas	20.52	20.52	49.15 ± 0.01	21.22 ± 0.01	21.73 ± 0.01	1.0162 ± 0.0043
16	Bare	35.92	35.92	35.54 ± 0.02	46.93 ± 0.03		0.9798 ± 0.0050
17	Bare	35.63	35.63	36.04 ± 0.60		48.04 ± 0.80	0.9865 ± 0.0050

Table 3.A.4.2 Critical assembly configurations and calculated k_{eff}'s for PuO_2-UO_2-Polystyrene fuel compacts of 11.46 wt% ^{240}Pu and 5.0 H/Pu

No.	Reflector	Critical Dimensions, cm			Critical Mass, kg of Pu		Calculated $k_{eff} \pm \sigma$
		Length	Width	Height	Experiment	Corrected	
		11.46 wt% ^{240}Pu					
1	Plexiglas	25.88	25.88	19.04±0.01	27.66±0.01	27.66±0.01	1.0184±0.0038
2	Plexiglas	31.24	30.96	14.77±0.02	30.94±0.04	30.94±0.04	1.0231±0.0047
3	Plexiglas	41.66	41.28	11.03±0.01	41.20±0.03	41.20±0.03	1.0180±0.0048
4	Plexiglas	52.07	51.60	9.38±0.01	54.78±0.02	54.78±0.02	1.0209±0.0043
5	Bare	36.59	36.11	28.60±0.05	82.88±0.13	---	0.9998±0.0038
6	Bare	35.84	35.84	28.82±0.05	---	85.03±0.2	1.0161±0.0042
						Average	1.0160

Table 3.A.4.3 Critical assembly configurations and calculated k_{eff}'s for PuO_2 fuel compacts of 18.35 wt% ^{240}Pu and 0.04 H/Pu

No.	Reflector	Critical Dimensions (cm)			Critical Mass (kg Pu)	Calculated $k_{eff} \pm \sigma$
		Length	Width	Height	18.35 wt% ^{240}Pu	
1	Plexiglas	25.65	25.65	10.03 ± 0.01	38.3 ± 0.3	1.0344 0.0048
2	Plexiglas	25.65	30.78	8.98 ± 0.01	41.1 ± 0.3	1.0262 ± 0.0046
3	Plexiglas	30.78	30.78	7.97 ± 0.03	43.8 ± 0.3	1.0252 ± 0.0053
4	Plexiglas	30.78	41.05	6.86 ± 0.0	40.3 ± 0.7	1.0282 ± 0.0051
5	Plexiglas	41.05	41.05	5.95 ± ----	58.2 ± 0.3	1.0130 ± 0.0053
6	Bare	30.78	30.78	20.90 ± 0.0	113.8 ± 0.9	1.0247 ± 0.0049
7	Bare	30.78	30.78	21.12 ± 0.06	115.1 ± 0.8	1.0350 ± 0.0042
					Average	1.0267

Table 3.A.5.1 Calculated k_{eff}'s for the minimally reflected single tank

No.	Tank		Location	Uranium concentration (g/ℓ)	Critical solution level (cm)	Calculated k_{eff}
	Material	Inner dia. (cm)	of tank			
1	Stainless steel	27.92	At center	145.68	31.20	0.9602±0.0058
2	〃	27.92	〃	346.73	28.93	0.9654±0.0061
3	Al	28.01	〃	142.92	33.55	0.9721±0.0060
4	〃	28.01	〃	357.71	30.91	0.9702± —
5	〃	33.01	〃	54.89	39.48	0.9609±0.0054
6	〃	33.01	〃	59.65	36.67	0.9831±0.0054
7	〃	33.01	〃	137.40	23.96	0.9687±0.0058
8	〃	33.01	〃	145.68	23.67	0.9734±0.0062
9	〃	33.01	〃	357.71	22.57	0.9712±0.0057
10	〃	50.69	〃	63.95	20.48	0.9721±0.0048
					Average	0.9697

Table 3.A.5.2 Calculated k_{eff}'s for the concrete-reflected single tank

No.	Tank		Location	Uranium concentration (g/ℓ)	Critical solution level (cm)	Calculated k_{eff}
	Material	Inner dia. (cm)	of tank			
11	Stainless steel	27.92	At center	144.38	29.79	0.9691±0.0058
12	〃	〃	〃	334.77	27.23	0.9642±0.0058
13	Aℓ	28.01	〃	144.38	31.37	0.9768±0.0063
14	〃	〃	〃	334.77	28.60	0.9790± —
15	〃	33.01	〃	59.65	34.01	0.9657±0.0051
16	〃	〃	〃	144.38	22.85	0.9833±0.0058
17	〃	〃	〃	334.77	21.50	0.9733±0.0057
18	Stainless steel	27.92	In corner	144.38	24.19	0.9753±0.0056
19	〃	〃	〃	334.77	21.79	0.9766±0.0062
20	Aℓ	28.01	〃	144.38	24.70	0.9947±0.0061
21	〃	〃	〃	334.77	22.33	0.9764±0.0059
22	〃	33.01	〃	59.65	27.27	0.9866±0.0053
23	〃	〃	〃	144.38	18.24	0.9822±0.0052
24	〃	〃	〃	334.77	16.78	0.9779±0.0060
					Average	0.9772

Table 3.A.5.3 Calculated k_{eff}'s for the plastic-reflected single tank

No.	Tank		Location	Uranium concetration (g/ℓ)	Critical solution level (cm)	Calculated k_{eff}
	Material	Inner dia. (cm)	of tank			
25	Stainless steel	27.92	At center	147.66	29.71	0.9674±0.0056
26	〃	〃	〃	345.33	27.60	0.9615±0.0055
27	Aℓ	27.88	〃	60.32	78.1	0.9746± —
28	〃	28.01	〃	147.66	31.26	0.9756±0.0058
29	〃	〃	〃	345.33	28.84	0.9691±0.0063
30	〃	33.01	〃	60.32	34.33	0.9775±0.0047
31	〃	〃	〃	147.66	22.78	0.9773±0.0060
32	〃	〃	〃	345.33	21.67	0.9785±0.0056
33	Stainless steel	27.93	In corner	60.32	50.52	0.9734±0.0052
34	〃	27.92	〃	147.66	25.03	0.9650±0.0057
35	〃	〃	〃	345.33	22.75	0.9697±0.0060
36	Aℓ	27.88	〃	60.32	51.67	0.9843±0.0048
37	〃	28.01	〃	147.66	25.26	0.9683±0.0050
38	〃	〃	〃	345.33	22.87	0.9711±0.0067
39	〃	33.01	〃	60.32	27.70	0.9683±0.0046
40	〃	〃	〃	66.33	25.10	0.9639±0.0051
41	〃	〃	〃	147.66	18.49	0.9851±0.0061
42	〃	〃	〃	345.33	17.20	0.9735±0.0051
43	Stainless steel	27.93	Centered on floor	60.32	67.48	0.9707±0.0052
44	Aℓ	27.88	〃	〃	77.1	0.9787± —
45	〃	33.01	〃	〃	31.75	0.9691±0.0054
					Average	0.9725

Table 3.A.6.1 Summary of characteristics of homogeneous plutonium benchmark experiments

No.	H/Pu atom ratio	%^{240}Pu	Pu density, g/cm	Geometry
1	3695	0	0.007	Infinite
2	125	5	0.172	Sphere
3	980	1	0.026	Sphere
4	758	5	0.034	Sphere
5	15	2	1.12	Parallelepiped
6	0	5	15.6	Sphere
7	422	5	0.058	Slab (Infinite)
8	910	14	0.028	Cylinder
9	50	18	0.37	Parallelepiped
10	210	8	0.116	Cylinder
11	0	18	5.8	Parallelepiped
12	5	11	2.3	Parallelepiped
13	0	20	15.7	Sphere
14	623	43	0.041	Cylinder

Table 3.A.6.2 Calculated results for homogeneous plutonium benchmark experiments

No.	H/Pu atom ratio	% ^{240}Pu	Pu density g/cm	Calculated k_{eff}
2	125	5	0.172	1.0001 ± 0.0064
3	980	1	0.026	0.9935 ± 0.0046
4	758	5	0.034	0.9844 ± 0.0046
5A	15	2	1.12	1.0181 ± 0.0030
5B	15	2	1.12	1.0243 ± 0.0047
6	0	5	15.6	0.9948 ± 0.0052
8	910	14	0.028	0.9882 ± 0.0042
9A	50	18	0.37	1.0007 ± 0.0030
9B	50	18	0.37	1.0101 ± 0.0044
11A	0.04	18	5.8	1.0308 ± 0.0024
11B	0.04	18	5.8	1.0303 ± 0.0048
12A	5	11	2.3	1.0206 ± 0.0029
12B	5	11	2.3	1.0275 ± 0.0041
13	0	20	15.7	1.0045 ± 0.0048
14	623	43	0.041	0.9942 ± 0.0028
			Average	1.0081

Table 3.A.7.1 Calculated k_{eff}'s for "30 degrees lateral" system

No.	Height of water (cm)	Critical height (cm)	Solution density (g/cm^3)	Calculated k_{eff}
1	210.1	128.2		———
2	209.3	128.4		———
3	209.8	128.3	2.0289	0.9814 ± 0.0040
4	144.9	128.55		0.9683 ± ——
5	144.9	128.45		———
6	129.2	129.1		0.9831 ± 0.0038
7	210.2	131.35		0.9860 ± 0.0044
8	147.2	131.6	2.0048	0.9787 ± 0.0045
9	132.8	132.2		0.9781 ± ——
10	210.2	132.1		0.9760 ± 0.0089
11	147.5	132.4	1.9952	0.9764 ± 0.0042
12	132.8	132.2		0.9800 ± 0.0041
13	209.9	141.65		0.9880 ± 0.0036
14	157.5	141.9	1.9367	0.9696 ± 0.0040
15	143.2	142.75		0.9762 ± 0.0038
16	210.1	155.25		0.9763 ± 0.0042
17	171.9	155.35	1.9108	0.9738 ± 0.0044
18	155.9	155.85		0.9733 ± 0.0039
19	210.1	169.10		0.9857 ± 0.0041
20	185.5	168.00	1.9059	0.9857 ± 0.0045
21	168.1	168.20		0.9736 ± 0.0045
22	209.5	204.60	1.8823	Subcritical
			Average	0.9781

Table 3.A.7.2 Calculated k_{eff}'s for "cross" system

No.	Height of water (cm)	Critical height (cm)	Solution density (g/cm^3)	Inside diameter (cm)	Calculated k_{eff}
23	210.5	115.45	2.020	26.67	0.9898±0.0043
24	210.5	115.6			——
25	115.9	115.9			0.9812±0.0037
26	116.0	116.0			——
27	117.3	117.2	2.015		0.9826±0.0042
28	210.5	133.9	1.970		0.9944±0.0038
29	134.1	134.1			0.9796±0.0041
30	210.5	109.6	2.026	27.30	0.9858±0.0045
31	110.6	110.6			0.9838±0.0040
32	210.5	115.55	1.971		0.9835±0.0048
33	116.05	116.05			0.9869±0.0041
34	210.5	106.3	2.024	27.94	0.9781±0.0041
35	107.9	107.9			0.9857±0.0042
36	210.5	110.0	1.971		0.9851±0.0041
37	110.95	110.95			0.9776±0.0039
38	210.5	117.0	1.920		0.9910±0.0043
39	117.5	117.5			0.9745±0.0043
40	210.5	104.45	2.023	28.57	0.9874±0.0040
41	105.7	105.7			0.9897±0.0039
42	210.5	107.8	1.967		0.9915±0.0040
43	109.0	109.0			0.9751±0.0044
44	210.5	111.0	1.921		0.9829±0.0034
45	111.9	111.9			0.9892±0.0038
46	210.5	115.4	1.892		0.9841±0.0043
47	115.95	115.95			0.9821±0.0039
48	210.5	122.65	1.866		0.9859±0.0037
49	123.15	123.15			0.9905±0.0037
50	210.5	150.05	1.844		0.9837±0.0043
51	150.05	150.05			0.9866±0.0041
				Average	0.9848

Table 3.A.8.1 Calculated results with experimental conditions for cylinders or spheres containing uranyl-fluoride solution

No.	Solution Concentration		Container (0.16-cm-thick wall)	Cylindrical Critical Dimensions				Calculated Results	
	$H/^{235}U$	g of U per liter		Diameter (cm)	Height (cm)	Volume (Liters)	^{235}U Mass (kg)	k_{eff}	σ
			Water-Reflected Units						
1	495	890	Aluminum	38.1	41.7	47.6	2.11	0.9743	0.0042
2	495	890	Aluminum	33.0	72.4	62.1	2.75	0.9740	0.0040
3	495	890	Aluminum	31.1	139.6	106.0	4.70	0.9741	0.0040
4	495	890	Aluminum	30.7	173.2	128.1	5.67	0.9657	0.0040
5	524	870	Stainless steel	50.8	29.3	59.4	2.53	0.9957	0.0043
6	524	870	Aluminum	38.1	44.8	51.1	2.17	0.9876	0.0045
7	524	870	Stainless steel	38.1	50.4	57.4	2.44	1.0015	0.0037
8	524	870	Stainless steel	30.5	>153	>111	>4.73	0.9546[a]	0.0043
9	643	728	Aluminum	76.2	23.9	109.2	3.89	0.9972	0.0036
10	643	728	Stainless steel	50.8	34.7	70.3	2.50	0.9903	0.0040
11	643	728	Stainless steel	38.1	75.5	86.1	3.06	0.9859	0.0041
12	735	650	Aluminum	76.2	24.2	110.4	3.50	0.9728	0.0034
13	735	650	Stainless steel	50.8	40.1	81.1	2.58	0.9859	0.0039
14	735	650	Stainless steel	38.1	153.0	174.4	5.54	0.9906	0.0035
15	994	496	Aluminum	76.2	37.9	173.1	4.20	0.9882	0.0035
16	994	496	Stainless steel	50.8	85.7	173.7	4.21	0.9815	0.0034
17	1099	452	Aluminum[b]	69.3		170.5	3.77	0.9850	0.0030
			Unreflected Units						
18	524	870	Stainless steel	50.8	38.7	78.3	3.33	0.9666	0.0044
19	524	870	Stainless steel	38.1	>147	>168	>7.13	0.9742[a]	0.0043
20	643	870	Aluminum	76.2	28.9	132	4.69	0.9594	0.0038
21	643	728	Stainless steel	50.8	45.7	92.6	3.30	0.9773	0.0041
22	643	728	Stainless steel	38.1	>166	>189	>6.73	0.9470[a]	0.0037
23	735	650	Aluminum	76.2	31.5	144	4.58	0.9530	0.0038
24	735	650	Stainless steel	50.8	54.3	110	3.50	0.9850	0.0045
25	994	496	Aluminum	76.1	44.8	204	4.96	0.9812	0.0034
26	994	496	Stainless steel	50.8	>140	>283	>6.84	0.9659[a]	0.0037
27	1002	492	Aluminum[c]	69.3		172.0	4.14	0.9836	0.0035

a Subcritical case.
b This was a spherical container 98 % filled when critical.
c This was a spherical container 99 % filled when critical.

Table 3.A.9.1 Calculated results with experimental conditions for cylinders containing uranyl-fluoride solution with combination of reflectors

Case No.	Cylinder Diameter (cm)	Combination of Reflector	Steel Thickness (cm)	Critical Height (cm)	Calculated Results $k_{eff} \pm \sigma$
1	33.02	Steel-Water	0	84.60	0.97886 ± 0.00457
2	33.02	Steel-Water	0.64	158.85	0.98556 ± 0.00426
3	33.02	Steel-Water	1.27	201.60	0.98106 ± 0.00451
4	33.02	Steel-Water	1.90	172.80	0.98547 ± 0.00462
5	33.02	Steel-Water	2.54	143.00	0.98936 ± 0.00389
6	33.02	Steel-Water	3.81	109.10	0.97785 ± 0.00424
7	33.02	Steel-Water	5.08	91.95	0.98536 ± 0.00399
8	39.09	Steel	0	98.80	0.99218 ± 0.00447
9	39.09	Steel	0.64	74.65	0.98724 ± 0.00401
10	39.09	Steel	1.27	64.75	0.98752 ± 0.00407
11	39.09	Steel	1.90	59.30	0.97833 ± 0.00455
12	39.09	Steel	2.54	55.70	0.97287 ± 0.00413
13	39.09	Steel	3.81	50.90	0.97928 ± 0.00473
14	39.09	Steel	5.08	48.20	0.98514 ± 0.00390
15	39.09	Steel-Water	0	44.70	0.97908 ± 0.00489
16	39.09	Steel-Water	0.64	48.70	0.98203 ± 0.00389
17	39.09	Steel-Water	1.27	49.40	0.97292 ± 0.00414
18	39.09	Steel-Water	1.90	48.95	0.99218 ± 0.00423
19	39.09	Steel-Water	2.54	48.20	0.97526 ± 0.00399
20	39.09	Steel-Water	3.81	46.50	0.97717 ± 0.00412
21	39.09	Steel-Water	5.08	45.10	0.98310 ± 0.00440
22	39.09	Cadmium-Steel-Water	0	64.90	0.98888 ± 0.00416
23	39.09	Cadmium-Steel-Water	2.54	54.45	0.99879 ± 0.00445
24	39.09	Cadmium-Steel-Water	5.08	50.30	0.98464 ± 0.00453

Table 3.A.10.1 Critical dimensions of piles of UF_4-paraffin compact fuel

	Critical Dimensions*			Worth of Support Structures of Unreflected Assemblies (cm of fuel height)
	Reflected (cm)		Unreflected (cm)	
		Mixture $U(2)F_4$-1		
(1)	56.22 X 56.22 X 112.88	(23)	71.47 X 71.47 X 94.14	0.89
(2)	61.33 X 61.33 X 79.46	(24)	76.65 X 76.65 X 78.08	0.77
(3)	71.55 X 71.55 X 58.03	(25)	81.75 X 86.75 X 66.71	0.63
(4)	74.11 X 74.11 X 54.71			
		Mixture $U(2)F_4$-2		
(5)	51.11 X 51.11 X 73.87	(26)	56.22 X 56.22 X 122.47	
(6)	61.33 X 61.33 X 49.12	(27)	61.33 X 61.33 X 79.60	c
(7)	71.55 X 71.55 X 40.70	(28)	71.55 X 71.55 X 57.92	
		(29)	92.00 X 92.00 X 46.18	
		Mixture $U(2)F_4$-3		
(8)	56.22 X 56.22 X 49.54	(30)	45.97 X 61.21 X 144.5	2.64
(9)	53.67 X 53.67 X 54.29	(31)	51.07 X 56.13 X 110.5	0.85
		(32)	51.07 X 61.21 X 88.27	0.60
		(33)	61.21 X 61.21 X 64.85	0.46
		(34)	61.21 X 71.57 X 56.68	0.61
		Mixture $U(2)F_4$-4		
(10)	46.00 X 46.00 X 96.57	(35)	45.99 X 61.3 X 144.83	2.37
(11)	51.11 X 51.11 X 62.97	(36)	51.1 X 56.23 X 112.09	1.11
(12)	61.33 X 61.33 X 44.53	(37)	51.1 X 61.3 X 88.74	0.59
		(38)	56.23 X 61.3 X 72.38	0.63
		(39)	61.3 X 61.3 X 64.64	0.42
		(40)	61.3 X 66.5 X 59.68	0.50
		Mixture $U(2)F_4$-5		
(13)	56.32 X 61.29 X 54.08	(41)	53.80 X 56.30 X 126.98	0.42
		(42)	61.30 X 66.54 X 66.52	0.43
		(43)	62.28 X 112.64 X 41.59	0.59
		Mixture $U(2)F_4$-6		
(14)	76.51 X 76.44 X 82.42	(44)	76.50 X 76.45 X 119.45	0.58
(15)	76.43 X 81.53 X 77.66	(45)	81.45 X 86.70 X 88.22	0.52
(16)	81.52 X 81.60 X 73.02	(46)	101.97 X 101.85 X 66.64	0.65
		Mixture $U(3)F_4$-1		
(17)	43.47 X 43.47 X 86.39	(47)	56.47 X 56.47 X 86.64	0.83
(18)	46.02 X 46.02 X 67.57	(48)	56.25 X 51.36 X 74.38	0.76
(19)	51.14 X 51.14 X 51.27	(49)	61.4 X 61.4 X 66.00	0.65
(20)	56.25 X 56.25 X 43.41			
(21)	61.36 X 61.36 X 38.67			
		Mixture $U(3)F_4$-2		
(22)	40.81 X 40.80 X 39.49	(50)	40.90 X 40.93 X 116.80	0.37
		(51)	48.59 X 51.14 X 48.53	0.42
		(52)	81.71 X 81.66 X 31.34	0.53

* The bottom reflector for all mixtures was 15.2 cm of methacrylate plastic (Plexiglass) while the top and sides of mixtures $U(2)F_4$-1, -2, -3, and -4 and $U(3)F_4$-1 were reflected with 15.2 cm of paraffin and mixtures $U(2)F_4$-5 and -6 and $U(3)F_4$-2 with 15.2 cm of polyethylene.

Table 3.A.10.2 Calculated results for piles of the UF_4-paraffin compact fuel

No.	$k_{eff} \pm \sigma$	No.	$k_{eff} \pm \sigma$
1	1.00976 ± 0.00414	23	1.01369 ± 0.00365
2	1.01015 ± 0.00374	24	1.00745 ± 0.00394
3	1.01606 ± 0.00406	25	1.00914 ± 0.00362
4	1.01374 ± 0.00369	26	1.00975 ± 0.00355
5	1.01050 ± 0.00357	27	1.00910 ± 0.00373
6	1.00360 ± 0.00354	28	1.00685 ± 0.00395
7	1.01518 ± 0.00419	29	1.00548 ± 0.00417
8	1.00576 ± 0.00367	30	1.00282 ± 0.00321
9	1.00410 ± 0.00358	31	0.99595 ± 0.00428
10	1.00074 ± 0.00362	32	0.99657 ± 0.00343
11	0.99733 ± 0.00367	33	1.00496 ± 0.00342
12	1.00031 ± 0.00344	34	1.00746 ± 0.00336
13	0.99438 ± 0.00310	35	1.00533 ± 0.00377
14	0.98392 ± 0.00289	36	1.00433 ± 0.00321
15	0.98879 ± 0.00284	37	0.99918 ± 0.00400
16	0.99010 ± 0.00287	38	0.99648 ± 0.00347
17	1.02039 ± 0.00381	39	0.99919 ± 0.00393
18	1.01887 ± 0.00398	40	1.00120 ± 0.00365
19	1.02039 ± 0.00432	41	0.99528 ± 0.00345
20	1.03095 ± 0.00367	42	0.99772 ± 0.00334
21	1.01969 ± 0.00413	43	0.99556 ± 0.00324
22	1.00754 ± 0.00382	44	0.98518 ± 0.00277
		45	0.99446 ± 0.00316
		46	0.99148 ± 0.00306
		47	1.02719 ± 0.00452
		48	1.01357 ± 0.00477
		49	1.01750 ± 0.00443
		50	1.00676 ± 0.00425
		51	1.02505 ± 0.00479
		52	1.00582 ± 0.00399

Table 3.A.11.1 Experimental configurations for spherical vessels containing uranyl-nitrate solution with various reflectors

No.	Reflector	Sp. Cr.	Crit. Conc. (gPu/Liter)	Molarity	Total Nitrate (gNO_3/Liter)	H_2O (g/Liter)	H/Pu Atomic Ratio	Crit.[a] Mass (kg/Pu)
	11.5-in. Stainless-Steel Sphere: 12.95 Liters (Vessel Wall Thickness 0.049 in.)							
1	Water	1.130	73	0.2	86	971	354	0.95
2		1.143	74.5	0.4	105	963	344	0.96
3		1.230	100	1.9	230	898	243	1.30
4		1.282	126	2.2	262	892	192	1.63
5		1.484	269	1.1	346	868	87	3.48
6		1.492	295[b]	0.8	303	893	81	3.82
7		1.680	435[b]	0.8	372	872	54	5.63
8	Concrete: 11.25-in.	1.145	75	0.44	109	961	341	0.97
9		1.433	236	1.16	318	878	100	3.06
	14-in. Stainless-Steel Sphere: 23.22 Liters (Vessel Wall Thickness 0.044 in.)							
10	½-in. Paraffin[c]		53.6	2.2	190	930	470	1.24
11			62.9	2.8	238	912	396	1.46
12			63.8	3.5	278	886	382	1.48
13			89	4.0	338	847	263	2.07
14			96.7	4.2	354	841	241	2.25
15			97.4	4.5	377	833	238	2.26
16	1-in. Paraffin[c]		53.6	4.3	323	855	443	1.24
17			95.1	6.4	482	763	256	1.98
18			97.6	6.1	473	765	223	2.27
19	4-in. Concrete and 0.03-in. Cadmium[c]		40	1.1	110	948	634	0.93
20			50.9	4.6	336	834	457	1.18
21			232	6.7	650	689	86	5.39
22	4-in. Concrete	1.093	32.8	1.1	118	949	770	0.75
23		1.143	35.5	2.9	216	889	684	0.82
24		1.253	45.2	5.62	410	792	495	1.05
25	10-in. Concrete	1.085	29.6	1.07	118	936	848	0.69
26		1.209	36.6	4.39	310	858	651	0.85
27		1.285	43.4	6.37	445	790	518	1.01
28	4-in. Air Gap;	1.250	67.9	4.29	336	842	344	1.58
29	6-in. Concrete	1.175	50.4	2.28	194	933	500	1.17
30	4-in. Air Gap; 6-in. Concrete Hemisphere	1.193	75.0	2.10	209	907	328	1.74
31	10-in. Concrete Hemisphere	1.146	46.4	2.05	175	923	538	1.08
32	4-in. Concrete +0.036-in. Stainless Steel	1.252	46.4	5.62	404	796	484	1.08
33	4-in. Concrete+0.72-in. Stainless Steel	1.258	46.9	5.62	416	790	476	1.09
34	Water	1.123	33.2	2.08	164	924	754	0.77
35		1.196	38.6	4.07	292	881	618	0.90
36		1.290	47.5	6.66	462	774	466	1.10
37	Water and 0.030-in.	1.126	46.9	1.4	136	942	540	1.09
38	Cadmium	1.238	69.0	3.9	313	852	341	1.60
39	Water + 0.072-in. Stainless Steel	1.268	49.5	6.01	424	789	452	1.15
	15.2-in. Stainless-Steel Sphere: 30.2 Liters (Vessel Wall Thickness 0.048 in.)							
40	Unreflected[d]	1.081	39.0	0.4	64	978	668	1.18
41		1.429	172.3	4.9	486	766	125	5.20
42	Stainless-Steel Shell 0.26-in. Thick	1.076	34.3	0.5	66	975	758	1.04
43	Concrete Shell: Air Gap (6-in. Thick Concrete, 3.63-in. Air Gap)	1.071	29.0	0.5	64	977	900	0.88
44	Water	1.060	24.4	0.5	58	977	1058	0.74
45		1.300	38.7	7.7	517	737	553	1.17
46	Water and 0.06-in. Stainless Steel	1.060	25.2	0.5	60	974	1032	0.76
47	Water Only[e]		23.6	0.5	55	979	1107	0.71
48	Unreflected[e]		41.0	0.4	67	976	634	1.24

[a] Includes 4.6% ^{240}Pu; experimental values not corrected for vessel walls or neck supports, except where noted. Correction values are discussed in the text.

[b] Contains Pu(VI) and plutonium polymer, increasing the uncertainty ±5%

[c] Values of nitrate corrected to full sphere from measurements close to full. Water calculated from nitric acid content and corrected by comparison to a known similar solution.

[d] These same solutions would be critical in spherical geometry at a volume of 31.1 liters with no stainless-steel walls or neck supports.

[e] Corrected for effect of vessel wall and neck supports.

Table 3.A.11.2 Calculated results for spherical vessels containing uranyl-nitrate solution with various reflectors

No.	k_{eff}	±σ	No.	k_{eff}	±σ
1	1.00059	0.00481	25	0.98562	0.00469
2	0.99331	0.00559	26	1.00285	0.00461
3	0.98141	0.00471	27	1.01424	0.00416
4	0.99620	0.00479	28	1.01460	0.00454
5	0.99997	0.00430	29	1.00981	0.00474
6	1.01679	0.00530	30	0.99243	0.00590
7	1.01845	0.00546	31	1.00839	0.00581
8	1.00975	0.00582	32	1.00871	0.00537
9	1.02079	0.00504	33	1.00546	0.00519
10	1.00054	0.00521	34	0.99789	0.00393
11	1.01352	0.00536	35	0.98364	0.00466
12	0.99792	0.00478	36	0.99520	0.00507
13	1.00934	0.00611	37	0.98357	0.00538
14	1.01286	0.00510	38	0.99087	0.00490
15	1.00342	0.00511	39	0.99520	0.00507
16	0.99881	0.00520	40	0.99324	0.00461
17	1.00714	0.00575	41	1.00440	0.00660
18	1.01158	0.00548	42	0.99786	0.00503
19	0.99971	0.00507	43	1.00301	0.00406
20	0.99852	0.00483	44	1.00917	0.00463
21	0.99851	0.00523	45	1.01300	0.00434
22	1.00293	0.00490	46	1.01295	0.00467
23	1.00129	0.00470	47	1.00461	0.00463
24	1.00212	0.00474	48	1.00122	0.00481

Table 3.A.12.1 Calculated results with experimental conditions for annular cylinders containing plutonium-nitrate solution with inner void region

No.	C(g/ℓ of Pu total) ±1.5%	NO_3^- (N)	H^+ (N)	Fer (g/ℓ)	Density	Temperature (°C)	Critical Height Hc(cm)	Calculated Results	
								k_{eff}	σ
1	152	6.68	3.85	3.4	1.386	21.0	36.88 ± 0.04	0.9919	0.0058
2	104	4.57	2.65	2.12	1.271	20.5	34.31 ± 0.03	0.9998	0.0049
3	62	3.02	1.88	1.28	1.171	20.5	37.13 ± 0.02	0.9910	0.0048
4	51	2.80	1.85	1.13	1.151	20.5	41.08 ± 0.06	1.0024	0.0049
5	40.9	2.63	1.87	0.92	1.135	20.5	49.16 ± 0.03	0.9927	0.0046
6	36.0	2.58	1.90	0.88	1.127	20.5	57.65 ± 0.03	1.0016	0.0037
7	33.1	2.51	1.90	0.71	1.121	20.5	66.64 ± 0.02	0.9968	0.0040
8	30.8	2.45	1.88	0.69	1.118	20.8	77.31 ± 0.02	0.9883	0.0034
9	28.7	2.47	1.94	0.65	1.114	20.3	93.34 ± 0.02	0.9916	0.0038

Table 3.A.12.2 Calculated results with experimental conditions for annular cylinders containing plutonium-nitrate solution with inner cadmium-paraffin region

No.	C(g/ℓ of Pu total) ±1.5%	NO_3^- (N)	H^+ (N)	Fer (g/ℓ)	Density	Temperature °C	Critical Height Hc(cm)	Calculated Results	
								k_{eff}	σ
10	165	6.17	3.11	3.8	1.393	21.8	60.72 ± 0.02	1.0058	0.0045
11	136	5.30	2.76	3.2	1.329	21.0	54.33 ± 0.02	0.9969	0.0049
12	105	4.14	2.17	2.5	1.261	21.5	51.46 ± 0.02	0.9858	0.0049
13	86	3.82	2.21	1.87	1.226	21.0	54.24 ± 0.03	0.9956	0.0049
14	74	3.59	2.22	1.56	1.202	21.5	59.33 ± 0.02	0.9910	0.0044
15	61	3.34	2.19	1.41	1.180	21.5	70.46 ± 0.02	0.9930	0.0044
16	55.8	3.17	2.12	1.33	1.168	21.0	83.61 ± 0.03	0.9849	0.0046
17	53.7	3.11	2.11	1.25	1.164	21.5	92.09 ± 0.04	0.9853	0.0044

Table 3.A.13.1 Calculated results with experimental conditions for cylinders containing plutonium-nitrate solution of 5.6 wt% ^{240}Pu in Pu

No.	Plutonium Concentration (g/ℓ)	Uranium Concentration (g/ℓ)	Acid Molarity	Specific Gravity	Critical Height (cm)	Critical Volume (ℓ)	Calculated Results	
							k_{eff}	±σ
1	97.3	200.4	4.8	1.562	19.96	58.37	1.0163	0.0049
2	87.9	184.3	4.4	1.512	19.48	57.00	0.9912	0.0050
3	75.4	168.5	3.7	1.450	18.82	55.04	1.0027	0.0045
4	63.1	147.7	2.9	1.389	18.72	54.76	1.0043	0.0044
5	49.6	122.3	2.4	1.320	19.35	56.59	1.0039	0.0055
6	39.9	96.7	2.2	1.257	20.32	59.44	1.0009	0.0049
7	30.2	72.5	2.1	1.213	22.89	66.97	1.0146	0.0041
8	25.3	60.9	2.0	1.182	25.12	73.48	0.9984	0.0041
9	20.3	48.9	1.8	1.154	29.92	87.53	0.9983	0.0038
10	17.2	41.5	1.7	1.132	36.04	105.44	1.0024	0.0042
11	14.1	34.4	1.5	1.117	52.60	153.91	0.9906	0.0036
12	13.3	32.2	1.4	1.110	64.01	187.24	1.0057	0.0033
13	12.4	29.9	1.3	1.103	95.20	278.50	0.9862	0.0039

Table 3.A.13.2 Calculated results with experimental conditions for spheres containing plutonium-uranyl-nitrate solution of 4.7 wt% ^{240}Pu in Pu

No.	Approximate Percent Plutonium	Sphere Wall Thickness (cm)	Plutonium Concentration (g/ℓ)	Uranium Concentration (g/ℓ)	Gadolinium Concentration (g/ℓ)	Acid Molarity	Specific Gravity	Critical Radius (cm)	Critical Volume (ℓ)	Calculated Results	
										k_{eff}	±σ
1	30	0.112	70.93	157.1	0.051	3.12	1.429	17.87	23.90	0.9945	0.0045
2	30	0.122	35.05	75.7	0.025	1.49	1.215	19.30	30.14	1.0096	0.0039
3	15	0.122	45.6	264.9	0.005	2.1	1.491	19.31	30.18	1.0120	0.0045

Table 3.A.13.3 Calculated results with experimental conditions for cylinders containing plutonium-uranyl-nitrate solution of 23.0 wt% ^{240}Pu in Pu

No.	Plutonium Concentration (g/liter)	Uranium Concentration (g/liter)	Acid Molarity	Specific Gravity	Critical Height (cm)	Critical Volume (liter)	Calculated Results	
							k_{eff}	±σ
1	30.63	390.2	0.45	1.5744	50.27	147.03	1.0046	0.0039
2	29.00	394.5	0.44	1.5799	54.66	159.89	0.9992	0.0040
3	27.32	399.0	0.44	1.5838	61.04	178.56	0.9928	0.0034
4	25.71	403.3	0.37	1.5840	70.49	206.20	0.9929	0.0034
5	24.28	407.1	0.36	1.5878	84.86	248.23	0.9909	0.0034
6	23.66	408.7	0.36	1.5889	94.56	276.62	0.9972	0.0033
7	30.44	390.7	0.43	1.5782	51.41	150.38	1.0036	0.0039
8	29.13	373.8	0.47	1.5536	52.29	152.98	0.9996	0.0034
9	27.28	351.1	0.54	1.5214	56.87	166.36	1.0019	0.0033
10	25.76	331.3	0.56	1.4914	60.99	178.39	1.0075	0.0035
11	24.35	312.5	0.56	1.4672	67.59	197.71	0.9955	0.0037
12	23.04	296.7	0.54	1.4416	76.96	225.13	0.9910	0.0031
13	21.85	281.9	0.56	1.4212	89.61	262.13	0.9925	0.0033

Table 3.A.14.1 Principal critical parameters and calculated k_{eff}'s for U_3O_8 package arrays

Type of Driver	Total Driver Mass (kg)	Metal Diameter of Solution Height*) (mm)	Critical Core Separation (mm)	Calculated k_{eff} MGCL(137-Group)
93.12 % Enriched Uranium Metal	29.870	0.0 (ID), 146.68(OD)	12.60±1.19[1)]	0.9997±0.0063
	29.870	0.0 (ID), 146.68(OD)	8.01±1.67[2)]	0.9855±0.0047
	33.543	40.02(ID), 153.32(OD)	14.64±2.26[3)]	0.9858±0.0057
High Concentration Solution (351.2 kg U/m^3)	14.066	105.47(S), 106.22(N)	6.68±1.79[1)]	1.0059±0.0045
	14.844	111.30(S), 112.10(N)	9.42±3.01[2)]	0.9874±0.0049
	16.143	121.04(S), 121.91(N)	9.04±1.44[3)]	0.9727±0.0052
Low Concentration Solution (86.4 kg U/m^3)	12.446	124.08(S), 124.42(N)	8.64±1.31[1)]	0.9998±0.0041
	12.875	128.28(S), 128.74(N)	9.12±1.42[2)]	0.9870±0.0045
	13.001	129.54(S), 129.99(N)	11.17±1.42[2)]	0.9942±0.0044
	13.999	139.46(S), 139.99(N)	6.30±1.66[3)]	0.9868±0.0050

*) ID = Inner diameter; OD = Outer diameter; S = South; N = North

1) Concrete reflector

2) Plastic reflector

3) Minimal reflector

Table 3.A.15.1 Principal critical parameters and calculated k_{eff}'s

No.	Concentration		Critical Values			Calculated k_{eff}
	Pu (g Pu/ℓ)	Gd (g Gd/ℓ)	Height (cm)	Volume (ℓ)	Mass (kg Pu)	
1	116	0.00	15.44	45.17	5.240	1.0009±0.0047
2	116	0.48	20.16	58.98	6.842	1.0008±0.0044
3	116	0.96	25.98	75.99	8.815	0.9838±0.0035
4	116	1.42	34.48	100.85	11.698	0.9833±0.0037
5	116	1.92	48.28	141.24	16.383	0.9879±0.0030
6	116	2.38	80.37	235.10	27.272	0.9853±0.0030
7	363	4.40	26.52	77.56	28.192	0.9938±0.0038
8	363	5.28	28.07	82.08	29.838	0.9842±0.0041
9	363	6.28	29.62	86.65	31.497	0.9858±0.0036
10	363	8.21	32.84	96.10	34.932	0.9860±0.0038
11	363	9.88	36.04	105.40	38.311	0.9875±0.0039
12	363	12.85	41.02	120.00	43.608	0.9883±0.0039
13	363	15.55	46.76	136.76	49.714	0.9840±0.0039
14	363	18.4	53.70	157.05	57.089	0.9818±0.0037
15	363	20.25	59.36	173.63	63.113	0.9881±0.0027

Table 3.A.16.1 Experimental condition for cylinders containing plutonium-uranyl-nitrate solution with soluble neutron absorbers

CASE No.	CRITICAL HEIGHT (cm)	PU CONC. (g/ℓ)	U CONC. (g/ℓ)	ACID MOLARITY	TOTAL NO_3 (g/ℓ)	SPECIFIC GRAVITY	Gd (g/ℓ)	B (g/ℓ)
01	15.44	116	0	1.85	238.9	1.255	0.00	0
02	20.16	116	0	1.85	238.9	1.255	0.48	0
03	25.98	116	0	1.85	238.9	1.255	0.96	0
04	34.48	116	0	1.85	238.9	1.255	1.42	0
05	48.28	116	0	1.85	238.9	1.255	1.92	0
06	80.37	116	0	1.85	238.9	1.255	2.38	0
07	26.52	363	0	4.10	634.1	1.701	4.40	0
08	28.07	363	0	4.10	634.1	1.701	5.28	0
09	29.62	363	0	4.10	634.1	1.701	6.28	0
10	32.84	363	0	4.10	634.1	1.701	8.21	0
11	36.04	363	0	4.10	634.1	1.701	9.88	0
12	41.02	363	0	4.10	634.1	1.701	12.85	0
13	46.76	363	0	4.10	634.1	1.701	15.55	0
14	53.70	363	0	4.10	634.1	1.701	18.4	0
15	59.36	363	0	4.10	634.1	1.701	20.25	0
16	19.10	75.6	171.9	3.27	371.4	1.446	0.042	0
17	21.93	76.3	173.4	3.26	377.0	1.452	0.180	0
18	24.61	76.3	174.6	3.42	383.8	1.450	0.288	0
19	29.47	76.6	174.7	3.07	375.8	1.456	0.459	0
20	33.42	76.6	175.3	3.05	365.2	1.454	0.581	0
21	37.15	77.0	175.9	3.14	370.8	1.456	0.679	0
22	43.71	77.1	175.1	3.13	380.7	1.456	0.800	0
23	53.12	77.3	177.7	3.24	376.4	1.461	0.923	0
24	62.12	77.2	176.3	3.27	381.3	1.455	1.01	0
25	75.32	77.3	176.8	3.25	383.8	1.462	1.06	0
26	18.13	85.0	182.5	1.55	320	1.433	0.04	0.0
27	18.65	84.9	182.2	1.61	311	1.434	0.04	0.1
28	19.68	84.8	182.6	1.67	290	1.433	0.04	0.3
29	21.13	84.5	182.1	1.75	296	1.438	0.128	0.27
30	82.16	82.8	180.6	1.95	309	1.443	0.293	0.9
31	43.03	82.2	179.5	2.12	319	1.446	0.388	1.2
32	52.12	81.2	180.0	2.18	321	1.447	0.424	1.35
33	67.83	81.0	180.4	2.09	316	1.451	0.519	1.5
34	75.44	81.0	180.3	2.21	318	1.452	0.537	1.54

Table 3.A.16.2 Calculated results for cylinders containing plutonium-uranyl-nitrate solution with soluble neutron absorbers

CASE No.	k_{eff}	$\pm\sigma$
01	1.02072	0.00451
02	1.00647	0.00413
03	0.99143	0.00361
04	0.99306	0.00379
05	0.98055	0.00316
06	0.98359	0.00324
07	0.99212	0.00448
08	0.98198	0.00418
09	0.98422	0.00408
10	0.98072	0.00392
11	0.98515	0.00376
12	0.98039	0.00327
13	0.97649	0.00341
14	0.97682	0.00341
15	0.98086	0.00368
16	1.00265	0.00509
17	1.00160	0.00448
18	0.99027	0.00365
19	0.99116	0.00400
20	0.98706	0.00414
21	0.97924	0.00374
22	0.97894	0.00407
23	0.97926	0.00333
24	0.97369	0.00317
25	0.97767	0.00270
26	1.00387	0.00466
27	0.98723	0.00454
28	0.99799	0.00446
29	1.00001	0.00415
30	0.98427	0.00383
31	0.98168	0.00330
32	0.97416	0.00341
33	0.96792	0.00332
34	0.96670	0.00314

Table 3.A.17.1 Calculated k_{eff}'s with experimental conditions for raschig rings in plutonium-uranyl solution

Exp. No.	Critical height (cm)	Pu Conc. (g/ℓ)	U Conc. (g/ℓ)	Calculated k_{eff}
106	57.56	92.3	147	0.9795 ± 0.0041
107	63.98	89.9	157	0.9891 ± 0.0042
108	70.46	86.1	173	0.9852 ± 0.0042
109	76.07	83.7	181	0.9765 ± 0.0037
110	79.78	82.4	191	0.9880 ± 0.0035
111	79.93	81.7	186	0.9800 ± 0.0038
112	81.51	80.8	185	0.9789 ± 0.0034
113	85.70	79.4	182	0.9893 ± 0.0040
			Average	0.9833

Table 3.B.1.1 Calculated k_{eff}'s for unreflected 3×4 arrays

No.	Cylinder center separation (cm)	Table separation at critical (cm)	Calculated k_{eff}
1	22.52	2.56	0.9548 ± 0.0040
2	22.68	0.74	0.9599 ± 0.0043
3	22.73	0.61	0.9588 ± 0.0037
4	22.81	0.12	0.9673 ± 0.0039
5	22.81	0.19	0.9597 ± 0.0040
6	22.81	1.01	0.9662 ± 0.0042
7	22.81	0.13	0.9695 ± 0.0044
8	22.81	1.26	0.9579 ± 0.0040
9	22.81	1.48	0.9585 ± 0.0042
10	22.81	1.21	0.9527 ± 0.0036
		Average	0.9605

Table 3.B.1.2 Calculated k_{eff}'s for unreflected 4×4 arrays

No.	Cylinder center separation (cm)	Table separation at critical (cm)	Calculated k_{eff}
11	24.50	4.10	0.9728 ± 0.0044
12	24.82	1.16	0.9652 ± 0.0040
13	24.91	0.88	0.9690 ± 0.0041
14	24.96	0.34	0.9688 ± 0.0043
15	24.96	1.14	0.9658 ± 0.0042
16	24.96	0.33	0.9640 ± 0.0040
		Average	0.9676

Table 3.B.1.3 Calculated k_{eff}'s for 2X2 arrays reflected on 5 sides by polyethylene and moderated by Plexiglas

No.	Cylinder center separation (cm)	Table separation at critical (cm)	Calculated k_{eff}
17	22.52	—	Sub-critical
18	23.66	—	"
19	25.05	1.22	0.9901 ± 0.0041
20	25.61	—	Sub-critical
21	26.24	—	"
22	25.13	0.59	0.9794 ± 0.0046
		Average	0.9848

Table 3.B.1.4 Calculated k_{eff}'s for 3X3 arrays reflected on 5 sides by polyethylene

No.	Cylinder center separation (cm)	Table separation at critical (cm)	Calculated k_{eff}
23	23.56	0.56	1.0069 ± 0.0043
24	24.17	~10.9	0.9880 ± 0.0044
25	24.84	~ 7.1	0.9934 ± 0.0040
26	26.09	0.31	1.0102 ± 0.0045
		Average	0.9996

Table 3.B.1.5 Calculated k_{eff}'s for 4X4 arrays with various polyethylene reflector conditions

No.	Cylinder center separation (cm)	Table separation at critical (cm)	Calculated k_{eff}
27	29.19	0.44	0.9990 ± 0.0045
28	29.19	0.60	0.9960 ± 0.0040
29	29.59	0.00	0.9909 ± 0.004*)
		Average	0.9953

*) k_{eff} of assembly was 0.9993

Table 3.B.1.6 Calculated k_{eff}'s for 2X2 arrays reflected on 5 sides by concrete and complete reflection

No.	Cylinder center separation (cm)	Table separation at critical (cm)	Calculated k_{eff}
30	22.52	0.96	0.9874 ± 0.0040
31	23.12	—	Sub-critical
32	23.12	1.52	0.9924 ± 0.0042
33	23.12	1.86	0.9964 ± 0.0042
34	23.12	2.01	1.0002 ± 0.0043
35	23.12	1.65	0.9960 ± 0.0044
36	22.84	0.18	0.9787 ± 0.0048
37	22.84	0.12	0.9809 ± 0.0044
38	22.68	0.54	0.9860 ± 0.0040
39	22.68	0.62	0.9862 ± 0.0043
		Average	0.9894

Table 3.B.1.7 Calculated k_{eff}'s for 2X2 arrays with various concrete reflector conditions

No.	Cylinder center separation (cm)	Table separation at critical (cm)	Calculated k_{eff}
40	25.70	—	Subcritical
41	25.70	1.04	1.0013 ± 0.0039
42	25.70	1.35	0.9933 ± 0.0044
43	25.70	1.56	0.9952 ± 0.0045
44	25.70	1.26	1.0065 ± 0.0038
45	25.01	—	Subcritical
46	25.01	—	Subcritical
		Average	0.9991

Table 3.B.1.8 Calculated k_{eff}'s for 3X3 arrays with various concrete reflector conditions

No.	Cylinder center separation (cm)	Table separation at critical (cm)	Calculated k_{eff}
47	30.78	1.35	0.9975 ± 0.0043
48	31.18	—	0.9901 ± 0.0036*)
49	31.18	2.31	0.9927 ± 0.0045
50	31.18	1.83	0.9989 ± 0.0040
		Average	0.9948

*) k_{eff} of assembly at table closure was 1.0009

Table 3.B.1.9 Calculated k_{eff}'s for 1X12 arrays with various concrete reflector conditions

No.	Cylinder center separation (cm)	Table separation at critical (cm)	Calculated k_{eff}
51	22.52	0.69	0.9994 ± 0.0038
52	22.52	0.62	0.9922 ± 0.0038
53	22.52	0.61	0.9996 ± 0.0052
54	22.52	—	Subcritical
		Average	0.9971

Table 3.B.1.10 Calculated k_{eff}'s for 1X5 arrays with various concrete reflector conditions

No.	Cylinder center separation (cm)	Table separation at critical (cm)	Calculated k_{eff}
55	26.66	—	Subcritical
56	26.66	0.00	0.9817 ± 0.0041*)
57	26.33	0.38	0.9859 ± 0.0043
58	26.33	0.72	1.0000 ± 0.0043
59	26.33	0.94	0.9892 ± 0.0044
60	26.33	—	Subcritical
61	26.33	0.28	0.9880 ± 0.0038
62	26.33	0.67	0.9920 ± 0.0040
		Average	0.9895

*) k_{eff} of assembly was 0.9997

Table 3.B.1.11 Calculated k_{eff}'s for 1X4 arrays with various concrete reflector conditions

No.	Cylinder center separation (cm)	Table separation at critical (cm)	Calculated k_{eff}
63	24.72	0.56	0.9985 ± 0.0047
64	24.72	0.65	0.9912 ± 0.0045
65	24.72	0.23	0.9964 ± 0.0047
		Average	0.9954

Table 3.B.1.12 Calculated k_{eff}'s for 1X3 arrays with various reflector conditions and with Plexiglas separating the cylinders

No.	Cylinder center separation (cm)	Table separation at critical (cm)	Calculated k_{eff}
66	22.52	—	Subcritical
67	23.66	0.69	0.9997 ± 0.0043
68	23.66	0.42	1.0010 ± 0.0049
69	23.66	0.12	0.9998 ± 0.0040
70	23.66	0.11	0.9965 ± 0.0046
		Average	0.9993

Table 3.B.1.13 Calculated k_{eff}'s for two linear three-cylinder arrays with close fitting concrete reflectors

No.	Cylinder center separation (cm)	Table separation at critical (cm)	Calculated k_{eff}
71	22.52	2.49	1.0057 ± 0.0041
72	22.52	3.54	1.0008 ± 0.0042
73	22.52	5.17	0.9967 ± 0.0042
74	22.52	1.06	1.0081 ± 0.0043
75	22.52	2.47	1.0100 ± 0.0041
		Average	1.0043

Table 3.B.1.14 Calculated k_{eff}'s for two linear three-cylinder arrays with concrete reflectors

No.	Cylinder center separation (cm)	Table separation at critical (cm)	Calculated k_{eff}
76	22.52	—	Subcritical
77	22.52	0.22	1.0134 ± 0.0039
78	22.52	0.13	1.0075 ± 0.0050
		Average	1.0105

Table 3.B.1.15 Calculated k_{eff}'s for two linear three-cylinder arrays with various reflector conditions

No.	Cylinder center separation (cm)	Table separation at critical (cm)	Calculated k_{eff}
79	22.52	—	Subcritical
80	22.52	0.39	1.0170 ± 0.0042
81	22.52	7.36	1.0135 ± 0.0045
		Average	1.0153

Table 3.B.2.1 Experimental data and calculated k_{eff}'s for the critical slab systems

No.	Slab with minimum reflector			
	Critical slab[a] thickness (cm)	Estimated[b] accuracy (cm)	Uranium concentrations (g/liter)	Calculated k_{eff}
1	12.7	± 0.3	465	0.9179 ± 0.0065
2	12.7	± 0.3	465	—
3	12.7	± 0.3	465	—
4	12.6	± 0.3	465	0.9192 ± 0.0053
5	12.7	± 0.3	465	—
6	12.8	± 0.2	495	—
7	13.0	± 0.2	500	0.9174 ± 0.0056
8	13.0	± 0.2	510	0.9326 ± 0.0054
9	13.0	± 0.2	520	—
			Average	0.9218
	Reflected slab[c]			
10	10.3	± 0.2	505	0.9961 ± 0.0057

a) Includes any precipitate present in the slab tank.
b) Repeatability of measurements was ±0.1 cm.
c) Reflected slab tank without cylinders.

Table 3.B.2.2 Experimental data and calculated k_{eff}'s for the critical slab-cylinder array configuration with the minimum reflector

No.	Cylinder diameter (cm)	Number of cylinders	Slab thickness (cm)	Array height (cm)	Uranium concentration (g/ℓ)	Calculated k_{eff}
11	11.0	1	12.6	87	465	0.9247 ±0.0057
12			12.6	37		0.9191 ±0.0060
13		4	12.3	88		0.9133 ±0.0051
14			12.4	5		0.9058 ±0.0055
15			12.5	0		0.9061 ±0.0055
16		9	12.1	88		0.9214 ±0.0057
17			12.2	39		0.9224 ±0.0052
18			12.3	18		0.9135 ±0.0062
19			12.6	2		0.9288 ±0.0054
20		16	11.4	88		0.9164 ±0.0057
21			11.7	38		0.9214 ±0.0061
22			11.9	19		0.9092 ±0.0050
23			12.5	2		0.9198 ±0.0058
24			12.7	0		0.9278 ±0.0058
25	13.6	16	10.0	108	520	0.9227 ±0.0055
26			10.4	69		0.9240 ±0.0058
27			11.3	26		0.9187 ±0.0051
28			12.3	4		0.9103 ±0.0057

Table 3.B.2.2 (continued)

No.	Cylinder diameter (cm)	Number of cylinders	Slab thickness (cm)	Array height (cm)	Uranium concentration (g/ℓ)	Calculated k_{eff}
29	16.3	1	12.2	88	470	0.9294±0.0052
30			12.2	40		0.9300±0.0055
31			12.3	19		0.9180±0.0057
32			12.3	14		0.9210±0.0053
33			12.5	6		0.9279±0.0051
34		4	12.0	88	480	0.9311±0.0057
35			12.2	25		0.9314±0.0054
36			12.3	12		0.9612±0.0051
37			12.6	1		0.9198±0.0055
38		9	10.5	90	485	0.9328±0.0054
39			11.0	40		0.9302±0.0062
40			11.8	14		0.9243±0.0058
41			12.4	3		0.9271±0.0060
42			12.7	0		0.9142±0.0058
43		16	0	78	495	0.9404±0.0065
44			2.6	64		0.9459±0.0058
45			5.5	50		0.9394±0.0056
46			7.7	37		0.9384±0.0056
47			10.0	20		0.9254±0.0061
48			11.4	8		0.9176±0.0053

Table 3.B.2.2 (continued)

No.	Cylinder diameter (cm)	Number of cylinders	Slab thickness (cm)	Array height (cm)	Uranium concentration (g/ℓ)	Calculated k_{eff}
49	16.3	16	12.4	3	495	0.9308±0.0054
50			12.6	0		0.9070±0.0057
51	21.3	1	11.1	88	500	0.9384±0.0058
52			11.1	39		0.9269±0.0068
53			12.4	3		0.9158±0.0059
54		4	8.3	91		0.9070±0.0059
55			10.1	39		0.9299±0.0064
56			11.0	19		0.9348±0.0059
57			11.8	10		0.9232±0.0053
58			12.7	2		0.9329±0.0064
59		9	0	47		0.9484±0.0060
60			1.5	43		0.9624±0.0053
61			5.9	32		0.9578±0.0068
62			8.6	23		0.9563±0.0062
63			10.0	15		0.9167±0.0055
64			11.6	7		0.9299±0.0062
65			12.7	1		0.9171±0.0054
66		16	0	26		0.9371±0.0063
67			2.7	22		0.9425±0.0051
68			7.5	14		0.9259±0.0051

Table 3.B.2.2 (continued)

No.	Cylinder diameter (cm)	Number of cylinders	Slab thickness (cm)	Array height (cm)	Uranium concentration (g/ℓ)	Calculated k_{eff}
69	21.3	16	9.1	11	500	0.9383±0.0051
70			9.5	9		0.9089±0.0054
71			11.8	3		0.9274±0.0054
72	22.4	1	10.8	108	505	0.9404±0.0057
73	22.9	1	10.1	110		0.9495±0.0062
74	23.4	1	8.9	111	525	0.9481±0.0060
75			10.3	33		0.9407±0.0057
76			11.4	15		0.9243±0.0052
77	23.9	1	0	112		0.9533±0.0055
78			7.7	66		0.9568±0.0052
79			9.7	34		0.9493±0.0057
80			11.9	8		0.9155±0.0061
					Average	0.9289

Table 3.B.2.3 Experimental data and calculated k_{eff}'s for the critical slab-cylinder configuration with the array suspended above the slab

No.	Spacing between top of solution slab to bottom of array (cm)	Slab thickness (cm)	Solution height in cylinders[a] (cm)	Calculated k_{eff}
81	9.4	4.7	66	0.9491±0.0063
82	6.9	7.3	49	0.9353±0.0053
83	3.6	10.5	19	0.9173±0.0052
84	2.7	11.4	8	0.9069±0.0061
85	20.4	7.8	67	0.9617±0.0056
86	18.2	10.0	49	0.9267±0.0059
87	16.7	11.4	19	0.9065±0.0059
88	16.4	11.7	10	0.8906±0.0058
89	28.2	12.4	0.3	0.9115±0.0050
			Average	0.9228

a) This height is measured from the bottom of the cylinders of the array.

Table 3.B.2.4 Experimental data and calculated k_{eff}'s for the critical slab-cylinder configuration with Plexiglas reflectors

No.	Number of cylinders	Top and side reflector thickness(cm)	Slab tank bottom reflector thickness (cm)	Slab thickness (cm)	Array height (cm)	Uranium concentration (g/ℓ)	Calculated k_{eff}
90	9	10.2	10.2	7.1 ± 0.2	112 ± 1	505	1.0138±0.0043
91				8.8 ± 0.2	42 ± 1		1.0040±0.0056
92				9.5 ± 0.2	20 ± 1		1.0070±0.0055
93				10.3 ± 0.2	0 ± 0		—
94	16	10.2	10.2	0 ± 0.2	92 ± 1		1.0085±0.0049
95				3.8 ± 0.2	61 ± 4		1.0070±0.0054
96				8.1 ± 0.2	26 ± 1		1.0057±0.0049
97				10.3 ± 0.2	0 ± 0		—
98	16	7.6	10.2	0 ± 0.5	96 ± 1	510	1.0049±0.0049
99				4.7 ± 0.2	59 ± 2		1.0000±0.0054
100				7.9 ± 0.2	26 ± 2		0.9850±0.0055
101				10.5 ± 0.2	0 ± 2		0.9826±0.0055
102	16	5.1	10.2	0 ± 0.5	105 ± 1		1.0034±0.0057
103				3.4 ± 0.2	75 ± 1		0.9969±0.0053
104				7.4 ± 0.2	36 ± 1		0.9928±0.0057
105				10.6 ± 0.2	2 ± 1		1.0056±0.0055
106	16	2.5	10.2	0 ± 0.5	149	515	0.9736±0.0059
107				3.3 ± 0.2	114 ± 1		0.9846±0.0055
108				6.0 ± 0.2	72 ± 1		0.9696±0.0058
109				8.6 ± 0.2	30 ± 1		0.9887±0.0051
110				9.8 ± 0.2	9 ± 1		0.9678±0.0052
111	16	0	10.2	8.3 ± 0.2	110 ± 0.6		0.9577±0.0055
112				8.7 ± 0.2	67.5±0.6		0.9715±0.0058
113				9.6 ± 0.2	27.5±0.6		0.9755±0.0054
114	16	0	5.1	8.7 ± 0.2	109.0 ± 0.5		0.9738±0.0056
115				9.0 ± 0.2	69.5 ± 0.5		0.9738±0.0056
116				9.9 ± 0.2	26.0 ± 0.5		0.9766±0.0057
117				11.0 ± 0.2	7.5 ± 0.5		0.9892±0.0059
118	16	0	0	10.0 ± 0.2	108 ± 1	520	—
119				10.4 ± 0.2	69 ± 1		—
120				11.3 ± 0.2	26 ± 1		—
121				12.3 ± 0.2	4 ± 1		—

Table 3.B.3.1 Calculated k_{eff}'s for the array of cylinders reflected by concrete

No.	Cylinder inner dia.(cm)	Stainless steel sleeve	Array size	Uranium concentration (g/ℓ)	Critical solution level(cm)	Calculated k_{eff}
1	21.12	Yes	4 × 4	67.28	28.63	0.9914±0.0050
2	21.12	No	4 × 4	67.28	27.15	0.9896±0.0043
3	21.12	Yes	2 × 2	76.09	60.70	0.9940±0.0054
4	21.12	No	2 × 2	76.09	62.34	0.9757±0.0051
5	21.12	No	2 × 2	80.72	57.88	0.9849±0.0052
6	16.12	Yes	4 × 4	83.49	57.34	0.9873±0.0045
7	16.12	No	4 × 4	83.49	51.21	0.9954±0.0054
8	21.12	Yes	4 × 4	369.96	17.24	0.9828±0.0063
9	21.12	No	4 × 4	364.11	17.13	0.9896±0.0065
10	21.12	Yes	2 × 2	360.37	29.49	0.9817±0.0051
11	21.12	No	2 × 2	364.11	31.11	0.9791±0.0058
12	16.12	Yes	4 × 4	360.37	32.32	0.9841±0.0054
13	16.12	No	4 × 4	359.55	31.82	0.9891±0.0059
14	16.12	No	2 × 4	359.55	51.45	0.9872±0.0055
15	16.12	No	2 × 3	359.55	65.49	0.9822±0.0057
16	16.12	Yes	2 × 2	359.55	101.45	0.9768±0.0049
17	16.12	No	2 × 2	359.55	104.04	0.9843±0.0052
					Average	0.9856

Table 3.B.3.2 Calculated k_{eff}'s for the array of cylinders reflected by plastic

No.	Cylinder inner dia.(cm)	Stainless steel sleeve	Array size	Uranium concentration (g/ℓ)	Critical solution level(cm)	Calculated k_{eff}
18	21.12	Yes	4 × 4	60.32	34.82	0.9823±0.0049
19	21.12	No	4 × 4	60.32	31.76	0.9791±0.0048
20	21.12	Yes	2 × 2	60.32	110.20	0.9844±0.0045
21	21.12	No	2 × 2	60.32	102.29	0.9771±0.0051
22	16.12	Yes	4 × 4	60.32	105.85	0.9820±0.0049
23	16.12	No	4 × 4	60.32	78.40	0.9739±0.0042
24	21.12	Yes	4 × 4	355.94	19.27	0.9724±0.0053
25	21.12	No	4 × 4	355.94	18.82	0.9735±0.0056
26	21.12	Yes	2 × 2	355.94	31.93	0.9681±0.0056
27	21.12	No	2 × 2	355.94	33.20	0.9757±0.0054
28	16.12	Yes	4 × 4	355.94	38.10	0.9776±0.0058
29	16.12	No	4 × 4	355.94	35.56	0.9814±0.0057
30	16.12	Yes	2 × 3	355.94	95.20	0.9741±0.0056
31	16.12	No	2 × 3	355.94	89.78	0.9856±0.0052
					Average	0.9777

Table 3.B.4.1 Calculated results for two aluminum cylindrical reactors

	Case No.	H/^{235}U Atomic Ratio	Surface Separation (cm)	Critical Height (cm)	Calculated Results	
					k_{eff}	σ
Cylinder Dia. = 8in	1- 1^{R}	29.9	0	13.4	1.0009*	0.0052
	2^{R}	52.9	0	13.2	0.9891**	0.0028
	3^{R}	52.9	3.5	14.9	0.9879*	0.0052
	4^{R}	52.9	7.0	17.0	0.9877*	0.0053
	5^{R}	52.9	14.7	19.1	0.9952*	0.0052
	6^{R}	52.9	20.1	18.6	0.9803**	0.0031
Cylinder Dia. = 10in	1- 7	169	15.6	35.8	0.9719*	0.0067
	8	329	16.6	64.7	0.9717*	0.0059
	9^{R}	329	0	16.9	0.9931*	0.0049
	10^{R}	329	8.0	21.1	0.9860**	0.0040
	11^{R}	52.9	13.0	12.9	0.9983*	0.0054
	12^{R}	52.9	20.0	13.0	0.9924*	0.0052
	13^{R}	29.9	0	11.0	1.0074*	0.0055
Cylinder Dia. = 15in	1-14	169	0.3	17.3	0.9493*	0.0060
	15	169	5.0	17.8	0.9574	0.0058
	16	169	15.0	18.0	0.9543*	0.0056
	17	329	0.2	20.1	0.9546*	0.0052
	18	329	5.0	20.8	0.9567*	0.0053
	19	329	9.7	21.0	0.9566*	0.0054
	20	329	31.3	21.3	0.9589*	0.0059
	21^{R}	52.9	0	7.3	0.9722*	0.0054
	22^{R}	52.9	5.8	7.65	0.9789*	0.0051
	23^{R}	52.9	11.6	7.7	0.9711*	0.0053
	24^{R}	169	0	9.0	0.9709**	0.0031
	25^{R}	169	3.0	9.3	0.9881*	0.0057
	26^{R}	169	22.0	9.7	0.9672*	0.0053
	27^{R}	329	0	11.5	0.9747*	0.0055
	28^{R}	329	5.0	12.3	0.9754*	0.0049
	29^{R}	329	20.0	12.6	0.9685**	0.0027

R: Experiment with water reflector.
*: Calculated with 30,000 neutron histories.
**: Calculated with 100,000 neutron histories.

Table 3.B.5.1 Calculated results for cubic arrays of uranium metal cylinders without reflectors

Case No.	Array	Cylinder		Critical Separation		Calculated Results	
		Radius (cm)	Height (cm)	Hori.	Vert.	k_{eff}	σ
2-1	3^3	5.7545	5.382	0	6.127	0.9957***	0.0017
2	2^3	5.747	8.077	0	3.417	0.9992***	0.0017
3	2^3	5.753	10.765	1.997	2.738	1.0105*	0.0044
4	3^3	5.742	10.765	6.118	6.837	1.0162**	0.0025
5	2^3	5.7545	13.459	4.269	2.319	1.0169*	0.0042

*: Calculated with 30,000 neutron histories.
**: Calculated with 100,000 neutron histories.
***: Calculated with 200,000 neutron histories.

Table 3.B.5.2 Calculated results for cubic arrays of uranium metal cylinders with reflectors

Case No.	Array	Cylinder Radius (cm)	Cylinder Height (cm)	Reflector Thickness (cm)	Critical Separation (cm)	Calculated Results k_{eff}	Calculated Results σ
2- 6	3^3	5.7545	5.382	0	2.007	1.0185*	0.0042
7				1.3	2.992	1.0050*	0.0047
8				3.8	5.872	1.0035*	0.0049
9				7.6	8.258	1.0090*	0.0049
10				15.2	8.689	1.0140*	0.0048
11	2^3	5.747	8.077	0	0.902	1.0144*	0.0043
12				1.3	1.905	1.0198*	0.0045
13				3.8	4.961	1.0058*	0.0050
14				7.6	7.391	1.0094*	0.0051
15				15.2	7.823	1.0117*	0.0049
16	2^3	5.753	10.765	0	2.248	1.0188*	0.0023
17				1.3	3.678	1.0130**	0.0028
18				2.5	5.710	1.0193**	0.0025
19				3.8	8.207	1.0153**	0.0025
20				7.6	11.509	1.0158**	0.0024
21				15.2	11.986	1.0121**	0.0023
22	3^3	5.742	10.765	0	6.363	1.0166**	0.0025
23				1.3	8.574	1.0035**	0.0024
24				3.8	14.764	1.0169**	0.0024
25				7.6	18.720	1.0148**	0.0022
26				15.2	19.147	1.0221**	0.0024
27	2^3	5.7545	13.459	0	3.543	1.0088*	0.0045
28				1.3	5.423	1.0038*	0.0045
29				3.8	11.532	1.0055*	0.0048
30				7.6	15.697	1.0139*	0.0047
31				15.2	16.378	1.0120*	0.0048

*: Calculated with 30,000 neutron histories

**: Calculated with 100,000 neutron histories

Table 3.B.6.1 Calculated results for arrays of plutonium metal billets

	Case No.	Array	Critical Separation (cm) Vertical	Critical Separation (cm) Horizontal	Moderator Thickness (cm)	Calculated Results k_{eff}	Calculated Results σ
3 kg Pu billet	3- 1	2^3	5.40	7.30	——	1.0018*	0.0051
	2	3^3	7.71	9.60	——	1.0088*	0.0048
	3	4^3	7.86	12.51	——	1.0033*	0.0047
	4^R	2^3	5.74	7.64	——	0.9982*	0.0028
	5^R	3^3	8.24	10.15	——	1.0121*	0.0028
	6	4^3	9.63	14.19	1.27	0.9761***	0.0017
	7	4^3	13.64	14.55	2.54	0.9878**	0.0027
	8	4^3	13.63	14.62	3.81	1.0055**	0.0029
6 kg Pu billet	9	2×2×1	——	7.59	——	1.0043**	0.0030
	10	2^3	11.98	9.76	——	1.0070*	0.0046
	11	3^3	13.68	14.51	——	0.9926*	0.0043
	12	4×4×1	——	10.91	——	0.9911*	0.0059
	13	4^3	47.12	11.93	——	1.0188***	0.0016
	14	4^3	32.12	13.09	——	1.0134***	0.0017
	15	4^3	22.12	15.23	——	1.0056**	0.0027
	16	4^3	17.12	17.28	——	0.9945**	0.0028
	17	4^3	13.12	20.19	——	0.9944**	0.0028
	18	4^3	25.79	17.50	1.27	0.9847**	0.0038
	19	4^3	25.82	21.24	2.54	0.9809**	0.0026

R: Experiment with polyethylene reflector

*: Calculated with 30,000 neutron histories

**: Calculated with 100,000 neutron histories

***: Calculated with 200,000 neutron histories

Table 3.B.7.1 Calculated results for cubic arrays of cylinders containing uranyl-nitrate solution with reflectors of various thicknesses

Case No.	Array	Surface Separation (cm)	Reflector Thickness (cm)	Calculated Results	
				k_{eff}	σ
4- 1	2^3	1.43	None	0.9763**	0.0031
2	2^3	3.28	Paraffin 1.27	0.9760**	0.0031
3	2^3	6.91	Paraffin 3.81	0.9919*	0.0053
4	2^3	8.48	Paraffin 7.62	1.0044*	0.0049
5	2^3	8.99	Paraffin 15.24	0.9967**	0.0030
6	2^3	3.00	Plexiglas 1.27	0.9815**	0.0029
7	3^3	6.48	None	0.9679**	0.0031
8	3^3	9.02	Paraffin 1.27	0.9797**	0.0030
9	3^3	13.69	Paraffin 3.81	0.9977*	0.0060
10	3^3	16.53	Paraffin 15.24	1.0025**	0.0032
11	3^3	8.76	Plexiglas 1.27	0.9756**	0.0032
12	4^3	10.67	None	0.9578**	0.0031
13	5^3	14.40	None	0.9584**	0.0031

* Calculated with 30,000 neutron histories

** Calculated with 100,000 neutron histories

Table 3.B.7.2 Calculated results for cubic arrays of cylinders containing uranyl-nitrate solution with reflectors of various thicknesses on five sides and a 15.24 cm thick paraffin reflector on the bottom

Case No.	Array	Surface Separation (cm)	Reflector Thickness	Calculated Results	
				k_{eff}	σ
4-14	2^3	3.86	Paraffin 1.27	0.9935*	0.0067
15	2^3	7.26	Paraffin 3.81	0.9870**	0.0031
16	2^3	8.71	Paraffin 7.62	1.0002*	0.0056
17	2^3	8.99	Paraffin 15.24	0.9967**	0.0030
18	2^3	3.61	Plexiglas 1.27	0.9842**	0.0030
19	2^3	5.41	Plexiglas 2.54	0.9963*	0.0053
20	2^3	7.39	Plexiglas 4.45	1.0061*	0.0061
21	2^3	8.64	Plexiglas 6.35	0.9974*	0.0053
22	2^3	9.53	Plexiglas 11.43	1.0008*	0.0058
23	2^3	9.60	Plexiglas 15.24	1.0026*	0.0028
24	3^3	9.88	Paraffin 1.27	0.9849**	0.0031
25	3^3	14.27	Paraffin 3.81	0.9950*	0.0055
26	3^3	15.85	Paraffin 7.62	1.0042*	0.0055
27	3^3	16.53	Paraffin 15.24	0.9917*	0.0058
28	3^3	9.58	Plexiglas 1.27	0.9786**	0.0032
29	3^3	11.94	Plexiglas 2.54	0.9856**	0.0031

* Calculated with 30,000 neutron histories

** Calculated with 100,000 neutron histories

Table 3.B.8.1 Description of parameters of $U(93.15)O_2$ container units

	Container type			
Container	I	II	III	IV
Number of containers	196	18	9	9
Inside radius, cm	3.735	7.65	6.76	6.76
Inside height, cm	11.59	21.76	25.18	25.18
Wall thickness, cm	0.055	0.03	0.03	0.03
Average weight, g	128	360	341	341
UO_2				
Height, cm	4.48	19.76	17.87	17.87
Density, g/cm^3	2.144	5.505	6.628	6.628
Mass, g	421	20,000	17,000	17,000
Uranium analysis, g of U/g of UO_2	0.8754	0.8780	0.8780	0.8780
C_2H_6O - 5% H_2O in UO_2 Region				
Density, g/cm^3			0.3458	0.3458
Mass, g			711.5	711.5
$H/^{235}U$ Atom ratio			1.556	1.556
C_2H_6O - 5% H_2O Layer above oxide				
Height, cm			3.14	0.53
Density, g/cm			0.8020	0.8020
Mass, g			36.1	61.5
Total alcohol mass, g			1,073	773

Table 3.B.8.2 Description of cells and experimental multiplication factors for $U(93)O_2$ moderated and unmoderated

Experiment number	Array size	Cell description: Material	Geometry	Dimensions, cm: R	±X	±Y	+Z	-Z	k(exp)
		421 g units of $U(93)O_2$, Type 1							
1	7X7X4	UO_2	Cylinder	3.735	–	–	+ 4.535	+0.055	1.0167
		Void	Cylinder	3.735	–	–	+11.645	+0.055	
		Steel	Cylinder	3.790	–	–	+11.71	0.0	
		Void	Cuboid	–	±4.025	±4.025	+11.71	0.0	
		$C_5O_2H_8$	Cuboid	–	±5.195	±5.195	+14.05	0.0	
2	7X7X4	Exp. 1 with 18 units removed from top layer							1.0012
3	7X7X4	UO_2					+ 3.639	+0.055	–
4	7X7X4	UO_2					+ 5.431	+0.055	–
		20 kg units of $U(93)O_2$, Type 2							
5	4X4X1	UO_2	Cylinder	7.65	–	–	+10.88	-10.88	1.0094
		Steel	Cylinder	7.68	–	–	+10.91	-10.91	
		Void	Cuboid	–	±7.85	±7.85	+11.15	-11.15	
6	3X2X2	See No.5 for cell description							0.9968
7	3X3X2	Void	Cuboid	–	±9.08	±9.08	+11.15	-11.15	1.0014
		20 kg units with methyl methacrylate between top and bottom units							

Table 3.B.8.2 (continued)

Experiment number	Array size	Cell description							k(exp)
				Dimensions, cm					
		Material	Geometry	R	±X	±Y	+Z	−Z	
8	3X3X2	Void	Cuboid	–	±10.22	±10.22	+11.15	−11.15	1.0001
		$C_5O_2H_8$	Cuboid	–	±10.22	±10.22	+ 1.18	− 1.18	
9	3X3X2	$C_5O_2H_8$	Cuboid	–	±10.22	±10.22	+ 1.81	− 1.81	1.0137
10	3X3X2	One corner unit removed from No.9							0.9996
11	3X3X2	$C_5O_2H_8$	Cuboid	–	±10.22	±10.22	+ 2.41	− 2.41	1.0129
12	3X3X2	One corner unit removed from No.11							0.9989
13	3X3X2	$C_5O_2H_8$	Cuboid	–	±10.22	±10.22	+ 3.04	− 3.04	1.0049
		20 kg units with 2-in-thick methyl methacrylate in three dimensions							
14	3X3X2	Void	Cuboid	–	±10.27	±10.27	+11.15	−11.15	–
15	3X3X2	Three units removed from top edge							1.010
16	3X3X2	Three units removed from top edge, 2 from opposite corners, and 1 from the middle of an edge							1.0018
17	3X3X2	Void	Cuboid	–	±10.27	±10.27	+11.15	−11.15	1.0012
		$C_5O_2H_8$	Cuboid	–	±12.70	±12.70	+11.15	−15.97	
		Void	Cuboid	–	±12.70	±12.70	+15.28	−15.97	
18	3X3X2	Void	Cuboid	–	±10.27	±10.27	+11.15	−11.15	1.009
		$C_5O_2H_8$	Cuboid	–	±12.70	±12.70	+11.15	−15.97	
		Void	Cuboid	–	±12.70	±12.70	+18.77	−15.97	
		20 kg units with 1-in-thick methyl methacrylate in three dimensions							
19	3X3X2	Void	Cuboid	–	±15.30	±10.22	+11.15	−11.15	1.0054
		17 kg units with C_2H_6O-5% H_2O, Type 3							
20	2X2X1	UO_2-C_2H_6O	Cylinder	6.76	–	–	+ 5.27	−12.60	1.0065
		C_2H_6O	Cylinder	6.76	–	–	+ 8.41	−12.60	
		Void	Cylinder	6.76	–	–	+12.58	−12.60	
		Steel	Cylinder	6.79	–	–	+12.63	−12.63	
		Void	Cuboid	–	±6.985	±6.985	+12.78	−12.78	
21	2X2X1	Void	Cuboid	–	±7.025	±7.025	+12.78	−12.78	1.0031
22	2X2X1	Void	Cuboid	–	±7.064	±7.064	+12.78	−12.78	1.0018
23	2X3X1	Void	Cuboid	–	±7.620	±7.620	+12.78	−12.78	1.0146
24	2X3X1	Void	Cuboid	–	±7.938	±7.938	+12.78	−12.78	1.0025
25	2X3X1	Void	Cuboid	–	±8.017	±8.017	+12.78	−12.78	0.9988
26	2X4X1	Void	Cuboid	–	±8.493	±8.493	+12.78	−12.78	1.0003
27	3X3X1	Void	Cuboid	–	±9.049	±9.049	+12.78	−12.78	0.9996
		17 kg units with C_2H_6O-5% H_2O, Type 4							
28	3X3X1	Void	Cuboid	–	±8.573	±8.573	+12.78	−12.78	1.0042
29	3X3X1	Void	Cuboid	–	±8.652	±8.652	+12.78	−12.78	0.9997

Table 3.B.8.3 Principal critical parameters and calculated k_{eff}'s

No.	Fuel					Unit Numbers	k_{eff} (Measured Value)	Calculated k_{eff}	C/E
	Type of Fuel	Density (g/cm^3)	Array	Pitch (cm) X, Y	Pitch (cm) Z				
1	I.D. = 3.735 cm UO_2 = 421 g	2.144	7X7X4	10.39	14.05	196	1.0167	1.0323±0.0049	1.015
2						178	1.0012	0.9988±0.0044	0.998
3		2.573				196	–	1.0006±0.0045	–
4		1.715					–	1.0515±0.0052	–
5	I.D. = 7.65 cm UO_2 = 20 kg	4.999	4X4X1	15.7	22.3	16	1.0094	1.0122±0.0044	1.003
6			3X2X2			12	0.9968	0.9875±0.0053	0.991
7			3X3X2	18.16		18	1.0014	1.0002±0.0046	0.999
8				20.44	24.66		1.0001	0.9869±0.0048	0.987
9					25.92		1.0137	1.0017±0.0050	0.988
10						17	0.9996	0.9759±0.0046	0.976
11					27.12	18	1.0129	1.0082±0.0048	0.995
12						17	0.9989	0.9891±0.0043	0.990
13					28.38	18	1.0049	1.0099±0.0047	1.005
14				25.4			–	1.0743±0.0051	–
15					27.12	15	1.010	1.0204±0.0051	1.010
16						12	1.0018	0.9555±0.0042	0.954
17					31.25	16	1.0012	1.0221±0.0048	1.021
18					34.74	18	1.009	1.0225±0.0048	1.013
19				33.03(X) 22.87(Y)	24.71		1.0054	0.9926±0.0047	0.987
20	I.D. = 6.76 cm UO_2 = 17 kg C_2H_6O -5% H_2O = 711.5 g	6.626	2X2X1	13.97		4	1.0065	0.9953±0.0049	0.989
21				14.05			1.0031	0.9966±0.0041	0.994
22				13.128			1.0018	0.9974±0.0052	0.996
23			2X3X1	15.24		6	1.0146	1.0175±0.0051	1.003
24				15.876			1.0025	1.0108±0.0043	1.008
25				16.034			0.9988	0.9884±0.0050	0.990
26			2X4X1	16.986		8	1.0003	0.9981±0.0049	0.998
27			3X3X1	18.098		9	0.9996	0.9929±0.0056	0.998
28				17.146			1.0042	0.9982±0.0042	0.994
29				17.304			0.9997	0.9944±0.0050	0.995

Table 3.C.1.1 Calculated results for $U(2.6)O_2$-H_2O systems

Lattice Name	Pattern	Critical Water Level [cm]	k_{eff}	± σ
1.50U (H/U = 4.33, Pitch = 1.849 cm)	19 × 19	99.45	0.99597	0.00312
	20^2	73.73	1.00010	0.00282
	21^2	60.81	0.99852	0.00293
	22^2	53.23	0.99276	0.00275
	23^2	47.81	0.99510	0.00282
	24^2	43.94	0.99469	0.00300
	25^2	40.89	0.98960	0.00288
1.83U (H/U = 5.28, Pitch = 1.956 cm)	12 × 29	131.94	0.99405	0.00311
	14 × 27	69.01	0.99113	0.00295
	14 × 24	85.36	0.99234	0.00321
	14 × 21	135.70	0.98645	0.00283
	15 × 19	139.72	0.99175	0.00271
	15 × 20	113.95	0.99717	0.00281
	15 × 21	94.58	0.99812	0.00289
	15 × 22	83.45	0.99068	0.00305
	15 × 23	75.74	0.99311	0.00290
	16 × 18	120.73	0.98465	0.00282
	17 × 17	114.59	0.99091	0.00328
	17×17+20	81.17	0.99218	0.00286
	18 × 18	75.32	0.99364	0.00302
	18 × 19	66.90	0.99321	0.00307
	19 × 19	60.38	0.99050	0.00279
	19 × 20	55.53	0.99597	0.00285
	20 × 20	51.65	0.99288	0.00351
	20 × 21	48.62	0.99277	0.00278
	21^2	46.01	0.99875	0.00285
	21 × 23	43.91	0.99278	0.00291
	22^2	42.12	0.99256	0.00286
	22 × 23	40.50	0.98987	0.00299
2.48U (H/U = 7.16, Pitch = 2.150 cm)	16 × 16	78.67	0.99121	0.00286
	17 × 17	59.96	0.99120	0.00294
	18 × 18	50.52	0.99181	0.00258
	19 × 19	44.55	0.99235	0.00295
	20 × 20	40.44	0.98858	0.00301
3.00U (H/U = 8.65, Pitch = 2.293 cm)	15 × 15	90.75	0.99343	0.00304
	16 × 16	64.42	0.98876	0.00299
	17 × 17	53.87	0.98980	0.00289
	18 × 18	46.06	0.98756	0.00305
	18 × 20	41.79	0.99043	0.00274
	19 × 19	41.54	0.99038	0.00292

Table 3.C.1.2 Calculated results for PuO_2-UO_2-H_2O systems

Lattice Name	Pattern	Critical Water Level [cm]	Date	k_{eff}	± σ
2.42PU	22^2	69.41	'72-6- 5	1.00128	0.00295
(H/(U+Pu) = 12.10	22 × 23	69.57	'74-5-14	0.99391	0.00311
Pitch = 1.825 cm)	23^2	59.55	'72-6- 7	0.99998	0.00304
	23^2	61.90	'73-5-14	0.99355	0.00304
	23^2	64.06	'74-5-14	0.99493	0.00305
	23^2	66.46	'75-5-16	0.99618	0.00320
	23 × 24	60.06	'74-5-14	0.99612	0.00277
	24^2	53.30	'72-6- 7	0.99423	0.00313
	24^2	56.68	'74-5-14	0.99815	0.00310
	24^2	58.36	'75-5-16	0.99559	0.00302
2.98PU	20 × 21	67.10	'72-5-18	0.99724	0.00300
(H/(U+Pu) = 14.87	21^2	61.50	'72-5-18	0.99734	0.00294
Pitch = 1.956 cm)	21^2	64.39	'73-5-22	0.99565	0.00283
	21^2	66.87	'74-5-28	0.99804	0.00297
	21^2	69.40	'75-5-21	1.00584	0.00282
	21 × 22	57.38	'72-5-18	0.99879	0.00278
	21 × 22	60.37	'73-5-22 '73-6- 6	1.00051	0.00282
	21 × 22	61.92	'74-5-28	0.99861	0.00306
	21 × 22	63.88	'75-5-21	0.99502	0.00311
	22^2	57.83	'74-5-28	0.99467	0.00296
	22 × 23	54.72	'74-5-28	0.99452	0.00262
	23^2	51.94	'74-5-28	0.99676	0.00290
	23 × 24	49.82	'74-5-28	0.99315	0.00303
	24^2	47.78	'74-5-28	0.99592	0.00275
	24^2	48.68	'75-5-21	1.00151	0.00306
4.24PU	19 × 20	68.67	'73-5-29	0.99338	0.00283
(H/(U+Pu) = 21.16	20^2	60.32	'72-4-13	0.99223	0.00288
Pitch = 2.225 cm)	20^2	62.95	'73-5-29	0.99556	0.00267
	20^2	65.63	'74-6- 5	0.98485	0.00297
	20^2	68.18	'75-5-28	1.00048	0.00285
	20 × 21	61.07	'74-6- 5	0.99072	0.00278
	21^2	53.41	'72-4-14	0.99066	0.00279
	21^2	55.48	'73-5-29	0.99490	0.00300
	21^2	57.28	'74-6- 5	1.00086	0.00291
	21^2	59.05	'75-5-28	0.99897	0.00265
	21 × 22	54.33	'74-6- 5	0.99886	0.00282
	22^2	51.74	'74-6- 6	0.99307	0.00289
	23^2	47.72	'74-6- 6	0.99349	0.00288
	24^2	44.67	'74-6- 6	0.99109	0.00285
	24^2	45.62	'75-5-28	0.99419	0.00311
5.55PU	20 × 21	69.16	'73-6- 6	0.99192	0.00257
(H/(U+Pu) = 27.72	21^2	62.05	'72-4-28	0.99662	0.00286
pitch = 2.474 cm)	21^2	64.53	'73-6- 7	0.99989	0.00279
	21 × 22	58.73	'72-4-26	0.98517	0.00271
	21 × 22	61.10	'73-6- 6	0.99048	0.00278
	22^2	58.08	'73-6- 6	0.98960	0.00248
	22 × 23	55.69	'73-6- 6	0.99557	0.00261
	23^2	53.50	'73-6- 6	0.99155	0.00286

Table 3.C.1.3 Calculated results for the water gap pattern

Lattice name	Pattern	Critical Water Level [cm]	k_{eff}	± σ
1.50U (H/U = 4.33, pitch = 1.849 cm)	24 × 25	42.42	0.99447	0.00448
	24 × 26	48.80	0.99836	0.00404
	24 × 27	64.05	0.99565	0.00414
	24 × 28	100.47	0.99850	0.00387
3.00U (H/U = 8.65, pitch = 2.293 cm)	20 × 19	46.84	0.99365	0.00429
	20 × 20	65.81	0.99438	0.00411
	20 × 21	130.77	0.99764	0.00394

Table 3.C.1.4 Calculated results for UO_2 lattices with boric acid solution

Lattice name	Pattern	Boron Concentration ppm	Critical Water Level [cm]	k_{eff}	± σ
1.83U (H/U = 5.28, pitch = 1.956 cm)	18 × 19	72.3	85.78	0.99828	0.00322
	19^2	146.6	96.85	0.99579	0.00298
	22^2	345.0	84.99	1.00547	0.00301
	25^2	554.0	85.79	1.00672	0.00277

Table 3.C.1.5 Calculated results for UO_2 lattices with the poison sheet

Lattice name	Poison Name	Position	Critical Water Level (cm)	k_{eff}	± σ
1.83U (H/U = 5.28, pitch = 1.956 cm)	Boral	16P16	120.4	1.00058	0.00297
		13P19	100.1	0.99959	0.00275
		11P21	83.9	1.00438	0.00296
1.83U	Al-Cd	13P14	86.62	0.99994	0.00284
	(No. 1)	10P17	83.92	0.99808	0.00323
		6P21	78.11	0.99762	0.00291
		3P24	73.96	0.98999	0.00315
		1P26	72.00	0.99794	0.00303
1.83U	Al-Cd	13P14	98.24	1.00262	0.00300
	(No. 2)	10P17	93.27	0.99671	0.00294
		6P21	82.46	0.99705	0.00315
		3P24	75.92	1.00237	0.00275
		1P26	73.10	0.99393	0.00305
1.83U	Al-Cd	13P14	115.87	1.00058	0.00283
	(No. 3)	10P17	105.85	1.00161	0.00307
		6P21	87.40	0.99796	0.00280
		3P24	78.08	0.99696	0.00292
		1P26	74.32	0.99988	0.00321
1.83U	Al-Cd	9P18	118.38	1.00036	0.00319
	(No. 4)	6P21	94.04	1.00153	0.00296
		3P24	80.39	0.99392	0.00271
		1P26	75.76	0.99998	0.00306
1.83U	Al-Cd	8P19	126.60	0.99526	0.00295
	(No. 5)	6P21	102.13	0.99535	0.00293
		3P24	83.32	0.99680	0.00321
		1P26	77.40	0.99616	0.00313

Table 3.C.2.1 Calculated results and experimental conditions for UO_2 rod clusters partially immersed in water without removal of rods

No.	Type	Pitch (mm)	Number of Rods	Number of Rods on Each Side	Critical Water Height (cm)	keff ±σ
1	Square	12.6	484	22×22	90.69 ±0.10	0.99090 ±0.00349
2		16.0	272	16×17	73.53 ±0.10	0.98616 ±0.00348
3		21.0	255	15×15	77.98 ±0.06	0.98527 ±0.00354
4		25.2	306	17×18	79.85 ±0.01	0.99280 ±0.00305
5	Triangular (hexagonal shape)	13.5	547	14 Each side	60.93 ±0 06	0.99141 ±0.00344
6		17.2	271	10 Each side	68.06 ±0 06	0.98307 ±0.00327
7		22.6	217	9 Each side	79.50 ±0.06	0.99182 ±0.00350
8	Triangular with irregular hexagonal shape	13.5	519	13/13/15/13/13/15	69.50 ±0.06	0.99379 ±0.00374
9			505	15/12/15/12/15/12	75.79 ±0.07	0.99573 ±0.00345
10			495	14/14/12/14/14/12	82.43 ±0.06	0.98754 ±0.00354
11	Triangular with pseudo-cylindrical shape	13.5	484	See Fig.3.C.2.1	85.21 ±0.06	0.98532 ±0.00342
12		17.2	277	See Fig.3.C.2.1	61.99 ±0.06	0.98319 ±0.00363.
13		22.6	225	See Fig.3.C.2.1	70.44 ±0.07	0.98929 ±0.00299

Table 3.C.2.2 Calculated results and experimental conditions for UO_2 rod clusters with systematic removal of rods

No.	Square Pitch (mm)	Pattern	Number of Rods	Number of Holes	Frequency of Hole	Critical Water Height (cm)	keff ±σ
14	12.6	22×22	459	25	1 in 5 spaces	81.36 ±0.07	0.99816 ±0.00398
15			448	36	1 in 4 spaces	77.69 ±0.07	0.99409 ±0.00337
16			420	64	1 in 3 spaces	73.05 ±0.06	0.99214 ±0.00345
17			363	121	1 in 2 spaces	58.77 ±0.06	0.99420 ±0.00382
18		21×21	392	49	1 in 3 spaces	89.07 ±0.07	0.98399 ±0.00361
19			320	121	1 in 2 spaces	84.37 ±0.06	0.98947 ±0.00292

Table 3.C.2.3 Calculated results and experimental conditions for UO_2 rod clusters with removal of rods in a small region

No.	Pitch (mm)	Pattern	Number of Rods	Number of Holes	Frequency of Holes	keff
	12.6	22×22	459	25	Alternate rods removed	±σ
	Configuration (See Fig. 3.C.2.2)	Locations of the Holes[a] Row Number ↓	Column Number →	Critical Water Height (cm)		
20		8-10-12-14-16	7-9-11-13-15	68.75 ±0.06	0.99072 ±0.00339	
21		9-11-13-15-17	6-8-10-12-14	69.40 ±0.06	0.99860 ±0.00331	
22		10-12-14-16-18	5-7- 9-11-13	69.88 ±0.06	0.98973 ±0.00407	
23		11-13-15-17-19	4-6- 8-10-12	71.14 ±0.06	0.98768 ±0.00360	
24		12-14-16-18-20	3-5- 7- 9-11	72.52 ±0.07	0.99290 ±0.00400	
25		13-15-17-19-21	2-4- 6- 8-10	75.38 ±0.07	0.99254 ±0.00356	
26		14-16-18-20-22	1-3- 5- 7-9	81.34 ±0.06	0.98948 ±0.00339	

[a] Rows and columns are numbered from the upper left corner.

Table 3.C.3.1 Calculated results for UO_2 rod clusters (^{235}U enrichment: 2.35 wt%, lattice pitch: 20.32 mm) submerged in water with various poison plates

Serial No.	Cluster Array Size	No. Clus	Plate Material	tp mm	G mm	Xc mm	keff	± σ
1	20×18.08	1	—	—	—	∞	0.99086	0.00294
2	20×17	3	—	—	—	119.2	0.98813	0.00276
3	20×16	3	—	—	—	83.9	—	—
4	20×16	3	—	—	—	84.1	—	—
5	20×16	3	—	—	—	84.2	0.99052	0.00299
6	20×16	3	—	—	—	84.4	—	—
7	22×16	3	—	—	—	100.5	0.98948	0.00320
8	20×15	3	—	—	—	63.9	0.98824	0.00268
9	24×14	3	—	—	—	80.1	1.00001	0.00297
10	20×16	3	—	—	—	44.6	0.99200	0.00324
11	20×16	3	304L Steel (B=0)	4.85	6.45	68.8	0.98874	0.00278
12	20×16	3	304L Steel (B=0)	4.85	27.32	76.4	0.98997	0.00301
13	20×16	3	304L Steel (B=0)	4.85	40.42	75.1	0.98686	0.00297
14	20×16	3	304L Steel (B=0)	3.02	6.45	74.2	0.98708	0.00305
15	20×16	3	304L Steel (B=0)	3.02	40.42	77.6	0.99188	0.00328
16	20×17	3	304L Steel (B=0)	3.02	6.45	104.4	0.99465	0.00279
17	20×17	3	304L Steel (B=0)	3.02	40.42	114.7	0.99699	0.00326
18	20×17	3	304L Steel (B=1.05%)	2.98	6.45	75.6	0.98370	0.00320
19	20×17	3	304L Steel (B=1.05%)	2.98	40.42	96.2	0.99023	0.00298
20	20×17	3	304L Steel (B=1.62%)	2.98	6.45	73.6	0.98839	0.00296
21	20×17	3	304L Steel (B=1.62%)	2.98	40.42	95.2	0.98983	0.00306
22	20×17	3	Boral	7.13	6.45	63.4	—	—
23	20×17	3	Boral	7.13	6.45	63.2	0.98876	0.00306
24	20×17	3	Boral	7.13	44.42	90.3	0.99262	0.00294
25	22.21×16	3	Boral	7.13	6.45	52.2	0.98828	0.00314
26	22×16	3	Boral	7.13	6.45	50.5	0.98653	0.00314
27	20×18.88	1	Boral	7.13	27.32	∞	0.99194	0.00311
28	20×18.48	1	Boral	7.13	27.32	∞	0.98686	0.00331
29	20×16	3	Copper (Cd=0)	6.46	6.45	66.2	0.98734	0.00313
30	20×16	3	Copper (Cd=0)	6.46	27.32	77.2	0.98574	0.00303
31	20×16	3	Copper (Cd=0)	6.46	44.42	75.1	0.98531	0.00290
32	24×15	3	Copper (Cd=0)	3.37	6.45	68.8	0.98846	0.00332
33	24×15	3	Copper (Cd=0)	3.37	40.42	70.0	0.99192	0.00276
34	24×15	3	Copper (Cd=0.989%)	3.57	6.45	51.5	0.99173	0.00300
35	24.21×15	3	Copper (Cd=0.989%)	3.57	6.45	52.2	0.98763	0.00291
36	24.83×15	3	Copper (Cd=0.989%)	3.57	40.42	52.2	0.99536	0.00300
37	20×17	3	Cadmium	0.61	6.45	67.4	0.98538	0.00294
38	20×17	3	Cadmium	0.61	14.82	76.0	0.98450	0.00296
39	20×17	3	Cadmium	0.61	40.42	98.7	0.99751	0.00294
40	20×17	3	Cadmium	0.291	14.82	77.8	0.98515	0.00294
41	20×17	3	Cadmium	0.291	40.42	94.0	0.98923	0.00286
42	20×17	3	Cadmium	0.291	14.82	75.4	0.99460	0.00288
43	20×17	3	Cadmium	0.291	40.42	93.9	0.98849	0.00288
44	20×16	3	Aluminum	6.25	6.45	86.6	0.99306	0.00299
45	20×16	3	Aluminum	6.25	40.42	87.8	0.99115	0.00311
46	20×16	3	Aluminum	6.25	44.42	88.3	0.99164	0.00290
47	20×16	3	Zircaloy 4	6.22	6.45	87.9	0.98436	0.00333
48	20×16	3	Zircaloy 4	6.52	40.42	87.8	0.99282	0.00289

Table 3.C.3.2 Calculated results for UO_2 rod clusters (^{235}U enrichment: 4.31 wt%, lattice pitch: 25.40 mm) submerged in water with various poison plates

No.	Fuel Cluster	Poison Plate				keff	± σ
		Material	Thickness (mm)	Distance G (mm)	Distance Xc (mm)		
1	1・10*11・51		0.0	0.0	0.0	0.98316	0.00323
2	1・ 9*13・35		0.0	0.0	0.0	0.99034	0.00301
3	1・ 8*16・37		0.0	0.0	0.0	0.99087	0.00331
4&5	3・15*8		0.0	0.0	106.200	0.99201	0.00335
6	3・15*8	304L S.S(B=0wt%)	4.850	2.450	85.80	0.98638	0.00300
7	3・15*8	304L S.S(B=0wt%)	4.850	32.770	96.50	0.99050	0.00325
8	3・15*8	304L S.S(B=0wt%)	3.020	4.280	92.20	0.99441	0.00321
9	3・15*8	304L S.S(B=0wt%)	3.020	32.770	97.60	0.98666	0.00312
10	3・15*8	304L S.S(B=1.05wt%)	2.980	4.320	61.00	0.98603	0.00348
11	3・15*8	304L S.S(B=1.05wt%)	2.980	32.770	80.8	0.98692	0.00299
12	3・15*8	304L S.S(B=1.62wt%)	2.980	4.320	57.6	0.98673	0.00324
13	3・15*8	304L S.S(B=1.62wt%)	2.980	32.770	79.0	0.98921	0.00339
14	3・15*8	Boral	7.130	32.770	67.2	0.98472	0.00357
15	3・15*8	Copper(Cd=0wt%)	6.460	0.840	81.5	0.99806	0.00332
16	3・15*8	Copper(Cd=0wt%)	6.460	32.770	94.2	0.98597	0.00357
17	3・15*8	Copper(Cd=0wt%)	3.370	−0.570	84.8	0.99475	0.00339
18	3・15*8	Copper(Cd=0wt%)	3.370	42.410	96.4	0.99372	0.00364
19	3・15*8	Copper(Cd=0.989wt%)	3.370	−0.570	66.6	0.99036	0.00328
20	3・15*8	Copper(Cd=0.989wt%)	3.370	32.770	83.5	0.98588	0.00322
21	3・15*8	Cadmium	0.291	7.009	59.3	0.98732	0.00360
22	3・15*8	Cadmium	0.291	32.770	74.2	0.99196	0.00320
23	3・15*8	Cadmium	0.610	6.69	59.6	0.98962	0.00306
24	3・15*8	Cadmium	0.610	32.770	74.2	0.98455	0.00323
25	3・15*8	Cadmium	0.901	6.40	58.7	0.98740	0.00314
26	3・15*8	Cadmium	0.901	32.770	73.8	0.98757	0.00346
27	3・15*8	Cadmium	2.006	5.290	56.8	0.98977	0.00339
28	3・15*8	Cadmium	2.006	32.770	72.8	0.99203	0.00282
29	3・15*8	Aluminium	6.250	1.050	107.2	0.98574	0.00330
30	3・15*8	Aluminium	6.250	32.770	107.7	0.99135	0.00335
31	3・15*8	Zircaloy−4	6.250	0.780	109.2	0.98764	0.00342
32	3・15*8	Zircaloy−4	6.250	32.770	108.6	0.99149	0.00350

Table 3.C.4.1 Calculated results for UO_2 rod clusters submerged in water with reflecting walls

No.	Fuel Cluster	Reflector Material	Pitch (mm)	Enrichment (wt %)	Distance Y(mm)	Distance Xc(mm)	keff	± σ
1	3・19*16	Uranium	20.32	2.35	0.0	118.30	0.99004	0.00264
2	3・19*16	Uranium	20.32	2.35	13.21	139.3	0.98970	0.00246
3	3・19*16	Uranium	20.32	2.35	19.56	141.1	0.99366	0.00263
4	3・19*16	Uranium	20.32	2.35	26.16	137.0	0.99342	0.00262
5	3・19*16	Uranium	20.32	2.35	54.05	106.9	0.99074	0.00286
6	3・19*16	Uranium	20.32	2.35	106.76	85.6	0.98342	0.00293
7	3・19*16	Uranium	20.32	2.35	∞	83.1	0.97858	0.00304
8	3・20*16	Uranium	20.32	2.35	∞	91.3	0.98147	0.00318
9	3・19*16	Lead	20.32	2.35	0.0	138.4	0.98981	0.00288
10	3・19*16	Lead	20.32	2.35	6.60	137.2	0.98256	0.00292
11	3・19*16	Lead	20.32	2.35	26.16	112.5	0.99099	0.00309
12	3・19*16	Lead	20.32	2.35	∞	83.1	0.98250	0.00318
13	3・20*16	Lead	20.32	2.35	∞	91.3	0.98336	0.00290
14	3・13* 8	Uranium	25.40	4.29	0.0	153.8	0.99111	0.00278
15	3・12* 8	Uranium	25.40	4.29	19.56	153.2	0.99239	0.00339
16	3・13* 8	Uranium	25.40	4.29	39.12	180.5	0.98900	0.00285
17	3・13* 8	Uranium	25.40	4.29	54.05	134.9	0.98850	0.00293
18	3・13* 8	Uranium	25.40	4.29	∞	82.4	0.98107	0.00320
19	3・13* 8	Lead	25.40	4.29	0.0	206.2	1.00077	0.00320
20	3・13* 8	Lead	25.40	4.29	6.6	207.8	0.99714	0.00360
21	3・13* 8	Lead	25.40	4.29	13.21	190.4	1.00175	0.00305
22	3・13* 8	Lead	25.40	4.29	54.05	103.0	1.00494	0.00315
23	3・19*16	Lead	25.40	4.29	∞	82.4	0.98353	0.00352

Table 3.C.5.1 Calculated results and critical experimental data for three lined rod-clusters in water with various poison plates

Serial No.	Fuel Clusters	Pitch mm	Plate Material	t_p mm	G mm	X_c mm	Enrich wt%	Calculated Results	
								k_{eff}	$\pm\sigma$
1	3–12X16	18.92	–	–	–	122.7	4.31	0.99680	0.00366
2	3–12X16	18.92	304L STEEL	3.02	–	105.2	4.31	0.99401	0.00302
3	3–12X16	18.92	304L STEEL, 1.1 wt% B	2.98	–	72.3	4.31	0.99512	0.00332
4	3–12X16	18.92	304L STEEL, 1.6 wt% B	2.98	–	66.3	4.31	0.99466	0.00371
5	3–12X16	18.92	COPPER	3.37	–	103.6	4.31	0.99292	0.00301
6	3–12X16	18.92	COPPER–CADMIUM	3.57	–	76.1	4.31	0.99606	0.00352
7	1–25X20, 2–17X20	16.84	–	–	–	98.8	2.35	0.99156	0.00335
8	1–18X25, 2–18X20	16.84	–	–	–	67.8	2.35	1.00976	0.00298
9	1–25X20, 2–17X20	16.84	304L STEEL	3.02	–	78.0	2.35	0.99224	0.00336
10	1–25X20, 2–17X20	16.84	304L STEEL, 1.1 wt% B	2.98	–	38.6	2.35	0.99472	0.00264
11	1–25X20, 2–17X20	16.84	304L STEEL, 1.6 wt% B	2.98	–	34.6	2.35	0.99270	0.00301
12	1–25X20, 2–17X20	16.84	BORAL B	2.92	–	16.8	2.35	0.98894	0.00293
13	1–25X20, 2–17X20	16.84	BORAL C	2.31	–	19.3	2.35	0.99020	0.00294
14	1–25X20, 2–17X20	16.84	BOROFLEX	5.46	–	18.4	2.35	0.99515	0.00284
15	1–25X20, 2–17X20	16.84	BOROFLEX	4.08	–	17.3	2.35	0.99406	0.00293
16	1–25X20, 2–17X20	16.84	CADMIUM	0.61	–	30.4	2.35	0.98568	0.00341
17	1–25X18, 2–20X18	16.84	COPPER	3.37	–	52.4	2.35	0.98636	0.00341
18	1–25X18, 2–20X18	16.84	COPPER–CADMIUM	3.57	–	26.0	2.35	0.99482	0.00295

Table 3.C.5.2 Calculated results and critical experimental data for four cross-arranged rod-clusters in water with various poison-plates

Serial No.	Fuel Clusters	Pitch (mm)	Plate Material	t_p (mm)	X_c (mm)	Y_c (mm)	Critical Size	Calculated Results	
								k_{eff}	$\pm\sigma$
19	1–(18X12+7)	18.92	–	–	0.0	0.0	223	0.99031	0.00320
20	2–(9X12), 1–(3X1), 1–(2X1)	18.92	–	–	28.3	28.3	221	0.99986	0.00346
21	2–(9X12), 2–(9X2+1)	18.92	–	–	47.2	47.2	254	0.99589	0.00353
22	2–(9X12), 1–(9X12), 1–(9X12+1)	18.92	–	–	66.1	66.1	433	0.99516	0.00299
23	1–(9X12+1), 1–(9X12+2)	18.92	–	–	28.3	0.0	219	0.98965	0.00312
24	2–(9X12), 1–(6X1), 1–(4X1)	18.92	–	–	28.3	83.8	225	0.99303	0.00297
25	2–(9X12), 2–(9X1)	18.92	–	–	28.3	108.6	234	0.99495	0.00391
26	2–(9X12), 2–(9X2)	18.92	–	–	28.3	112.9	252	0.99093	0.00336
27	2–(9X12), 2–(9X4)	18.92	–	–	28.3	120.2	288	0.98944	0.00292
28	2–(9X12), 2–(9X8)	18.92	–	–	28.3	136.4	360	0.99599	0.00356
29	2–(9X12), 2–(9X10)	18.92	–	–	28.3	149.8	396	0.98639	0.00357
30	4–(9X12)	18.92	–	–	28.3	198.1	432	0.99896	0.00314
31	2–(9X12), 2–(9X1)	18.92	ALUMINUM	6.25	28.3	85.0	234	0.99232	0.00341
32	2–(9X12), 2–(9X1)	18.92	ALUMINUM	6.25	28.3	90.4	234	0.99193	0.00375
33	2–(9X12), 2–(9X1)	18.92	ZIRCALOY–4	6.52	28.3	110.4	234	1.00146	0.00299
34	2–(9X10), 2–(9X8+5)	18.92	ZIRCALOY–4	6.52	28.3	85.0	334	0.99078	0.00329
35	2–(8X10), 1–(9X9+2), 1–(9X9+3)	18.92	–	–	28.3	85.0	347	0.99977	0.00360
36	2–(9X12), 1–(9X1+6), 1–(9X1+7)	18.92	304L STEEL	3.02	28.3	28.3	247	0.99786	0.00330

Table 3.C.5.2 (continued)

Serial No.	Fuel Clusters	Pitch (mm)	Plate Material	t_p (mm)	X_c (mm)	Y_c (mm)	Critical Size	Calculated Results	
								k_{eff}	$\pm\sigma$
37	2–(9X12), 2–(9X2)	18.92	304L STEEL	3.02	28.3	33.8	252	0.99924	0.00370
38	2–(9X12), 2–(9X3)	18.92	304L STEEL	3.02	28.3	45.4	270	0.99395	0.00380
39	2–(9X12), 2–(9X7)	18.92	304L STEEL	3.02	28.3	64.9	342	0.99024	0.00392
40	2–(9X12), 2–(9X10)	18.92	304L STEEL	3.02	28.3	81.0	396	0.99044	0.00364
41	4–(9X12)	18.92	304L STEEL	3.02	28.3	99.6	432	1.00473	0.00320
42	2–(9X12), 2–(9X13)	18.92	304L STEEL	3.02	28.3	115.5	450	0.98971	0.00323
43	2–(9X12), 2–(9X13+2)	18.92	304L STEEL	3.02	28.3	122.9	454	0.99728	0.00387
44	2–(9X12), 2–(9X3+1)	18.92	304L STEEL	4.85	28.3	28.3	272	1.00229	0.00325
45	2–(9X12), 2–(9X5)	18.92	304L STEEL	4.85	28.3	44.7	306	0.99042	0.00346
46	4–(9X12)	18.92	304L STEEL	4.85	28.3	83.6	432	0.99613	0.00337
47	3–(9X12), 1–(9X2+2), 1–(9X2+3)	18.92	COPPER	3.37	28.3	28.3	257	0.99675	0.00351
48	2–(9X12), 2–(9X7)	18.92	COPPER	3.37	28.3	59.4	342	0.99368	0.00310
49	4–(9X12)	18.92	COPPER	6.46	28.3	90.2	432	0.99169	0.00317
50	2–(9X12), 2–(9X5)	18.92	COPPER	6.46	28.3	26.7	306	0.99520	0.00398
51	2–(9X12), 2–(9X5+2)	18.92	COPPER	6.46	28.3	28.3	310	0.99922	0.00350
52	2–(9X12), 2–(9X6)	18.92	COPPER	6.46	28.3	34.7	324	0.99236	0.00385
53	2–(9X12), 1–(9X8+4), 1–(9X8+3)	18.92	COPPER	6.46	28.3	47.2	367	1.00026	0.00292
54	4–(9X12)	18.92	COPPER	6.46	28.3	71.0	432	0.98935	0.00301
55	2–(9X12), 2–(9X13)	18.92	COPPER	6.46	28.3	81.2	450	0.99433	0.00304
56	2–(9X12), 2–(9X14)	18.92	COPPER	6.46	28.3	102.1	468	0.98845	0.00341
57	2–(11X14), 1–(11X15), 1–(11X15+1)	18.92	BORAL–A	7.13	28.3	28.3	639	0.99910	0.00309
58	2–(11X14), 2–(11X16)	18.92	BORAL–A	7.13	28.3	48.0	660	0.99289	0.00337
59	2–(11X14), 1–(11X16+7), 1–(11X16+8)	18.92	BORAL–A	7.13	28.3	85.0	675	0.99617	0.00296
60	2–(11X14), 2–(11X16+10)	18.92	BORAL–A	7.13	28.3	103.9	680	0.98829	0.00347
61	2–(11X14), 2–(11X13+5)	18.92	BORAL–B	2.92	28.3	28.3	604	0.99291	0.00343
62	4–(11X14)	18.92	BORAL–B	2.92	28.3	31.7	616	1.00013	0.00371
63	2–(11X14), 2–(11X14+9)	18.92	BORAL–B	2.92	28.3	47.2	634	0.98486	0.00338
64	2–(11X14), 2–(11X15)	18.92	BORAL–B	2.92	28.3	52.4	638	1.00120	0.00290
65	2–(11X14), 2–(11X16)	18.92	BORAL–B	2.92	28.3	85.0	660	0.99179	0.00357
66	2–(11X14), 2–(11X13+6)	18.92	BORAL–C	2.31	28.3	28.3	606	0.99689	0.00376
67	4–(11X14)	18.92	BORAL–C	2.31	28.3	35.3	616	1.00034	0.00338
68	2–(11X14), 2–(11X16+1)	18.92	BORAL–C	2.31	28.3	85.0	662	0.99838	0.00319
69	2–(11X14), 1–(11X13+3), 1–(11X13+4)	18.92	BOROFLEX	5.46	28.3	28.3	601	1.00044	0.00330
70	4–(11X14)	18.92	BOROFLEX	5.46	28.3	36.0	616	0.99672	0.00355
71	2–(11X14), 2–(11X14+9)	18.92	BOROFLEX	5.46	28.3	47.2	634	0.99910	0.00337
72	2–(11X14), 1–(11X16+1), 1–(11X16+2)	18.92	BOROFLEX	5.46	28.3	85.0	663	0.99530	0.00306
73	2–(11X14), 2–(11X13+2)	18.92	BOROFLEX	4.08	28.3	28.3	598	0.99623	0.00332
74	2–(11X14), 1–(11X14+7), 1–(11X14+8)	18.92	BOROFLEX	4.08	28.3	47.2	631	1.00086	0.00388
75	2–(11X14), 1–(11X15+6), 1–(11X15+7)	18.92	BOROFLEX	4.08	28.3	66.1	651	1.00011	0.00339
76	2–(11X14), 1–(11X15+2), 1–(11X15+3)	18.92	BOROFLEX	7.72	28.3	28.3	643	0.99458	0.00312
77	2–(11X14), 2–(11X16)	18.92	BOROFLEX	7.72	28.3	49.4	660	0.99673	0.00408
78	2–(11X14), 2–(11X16+6)	18.92	BOROFLEX	7.72	28.3	66.1	672	0.99210	0.00340

Table 3.C.5.2 (continued)

Serial No.	Fuel Clusters	Pitch (mm)	Plate Material	t_p (mm)	X_c (mm)	Y_c (mm)	Critical Size	Calculated Results	
								k_{eff}	$\pm\sigma$
79	2–(11X14), 1–(11X15+2), 1–(11X15+3)	18.92	BOROFLEX	6.34	28.3	28.3	643	0.99773	0.00298
80	2–(11X14), 2–(11X16+5)	18.92	BOROFLEX	6.34	28.3	66.1	670	0.99250	0.00395
81	2–(11X14), 2–(11X16+8)	18.92	BOROFLEX	6.34	28.3	85.0	676	0.99455	0.00289
82	2–(11X14), 1–(11X9), 1–(11X8+10)	18.92	CADMIUM	0.61	28.3	28.3	505	0.99433	0.00312
83	2–(11X14), 2–(11X13)	18.92	CADMIUM	0.61	28.3	53.0	594	0.99363	0.00333
84	4–(11X14)	18.92	CADMIUM	0.61	28.3	64.3	616	0.99646	0.00321
85	1–(34X17+17)	16.84	–	–	0.0	0.0	595	0.99819	0.00348
86	2–(17X17), 2–(11X1)	16.84	–	–	25.9	25.9	600	1.00270	0.00263
87	1–(17X17+5), 1–(17X17+4)	16.84	–	–	16.8	0.0	587	0.99014	0.00330
88	2–(17X17), 1–(17X3+15), 1–(17X3+14)	16.84	–	–	42.7	42.7	709	0.99500	0.00325
89	2–(17X17), 2–(17X15+2)	16.84	–	–	59.5	59.5	1,092	0.99790	0.00284
90	2–(17X17), 2–(17X1)	16.84	–	–	25.9	51.1	612	0.99564	0.00288
91	2–(17X17), 2–(17X2)	16.84	–	–	25.9	66.6	646	0.99565	0.00259
92	2–(17X17), 2–(17X4)	16.84	–	–	25.9	75.3	714	0.99117	0.00299
93	2–(17X17), 2–(17X9)	16.84	–	–	25.9	90.0	884	0.99232	0.00312
94	2–(17X17), 2–(17X12)	16.84	–	–	25.9	99.7	986	0.99346	0.00281
95	2–(17X17), 2–(17X15)	16.84	–	–	25.9	114.5	1,088	0.99438	0.00301
96	4–(17X17)	16.84	–	–	25.9	138.7	1,156	0.99544	0.00336
97	2–(17X17), 1–(12X1), 1–(13X1)	16.84	ALUMINUM	6.25	25.9	25.9	603	0.99568	0.00328
98	2–(17X17), 2–(10X1)	16.84	ZIRCALOY–4	6.52	25.9	25.9	598	0.99742	0.00294
99	2–(17X17), 1–(17X3+13), 1–(17X3+14)	16.84	304L STEEL	3.02	25.9	25.9	707	0.99585	0.00289
100	2–(17X17), 2–(17X11+11)	16.84	304L STEEL	3.02	25.9	59.5	974	0.99284	0.00299
101	2–(17X17), 2–(17X15+15)	16.84	304L STEEL	3.02	25.9	76.4	1,118	0.99424	0.00299
102	2–(17X17), 2–(17X17+16)	16.84	304L STEEL	3.02	25.9	93.2	1,188	0.99936	0.00362
103	2–(17X17), 1–(17X5+15), 1–(17X5+14)	16.84	304L STEEL	4.85	25.9	25.9	777	0.99616	0.00371
104	2–(17X17), 2–(17X9+7)	16.84	304L STEEL	4.85	25.9	42.7	898	0.99407	0.00295
105	2–(17X17), 1–(17X19), 1–(17X18+16)	16.84	304L STEEL	4.85	25.9	93.2	1,223	0.99682	0.00334
106	2–(17X17), 1–(17X5), 1–(17X4+16)	16.84	COPPER	3.37	25.9	25.9	747	0.99457	0.00315
107	2–(17X17), 1–(17X8+5), 1–(17X8+6)	16.84	COPPER	3.37	25.9	42.7	861	0.99045	0.00322
108	3–(17X17), 1–(17X16+16)	16.84	COPPER	3.37	25.9	76.4	1,155	0.99111	0.00361
109	2–(17X17), 1–(17X8+8), 1–(17X8+9)	16.84	COPPER	6.46	25.9	25.9	867	0.99411	0.00299
110	2–(17X17), 2–(17X16+10)	16.84	COPPER	6.46	25.9	59.5	1,142	0.99436	0.00339

Table 3.C.6.1 Calculated results and critical experimental data for three aligned UO_2 rod clusters in water with side reflectors

Serial No.	Fuel Cluster	Reflector Material	Pitch (mm)	Enrichment (wt %)	Distance Y (mm)	Distance X_c (mm)	500 neutrons/gen.	
							k_{eff}	$\pm\sigma$
1	1·23×18, 2·20×18	Uranium	16.84	2.35	0.0	80.6	0.98039	0.00292
2	1·23×28, 2·20×18	Uranium	16.84	2.35	13.21	95.0	0.98954	0.00294
3	1·23×28, 2·20×18	Uranium	16.84	2.35	26.16	98.3	0.99070	0.00278
4	1·23×28, 2·20×18	Uranium	16.84	2.35	39.12	91.9	0.99454	0.00291
5	1·23×18, 2·20×18	Lead	16.84	2.35	0.0	100.6	0.98930	0.00310
6	1·23×18, 2·20×18	Lead	16.84	2.35	6.60	101.1	0.98928	0.00342
7	1·23×18, 2·20×18	Lead	16.84	2.35	32.76	85.0	0.99376	0.00312
8	1·23×18, 2·20×18	Lead	16.84	2.35	∞	65.9	0.98444	0.00295
9	1·23×18, 2·20×18	Lead	16.84	2.35	∞	72.2	0.98274	0.00320
10	3·12×16	Uranium	18.92	4.31	0.0	153.3	0.98676	0.00292
11	3·12×16	Uranium	18.92	4.31	6.60	167.1	0.98918	0.00338
12	3·12×16	Uranium	18.92	4.31	13.21	182.7	0.99466	0.00348
13	3·12×16	Uranium	18.92	4.31	19.56	192.4	0.98730	0.00350
14	3·12×16	Uranium	18.92	4.31	26.16	193.7	0.98936	0.00318
15	3·12×16	Uranium	18.92	4.31	32.76	187.8	0.99898	0.00323
16	3·12×16	Uranium	18.92	4.31	54.05	164.0	0.99046	0.00367
17	3·12×16	Uranium	18.92	4.31	∞	123.5	0.99252	0.00343
18	3·12×16	Lead	18.92	4.31	0.0	177.4	0.98862	0.00339
19	3·12×16	Lead	18.92	4.31	6.60	181.8	0.99083	0.00338
20	3·12×16	Lead	18.92	4.31	19.56	174.3	0.99372	0.00304
21	3·12×16	Lead	18.92	4.31	54.05	143.5	0.99016	0.00322
22	3·12×16	Lead	18.92	4.31	∞	129.7	0.98013	0.00348

Table 3.C.7.1 Calculated results and critical experimental data for three UO_2 rod clusters in water with absorbers and reflecting walls

Serial No.	Fuel Clusters	Pitch (mm)	Plate Material	t_p (mm)	G (mm)	X_c (mm)	Y (mm)	k_{eff}	$\pm\sigma$
1	3–19X16	20.32	–	–	–	106.5	0.0	0.98658	0.00286
2	3–19X16	20.32	–	–	–	112.0	6.60	0.99139	0.00303
3	3–19X16	20.32	–	–	–	112.0	13.21	0.98965	0.00275
4	3–19X16	20.32	–	–	–	103.6	26.16	0.98721	0.00300
5	3–19X16	10.32	–	–	–	95.1	39.12	0.99097	0.00302
6	3–19X16	20.32	–	–	–	83.1	∞	0.98323	0.00296
7	3–19X16	20.32	–	–	–	82.3	∞	0.97993	0.00290
8	1–25X18, 2–20X18	16.84	–	–	–	89.8	0.0	0.99531	0.00287
9	1–25X18, 2–20X18	16.84	–	–	–	95.8	6.60	0.99609	0.00307
10	1–25X18, 2–20X18	16.84	–	–	–	95.1	13.21	0.99524	0.00353
11	1–25X18, 2–20X18	16.84	–	–	–	96.6	16.84	0.99509	0.00306
12	1–25X18, 2–20X18	16.84	–	–	–	92.8	23.44	0.98976	0.00310
13	1–25X18, 2–20X18	16.84	–	–	–	90.6	30.05	0.99570	0.00280
14	1–25X18, 2–20X18	16.84	–	–	–	85.4	39.12	0.99078	0.00326
15	1–25X18, 2–20X18	16.84	–	–	–	76.7	67.26	0.98555	0.00288
16	1–25X28, 2–20X18	16.84	–	–	–	72.4	∞	0.98809	0.00314
17	1–25X18, 2–20X18	16.84	–	–	–	71.9	∞	0.98374	0.00327
18	1–25X18, 2–20X18	16.84	–	–	–	95.1	13.21	0.99524	0.00353
19	1–25X18, 2–20X18	16.84	304L STEEL	3.02	0.0	82.8	13.21	0.99107	0.00303
20	1–25X18, 2–20X18	16.84	304L STEEL, 1.1 wt% B	2.98	0.0	48.0	13.21	0.98961	0.00318
21	1–25X18, 2–20X18	16.84	BORAL B	2.92	0.0	26.9	13.21	0.98916	0.00308
22	1–25X18, 2–20X18	16.84	BOROFLEX	5.46	0.0	29.8	13.21	0.99575	0.00291
23	1–25X18, 2–20X18	16.84	CADMIUM	0.61	0.0	38.6	13.21	0.99094	0.00322
24	1–25X18, 2–20X18	16.84	COPPER	3.37	0.0	77.9	13.21	0.98696	0.00297
25	1–25X18, 2–20X18	16.84	COPPER–CADMIUM	3.57	0.0	54.3	13.21	0.98634	0.00302
26	3–13X8	25.40	–	–	–	128.9	0.0	0.99502	0.00370
27	3–13X8	25.40	–	–	–	142.5	6.60	0.99130	0.00356
28	3–13X8	25.40	–	–	–	141.2	13.21	0.99103	0.00339
29	3–13X8	25.40	–	–	–	124.4	26.16	0.98769	0.00342
30	3–13X8	25.40	–	–	–	98.0	54.05	0.98502	0.00316
31	3–13X8	25.40	–	–	–	82.3	∞	0.98269	0.00303
32	3–13X8	25.40	–	–	–	82.4	∞	0.98870	0.00364
33	3–12X16	18.92	–	–	–	148.7	0.0	0.99304	0.00359
34	3–12X16	18.92	–	–	–	157.4	6.60	0.99105	0.00276
35	3–12X16	18.92	–	–	–	158.7	13.21	0.99709	0.00332
36	3–12X16	18.92	–	–	–	158.4	19.56	0.99549	0.00345
37	3–12X16	18.92	–	–	–	154.5	26.16	1.00108	0.00321
38	3–12X16	18.92	–	–	–	138.2	54.05	0.99802	0.00350
39	3–12X16	18.92	–	–	–	129.6	∞	0.99537	0.00342
40	3–12X16	18.92	–	–	–	129.8	∞	0.99088	0.00349
41	3–12X16	18.92	–	–	–	127.5	∞	0.99050	0.00381
42	3–12X16	18.92	–	–	–	158.4	19.56	0.99549	0.00345
43	3–12X16	18.92	304L STEEL	3.02	0.0	137.5	19.56	0.99255	0.00317
44	3–12X16	18.92	304L STEEL, 1.1 wt% B	2.98	0.0	98.3	19.56	0.98899	0.00353
45	3–12X16	18.92	BORAL B	2.92	0.0	83.0	19.56	0.99635	0.00302
46	3–12X16	18.92	BOROFLEX	5.46	0.0	83.7	19.56	0.99275	0.00328
47	3–12X16	18.92	CADMIUM	0.61	0.0	89.4	19.56	0.99705	0.00332
48	3–12X16	18.92	COPPER	3.37	0.0	134.7	19.56	0.98733	0.00367
49	3–12X16	18.92	COPPER–CADMIUM	3.57	0.0	105.7	19.56	0.99261	0.00362

Table 3.C.8.1 Summary of characteristics of heterogeneous plutonium benchmark experiments

No.	H/Pu atom ratio	$\%^{240}Pu$	Core radius, cm	Fuel type
16	632	6	23.3	Aℓ-1.8 wt% Pu
17	1003	6	25.0	Aℓ-1.8 wt% Pu
18	1333	6	29.4	Aℓ-1.8 wt% Pu
19	583	16	29.3	Aℓ-2 wt% Pu
20	926	16	32.6	Aℓ-2 wt% Pu
21	1230	16	41.4	Aℓ-2 wt% Pu
22	355	5	16.8	Aℓ-5 wt% Pu
23	666	5	18.1	Aℓ-5 wt% Pu
24	1148	5	25.4	Aℓ-5 wt% Pu
25*	666	5	20.2	Aℓ-5 wt% Pu
26*	666	5	23.8	Aℓ-5 wt% Pu
27	238	8	19.1	UO_2-2 wt% PuO_2
28	554	8	17.3	UO_2-2 wt% PuO_2
29	1113	8	24.3	UO_2-2 wt% PuO_2
30	185	8	27.7	UO_2-2 wt% PuO_2
31*	185	8	27.7	UO_2-2 wt% PuO_2
32	391	8	17.4	UO_2-2 wt% PuO_2
33*	391	8	34.4	UO_2-2 wt% PuO_2
34	564	8	17.9	UO_2-2 wt% PuO_2
35*	564	8	37.2	UO_2-2 wt% PuO_2
36	238	24	24.3	UO_2-2 wt% PuO_2
37	554	24	21.4	UO_2-2 wt% PuO_2
38	1113	24	35.3	UO_2-2 wt% PuO_2
39	153	18	18.0	UO_2-4 wt% PuO_2
40	289	18	16.5	UO_2-4 wt% PuO_2
41	922	18	37.4	UO_2-4 wt% PuO_2

* With boron in the moderator

Table 3.C.8.2 Calculated results for heterogeneous plutonium benchmark experiments

No.	Fuel type	H / Pu atom ratio (boron PPM)	% ^{240}Pu	Core radius cm	Calculated k_{eff}
16	Aℓ-1.8wt%Pu	632	6	23.3	0.9993 ± 0.0040
17	〃	1003	〃	25.0	0.9852 ± 0.0041
18	〃	1333	〃	29.4	1.0047 ± 0.0039
19	Aℓ-2wt% Pu	583	16	29.3	1.0102 ± 0.0044
20	〃	926	〃	32.6	1.0110 ± 0.0034
21	〃	1230	〃	41.4	1.0228 ± 0.0035
22	Aℓ-5wt%Pu	355	5	16.8	0.9976 ± 0.0052
23	〃	666	〃	18.1	1.0001 ± 0.0043
24	〃	1148	〃	25.4	1.0039 ± 0.0048
25	〃	666(100)	〃	20.2	1.0032 ± 0.0048
26	〃	666(285)	〃	23.8	0.9964 ± 0.0046
27	UO_2-2wt%PuO_2	238	8	19.1	0.9954 ± 0.0045
28	〃	554	〃	17.3	0.9913 ± 0.0041
29	〃	1113	〃	24.8	1.0256 ± 0.0038
36	〃	238	24	24.3	0.9936 ± 0.0042
37	〃	554	〃	21.4	1.0035 ± 0.0042
38	〃	1113	〃	35.3	1.0064 ± 0.0036
39	UO_2-4wt%PuO_2	153	18	18.0	1.0104 ± 0.0046
40	〃	289	〃	16.5	1.0058 ± 0.0049
41	〃	522	〃	37.4	1.0115 ± 0.0036
				Average	1.0039

Table 3.C.9.1 Principal critical parameters and calculated results

No.	Fuel type	Pitch (mm)	Critical number of rods	Boron concentration (wppm)	Calculated k_{eff}
1	UO_2 - 2.35% ^{235}U	1.5621	708	0.9	0.9910±0.0043
2	〃	1.5621	1201	463.8	1.0039±0.0037
3	〃	1.905	383	0.5	0.9911±0.0043
4	〃	1.905	1201	568.0	0.9831±0.0035
5	〃	2.2098	342	0.9	0.9921±0.0041
6	〃	2.2098	885	285.8	0.9963±0.0033
7	UO_2 - 2 w/o PuO_2 (8% ^{240}Pu)	1.778	469	1.7	1.0051±0.0047
8	〃	1.778	761	680.9	1.0066±0.0042
9	〃	2.2098	195	0.9	0.9947±0.0048
10	〃	2.2098	761	1090.4	1.0222±0.0033
11	〃	2.5146	160	1.6	0.9999±0.0039
12	〃	2.5146	689	767.2	1.0147±0.0034
				Average	1.000

Table 3.C.10.1 Measured and calculated k_{eff} values

Core No.	Measured values	Calculated values	C/E
1	1.0002±0.0005	0.9898±0.0039	0.9896
2	1.0001±0.0005	1.0148±0.0036	1.0147
3	1.0000±0.0006	1.0158±0.0035	1.0158
4	0.9999±0.0006	0.9979±0.0040	0.9980
5	1.0000±0.0007	0.9958±0.0041	0.9958
6	1.0097±0.0012	1.0056±0.0038	0.9959
7	0.9998±0.0009	0.9935±0.0040	0.9937
8	1.0083±0.0012	1.0046±0.0038	0.9963
9	1.0030±0.0009	1.0024±0.0043	0.9994
10	1.0001±0.0009	1.0100±0.0039	1.0099
11	1.0000±0.0006	1.0120±0.0037	1.0120
12	1.0000±0.0007	0.9935±0.0042	0.9915
13	1.0000±0.0010	0.9962±0.0045	0.9962
14	1.0001±0.0010	0.9984±0.0038	0.9983
15	0.9998±0.0016	1.0056±0.0042	1.0058
16	1.0001±0.0019	0.9951±0.0037	0.9950
17	1.0000±0.0010	1.0034±0.0035	1.0034
18	1.0002±0.0011	1.0064±0.0035	1.0062
19	1.0002±0.0010	1.0075±0.0037	1.0073
20	1.0003±0.0011	1.0089±0.0034	1.0086
21	0.9997±0.0015	1.0065±0.0034	1.0068
Average	1.001	1.003	

Table 3.C.10.2 Comparison of the group averaged k_{eff}'s for different spacings between assemblies

Spacing between assemblies (cm)	Core No.	Moderator boron Concentration (ppm)	Measured k_{eff}	Calculated k_{eff}
None	1	0	1.0002 ± 0.0005	0.9898 ± 0.0039
	2	1037	1.0001 ± 0.0005	1.0148 ± 0.0036
Average k_{eff}			1.0002	1.0023
1.636 (1 pitch)	3	764	1.0000 ± 0.0006	1.0158 ± 0.0035
	4	0	0.9999 ± 0.0006	0.9979 ± 0.0040
	11	514	1.0000 ± 0.0006	1.0120 ± 0.0037
	13	15	1.0000 ± 0.0010	0.9962 ± 0.0045
	14	92	1.0001 ± 0.0010	0.9984 ± 0.0038
	15	395	0.9998 ± 0.0016	1.0056 ± 0.0042
	17	487	1.0000 ± 0.0010	1.0034 ± 0.0035
	19	634	1.0002 ± 0.0010	1.0075 ± 0.0037
Average k_{eff}			1.0000	1.0046
3.272 (2 pitches)	5	0	1.0000 ± 0.0007	0.9958 ± 0.0041
	6	0	1.0097 ± 0.0012	1.0056 ± 0.0038
	12	217	1.0000 ± 0.0007	0.9935 ± 0.0042
	16	121	1.0001 ± 0.0019	0.9951 ± 0.0037
	18	197	1.0002 ± 0.0011	1.0064 ± 0.0035
	20	320	1.0003 ± 0.0011	1.0089 ± 0.0034
Average k_{eff}			1.0017	1.0009
4.908 (3 pitches)	7	0	0.9998 ± 0.0009	0.9935 ± 0.0040
	8	0	1.0083 ± 0.0012	1.0046 ± 0.0038
	10	143	1.0001 ± 0.0009	1.0100 ± 0.0039
	21	72	0.9997 ± 0.0015	1.0065 ± 0.0034
Average k_{eff}			1.0020	1.0037
6.544 (4 pitches)	9	0	1.0030 ± 0.0009	1.0024 ± 0.0043

Table 3.C.11.1 Principal critical parameters and calculated k_{eff}

No.	Number of pins	Center separation (cm)	Critical water height above fuel (cm)	Calculated k_{eff}
NUSW001	380	1.054	15.2	——
NUSW002	222	1.242	15.2	0.9556±0.0045
NUSW003	138	1.488	30.8	0.9514±0.0047
NUSW004	102	1.742	−21.3	0.9526±0.0054
NUSW005	85	1.999	15.2	0.9593±0.0053
NUSW006	78	2.276	15.2	0.9637±0.0050
NUSW007	77	2.253	− 3.9	0.9718±0.0045
NUSW008	75	2.507	15.2	0.9682±0.0050
NUSW009	77	2.779	−43.2	0.9799±0.0044
NUSW010	83	2.995	−34.1	0.9859±0.0040
NUSW011	96	2.497	−10.4	0.9615±0.0047
NUSW012	75	1.250	−12.2	——
			Average	0.9650

Table 3.C.11.2 Principal critical parameters and calculated k_{eff}'s

No.	Number of pins	Solution characteristic		Calculated k_{eff}
		B (%)	^{235}U (%)	
NUSS001	99	—	—	0.9760±0.0046
NUSS002	114	0.039	—	0.9674±0.0050
NUSS003	113	0.039	—	0.9807±0.0049
NUSS004	133	0.190	—	0.9774±0.0048
NUSS005	83	—	3.68	0.9776±0.0039
NUSS006	133	0.315	3.68	0.9794±0.0042
			Average	0.9764

Table 3.C.12.1 Critical experimental data for UO_2 rod clusters fully immersed in borated water

No.	Square Pitch (cm)	Boron[(a)] Concentration g/ℓ	Critical Array Width No. of Rods	Critical[(b)(c)] Array Length No. of Rods	Total Rods[(d)] for Criticality
1	1.890	0.0	40	8.92	357
2	1.890	0.49 ± 0.06	40	10.72	429
3	1.890	1.25 ± 0.21	40	14.05	562
4	1.890	2.15 ± 0.35	40	23.07	923
5	1.890	2.55 ± 0.07	40	30.92	1237
6	1.715	0.0	44	11.57	509
7	1.715	1.03 ± 0.05	44	16.75	737
8	1.715	1.82 ± 0.30	44	20.84	917
9	1.715	2.55 ± 0.21	44	27.09	1192

(a) Boron added in the form of H_3BO_3.

(b) This has the same interpretation as all experiments performed before in this program. A fraction of a row is a row which extends full width but is thinner in length. This is the best interpretation for computer modeling.

(c) The cell boundary of the first fuel row is next to the plexiglas wall of the box.

(d) The error in critical rod number is <0.5%.

Table 3.C.12.2 Calculated k_{eff}'s with different Monte Carlo calculational conditions

ケース NO.	500n/b		1000n/b	
	k_{eff}	±σ	k_{eff}	±σ
1-01	0.99158	0.00323	0.99361	0.00202
1-02	0.95701	0.00331	0.96186	0.00247
1-03	0.94702	0.00301	0.94811	0.00212
1-04	0.97890	0.00280	0.97504	0.00215
1-05	0.98931	0.00287	0.98485	0.00197
1-06	0.99780	0.00371	0.99799	0.00248
1-07	0.98254	0.00324	0.98309	0.00223
1-08	0.98874	0.00298	0.97800	0.00211
1-09	0.98341	0.00275	0.98428	0.00192

Table 3.C.13.1 Calculated results for UO_2 fuel rods in $NaNO_3$ solution

No	Lattice			Solution Data				Calculation	
	Square Pitch (mm)	Configuration	Total Number of Rods	Density (g/cm^3)	Concentration $NaNO_3$ (g/cm^3)	Normality NO_3^- ± 2%	Critical Height (cm ± 0.1)	k_{eff}	σ
1	12.6	24 × 25	600	1.1521	0.247	2.91	80.9	0.99293	0.00352
2	16	18 × 18	324	1.1503	0.243	2.86	76.1	0.99475	0.00327
3		17 × 17	289	1.1523	0.246	2.89	76.2	0.95977	0.00349
4	21.0	16 × 16	256	1.1094	0.178	2.10	89.5	0.98743	0.00348
5		15 × 16	240	1.0565	0.090	1.06	84.8	0.99616	0.00324
6	25.2	20 × 21	420	1.1523	0.246	2.89	85.9	0.98815	0.00308

Table 3.C.14.1 Calculated results with experimental conditions for each case of triangular lattices in poisonous water

Case No.	Triangular Lattice Pitch (mm)	Number of Fuel Rods Required for Criticality	Neutron Absorber Concentration (g/ℓ)	Total NO_3 (g/ℓ)	Excess Acid Molarity M	Calculated Results	
						k_{eff}	σ
1	22.86	223.3	0	---	---	0.95990	0.00339
2	22.86	289.8	0.2307 B	---	---	0.95837	0.00308
3	22.86	363.0	0.4514 B	---	---	0.97193	0.00301
4	22.86	433.2	0.6053 B	---	---	0.97151	0.00309
5	22.86	282.6	0.4293 Cd	0.722	0.004	0.95580	0.00364
6	22.86	391.7	1.060 Cd	1.418	0.004	0.97888	0.00319
7	22.86	283.4	0.0722 Gd	0.230	0.0023	0.95653	0.00348
8	22.86	349.5	0.145 Gd	0.398	0.0036	0.96767	0.00305
9	22.86	422.4	0.213 Gd	0.527	0.0044	0.97949	0.00320
10	27.94	166.6	0	---	---	0.97951	0.00353
11	27.94	225.6	0.158 B	---	---	0.98852	0.00301
12	27.94	349.9	0.380 B	---	---	1.00229	0.00262
13	27.94	232.3	0.0547 Gd	0.1927	0.0021	0.99138	0.00314
14	27.94	341.8	0.1169 Gd	0.2707	0.0021	1.00067	0.00289
15	33.02	187.4	0	---	---	1.01526	0.00308
16	33.02	234.0	0.0643 B	---	---	1.00967	0.00309
17	33.02	434.0	0.2154 B	---	---	1.03261	0.00288
18	33.02	327.5	0.1507 B	---	---	1.01870	0.00318
19	33.02	252.7	0.0257 Gd	0.1571	0.00204	1.01943	0.00290
20	33.02	316.8	0.0440 Gd	0.1805	0.00207	1.02042	0.00303

Table 3.C.15.1 Calculated results with experimental conditions for UO_2 rod clusters partially immersed in uranyl-nitrate solution

Case No.	Number of Fuel Rods	Triangular Lattice Pitch (mm)	Gadolinium Concentration (g/ℓ)	Critical Solution Height (mm)	Calculated Results	
					k_{eff}	σ
1	451	22.86	0	373	0.8962	0.0038
2			0.124	552	0.9191	0.0040
3			0.148	612	0.9197	0.0039
4			0.184	744	0.9323	0.0042
5	443	27.94	0	309	0.9084	0.0040
6			0.074	413	0.9314	0.0038
7			0.099	481	0.9467	0.0040
8			0.124	565	0.9622	0.0040
9	421	33.02	0	333	0.9459	0.0041
10			0.025	388	0.9542	0.0042
11			0.049	460	0.9629	0.0039
12			0.074	577	0.9739	0.0038

Table 3.C.16.1 Calculated results with experimental conditions for mixed-oxide fuel rods in plutonium-uranyl-nitrate solution containing gadolinium and boron

Case No.	Critical Height (cm)	Pu Conc. (g/ℓ)	U Conc. (g/ℓ)	Acid Molarity	Total NO_3 (g/ℓ)	Specific Gravity	Gd (g/ℓ)	B (g/ℓ)	Calculated Result	
									k_{eff}	σ
1	19.205	77.63	180.0	3.4	384.0	1.463	0.02	0	1.0202	0.0050
2	23.066	77.63	180.0	3.4	384.0	1.463	0.258	0	1.0126	0.0041
3	28.227	77.63	180.0	3.4	384.0	1.463	0.515	0	1.0088	0.0040
4	45.753	77.63	180.0	3.4	384.0	1.463	1.040	0	1.0047	0.0039
5	64.506	77.63	180.0	3.4	384.0	1.463	1.280	0	1.0093	0.0033
6	68.862	77.63	180.0	3.4	384.0	1.463	1.338	0	1.0042	0.0036
7	21.20	84.5	182.1	1.75	296	1.438	0.13	0.27	1.0192	0.0044
8	25.37	84.0	183.2	1.88	302	1.442	0.235	0.6	1.0098	0.0039
9	30.49	82.7	180.6	2.01	308	1.444	0.309	0.9	1.0148	0.0041
10	43.86	81.2	180.0	2.18	321	1.447	0.424	1.35	1.0015	0.0034
11	51.97	81.0	180.4	2.09	316	1.451	0.519	1.5	1.0088	0.0030
12	55.18	81.0	180.3	2.21	318	1.452	0.537	1.548	1.0078	0.0030
13	65.42	80.5	180.5	2.24	321	1.454	0.541	1.662	1.0091	0.0031

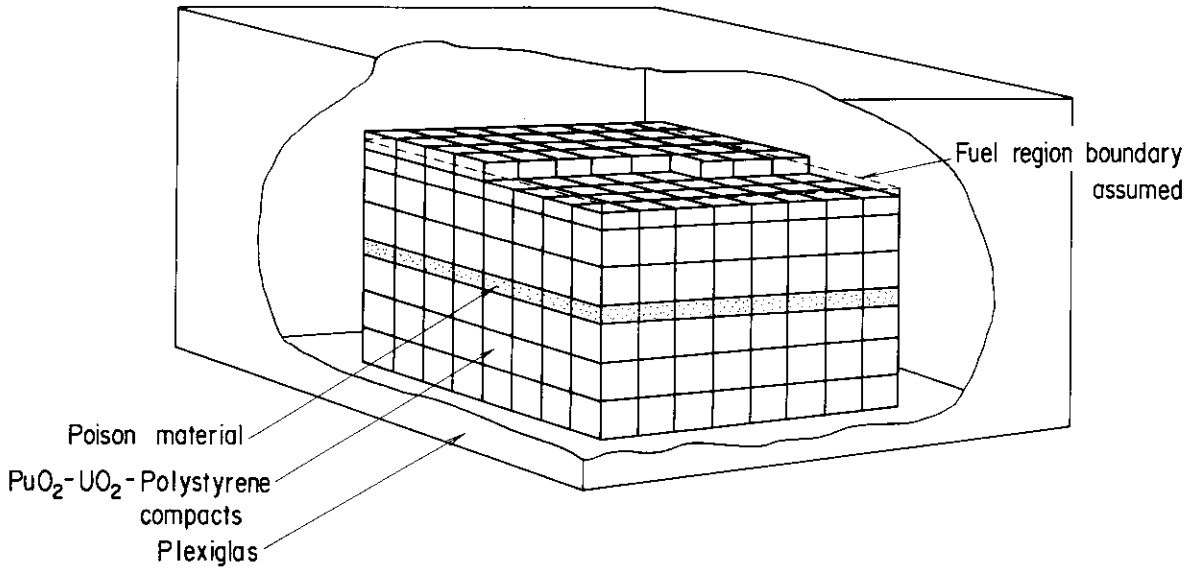

Fig. 3.A.1.1 Configuration of PuO_2-UO_2 polystyrene compacts.

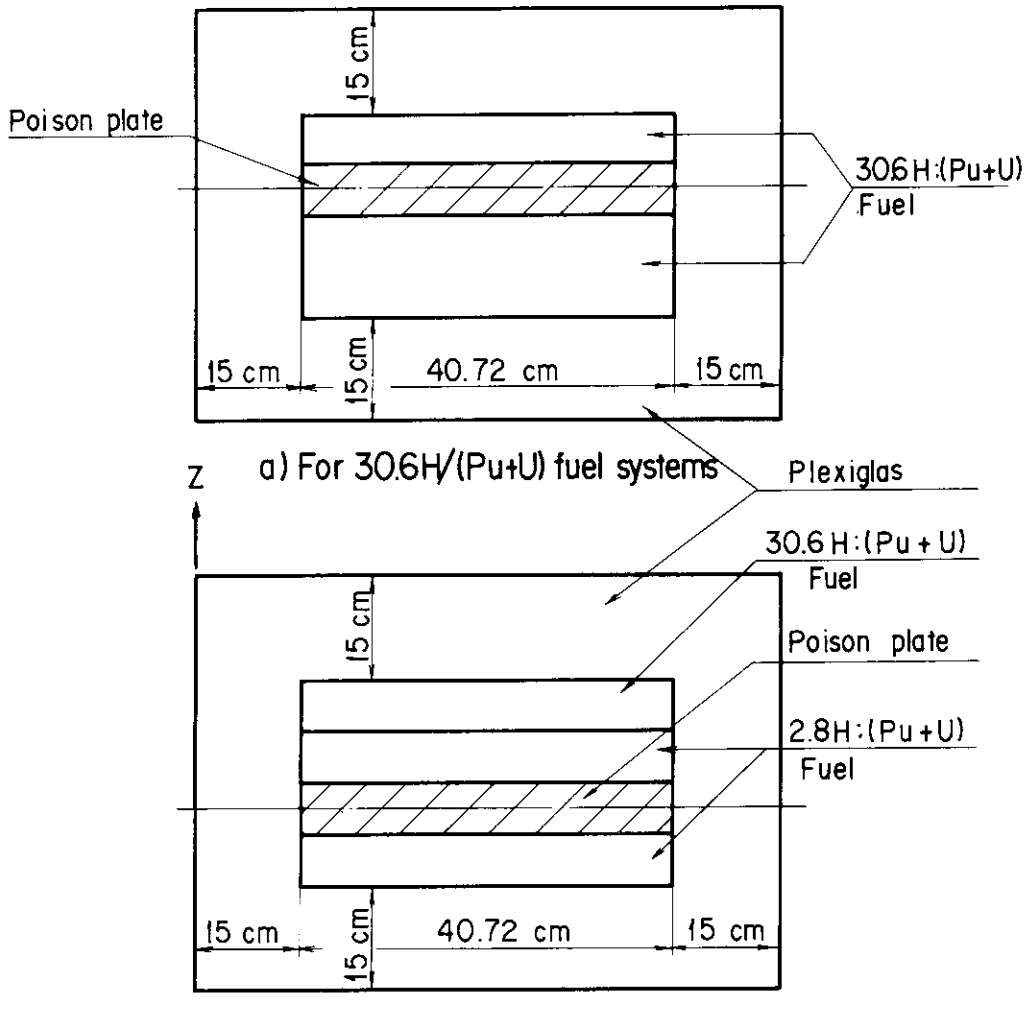

Fig. 3.A.1.2 Calculational model for PuO_2-UO_2 polystyrene compacts.

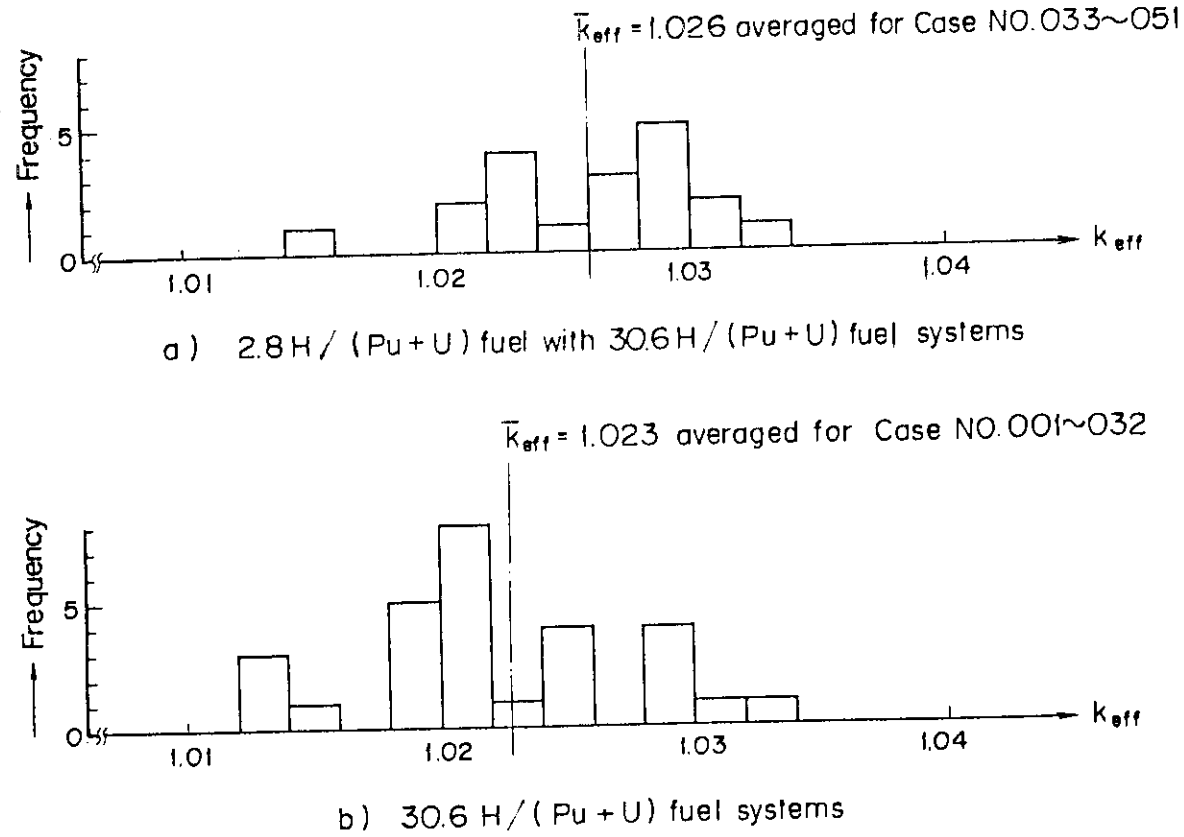

Fig. 3.A.1.3 Histogram of calculated k_{eff}'s for the two different fuel systems.

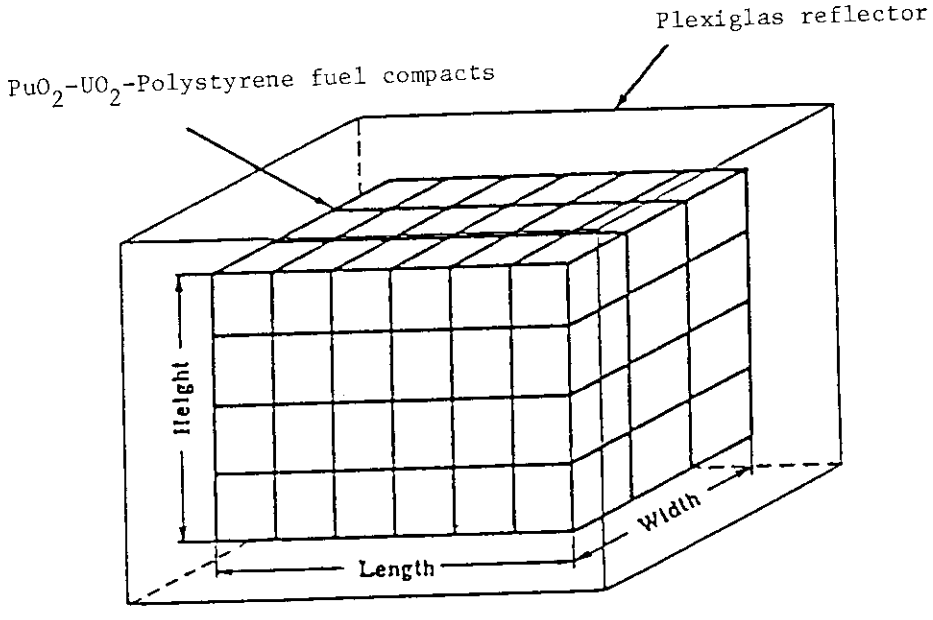

Fig. 3.A.2.1 Calculational model for PuO_2-UO_2 polystyrene fuel compacts.

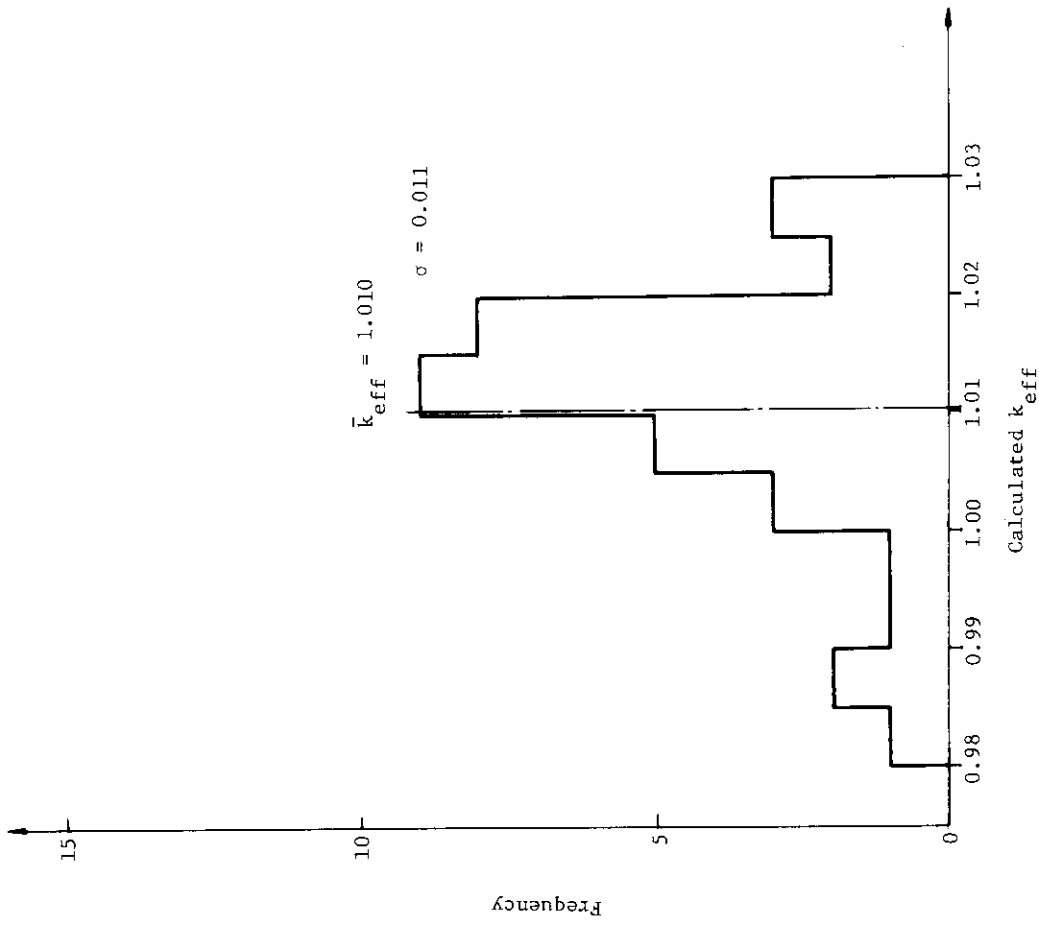

Fig. 3.A.2.3 Histogram of calculated k_{eff}'s for PuO_2-UO_2 polystyrene fuel compacts of high (30–50)H/(Pu+U) atomic ratio (35 cases).

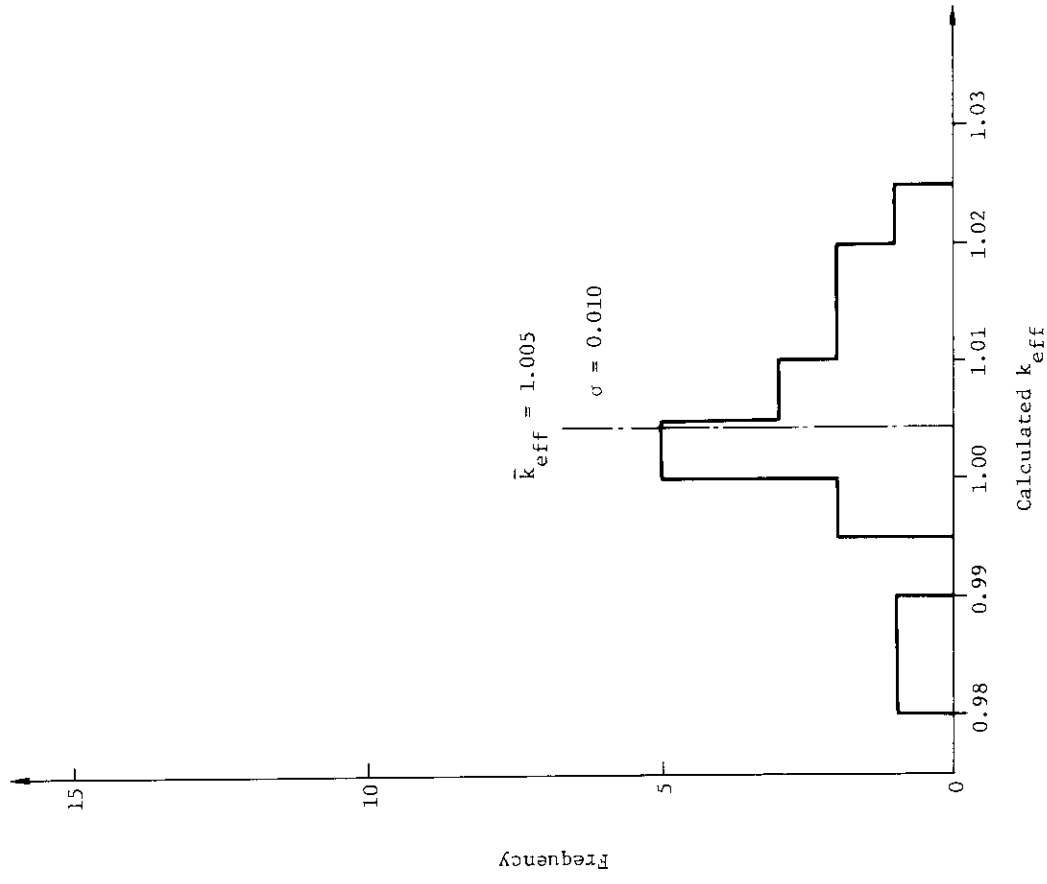

Fig. 3.A.2.2 Histogram of calculated k_{eff}'s for PuO_2-UO_2 polystyrene fuel compacts of low (2–8)H/(Pu+U) atomic ratio (17 cases).

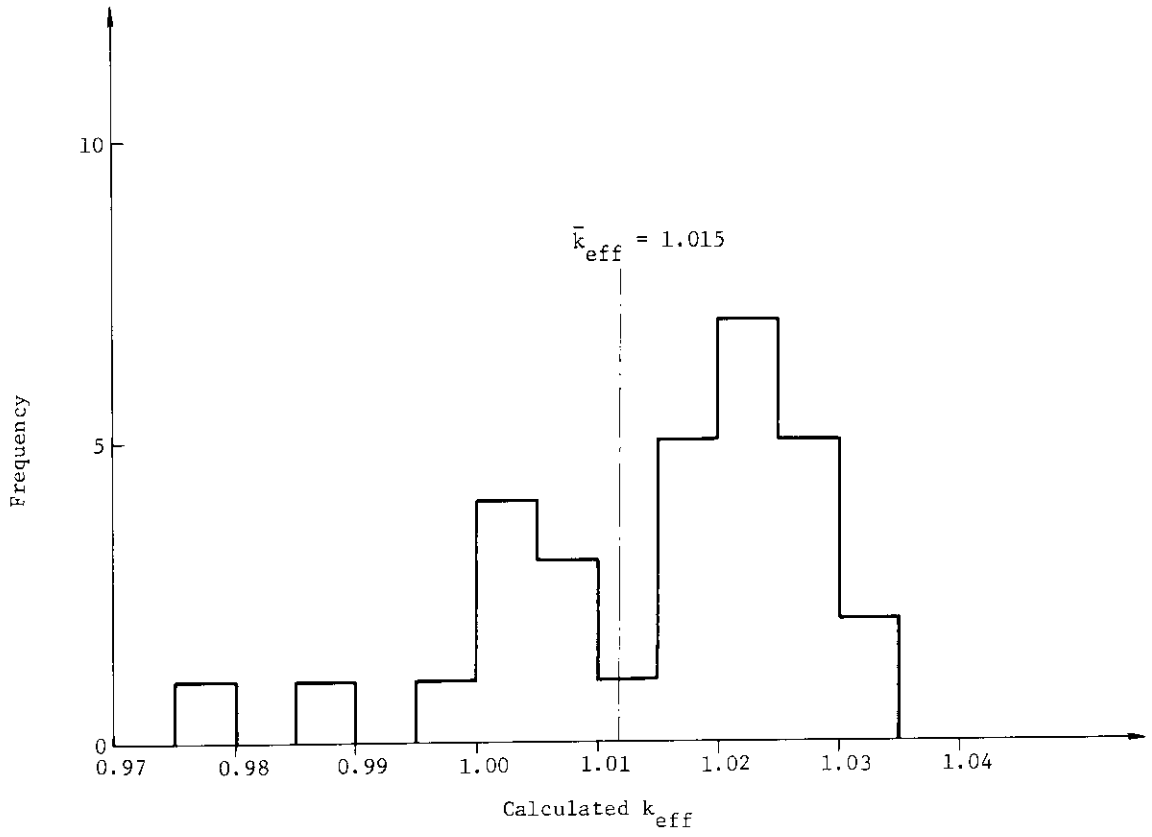

Fig. 3.A.4.1 Histogram of calculated k_{eff}'s for PuO_2 polystyrene fuel compacts.

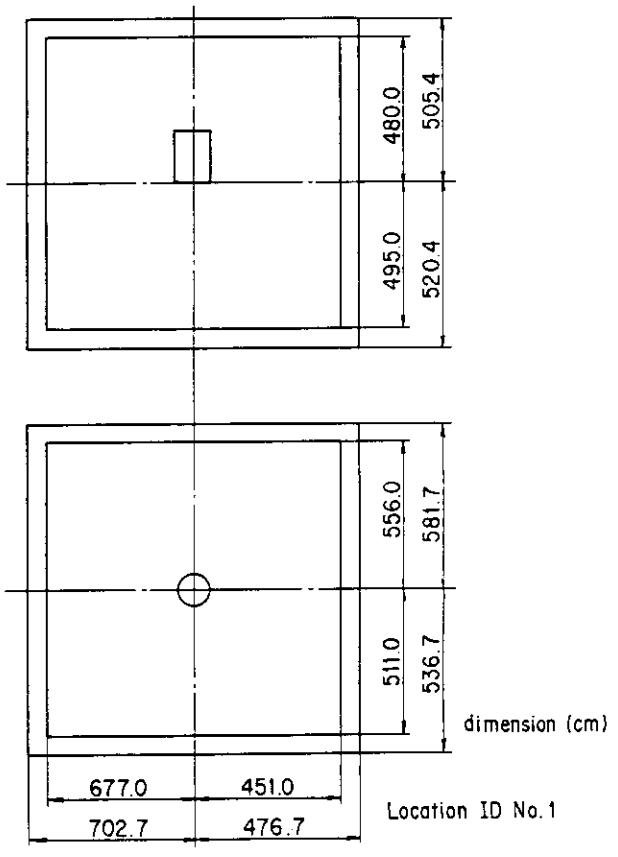

Fig. 3.A.5.1 Calculational model of a reflected single tank.

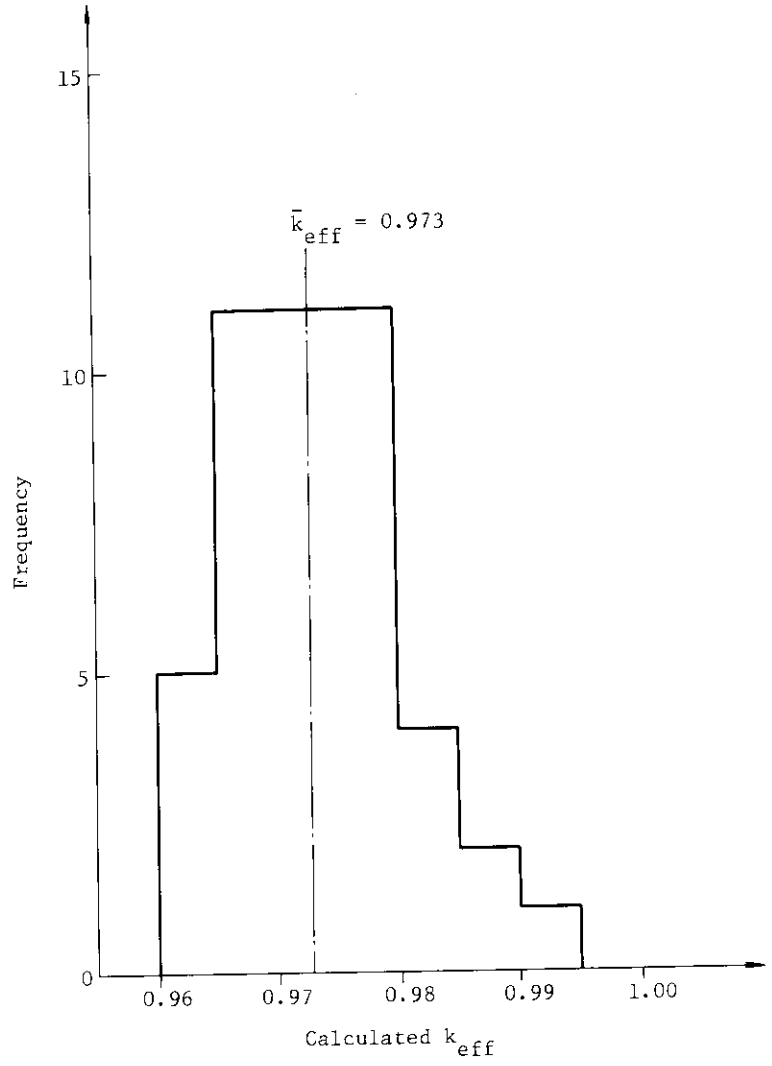

Fig. 3.A.5.2 Histogram of calculated k_{eff}'s for a single tank (45 cases).

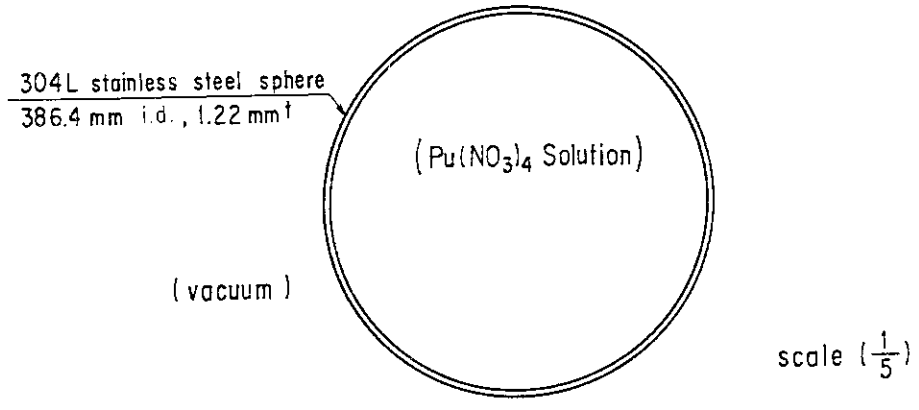

Fig. 3.A.6.1 Calculational model of B.M. No.2.

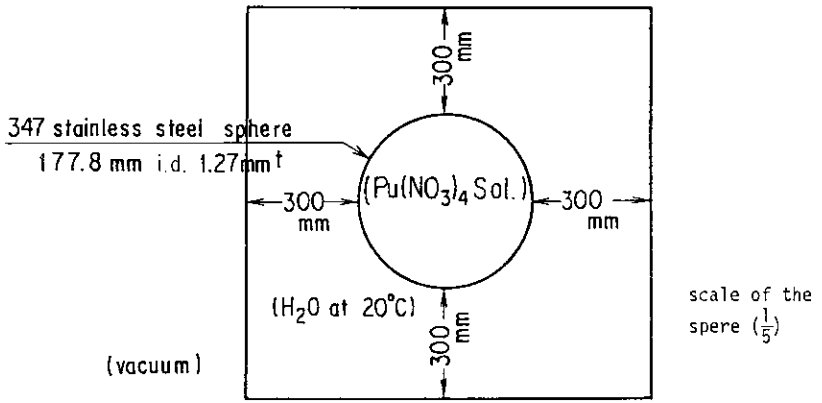

The sphere is at the center of water cubic 300 mm apart from the cubical surface

Fig. 3.A.6.2 Calculational model of B.M. No.3.

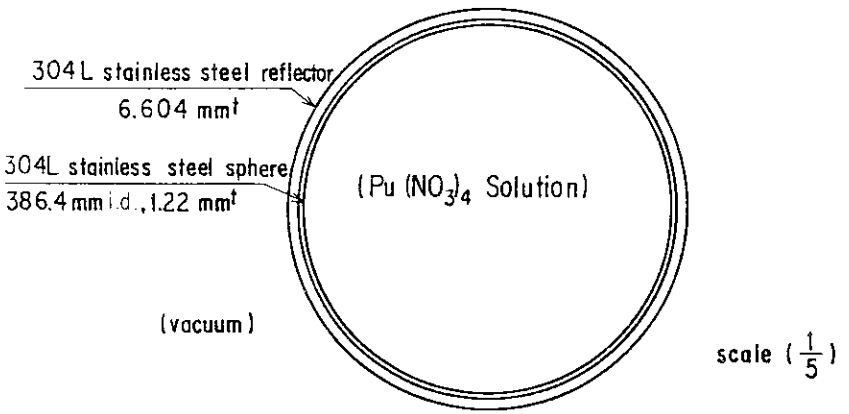

Fig. 3.A.6.3 Calculational model of B.M. No.4.

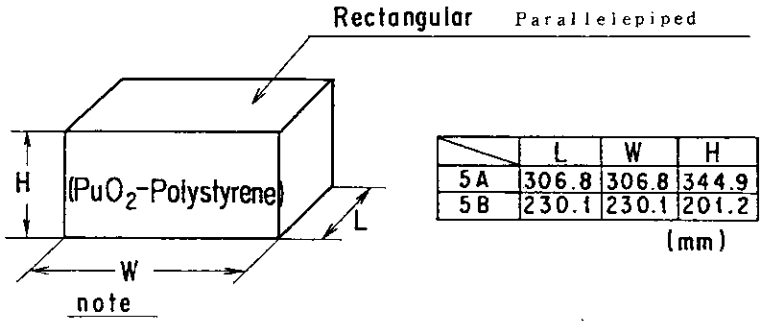

	L	W	H
5A	306.8	306.8	344.9
5B	230.1	230.1	201.2

(mm)

note

Serial No 5A has no reflector
Serial No 5B has 15 cm thick Plexiglas reflector.

Fig. 3.A.6.4 Calculational model of B.M. No.5.

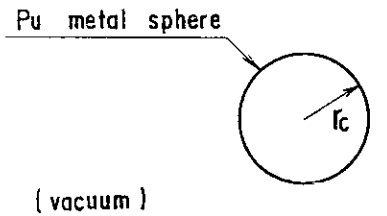

r_c is 63.85mm for B.M. No 6,
and 66.6 mm for B.M. No 13,

Fig. 3.A.6.5 Calculational model of B.M. No.6 and No.13.

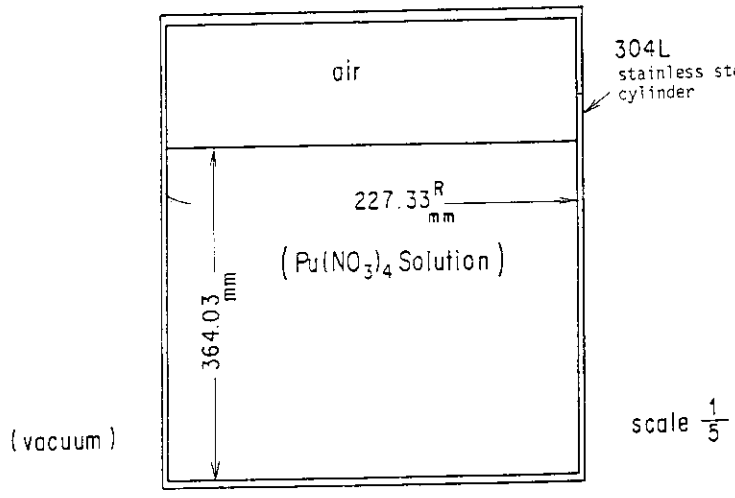

This calculation was performed without the cylinder vessel due to lack of dimensional data

Fig. 3.A.6.6 Calculational model of B.M. No.8.

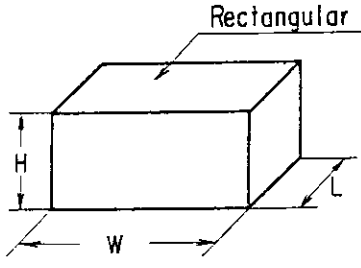

No	L	W	H
9A	458.1	407.12	491.1
9B1	407.2	407.2	235.8
9B2	509.0	509.0	186.8
9B3	610.8	509.0	174.7
9B4	610.8	610.8	163.5
9B5	∞	∞	108.7

(mm)

note

Serial No 9A has no reflector

Serial No 9B1 ~ B5 have 15 cm thick Plexiglas reflector

Fig. 3.A.6.7 Calculational model of B.M. No.9.

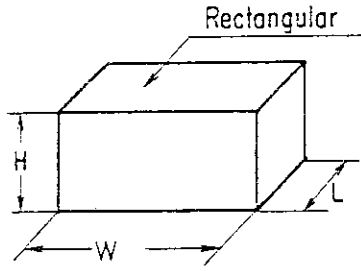

No	L	W	H
11A	307.8	307.8	209.9
11B1	256.5	256.5	100.3
11B2	256.5	307.8	89.8
11B3	307.8	307.8	79.6
11B4	307.8	410.4	68.5
11B5	410.4	410.4	61.6
11B6	∞	∞	33.4

(mm)

note

Serial No 11A has no reflector.

Serial No 11B1 ~ B6 have 15 cm thick Plexiglas reflector.

Fig. 3.A.6.8 Calculational model of B.M. No.11.

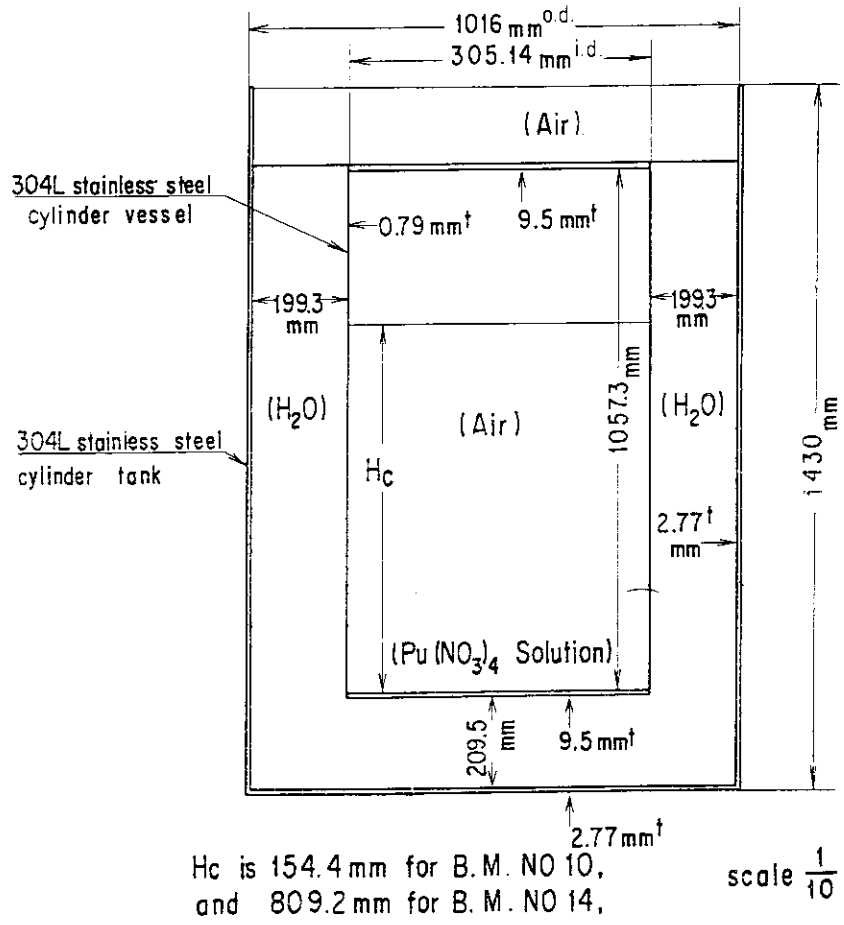

Fig. 3.A.6.9 Calculational model of B.M. No.10 and No.14.

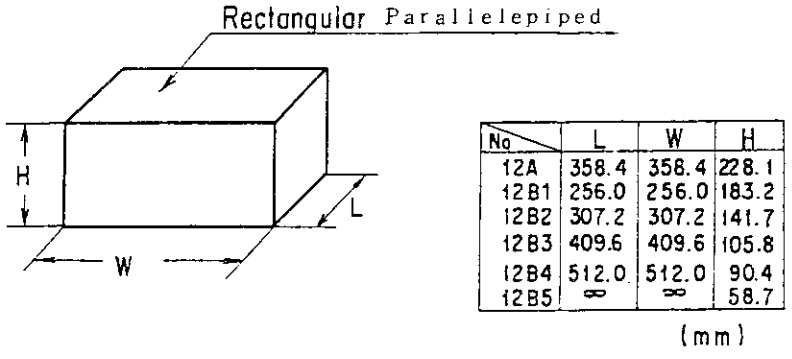

No	L	W	H
12A	358.4	358.4	228.1
12B1	256.0	256.0	183.2
12B2	307.2	307.2	141.7
12B3	409.6	409.6	105.8
12B4	512.0	512.0	90.4
12B5	〃	〃	58.7

(mm)

Serial No 12A has no reflector.

Serial No 12B1 ~ B5 have 15 cm thick Plexiglas reflector

Fig. 3.A.6.10 Calculational model of B.M. No.12.

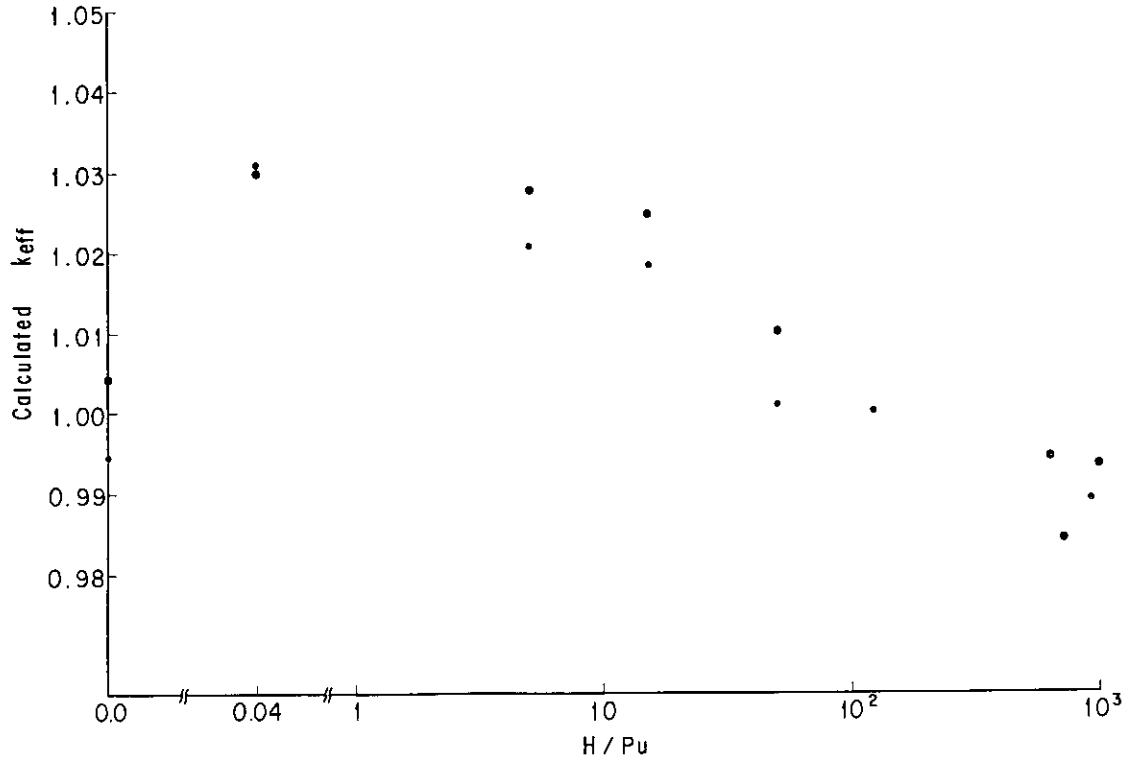

Fig. 3.A.6.11 Decreasing trend of calculated k_{eff} with increasing H/Pu.

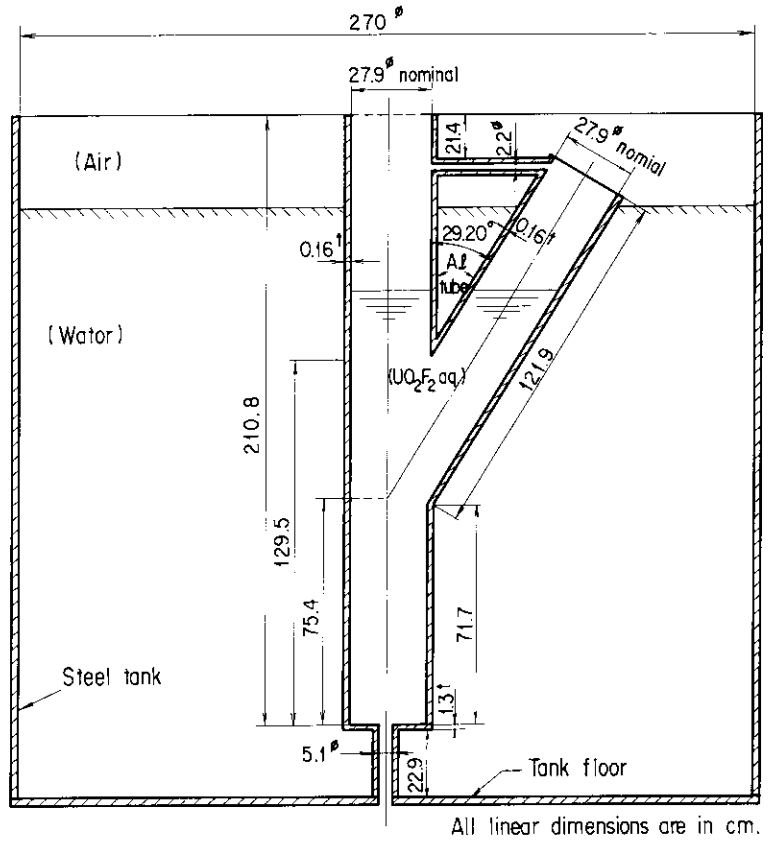

Fig. 3.A.7.1 Cut-out view of the experimental arrangement of "30 degrees lateral".

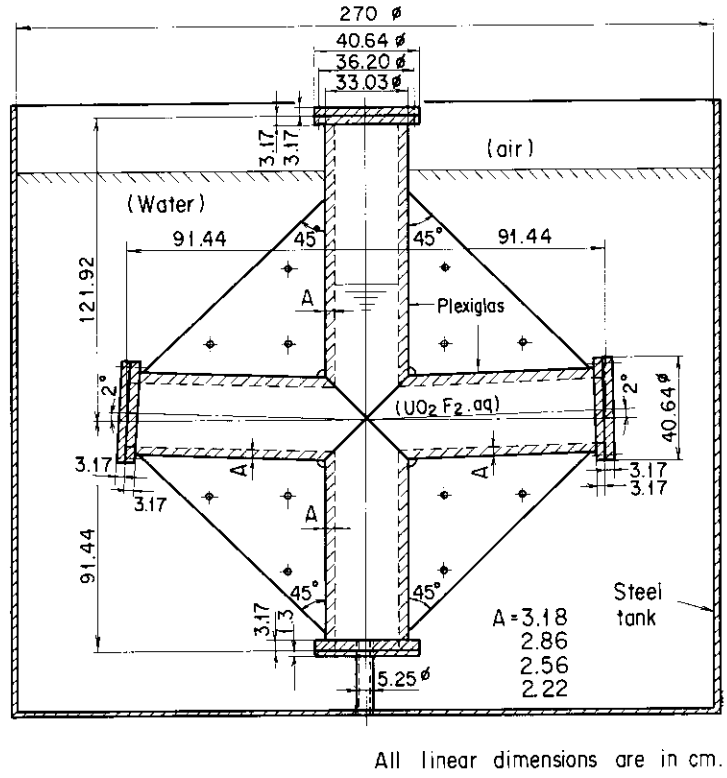

Fig. 3.A.7.2 Cut-out view of the experimental arrangement of "cross".

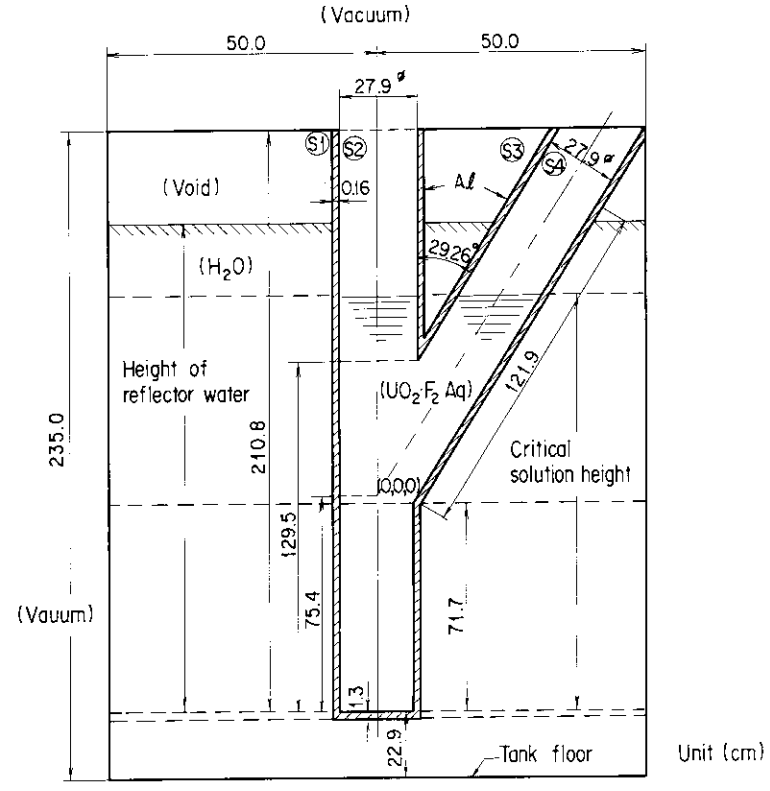

Surface equations

(S1) $X^2 + y^2 - 199.09 = 0$

(S2) $X^2 + y^2 - 194.60 = 0$

(S3) $1.3139\,X^2 + y^2 + 0.3139\,Z^2 - 1.1205\,yZ - 258.63 = 0$

(S4) $1.3139\,X^2 + y^2 + 0.3139\,Z^2 - 1.1205\,yZ - 255.69 = 0$

Fig. 3.A.7.3 Calculational model for "30 degrees lateral".

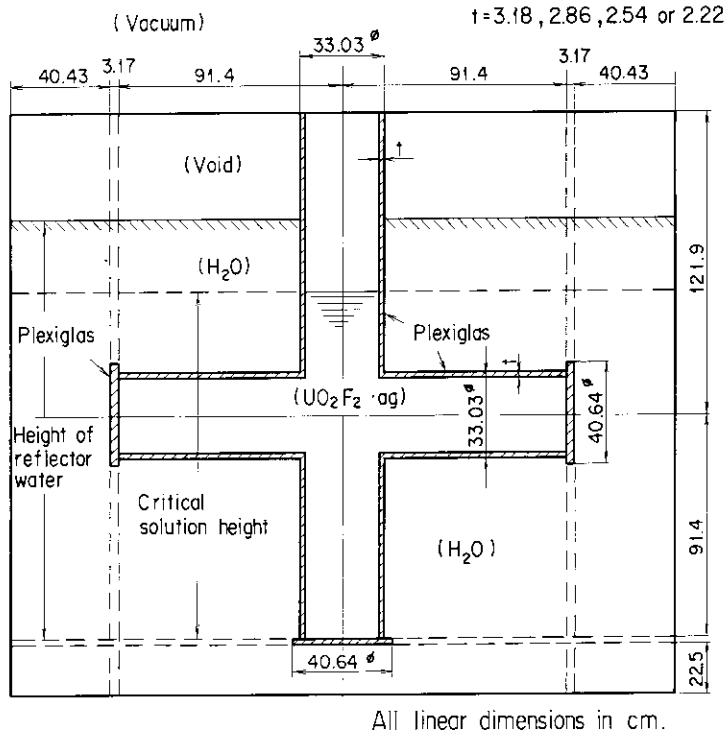

Fig. 3.A.7.4 Calculational model for "cross".

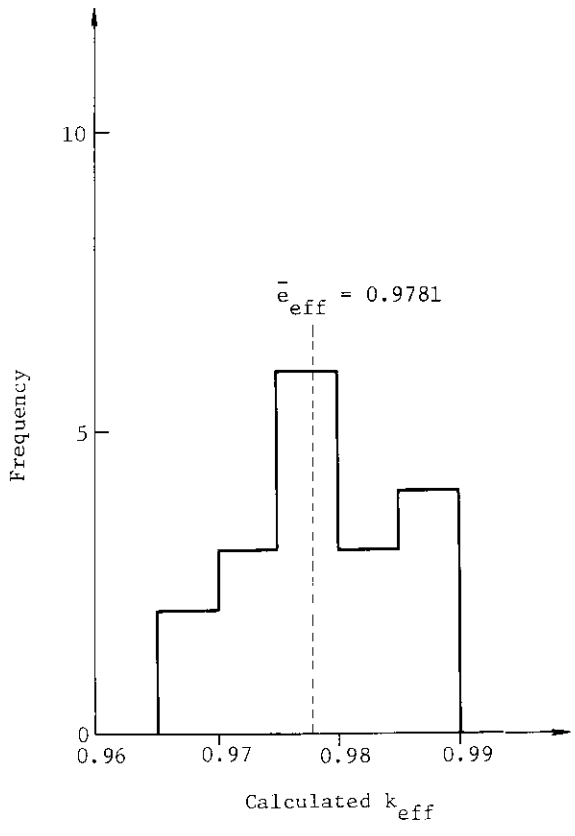

Fig. 3.A.7.5 Histogram of calculated k_{eff}'s for "30 degrees lateral" system (18 cases).

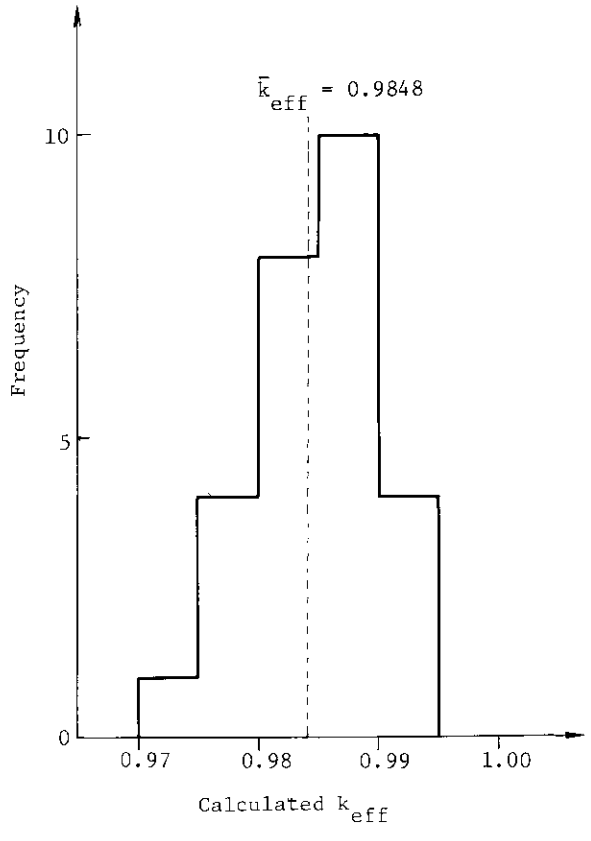

Fig. 3.A.7.6 Histogram of calculated k_{eff}'s for "cross" systems (27 cases).

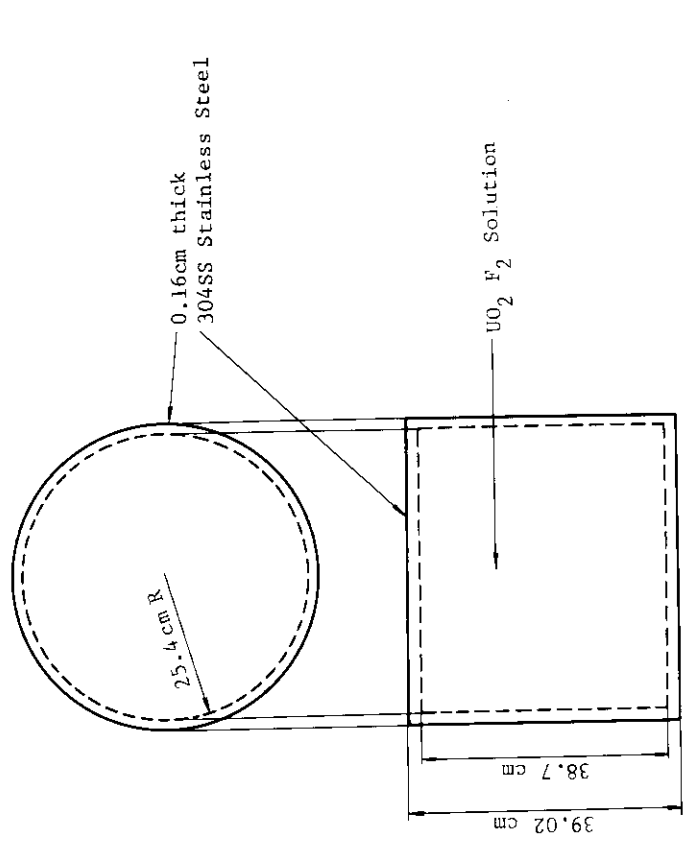

Fig. 3.A.8.2 Calculational model for a typical unreflected cylinder containing uranyl-fluoride solution.

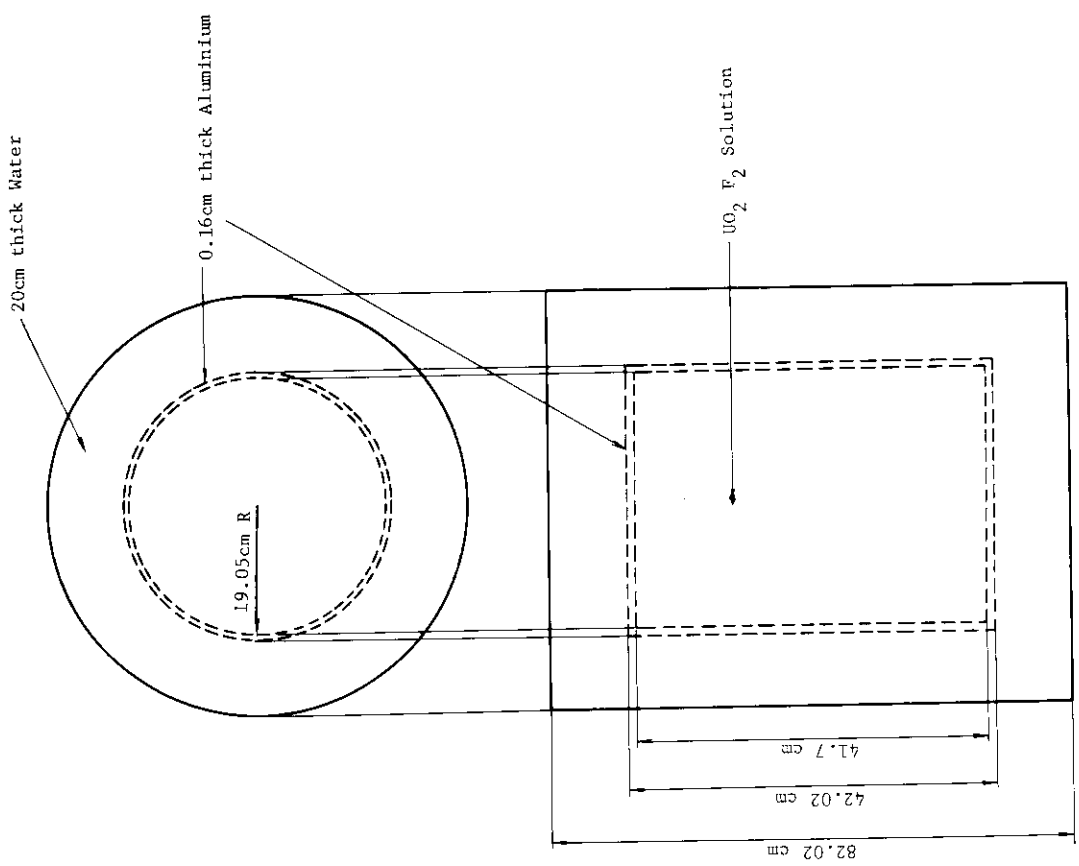

Fig. 3.A.8.1 Calculational model for a typical water-reflected cylinder containing uranyl-fluoride solution.

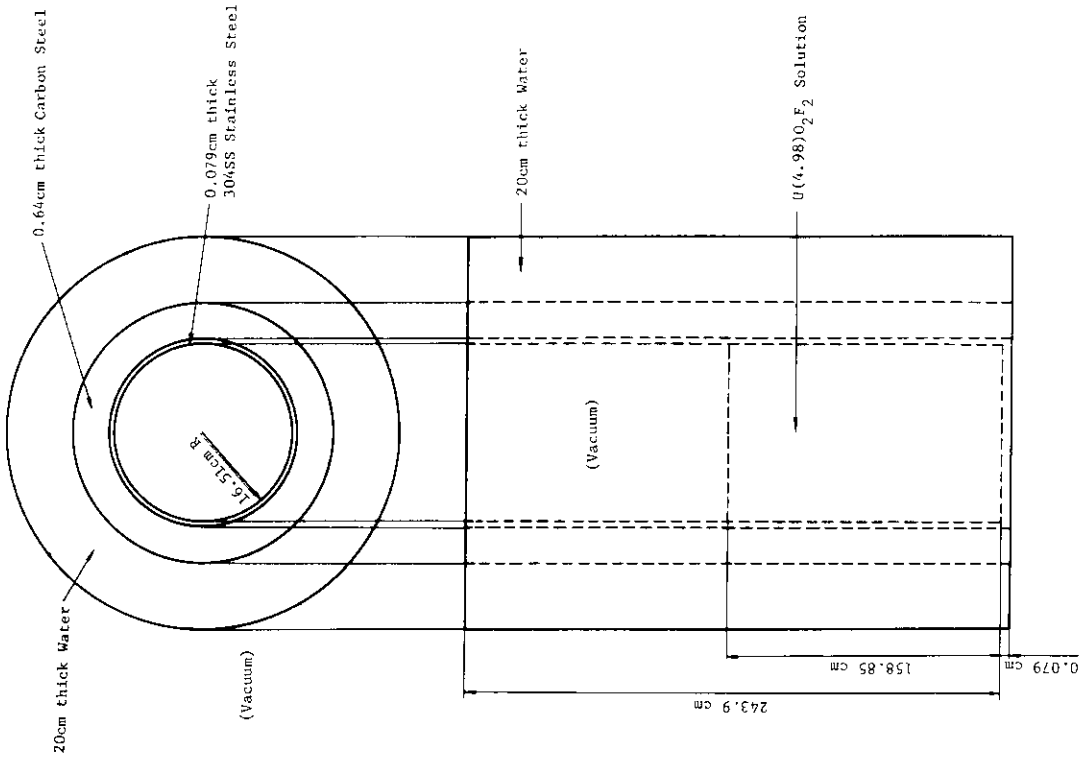

Fig. 3.A.9.1 Calculational model for a typical experimental case of $U(4.98)O_2F_2$ solution cylinder surrounded by composite reflector of steel/water.

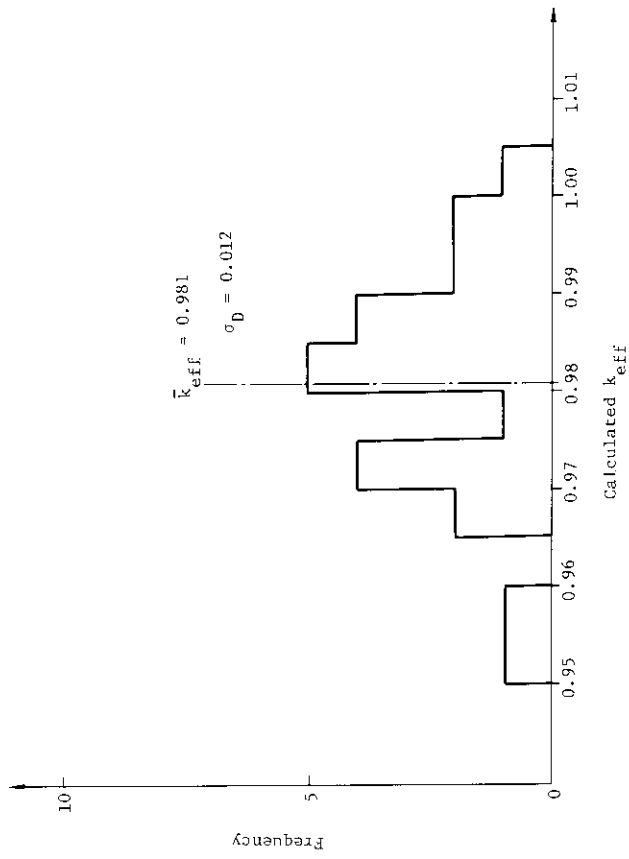

Fig. 3.A.8.3 Histogram of calculated k_{eff}'s for cylinders or spheres containing uranyl-fluoride solution.

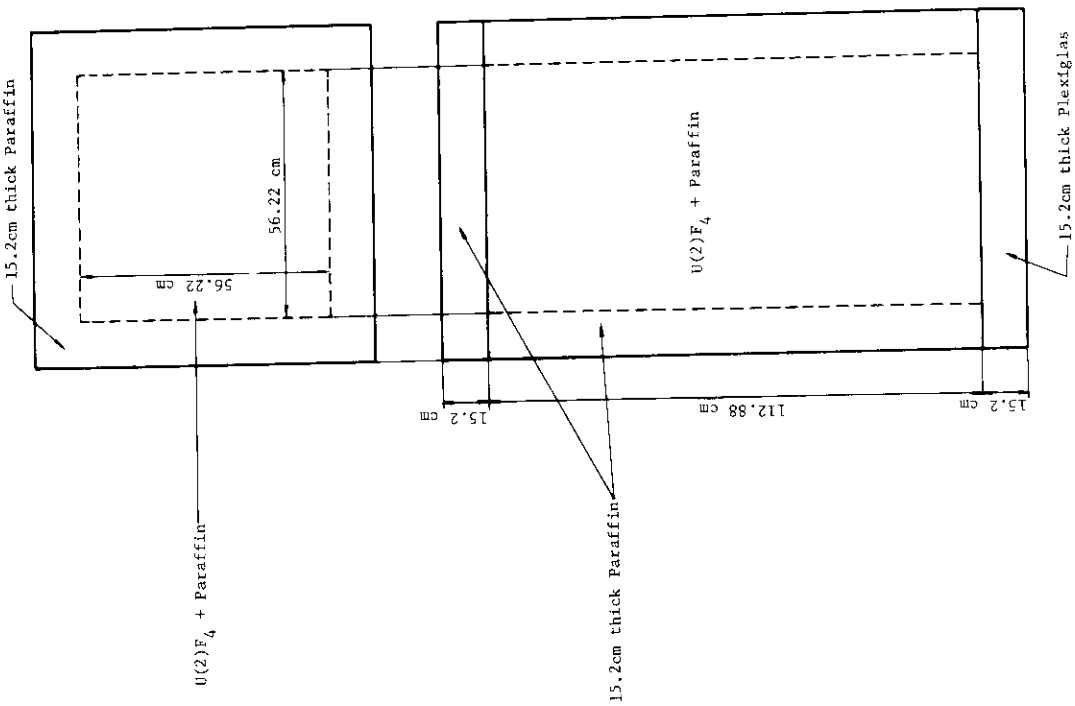

Fig. 3.A.10.1 Calculational model for a typical reflected pile of UF_4-paraffin compact fuel.

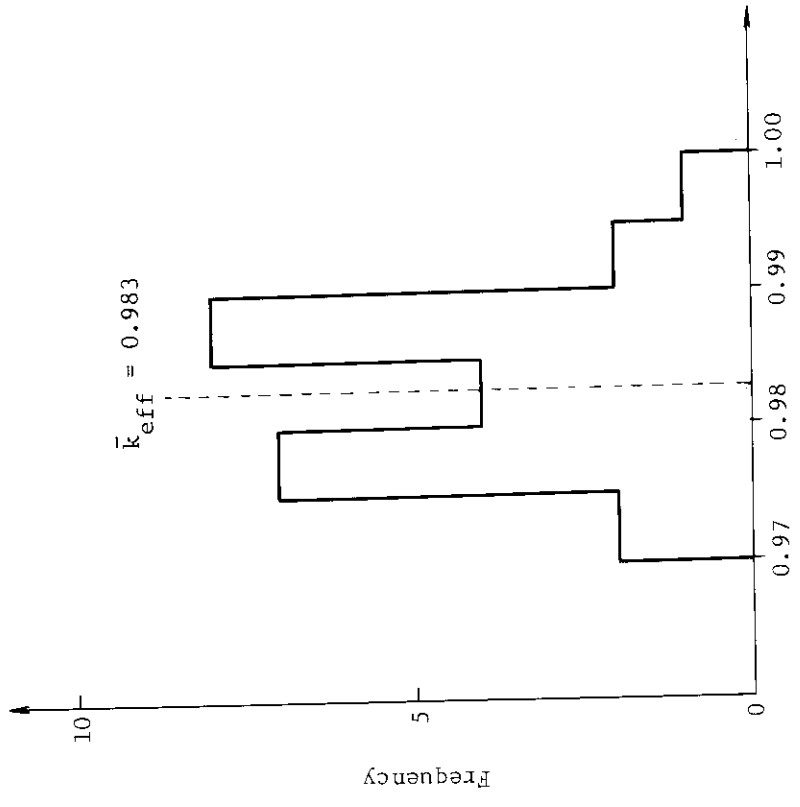

Fig. 3.A.9.2 Histogram of calculated k_{eff}'s for cylinders containing uranyl-fluoride solution surrounded by composite reflector.

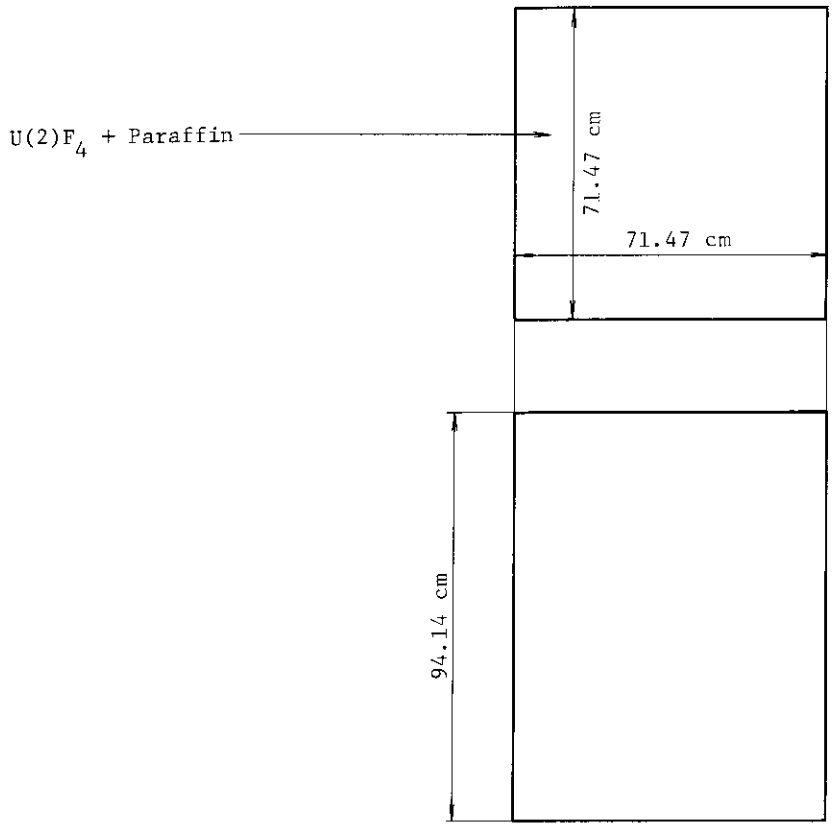

Fig. 3.A.10.2 Calculational model for a typical unreflected pile of UF_4-paraffin compact fuel.

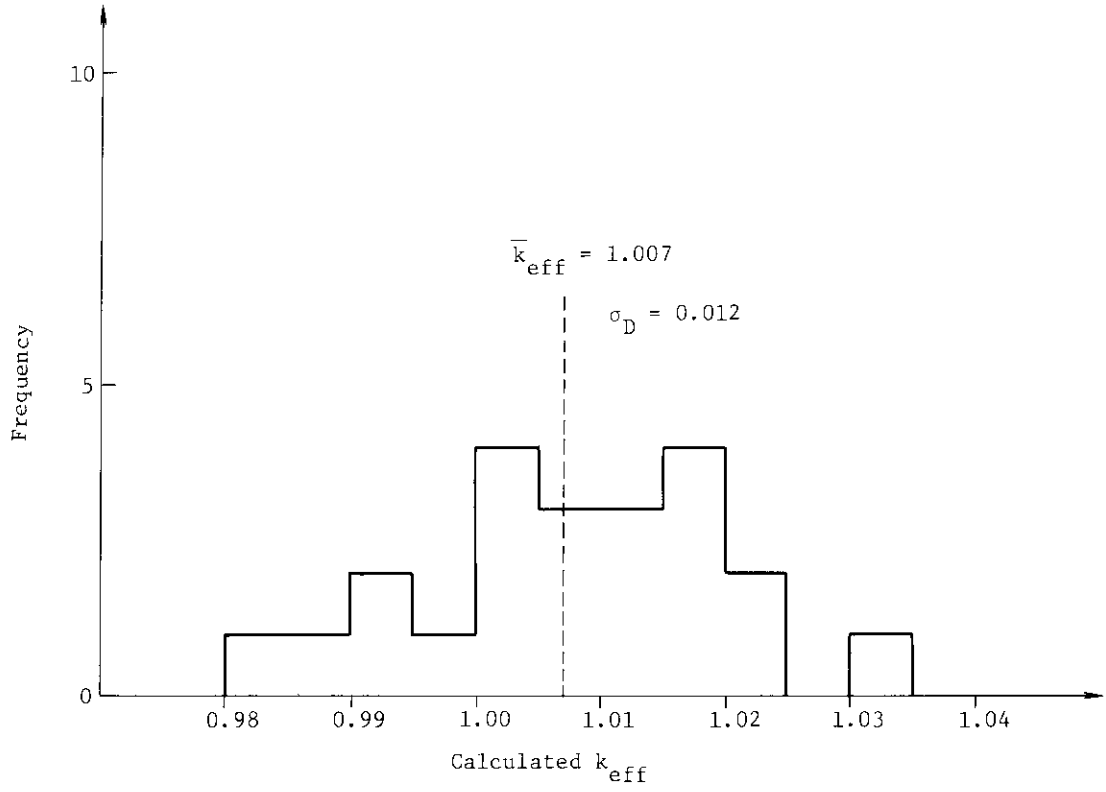

Fig. 3.A.10.3 Histogram of calculated k_{eff}'s for reflected pile of UF_4-paraffin compact fuel.

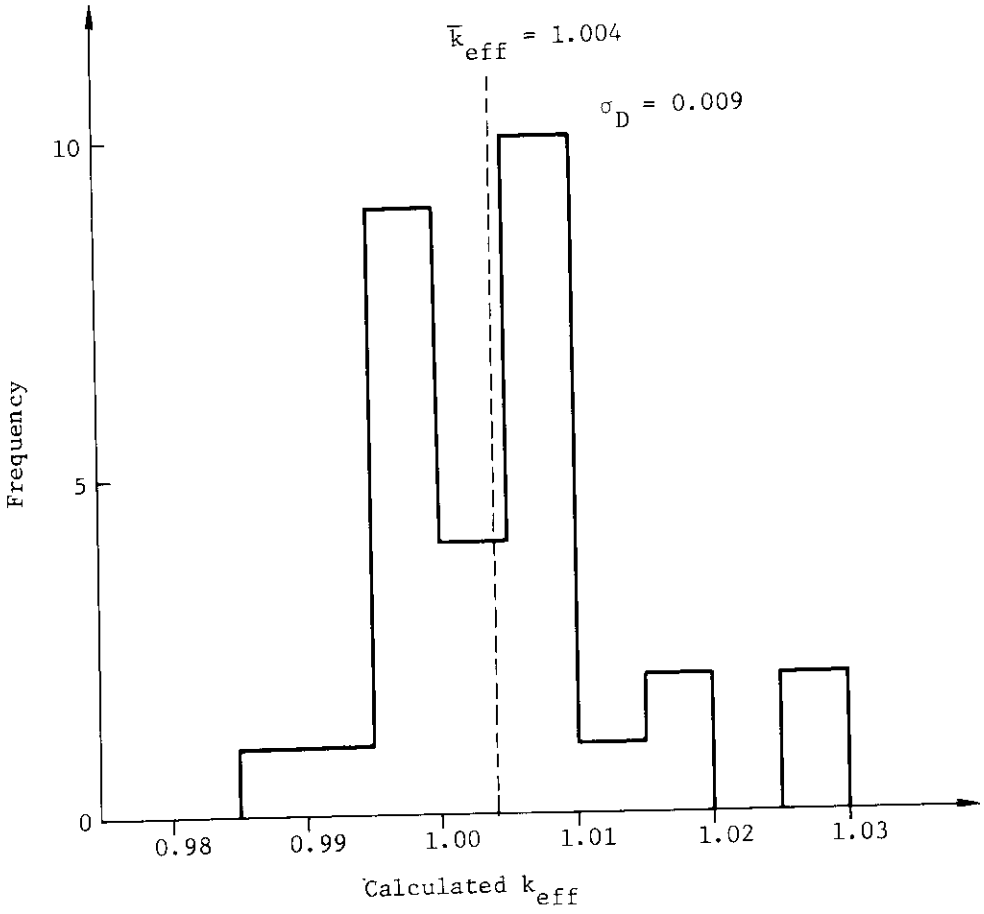

Fig. 3.A.10.4 Histogram of calculated k_{eff}'s for unreflected pile of UF_4-paraffin compact fuel.

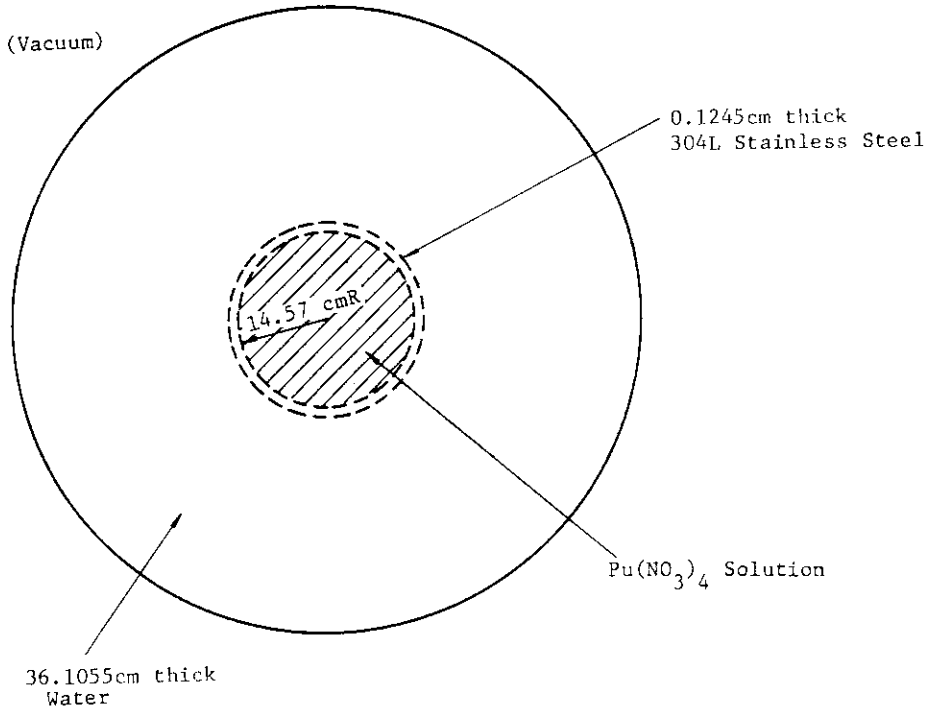

Fig. 3.A.11.1 Calculational model for a typical experimental system, case No.1.

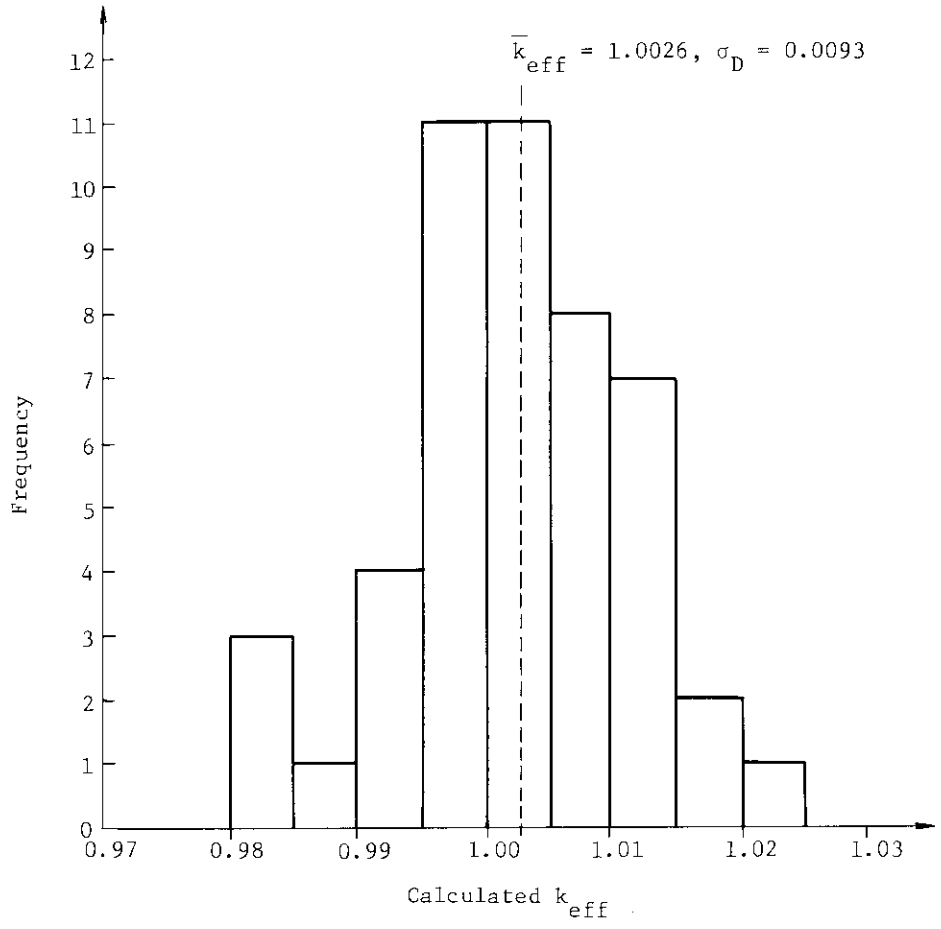

Fig. 3.A.11.2 Histogram of calculated k_{eff}'s for 48 spherical vessels containing uranyl-nitrate solution with various reflectors.

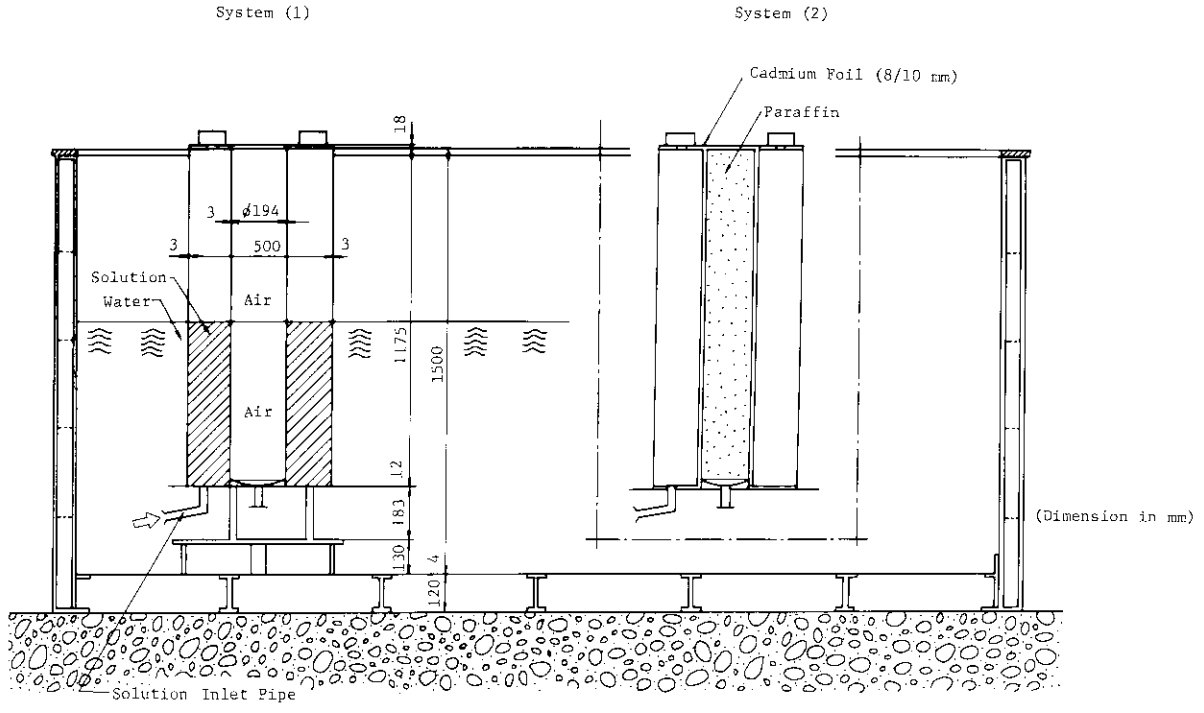

Fig. 3.A.12.1 Experimental arrangement of annular cylinders containing plutonium-nitrate solution.

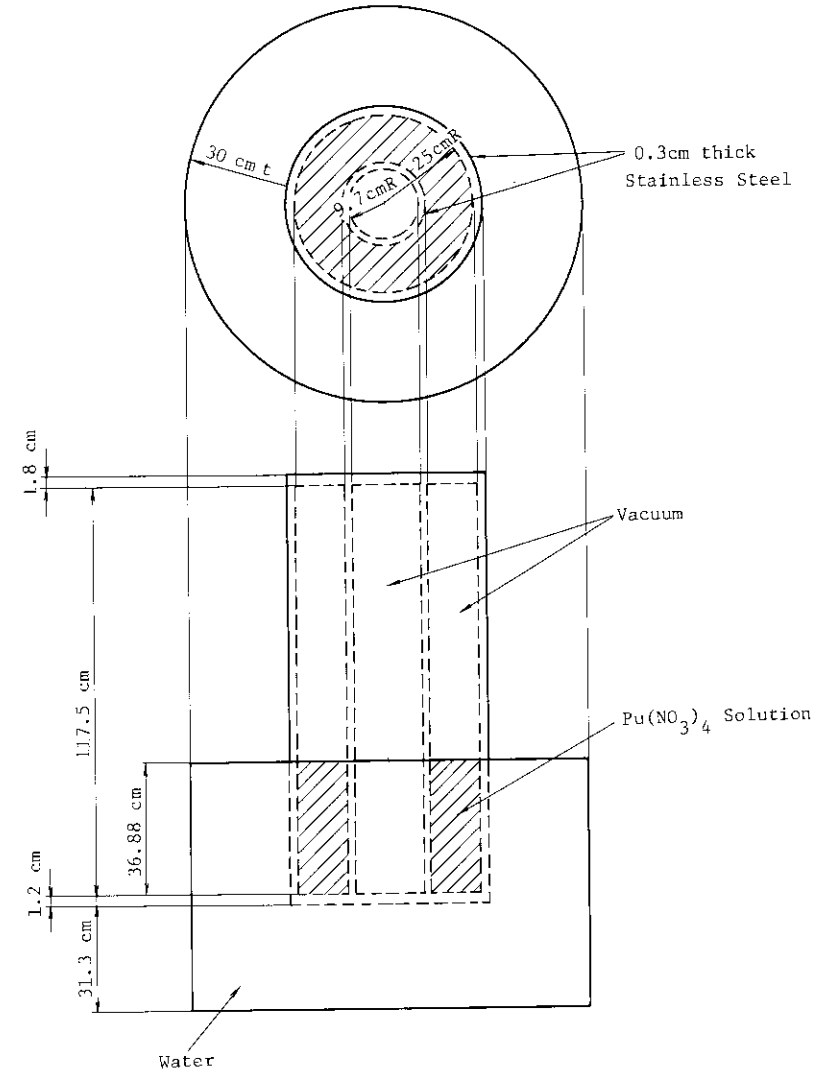

Fig. 3.A.12.2 Calculational model for a typical case of annular cylinder containing plutonium-nitrate solution.

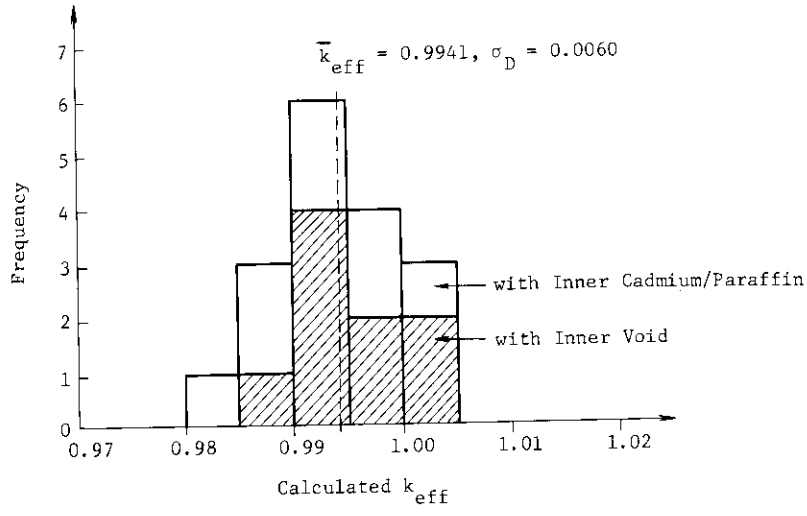

Fig. 3.A.12.3 Histogram of calculated k_{eff}'s for annular cylinders containing plutonium-nitrate solution with or without inner cadmium/paraffin.

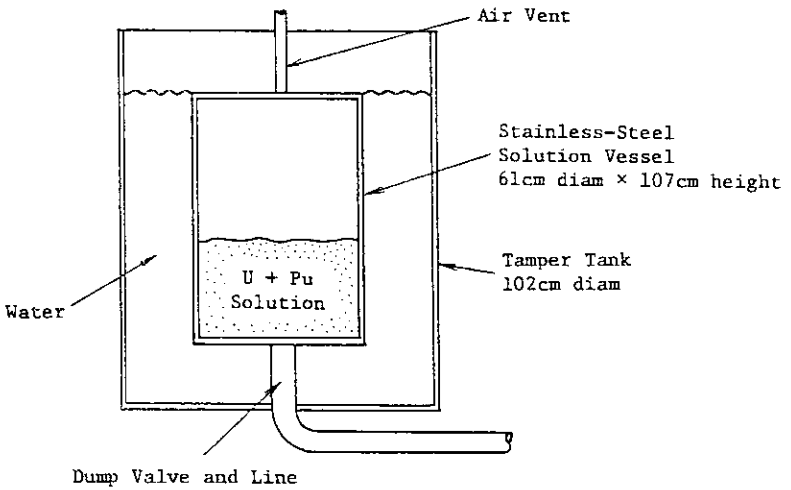

Fig. 3.A.13.1 Experimental set-up for cylinder containing plutonium-uranyl nitrate solution.

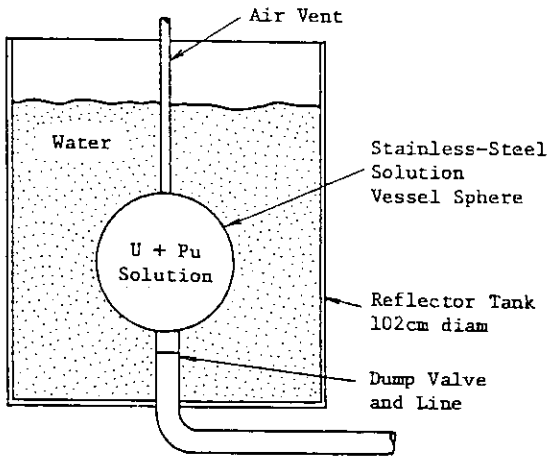

Fig. 3.A.13.2 Experimental set-up for sphere containing plutonium-uranyl nitrate solution.

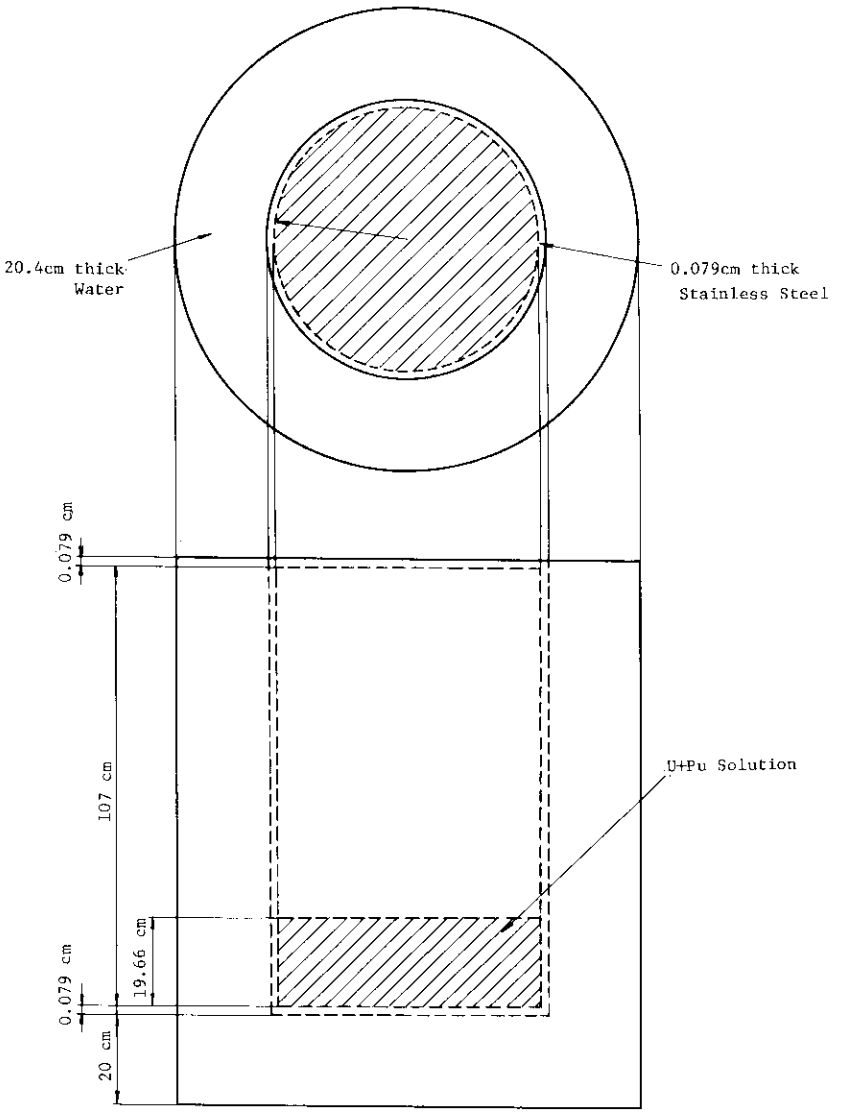

Fig. 3.A.13.3 Calculational model for a typical cylinder containing plutonium-uranyl nitrate solution.

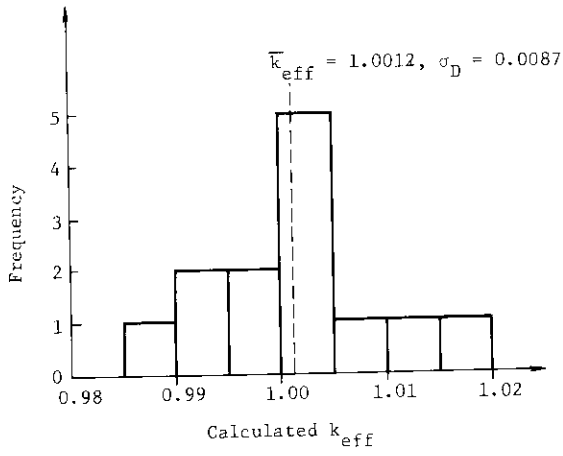

Fig. 3.A.13.4 Histogram of calculated k_{eff}'s for cylinders containing (Pu+U) nitrate solution of 5.6 wt% ^{240}Pu in Pu.

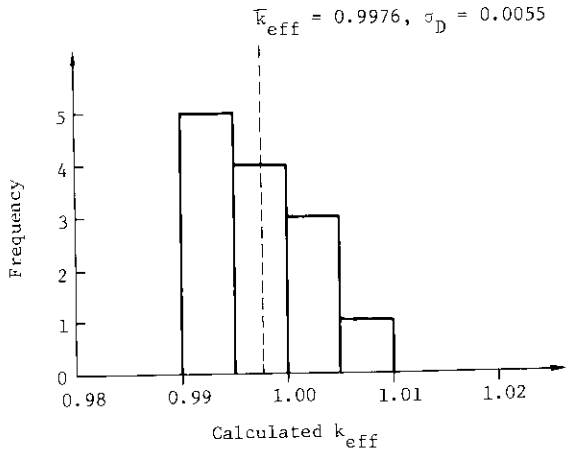

Fig. 3.A.13.5 Histogram of calculated k_{eff}'s for cylinders containing (Pu+U) nitrate solution of 23.0 wt% ^{240}Pu in Pu.

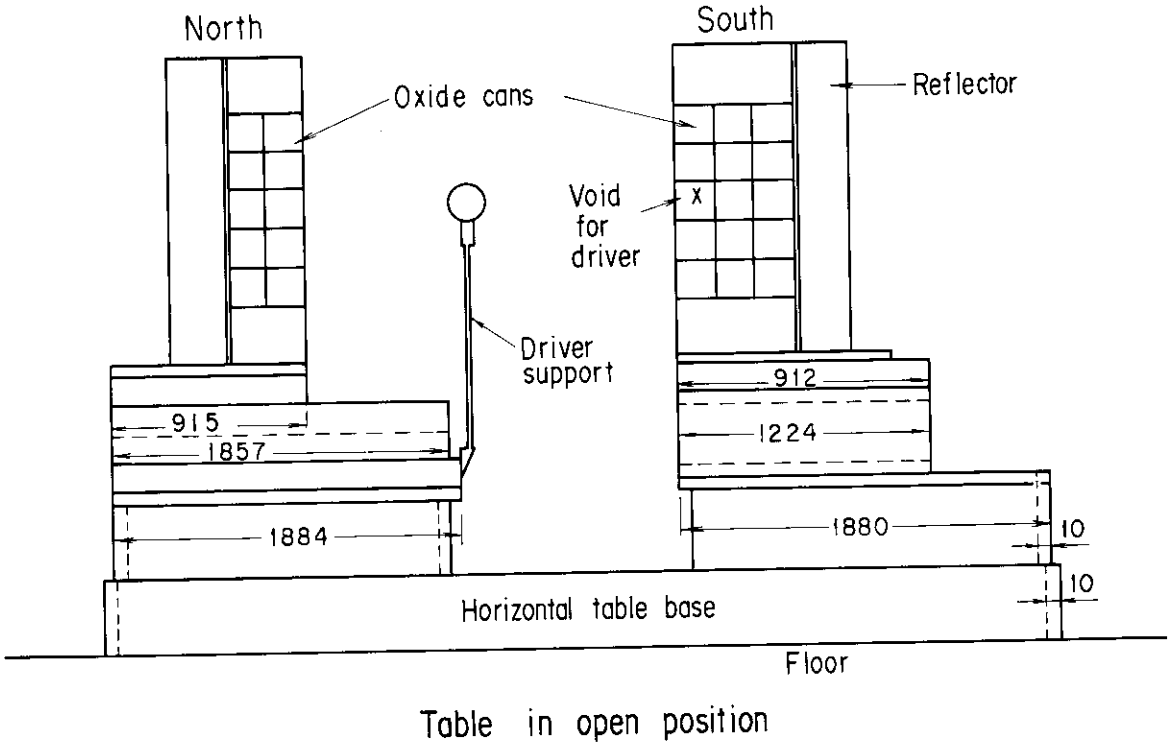

Fig. 3.A.14.1 Experimental arrangement of the array of compacted low-enriched uranium-oxide packages.

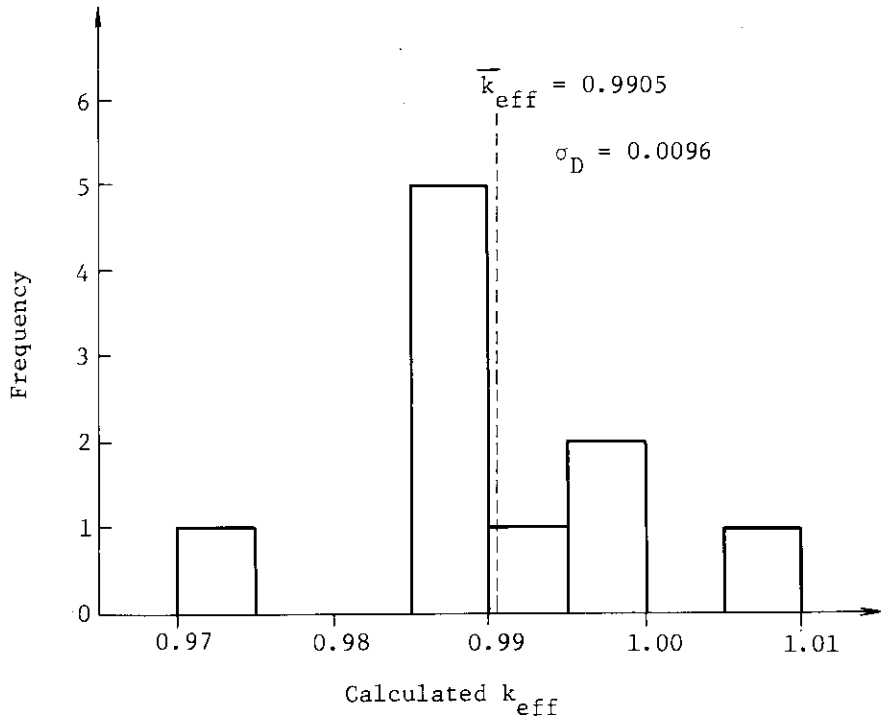

Fig. 3.A.14.2 Histogram of calculated k_{eff}'s for U_3O_8 package arrays.

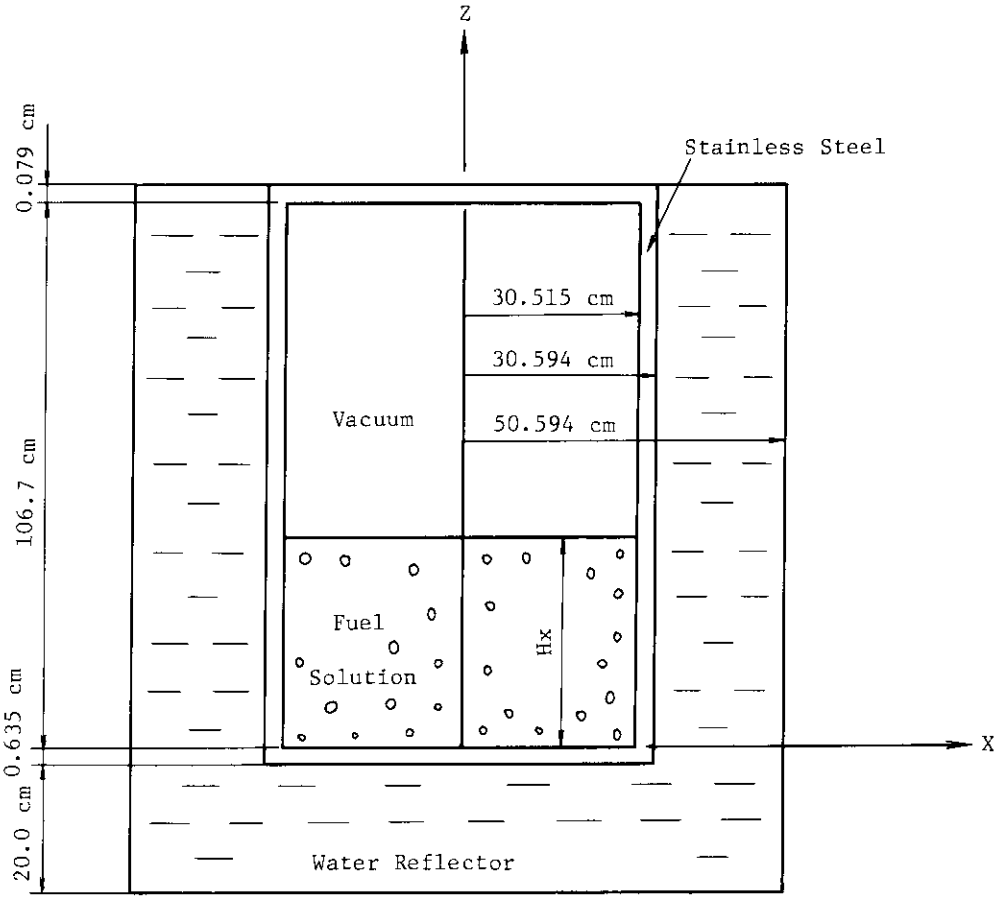

Fig. 3.A.15.1 Calculational model for plutonium-nitrate solution with gadolinium poison in a cylindrical vessel.

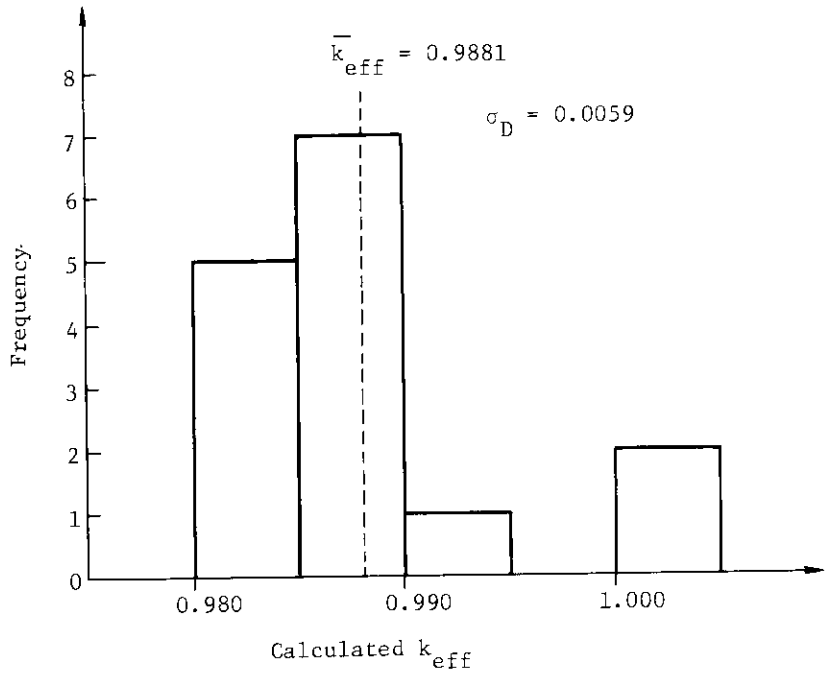

Fig. 3.A.15.2 Histogram of calculated k_{eff}'s for plutonium-nitrate solution with gadolinium.

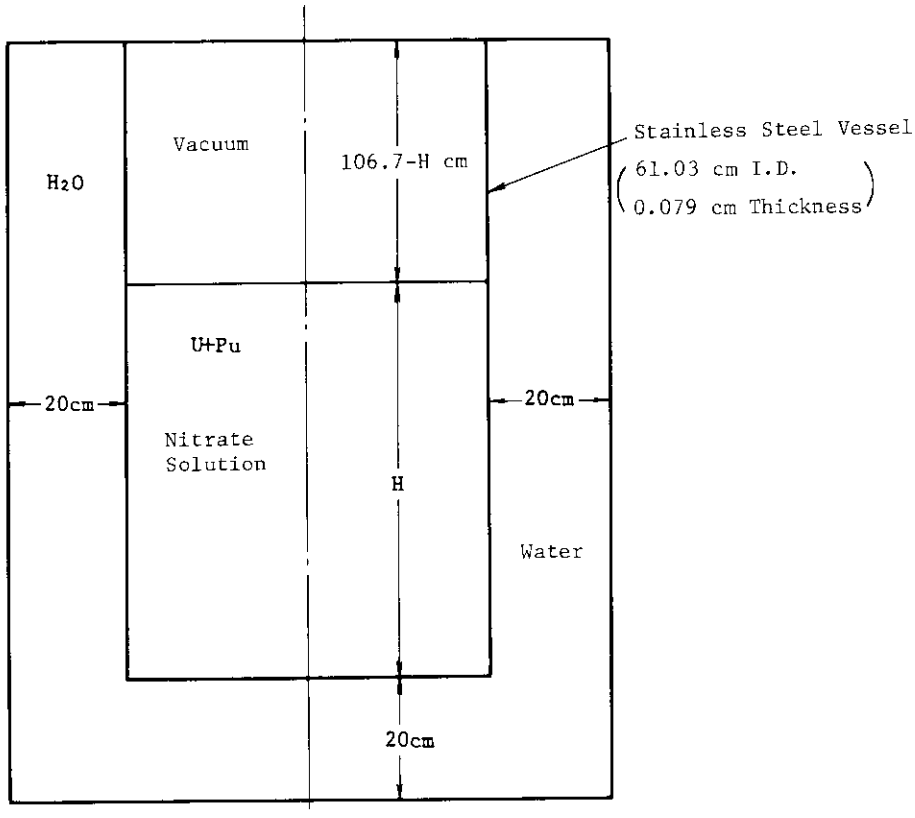

Fig. 3.A.16.1 Calculational model for a cylinder containing (U+Pu) nitrate solution with soluble neutron absorbers.

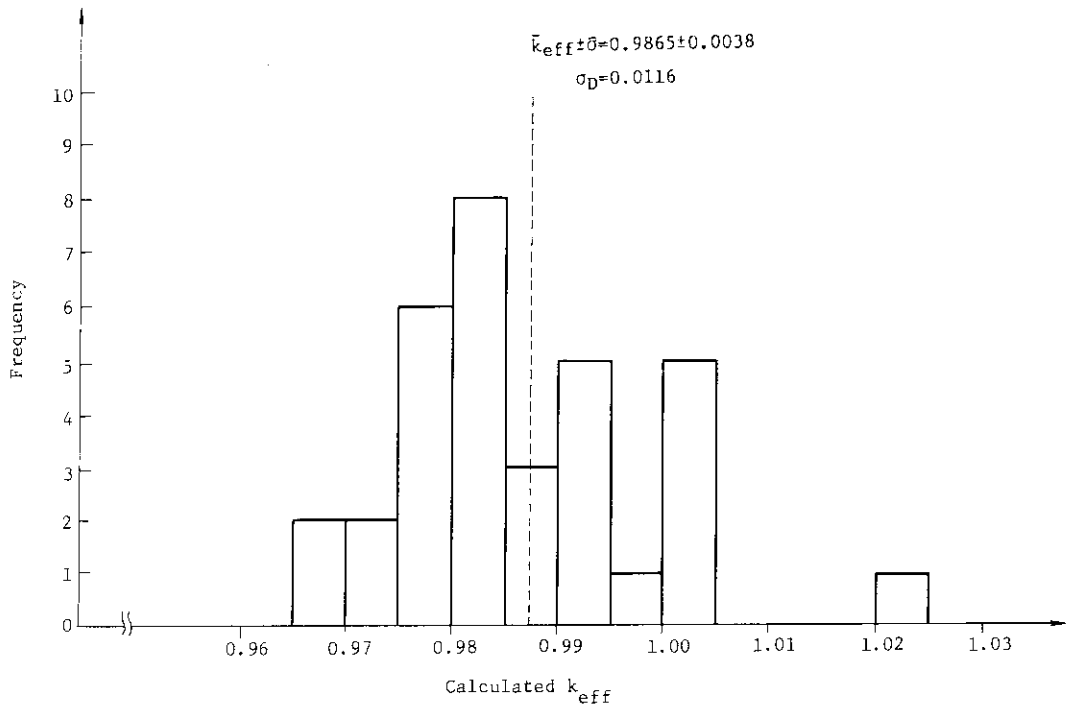

Fig. 3.A.16.2 Histogram of 34 calculated k_{eff}'s for cylinders containing Plutonium-uranyl nitrate solution with soluble neutron absorbers.

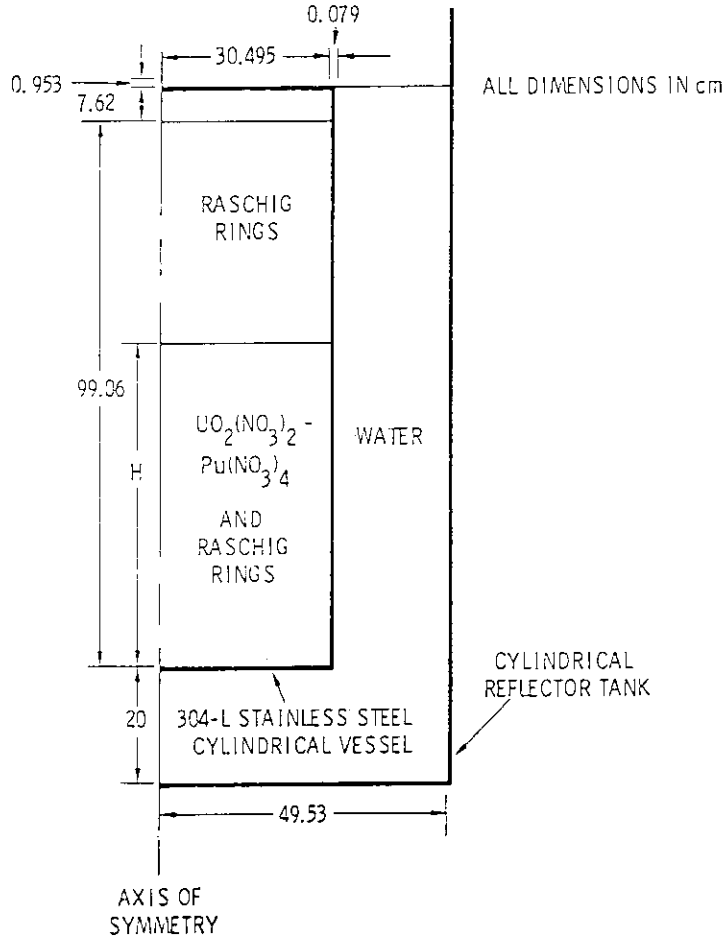

Fig. 3.A.17.1 Schema of experimental set up for raschig rings in uranium-plutonium nitrate solution.

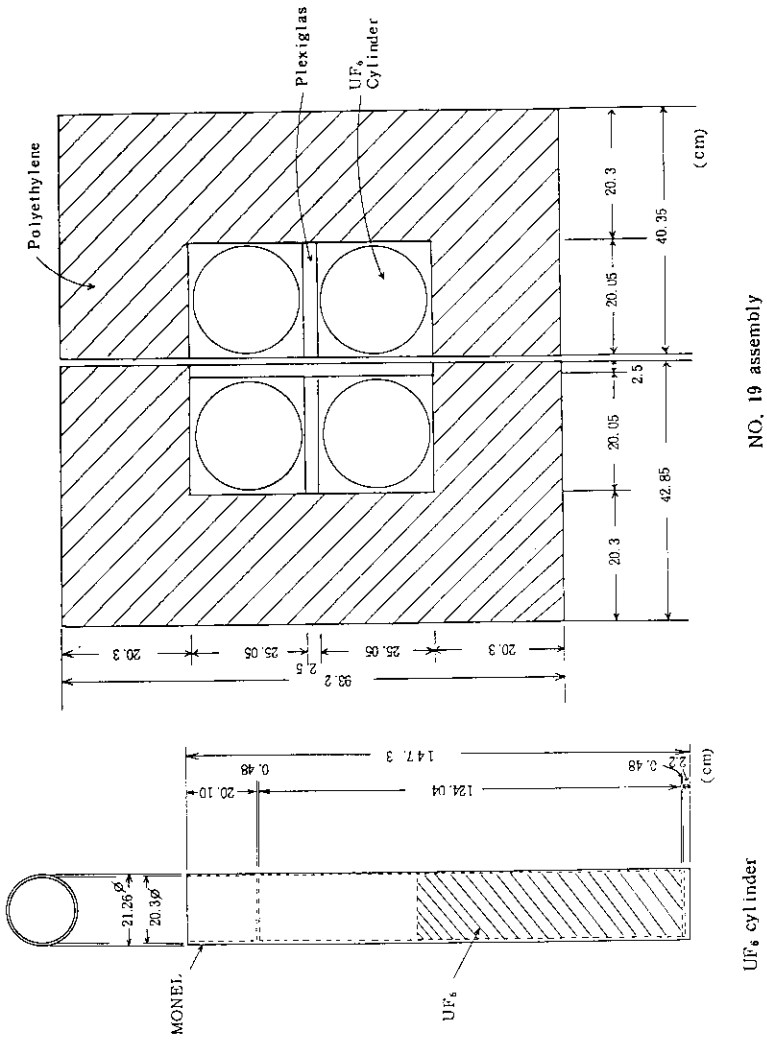

Fig. 3.B.1.1 Calculational models of a UF_6 cylinder and its typical arrangement.

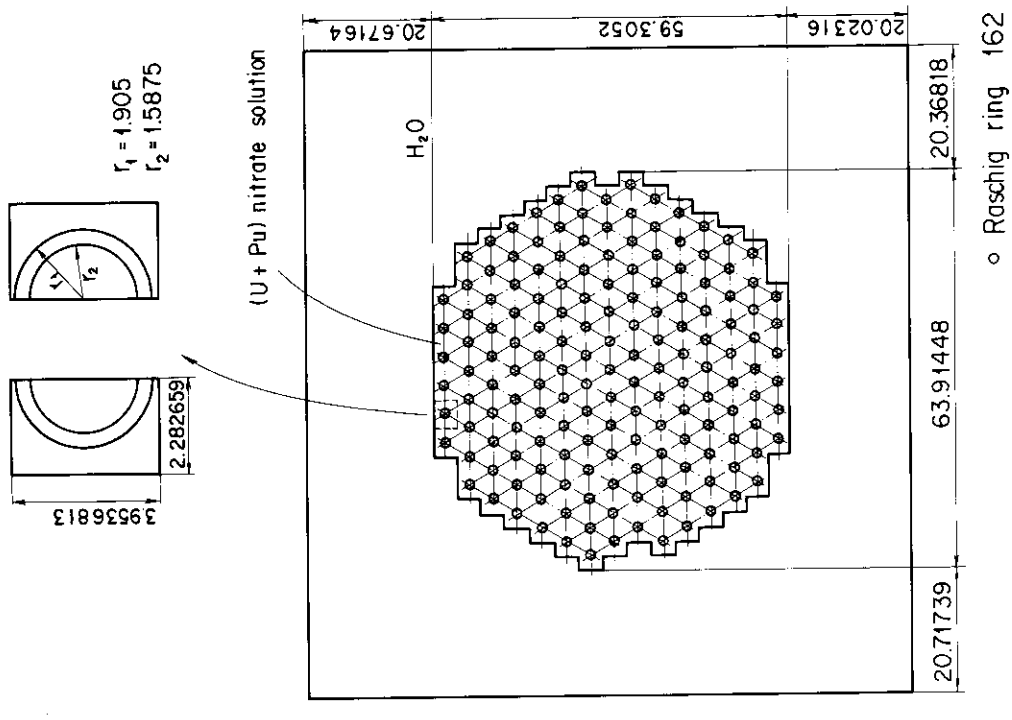

Fig. 3.A.17.2 Calculational model for raschig rings in uranium-plutonium nitrate solution.

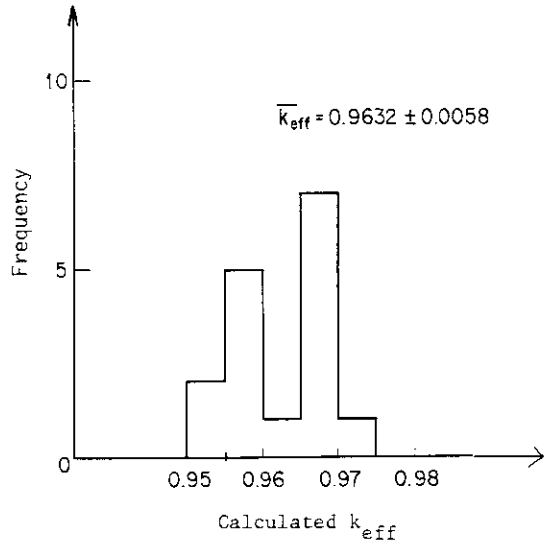

Fig. 3.B.1.2 Histogram of calculated k_{eff}'s for the unreflected UF_6 cylinder systems (16 cases).

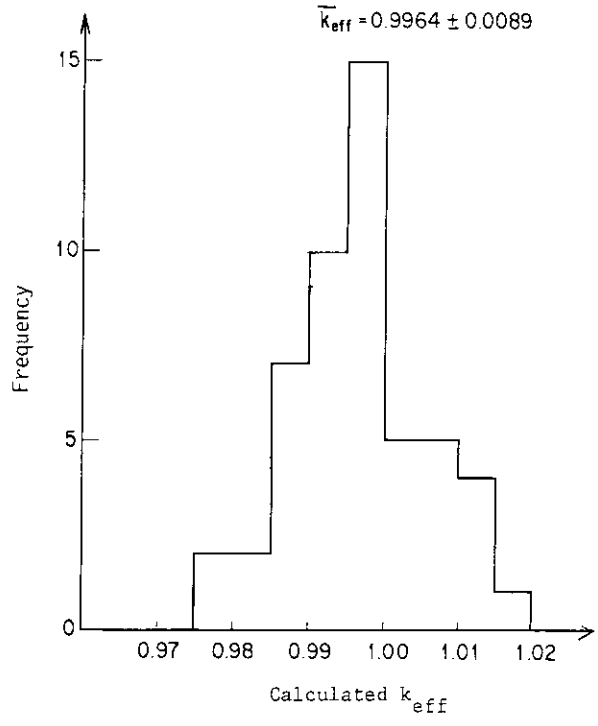

Fig. 3.B.1.3 Histogram of calculated k_{eff}'s for the reflected UF_6 cylinder systems (51 cases).

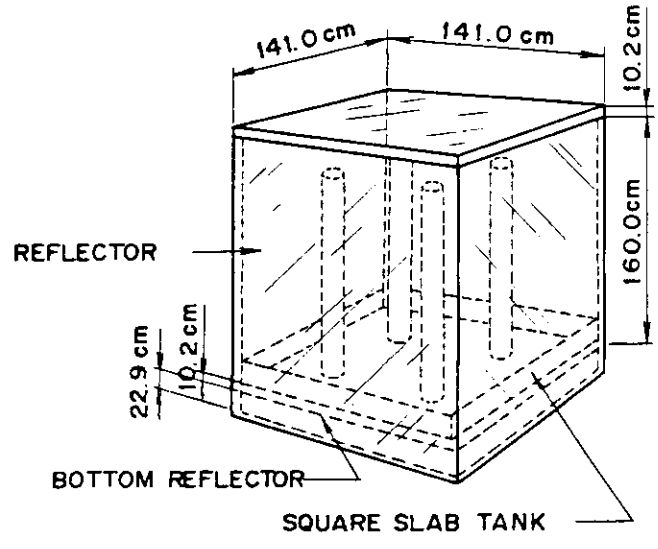

Fig. 3.B.2.1 Typical reflected experimental configuration.

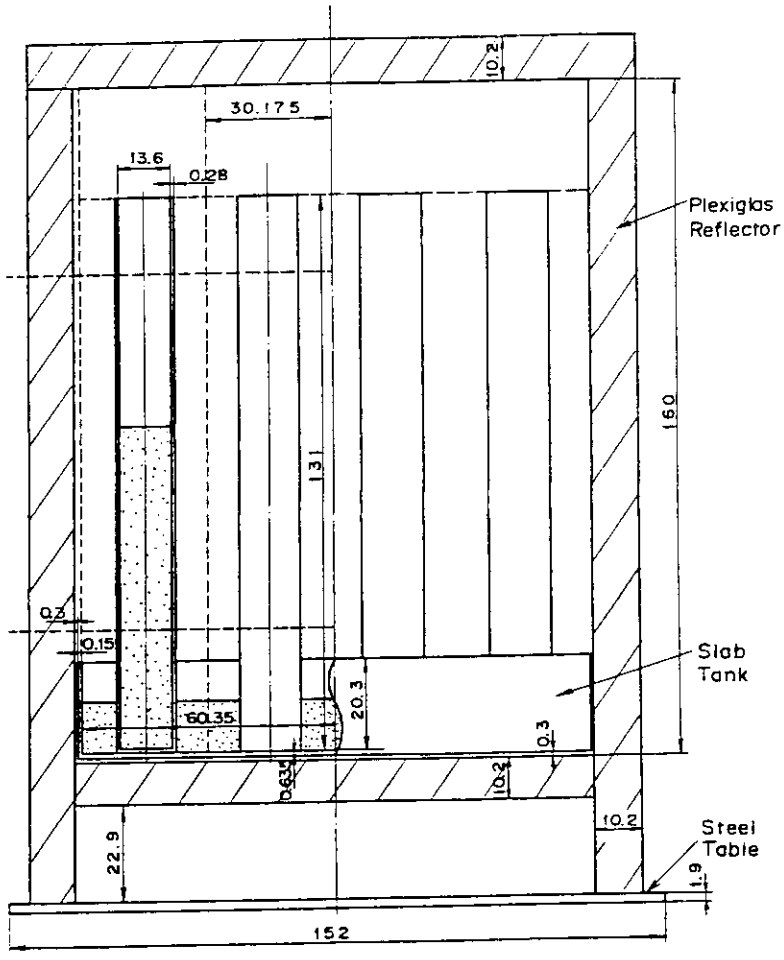

Fig. 3.B.2.2 Calculational model for a reflected 4×4 cylinder array.

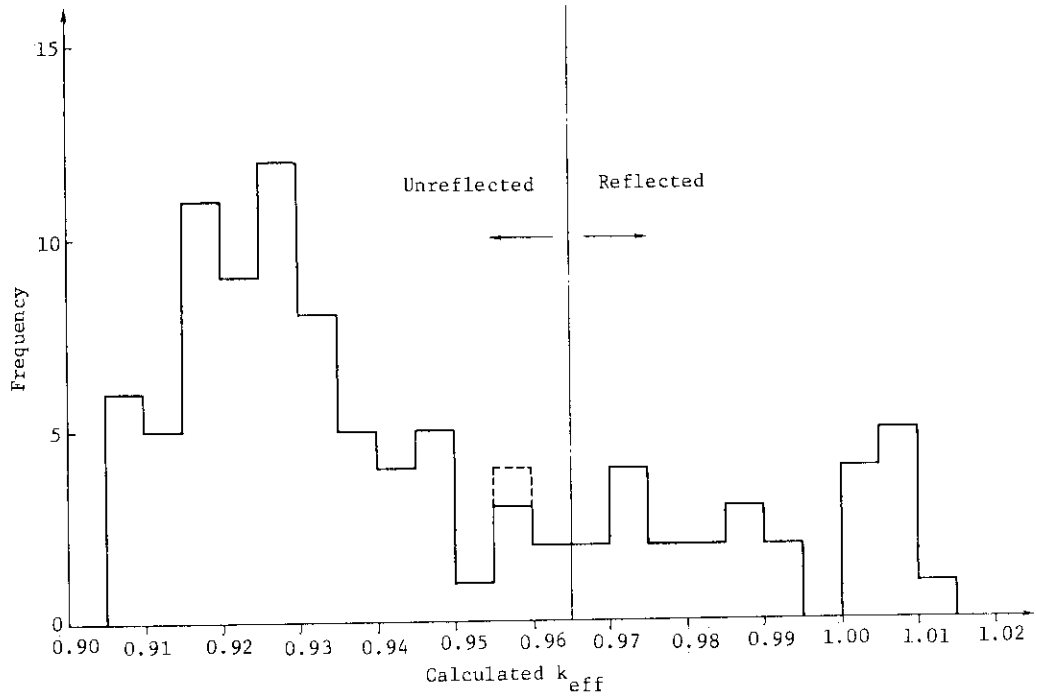

Fig. 3.B.2.3 Histogram of calculated multiplication factor (k_{eff}). Calculated k_{eff}'s are divided into two groups; one has the values lower than 0.965 corresponding to the unreflected systems (70 cases); the other has the values greater than 0.965 corresponding to the reflected systems (26 cases).

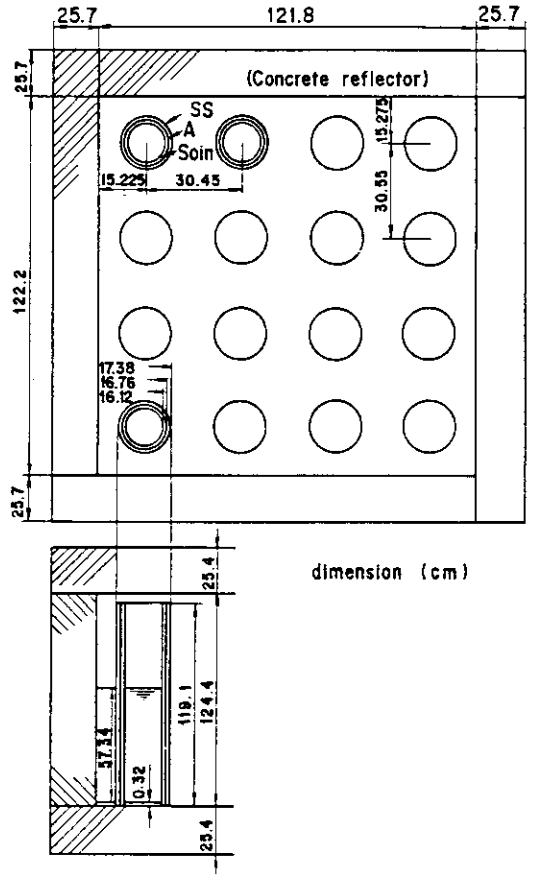

Fig. 3.B.3.1 Calculational model of reflected sleeved cylinders.

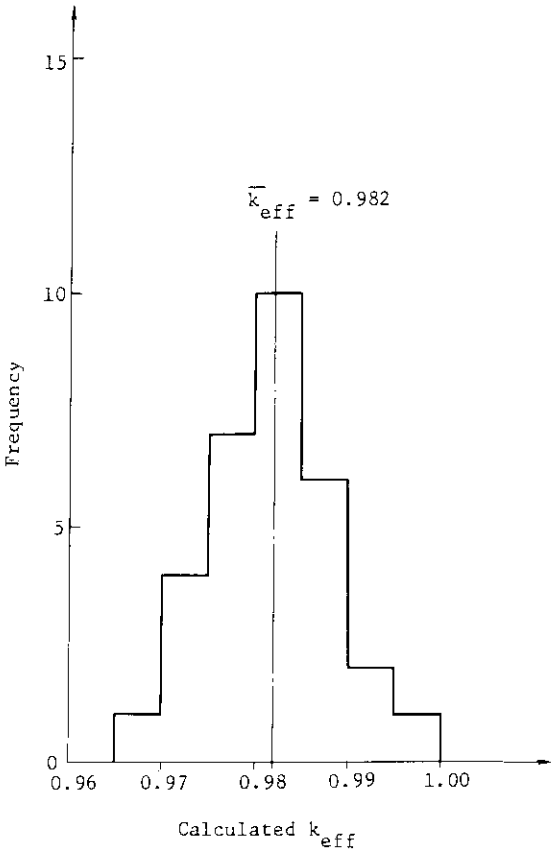

Fig. 3.B.3.2 Histogram of calculated k_{eff}'s for the reflected array of cylinders (31 cases).

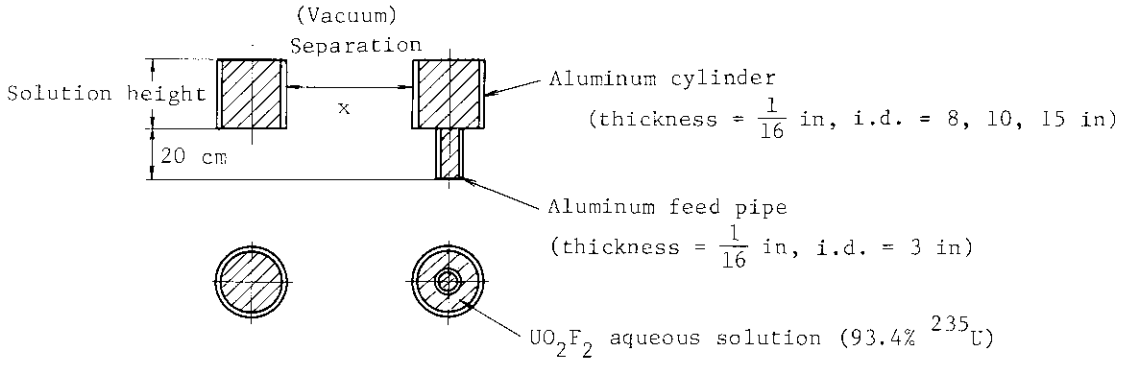

Fig. 3.B.4.1 Calculational model for two aluminum reactors without water reflector.

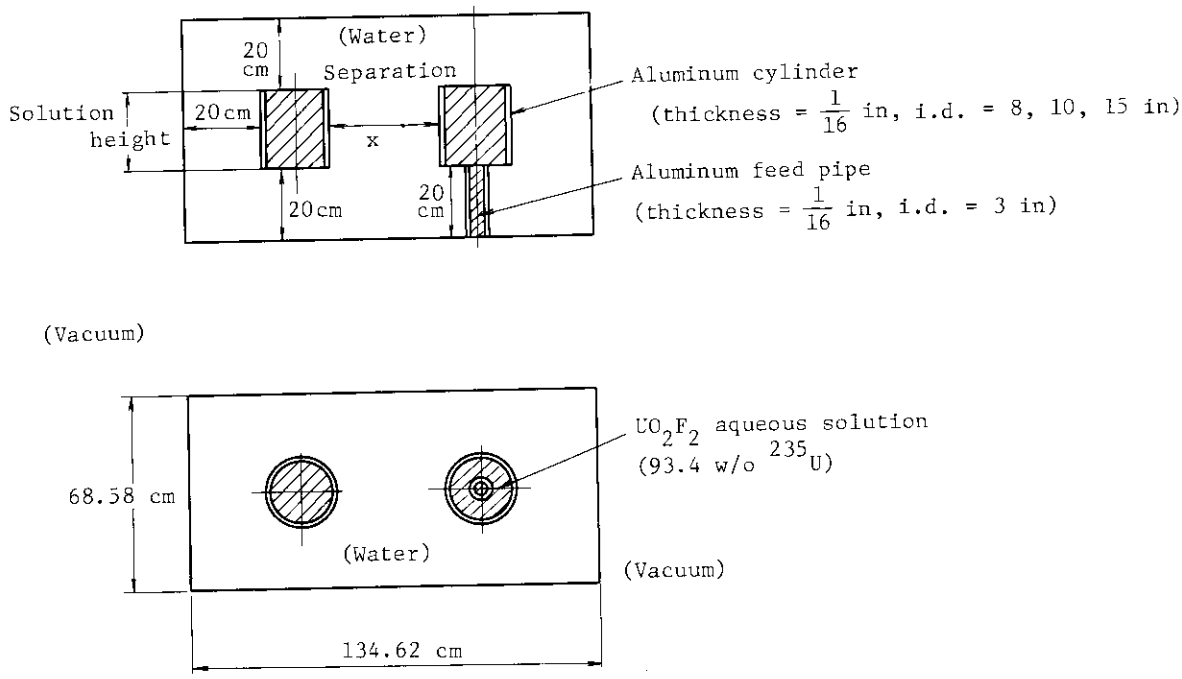

Fig. 3.B.4.2 Calculational model for two aluminum reactors with water reflector.

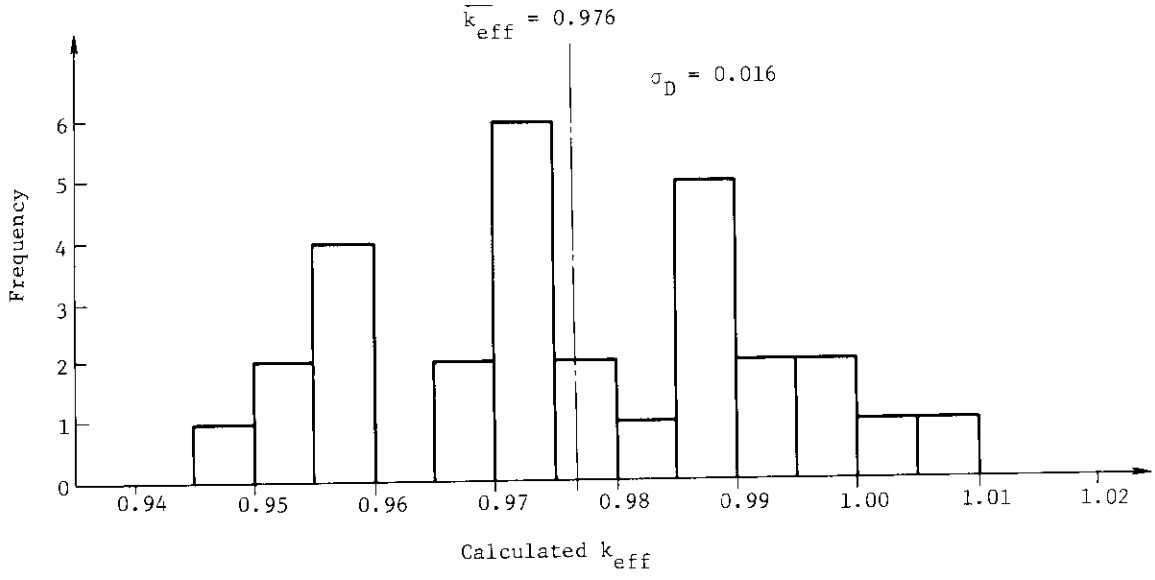

Fig. 3.B.4.3 Histogram of calculated k_{eff}'s for two aluminum reactors (29 cases).

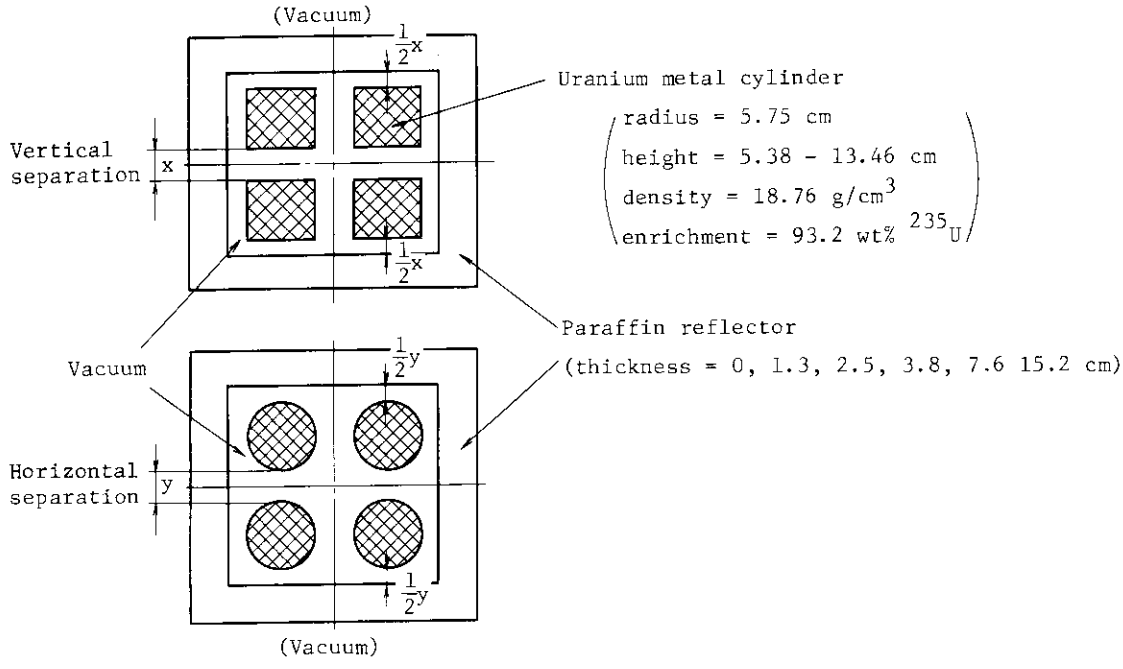

Fig. 3.B.5.1 Calculational model for a 2X 2X 2 array of uranium-metal cylinders with paraffin reflector.

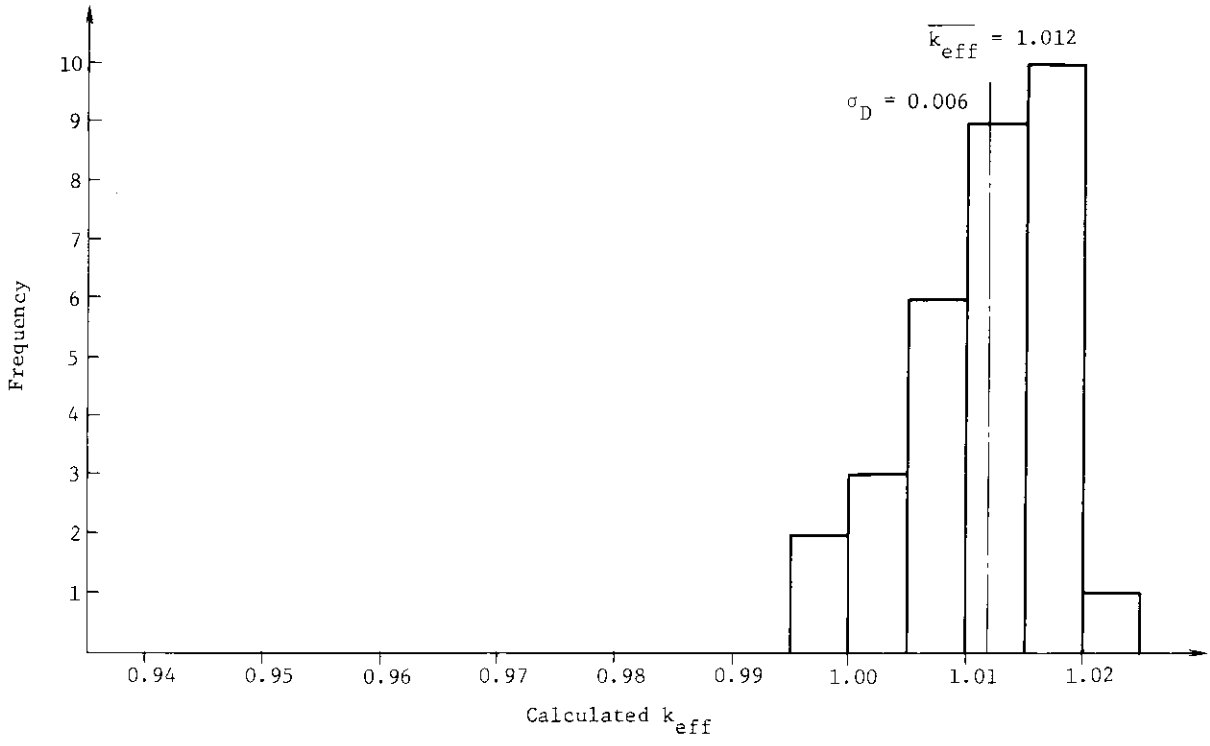

Fig. 3.B.5.2 Histogram of calculated k_{eff}'s for cubic arrays of uranium-metal cylinders (31 cases).

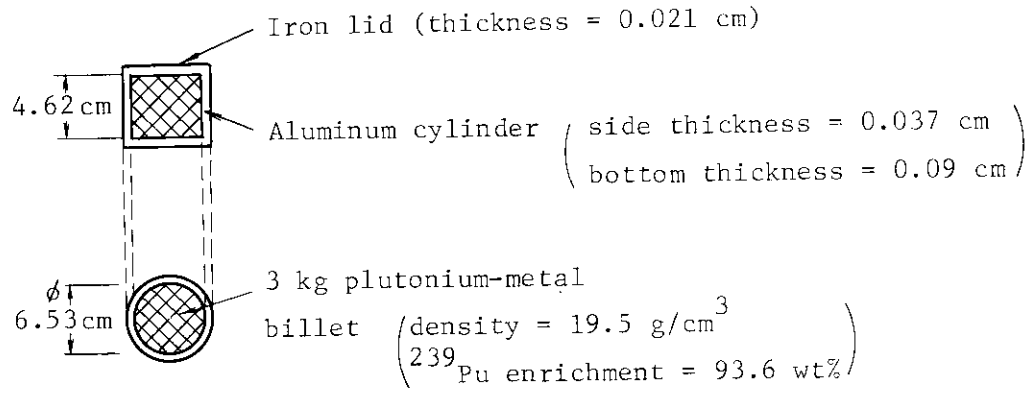

Fig. 3.B.6.1 Calculational model for a 3 kg plutonium-metal billet.

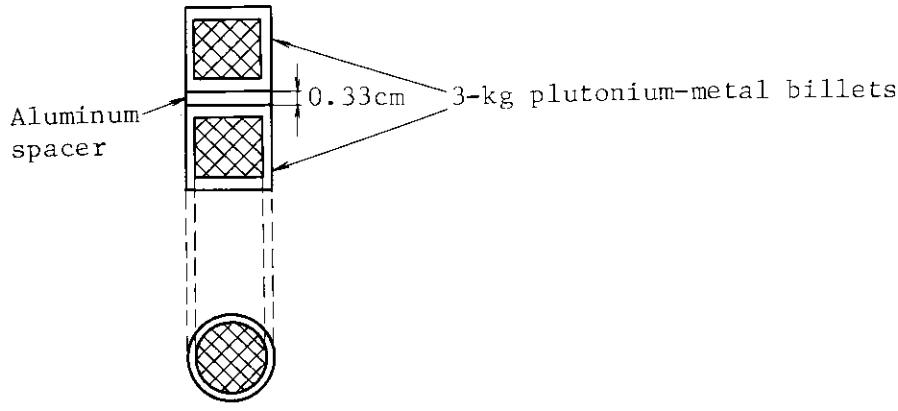

Fig. 3.B.6.2 Calculational model for a 6 kg plutonium-metal billet.

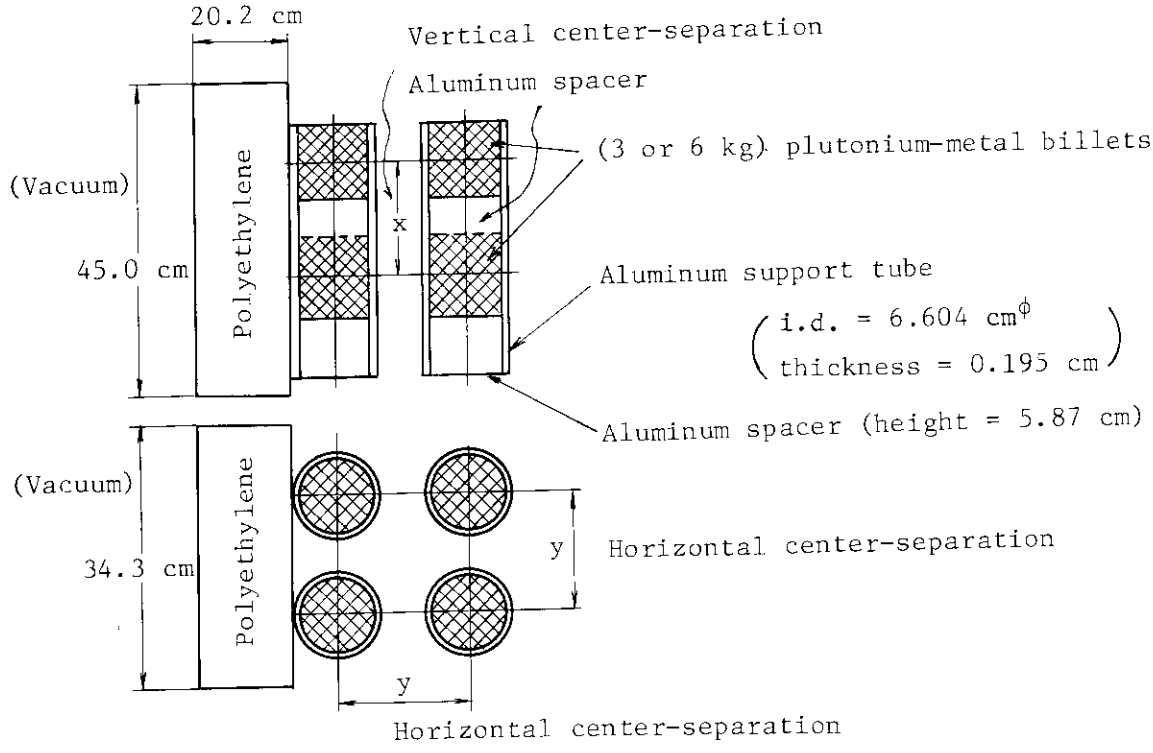

Fig. 3.B.6.3 Calculational model for a 2X2X2 array of plutonium-metal billets unmoderated with partial reflection.

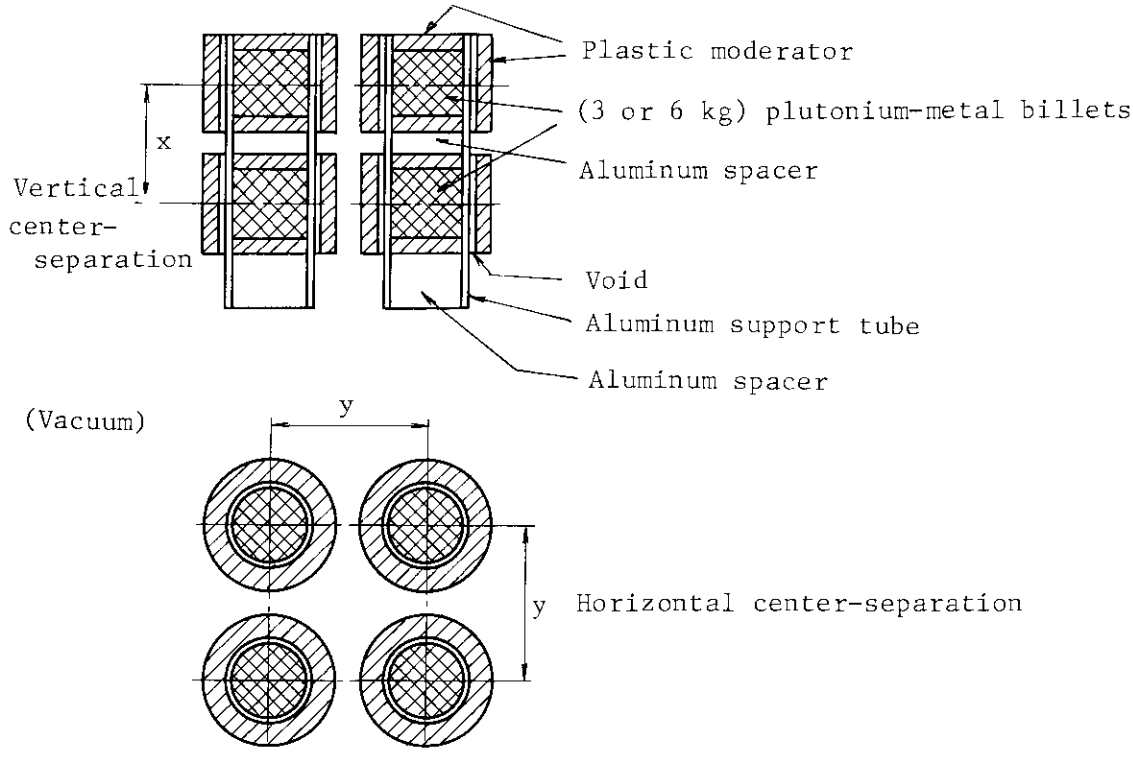

Fig. 3.B.6.4 Calculational model for a 2X2X2 array of plutonium-metal billets moderated without reflectors.

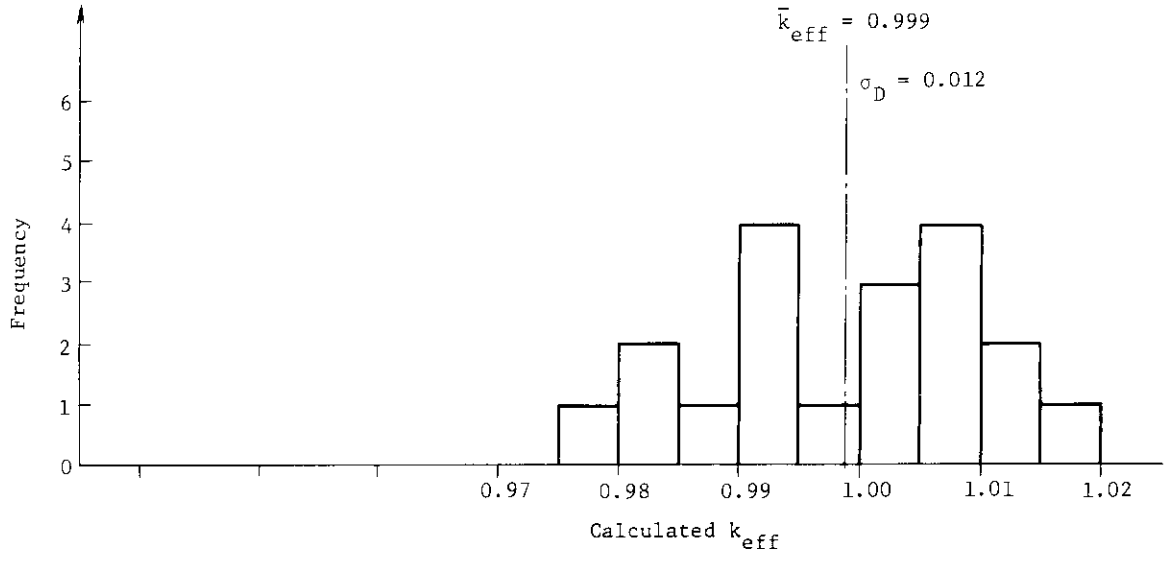

Fig. 3.B.6.5 Histogram of calculated k_{eff}'s for arrays of plutonium (19 cases).

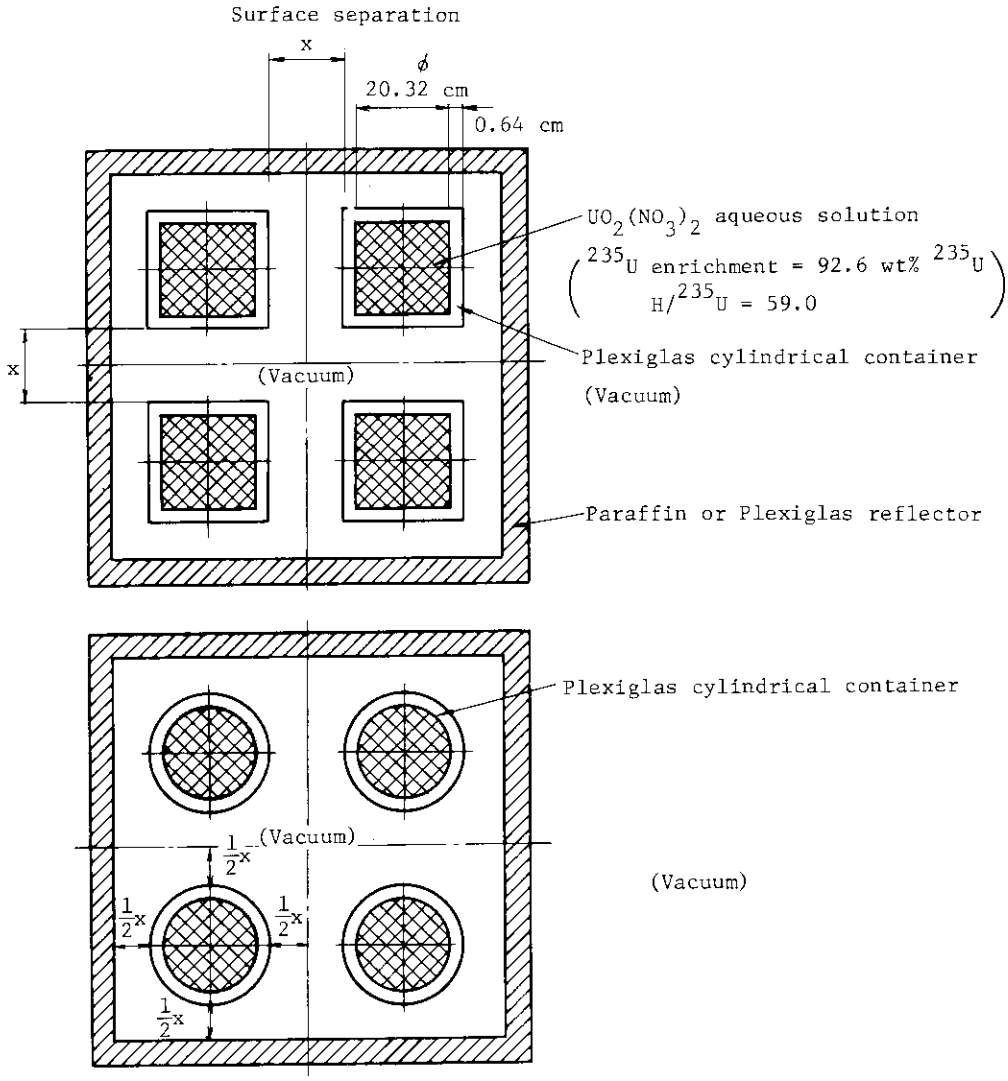

Fig. 3.B.7.1 Calculational model for a 2X2X2 array of $UO_2(NO_3)_2$ aqueous solution with reflectors.

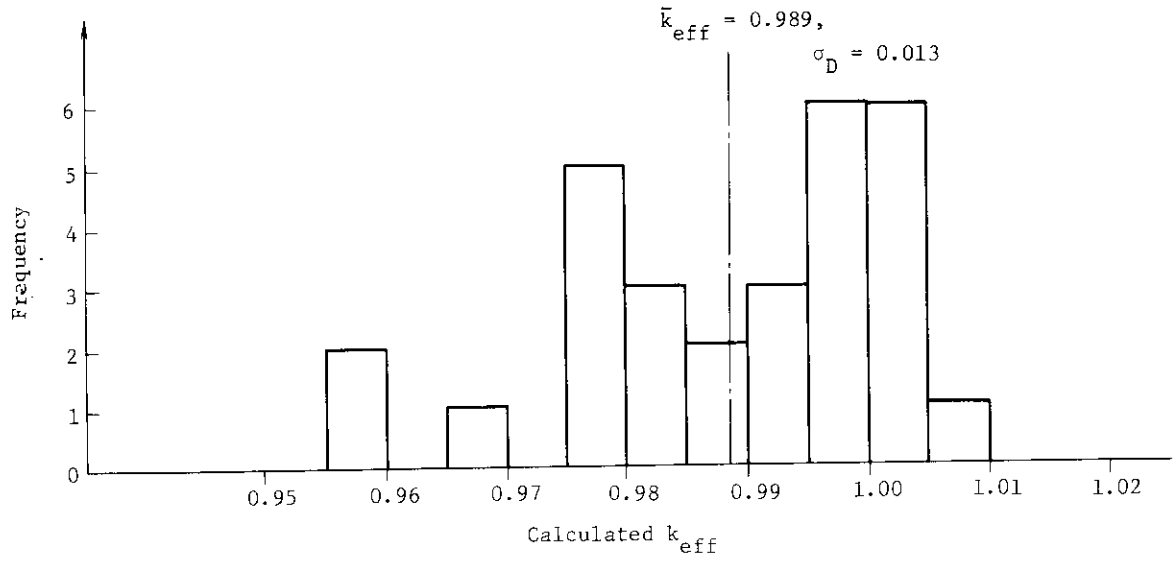

Fig. 3.B.7.2 Histogram of calculated k_{eff}'s for cubic arrays of uranyl-nitrate cylinders (29 cases).

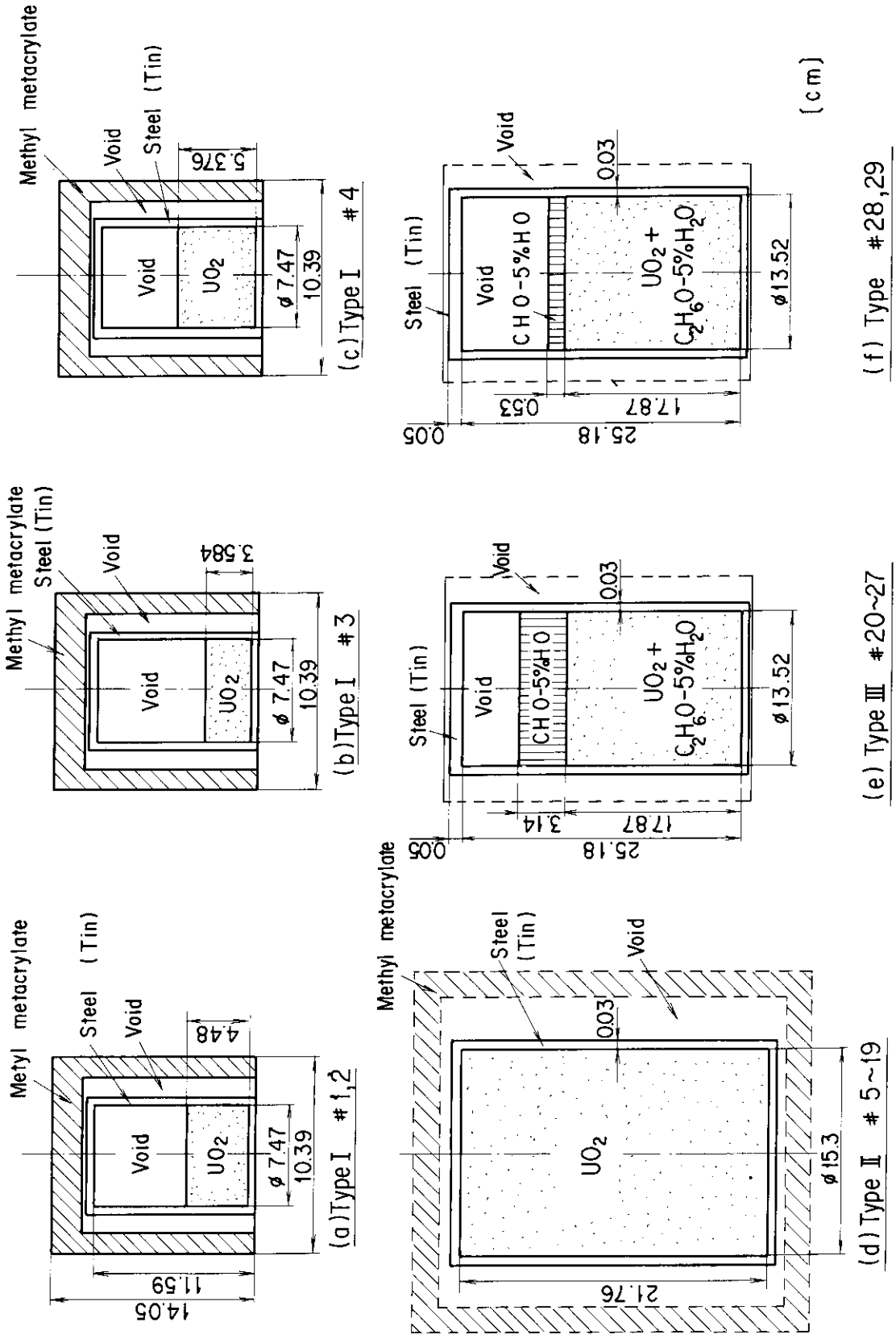

Fig. 3.B.8.1 Modeling of fuel unit.

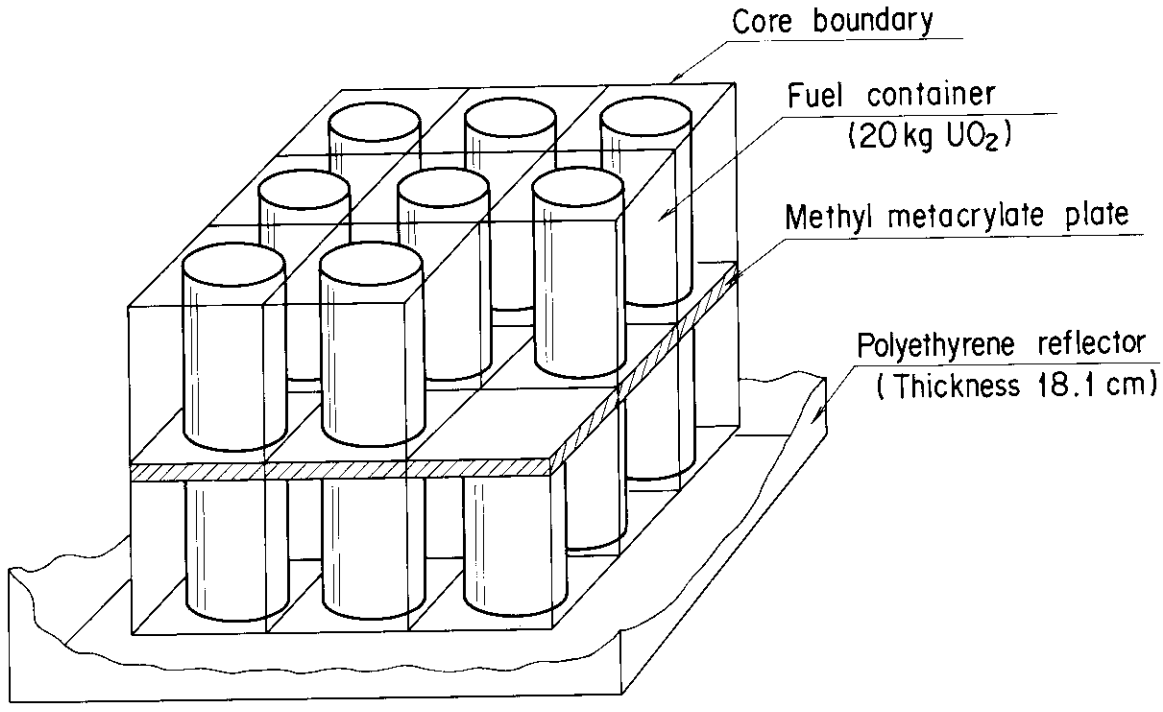

Fig. 3.B.8.2 Example of calculational model for array.

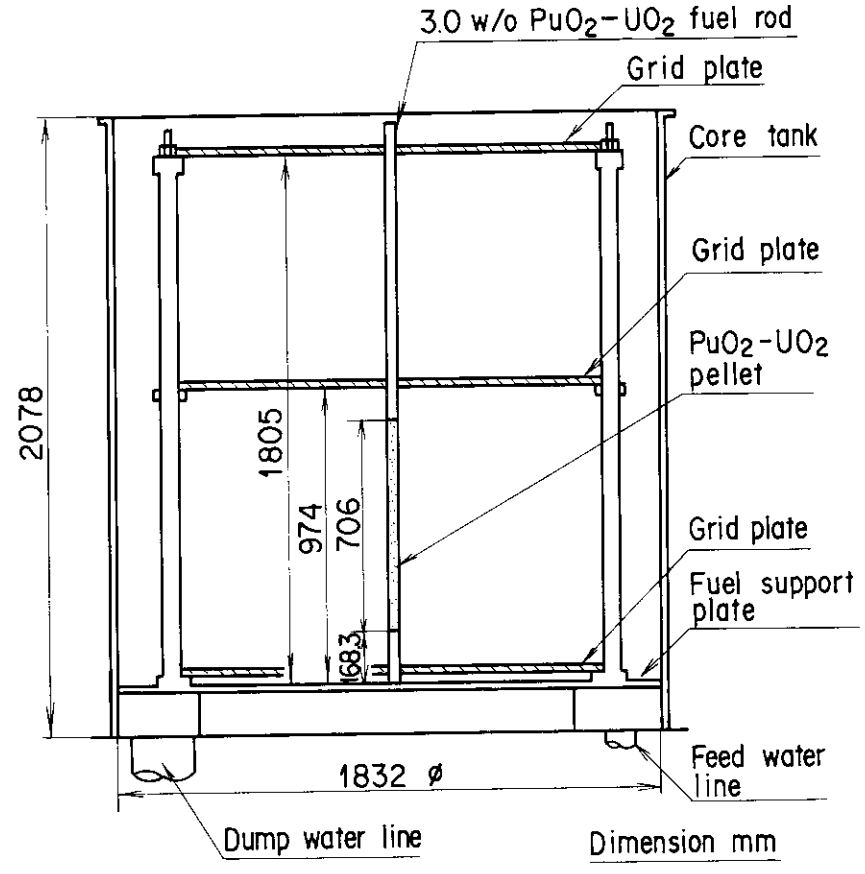

Fig. 3.C.1.1 Vertical cross-sectional view of core tank.

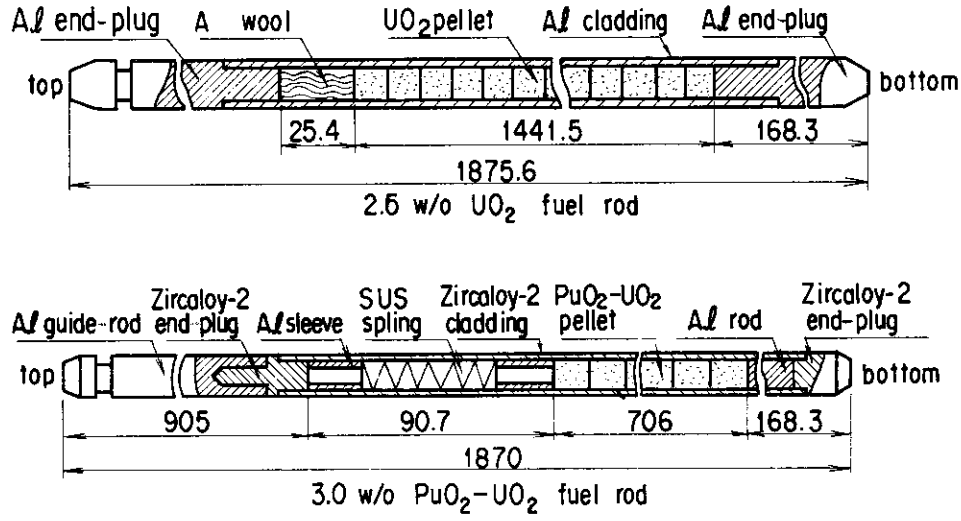

Fig. 3.C.1.2 2.6 wt% UO_2 and 3.0 wt% PuO_2-natural UO_2 fuel rods.

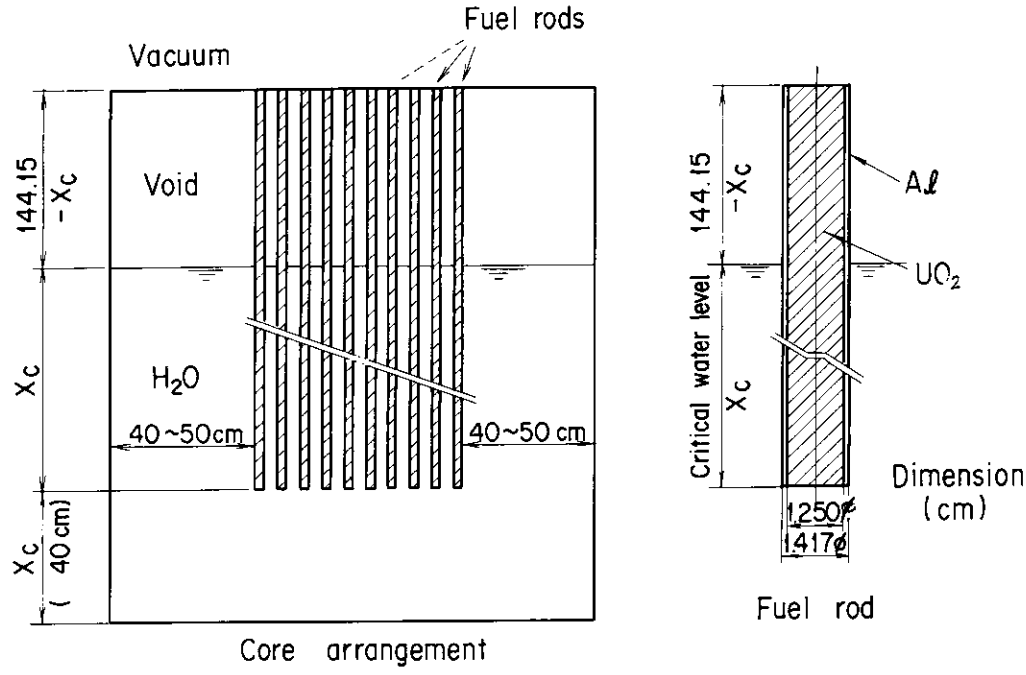

Fig. 3.C.1.3 Calculational model for UO_2 fuel lattice.

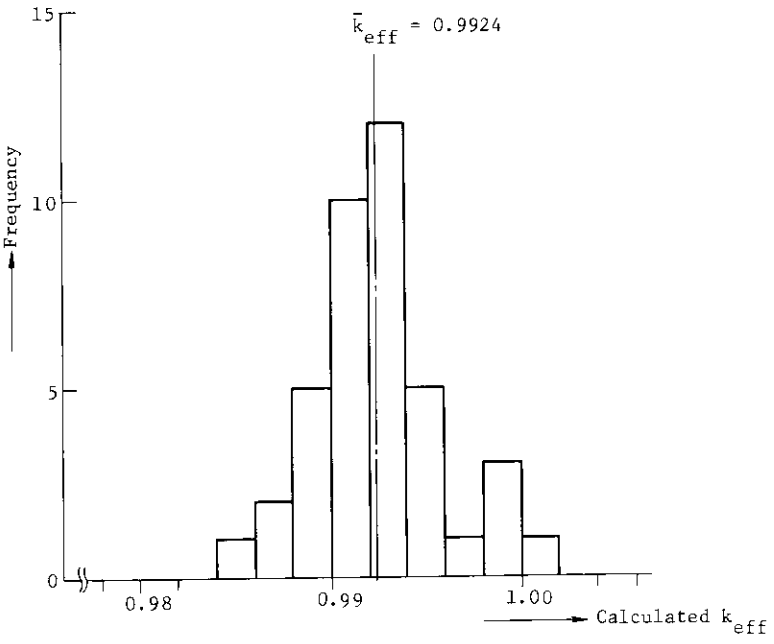

Fig. 3.C.1.4
Histogram of calculated k_{eff}'s for U(2.6)O_2-H_2O systems.

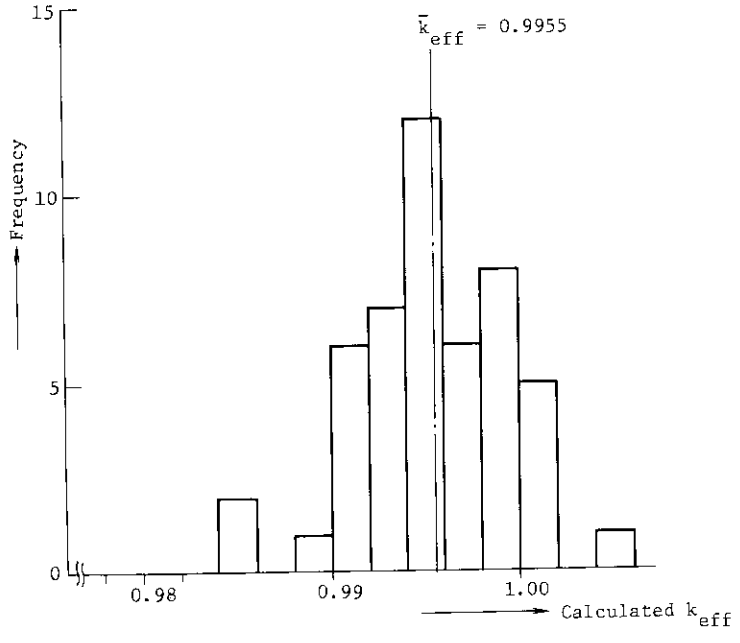

Fig. 3.C.1.5
Histogram of k_{eff}'s for PuO_2-U(Natural)O_2-H_2O systems.

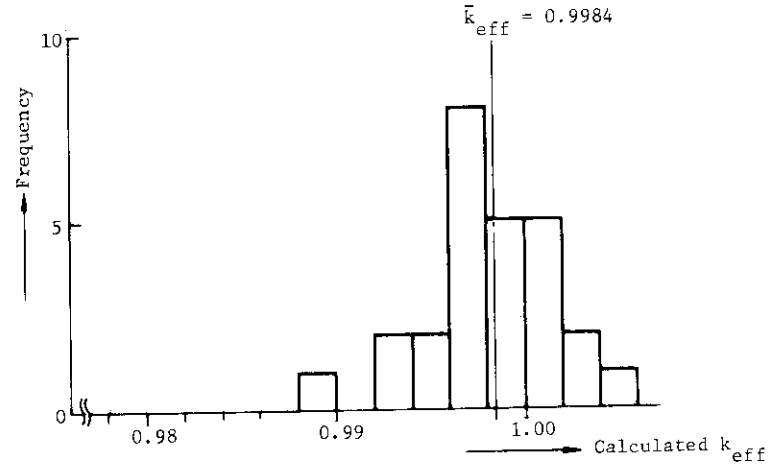

Fig. 3.C.1.6
Histogram of k_{eff}'s for U (2.6)O_2-poison sheet-H_2O systems.

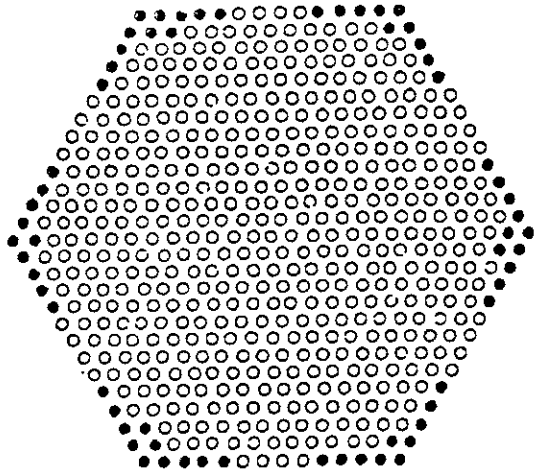

Pitch = 13.5 mm
Rods = 484
Holes = 63
Critical water height = 85.21 cm

Case No. 11

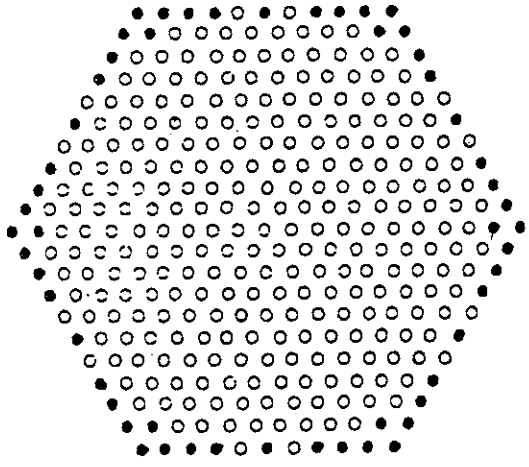

Pitch = 17.2 mm
Rods = 277
Holes = 54
Critical water height = 61.99 cm

Case No. 12

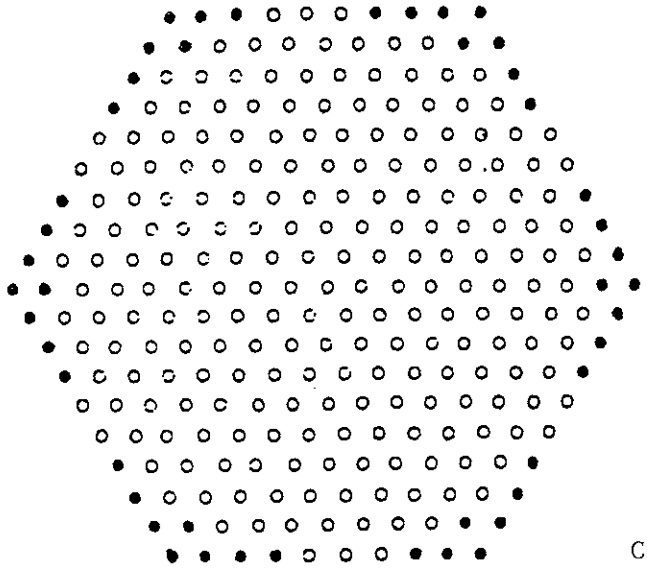

Pitch = 22.6 mm
Rods = 225
Holes = 48
Critical water height = 70.44 cm

Case No. 13

Fig. 3.C.2.1 Calculational models for representative cases of UO_2 rod hexagonal lattices. Solid circle indicates the removal of rods.

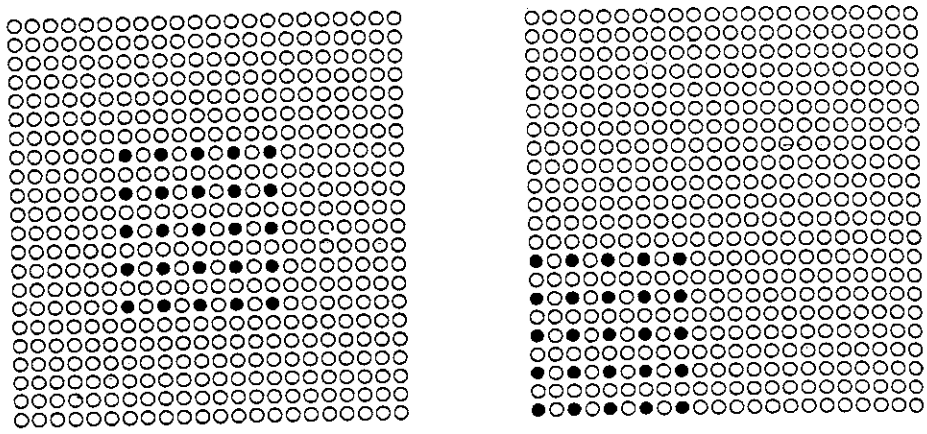

Fig. 3.C.2.2 Calculational models for representative cases of UO_2 rod square lattices. Solid circle indicates the removal of rods.

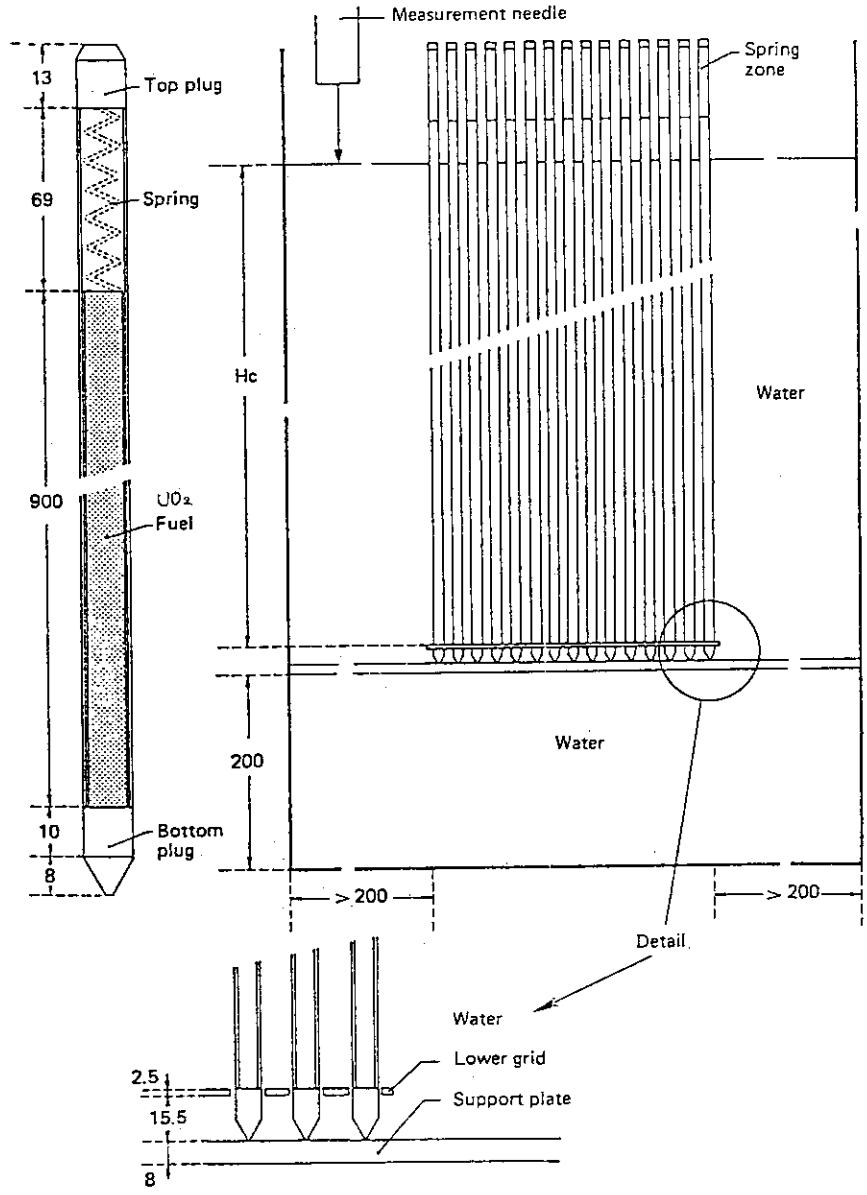

Fig. 3.C.2.3 Experimental arrangement of UO_2 rod clusters partially immersed in water.

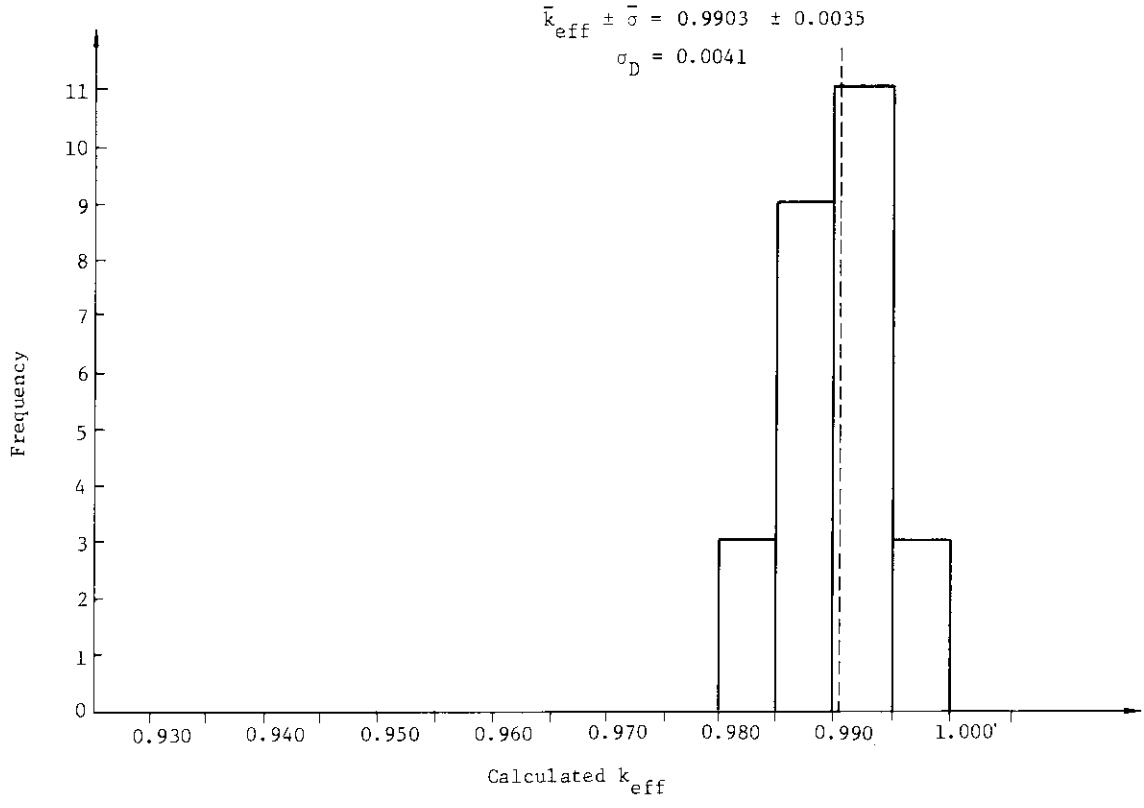

Fig. 3.C.2.4 Histogram of calculated k_{eff}'s for UO_2 rod clusters partially immersed in water (26 cases).

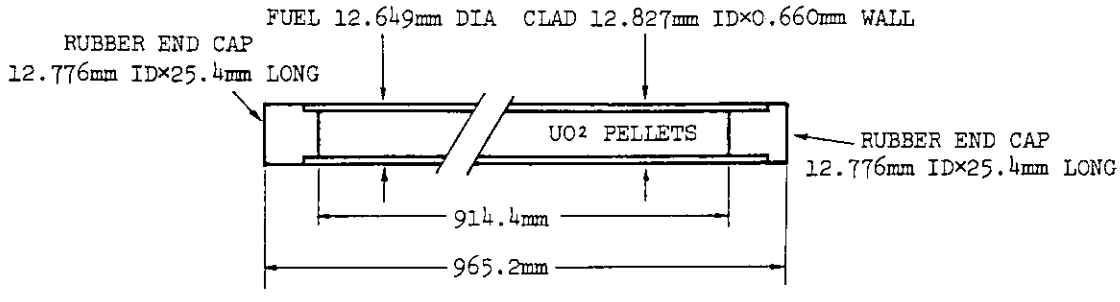

CLADDING: 6061 ALUMINUM TUBING

LOADING:

ENRICHMENT - 4.289±0.006wt% ^{235}U

FUEL DENSITY - 94.9±0.55% OF THEORETICAL DENSITY

URANIUM ASSAY - 88.055±0.261wt% OF TOTAL FUEL COMPOSITION

UO_2 - 1203.33±4.12g/ROD

Fig. 3.C.3.1 4.29 wt% ^{235}U enriched UO_2 rods.

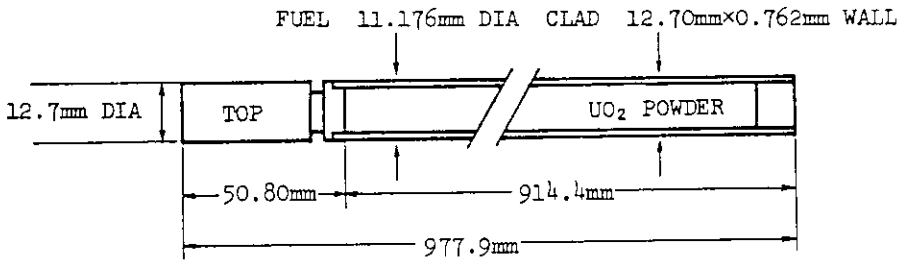

CLADDING: 6061 ALUMINUM TUBING SEAL WELDED WITH A LOWER END PLUG OF 5052-H32 ALUMINUM AND A TOP PLUG OF 1100 ALUMINUM

LOADING:

ENRICHMENT - 2.35±0.05wt% ^{235}U

FUEL DENSITY - 9.20mg/mm^3 (84% THEORETICAL DENSITY)

URANIUM ASSAY - 88.0wt%

UO_2- 825g/ROD (AVERAGE)

Fig. 3.C.3.2 2.35 wt% ^{235}U enriched UO_2 rods.

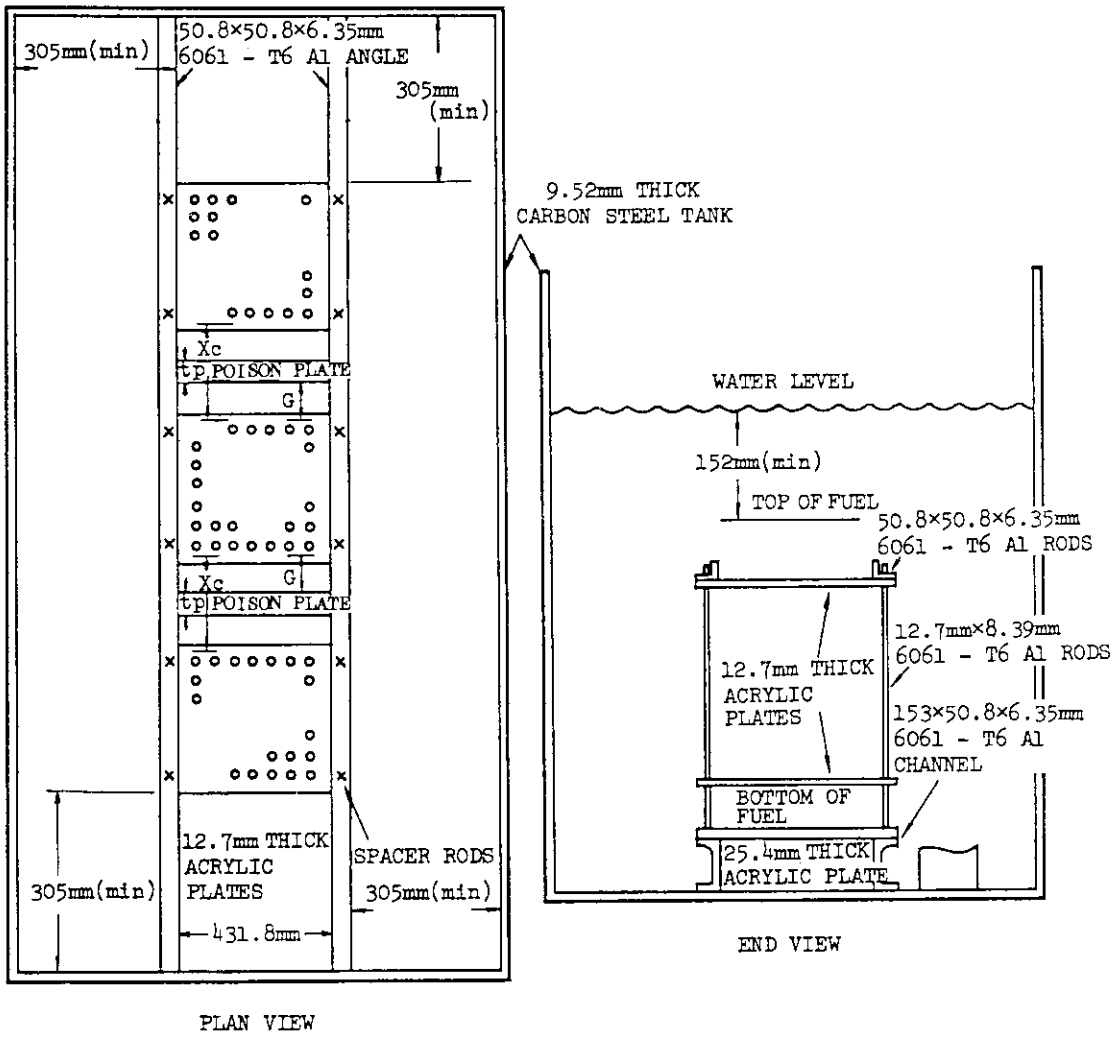

Fig. 3.C.3.3 Experimental arrangement of simulated shipping containers with poison plates.

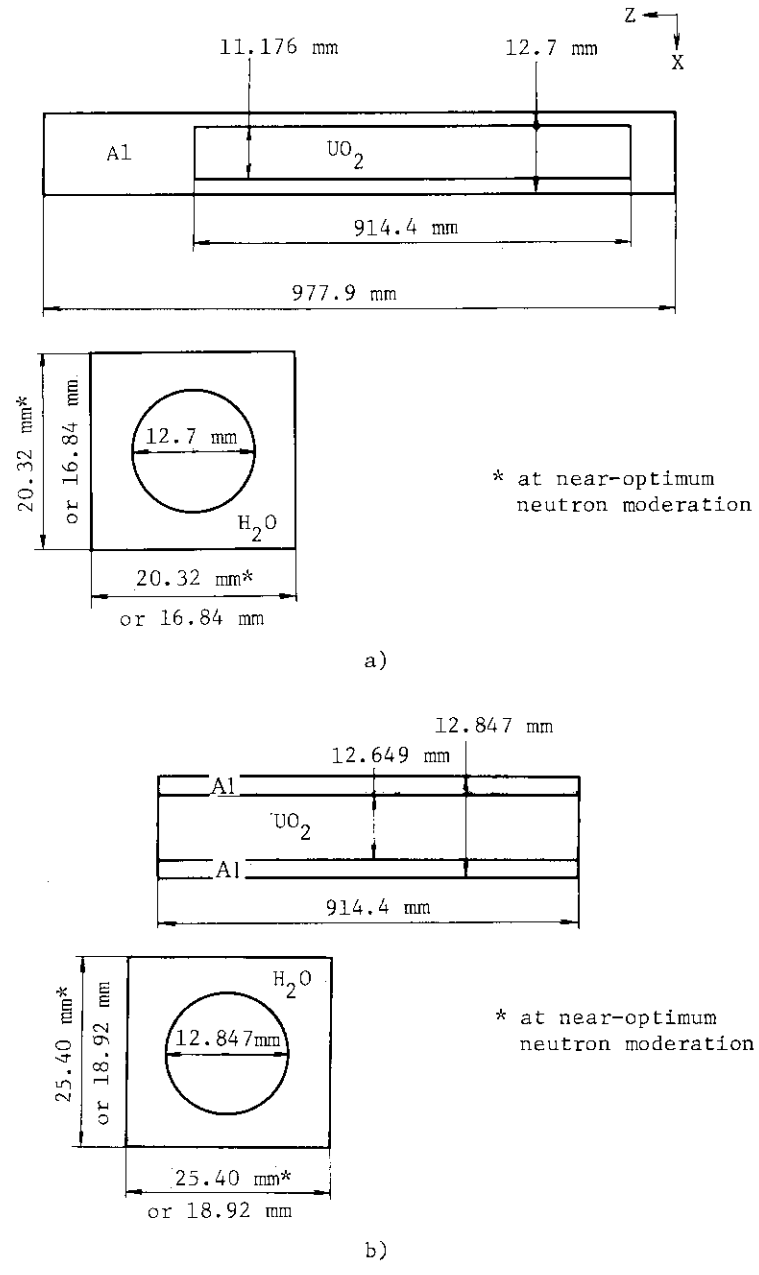

Fig. 3.C.3.4 Calculational model for UO_2 lattice cell.
a) 2.35 wt% ^{235}U fuel rod cell model.
b) 4.31 wt% ^{235}U fuel rod cell model.

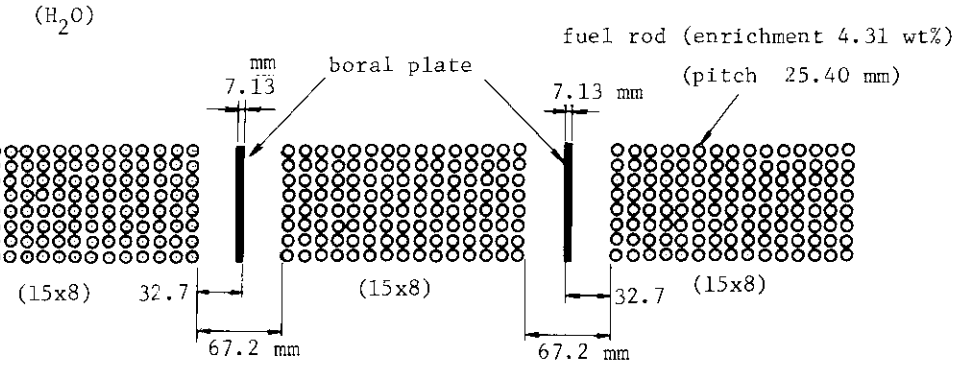

Fig. 3.C.3.5 A typical KENO-IV calculational model for UO_2 rod clusters submerged in water with boral poison plates.

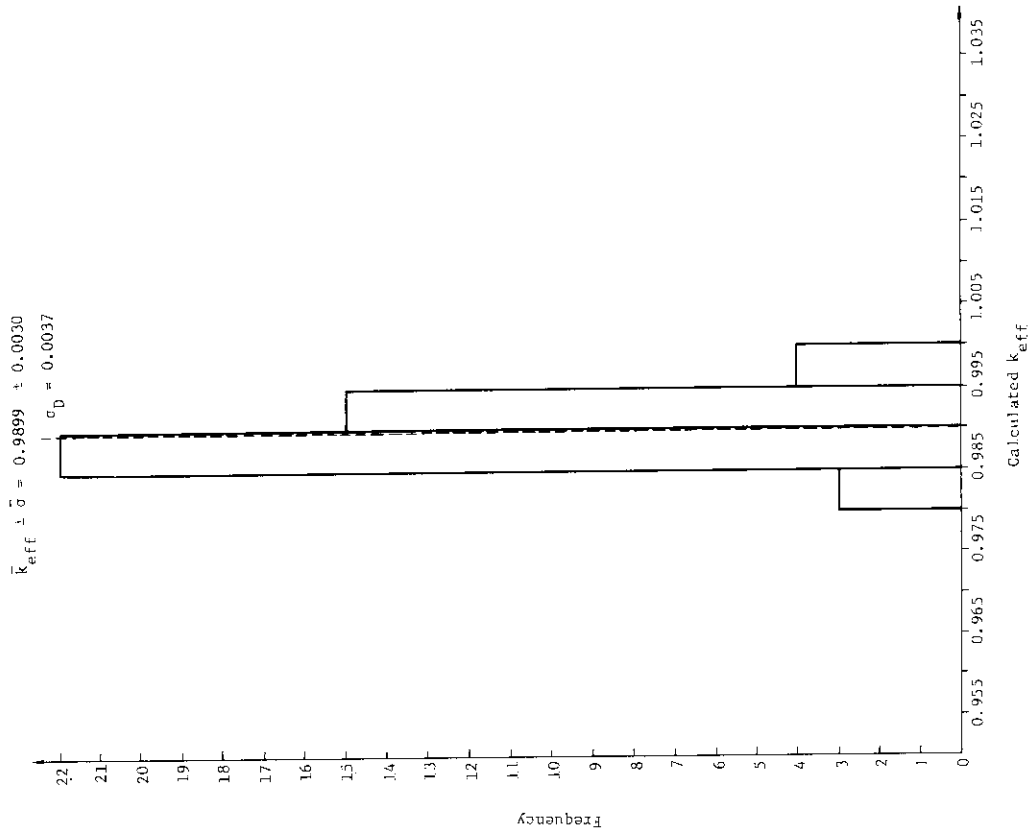

Fig. 3.C.3.7 Histogram of calculated k_{eff}'s for UO_2 rod clusters (^{235}U enrichment: 2.35 wt%, lattice pitch 20.32 mm) in water with various poison plates (44 cases).

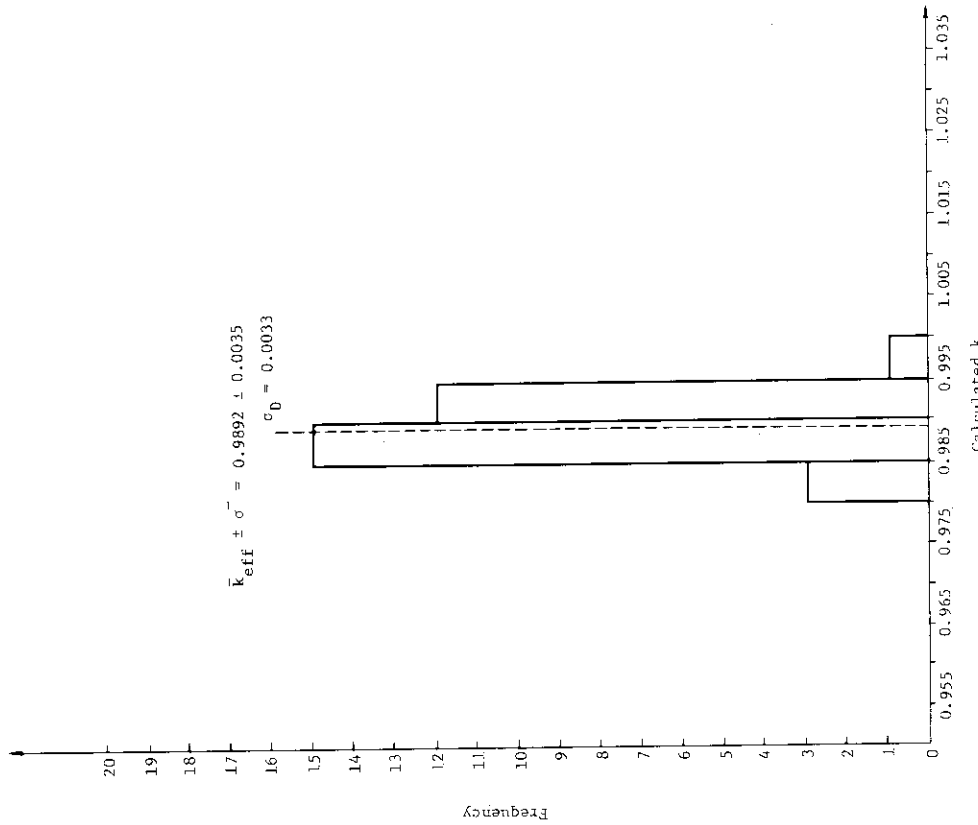

Fig. 3.C.3.6 Histogram of calculated k_{eff}'s for UO_2 rod clusters (^{235}U enrichment: 4.31 wt%, lattice pitch: 25.40 mm) in water with various poison plates (31 cases).

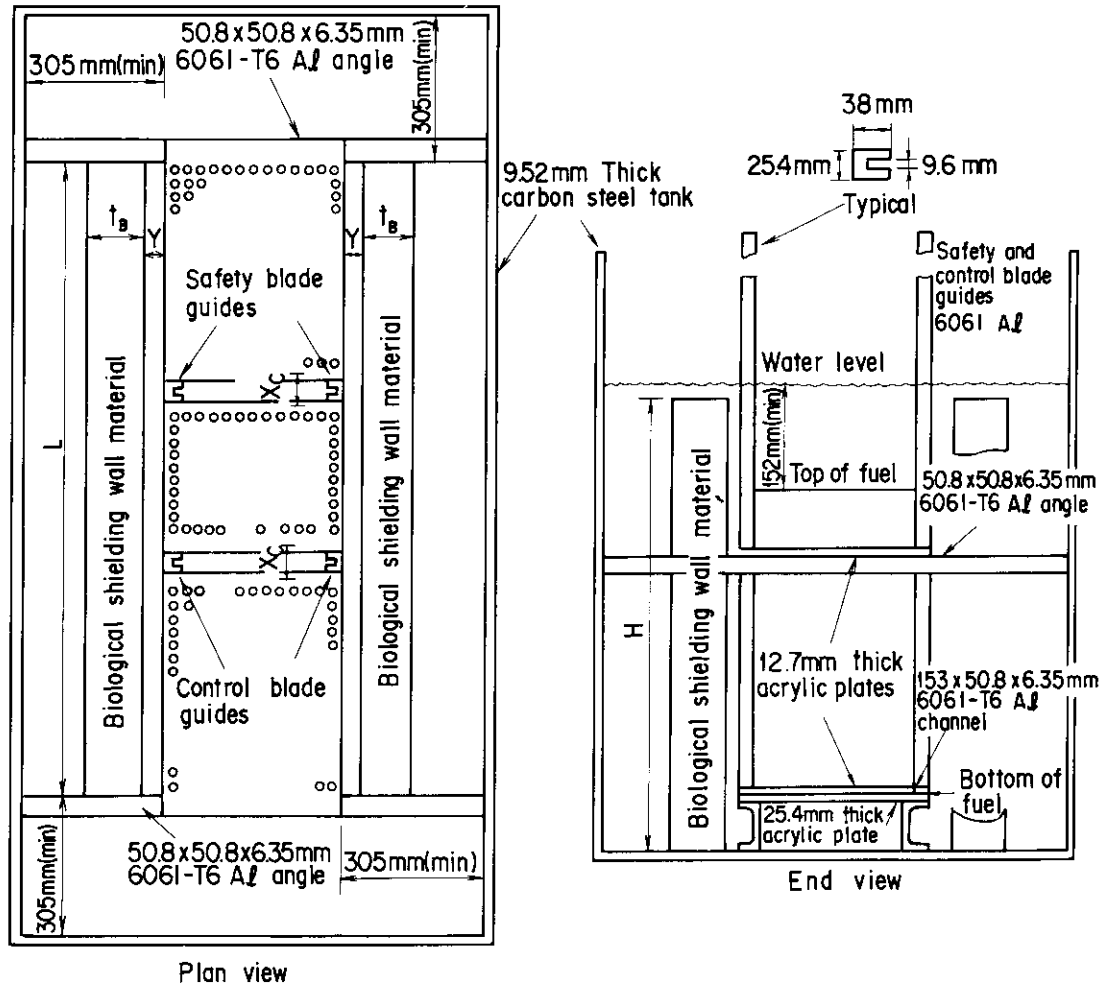

Fig. 3.C.4.1 Graphical arrangement of simulated shipping container critical experiments.

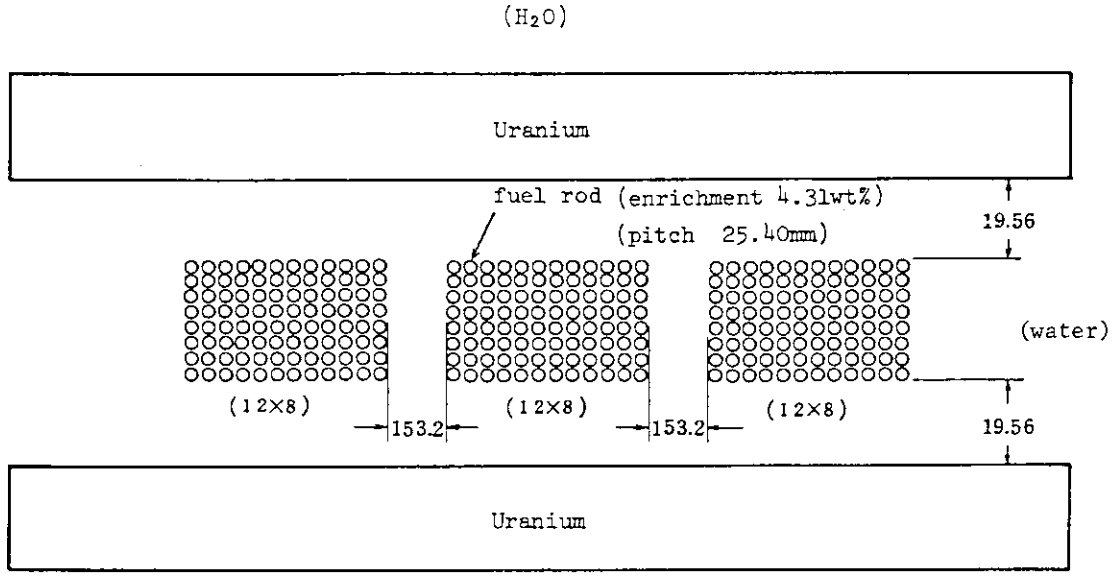

Fig. 3.C.4.2 A typical KENO-IV calculational model for UO_2 rod clusters submerged in water with reflecting walls.

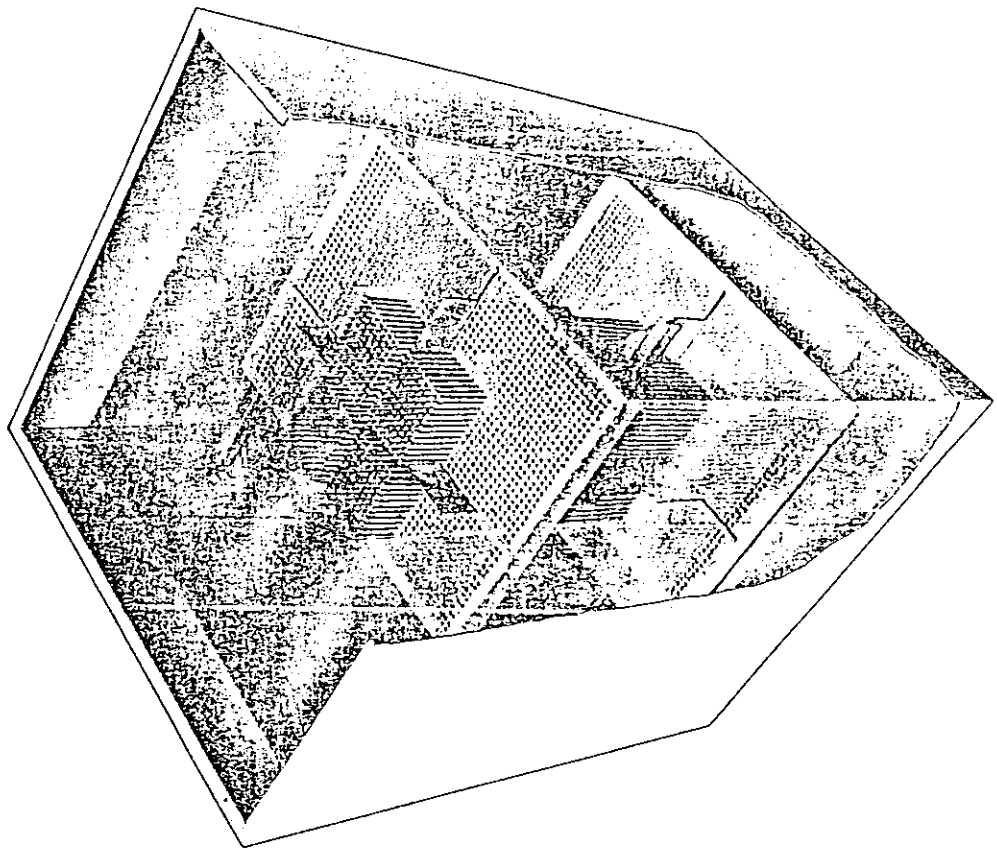

Fig. 3.C.5.1 Bird's eye view of typical four cross arranged clusters in water pool.

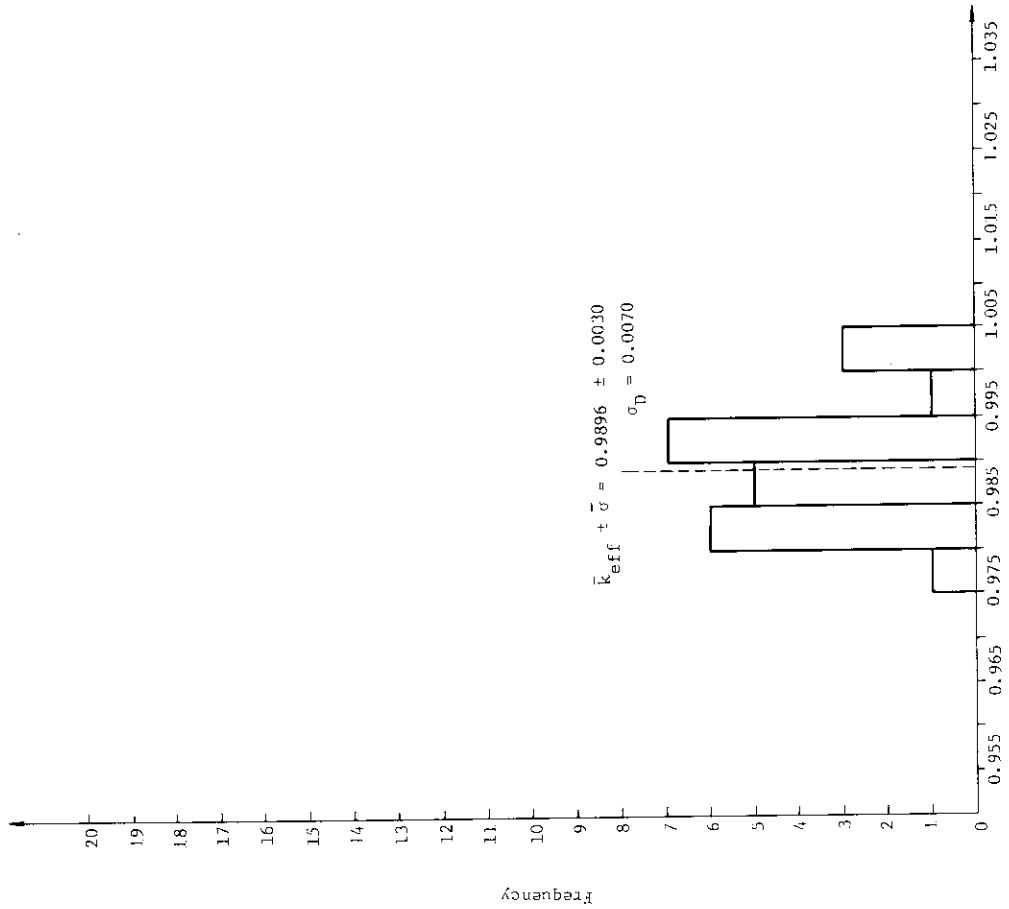

Fig. 3.C.4.3 Histogram of calculated k_{eff}'s for UO_2 rod clusters submerged in water with reflecting walls (23 cases).

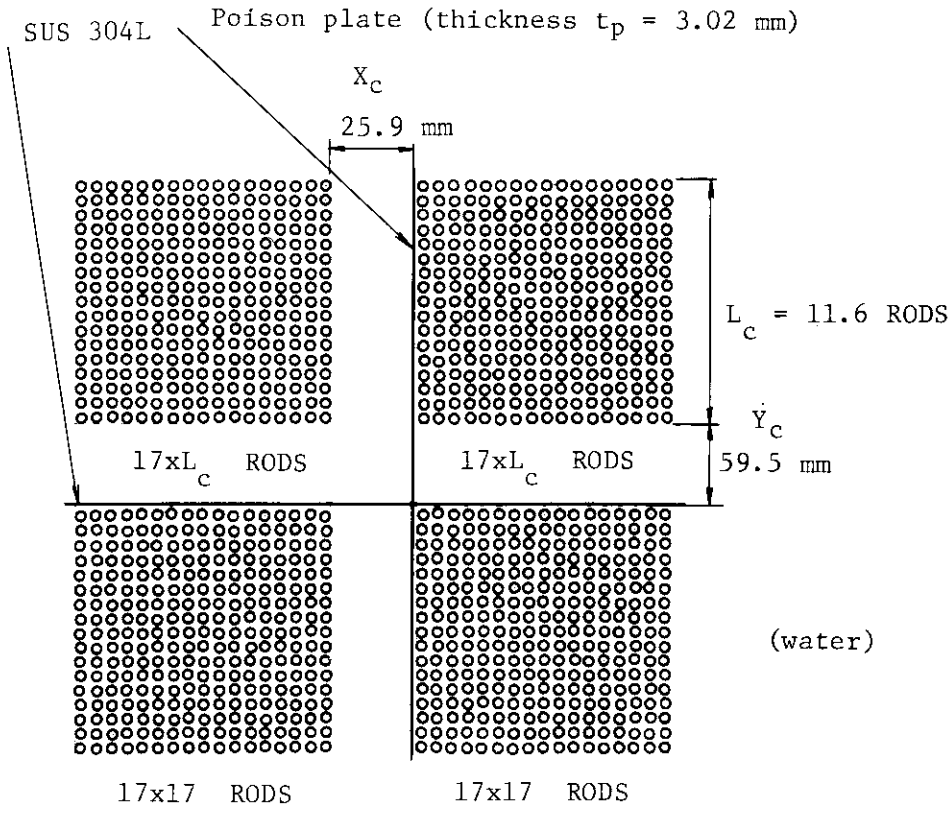

Fig. 3.C.5.2 Typical calculational model for four cross arranged clusters (Case No.100).

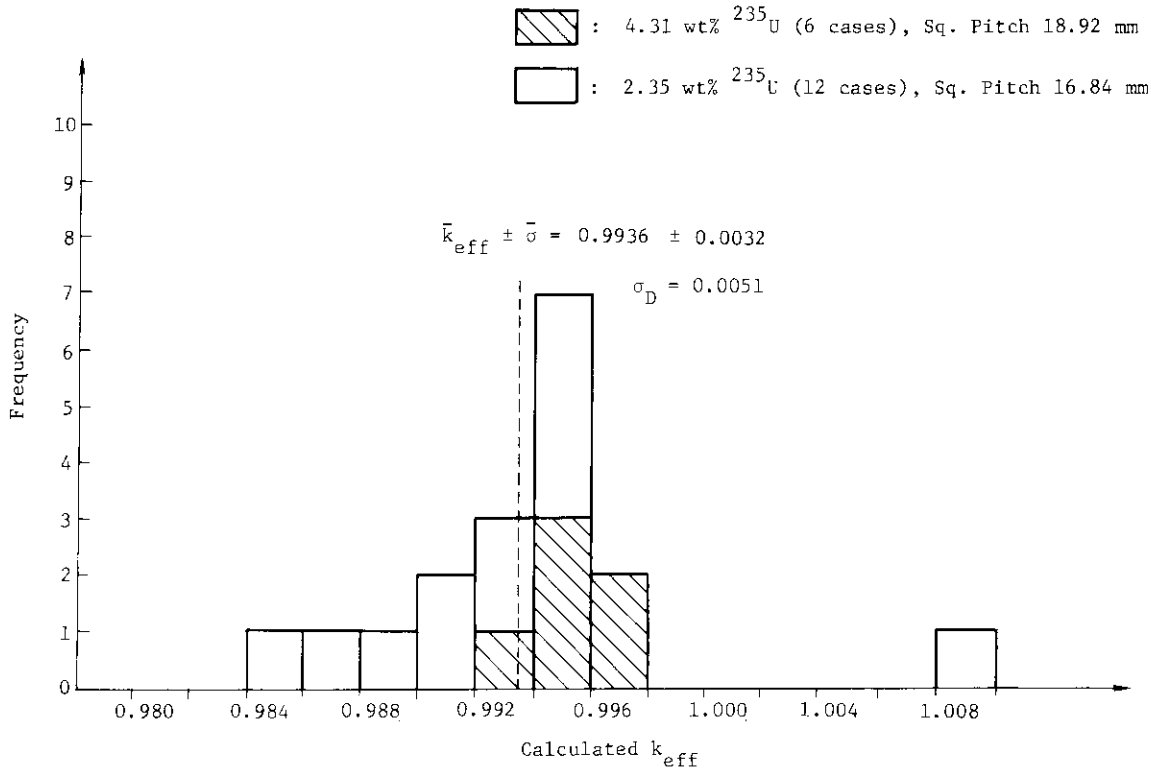

Fig. 3.C.5.3 Histogram of calculated k_{eff}'s for three lined clusters (18 cases).

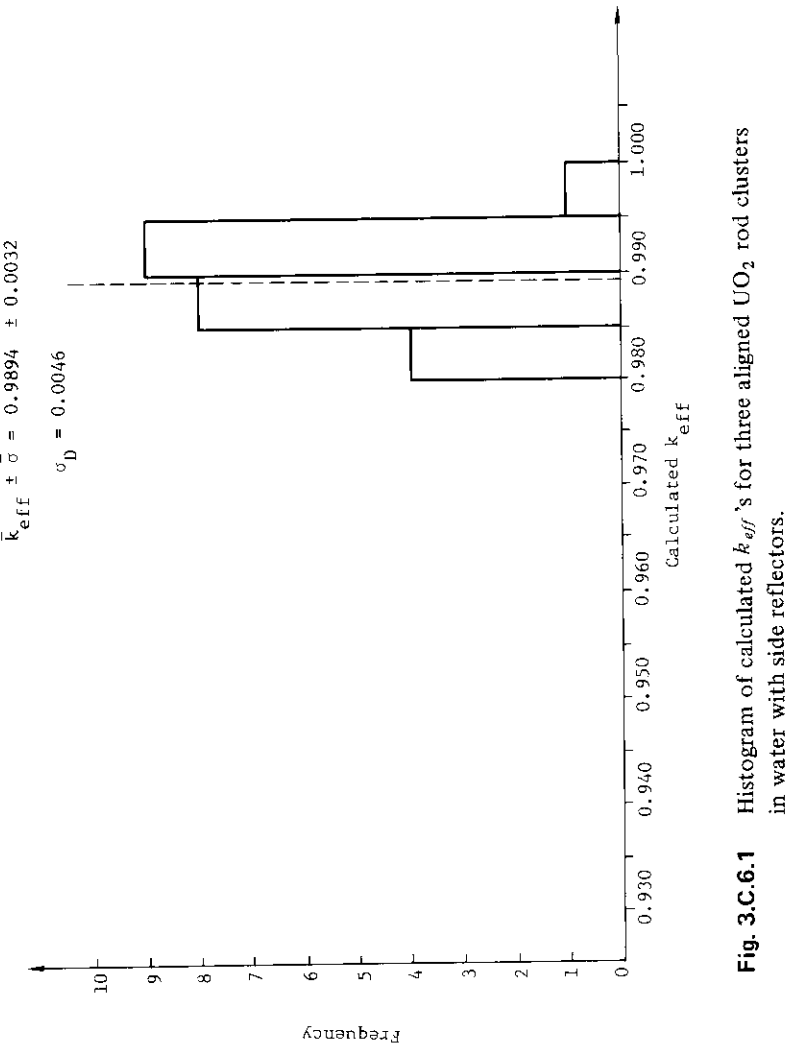

Fig. 3.C.6.1 Histogram of calculated k_{eff}'s for three aligned UO_2 rod clusters in water with side reflectors.

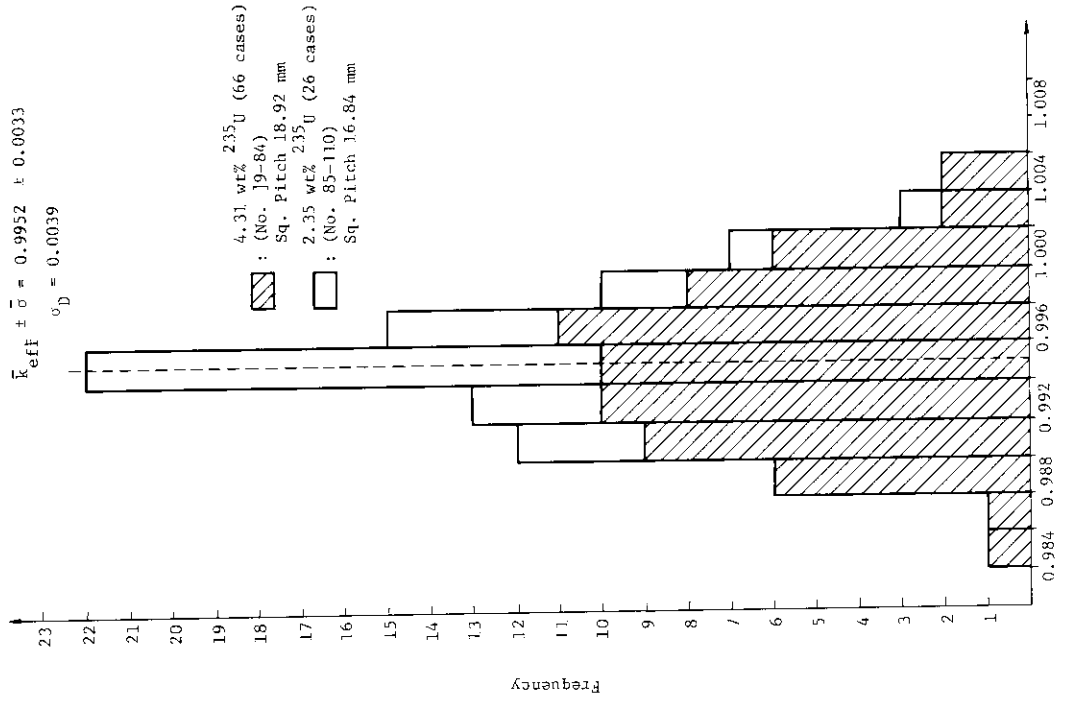

Fig. 3.C.5.4 Histogram of calculated k_{eff}'s for four cross arranged clusters (92 cases).

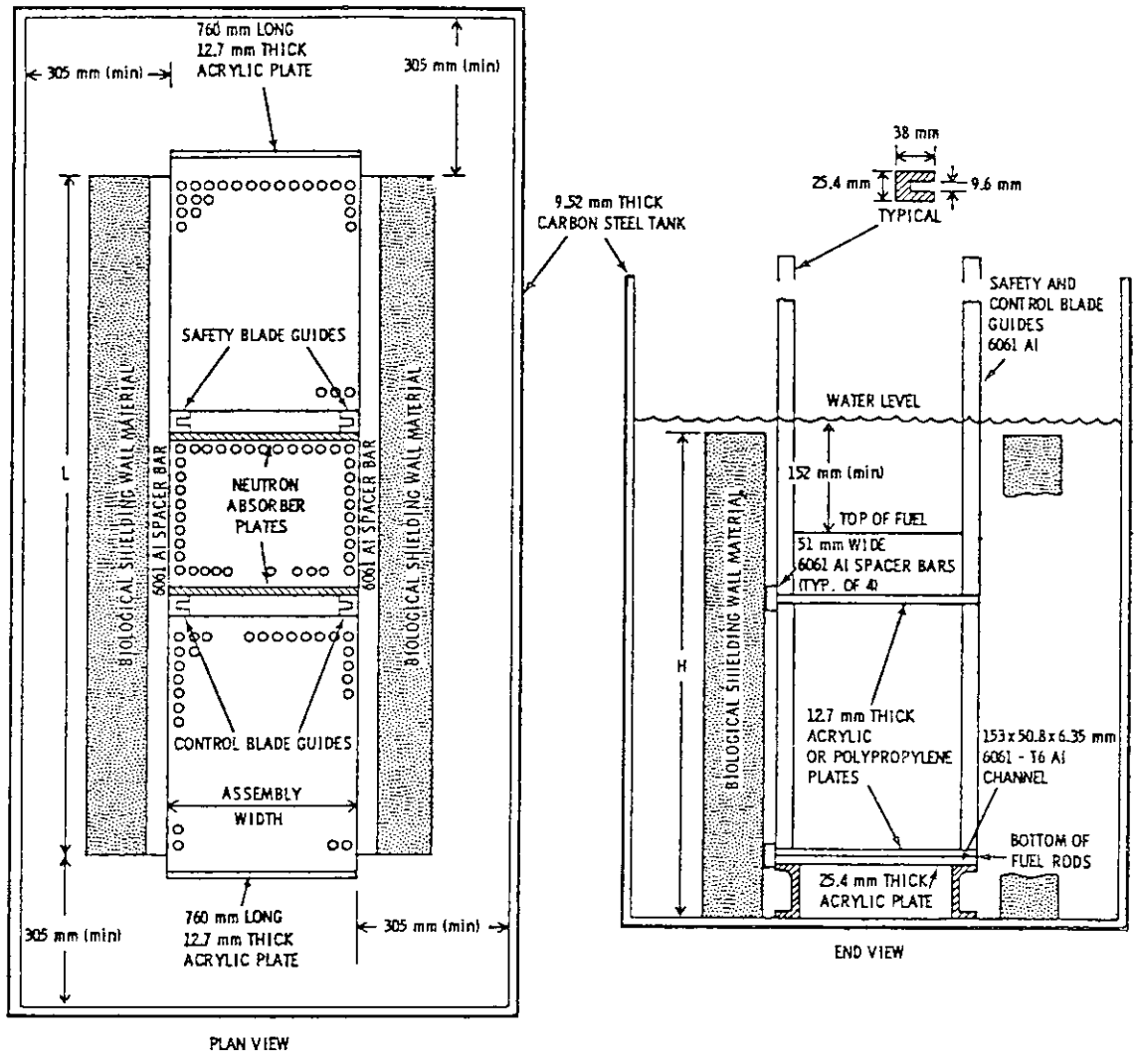

Fig. 3.C.7.1 Experimental arrangement of three UO_2 rod clusters in water with absorbers and reflecting walls.

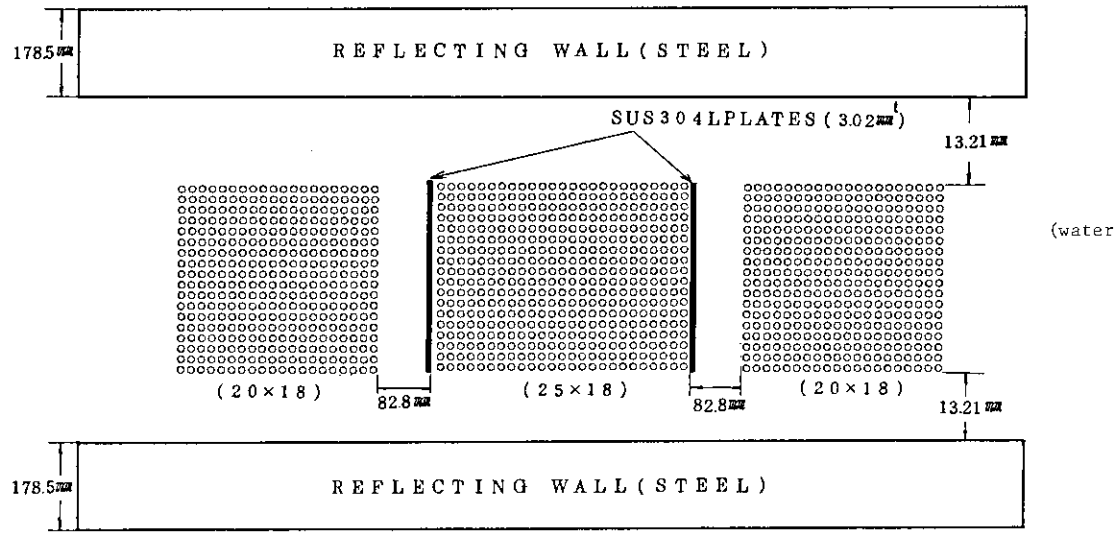

Fig. 3.C.7.2 Calculational model for three UO_2 rod clusters in water with absorbers and reflecting walls.

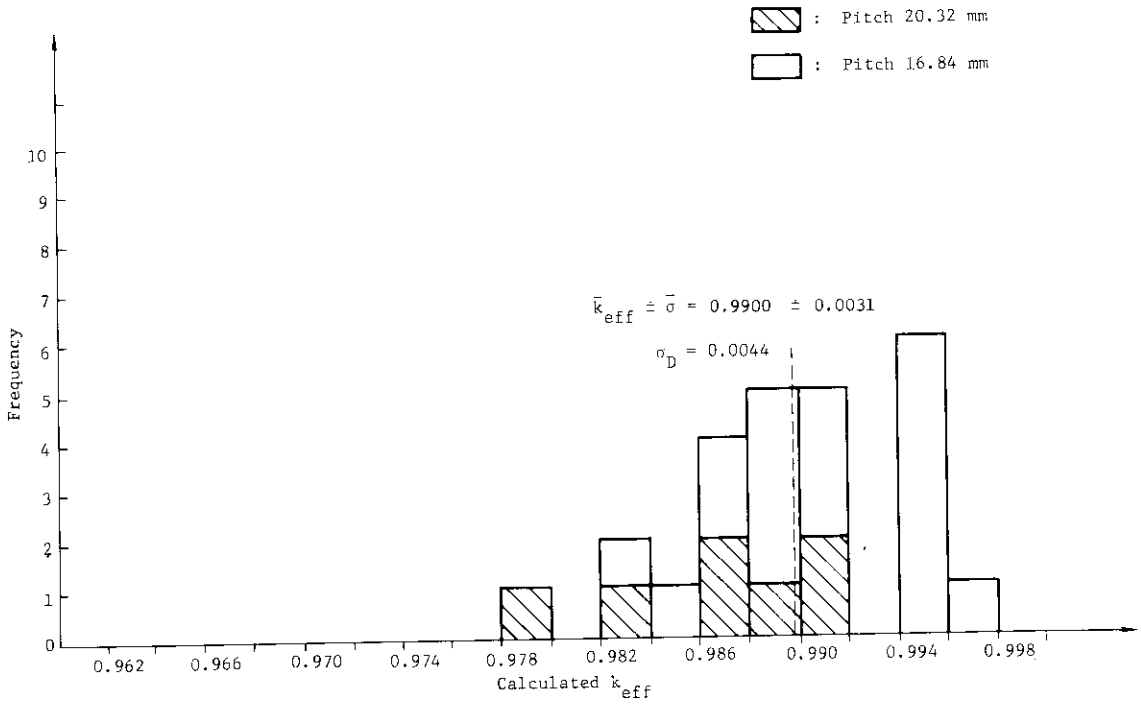

Fig. 3.C.7.3 Histogram of calculated k_{eff}'s for three UO_2 rod clusters (^{235}U enrichment: 2.35 wt%) in water with neutron absorbers and reflecting walls (25 cases).

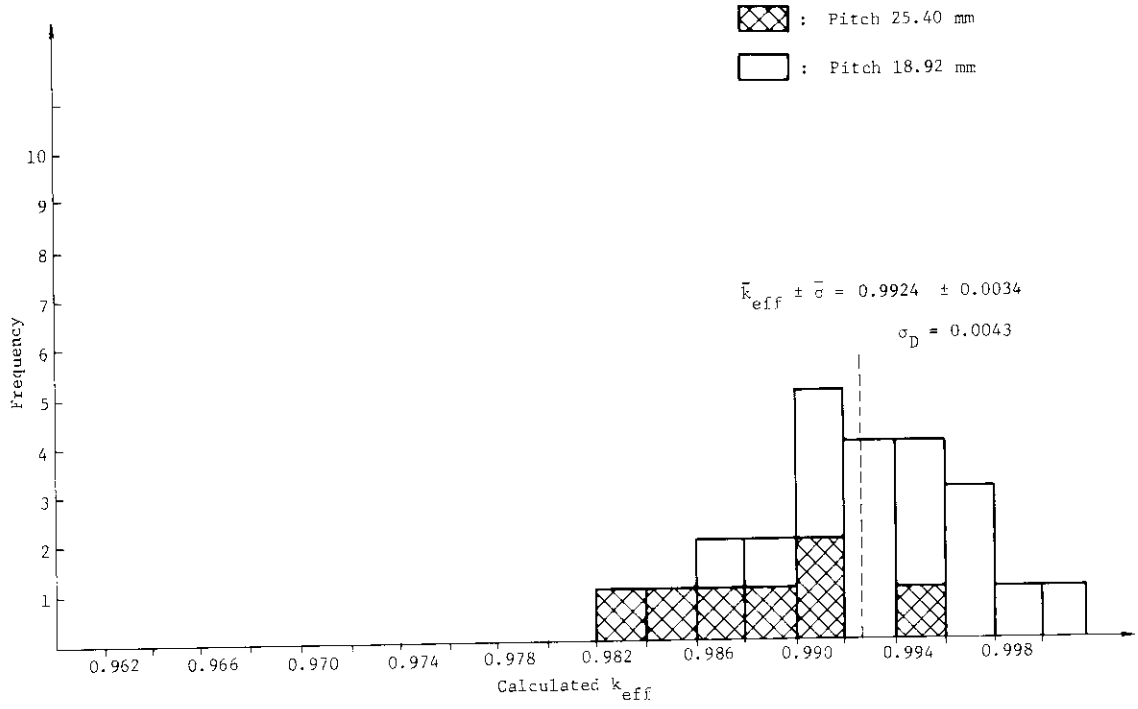

Fig. 3.C.7.4 Histogram of calculated k_{eff}'s for three UO_2 rod clusters (^{235}U enrichment: 4.31 wt%) in water with neutron absorbers and reflecting walls (24 cases).

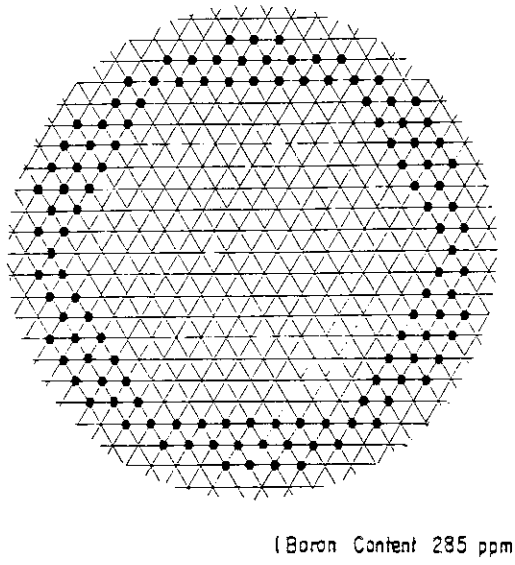

Fig. 3.C.8.1 Calculational model for B.M. No.26, N_c=288.

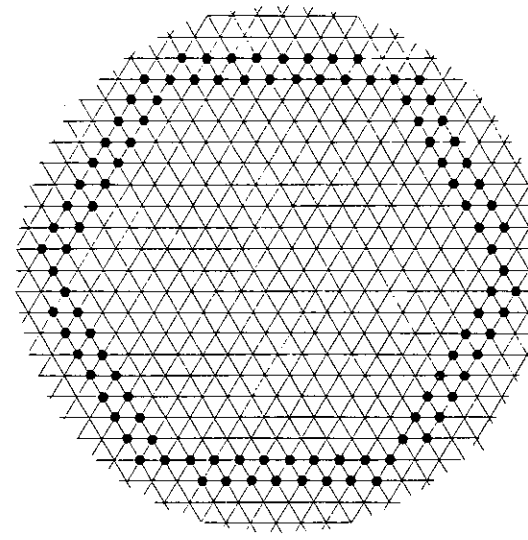

Fig. 3.C.8.2 Calculational model for B.M. No.27, N_c=320.

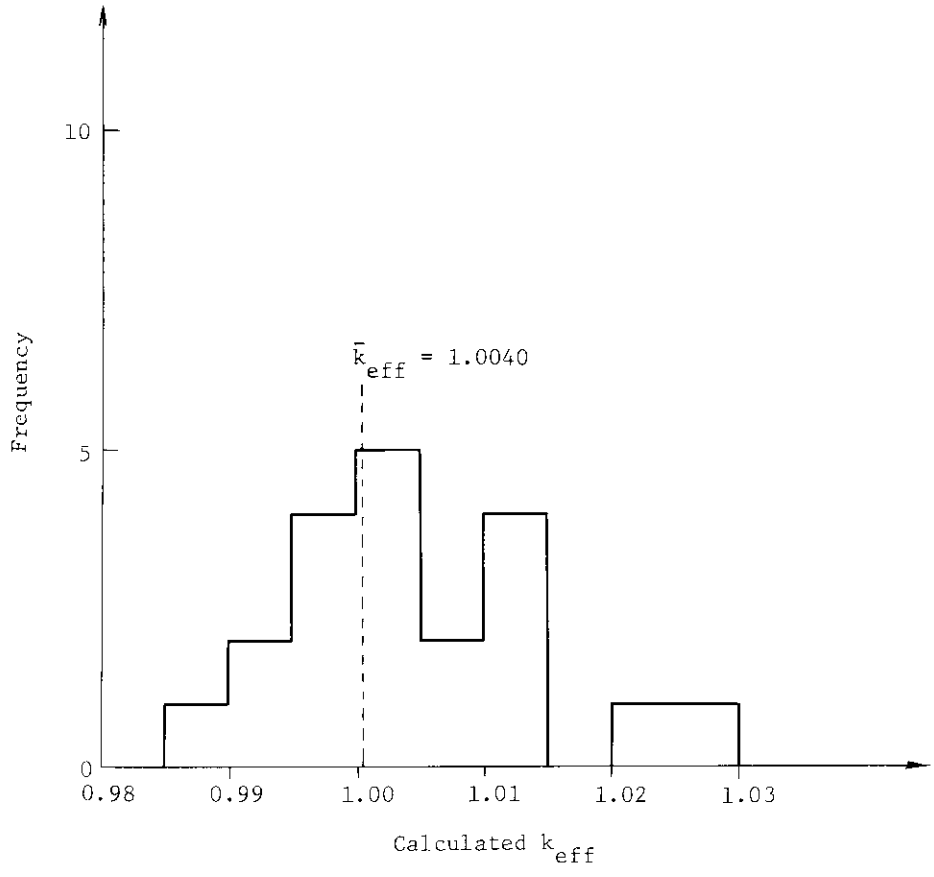

Fig. 3.C.8.3 Histogram of calculated k_{eff}'s for the heterogeneous plutonium benchmark experiments (20 cases).

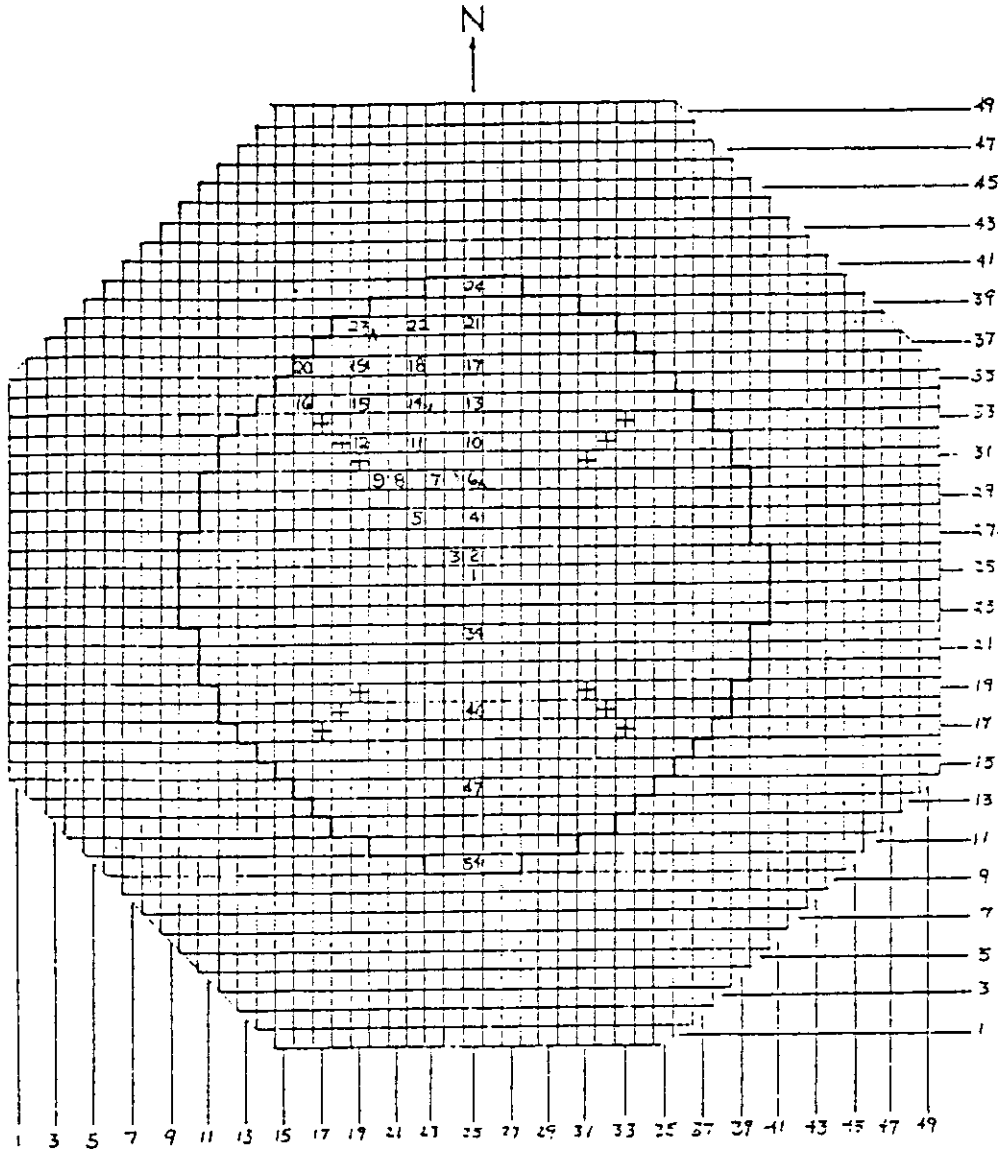

0.615-INCH UO_2 CORE, UNBORATED, GAMMA SCAN IRRADIATION

Top Reflector thickness 6.0 inches. Moderator Temp. 21.90 °C

Excess Reactivity 6.88 cents. Boron concentration, < 1 wppm.

Number and Type of Fuel Rods in Core:

UO_2-2.35% ^{235}U 708

β_{eff} = 6.99 $\times 10^{-3}$

Top Reflector thickness during Irradiation 6.0 inches.

A=Axial Scan D=Decay Rod

N=Normalization Rod

Fig. 3.C.9.1 Example of fuel pins loading pattern.

FUEL SPECIFICATIONS: 2.35% ENRICHED UO_2

FUEL RODS

1. ROD DIMENSIONS

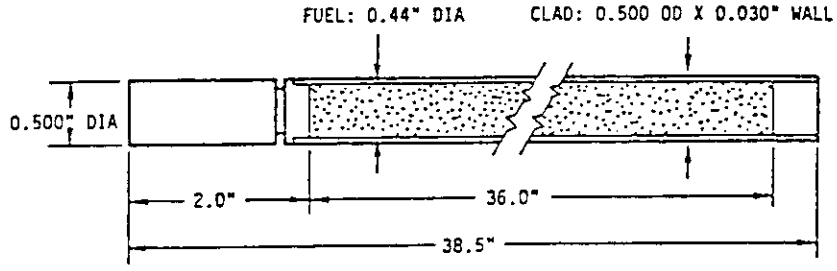

2. CLADDING: 6061 ALUMINUM TUBING SEAL WELDED WITH A LOWER END PLUG OF 5052-H32 ALUMINUM AND A TOP PLUG OF 1100 ALUMINUM.
3. TOTAL WEIGHT OF LOADED FUEL RODS: 917 gm (AVERAGE)

FUEL LOADING

1. FUEL MIXTURE VIBRATIONALLY COMPACTED.
2. 825 gm OF UO_2 POWDER/ROD, 726 gm OF U/ROD, 17.08 gm OF U-235/ROD.
3. ENRICHMENT - 2.35 ± 0.05 w/o U-235.
4. FUEL DENSITY - 9.20 gm/cm^3 (84% THEORETICAL DENSITY).

Fig. 3.C.9.2 UO_2-2.35 wt% ^{235}U fuel description.

FUEL SPECIFICATIONS: UO_2 - 2 WT% PuO_2

FUEL RODS

1. ROD DIMENSIONS

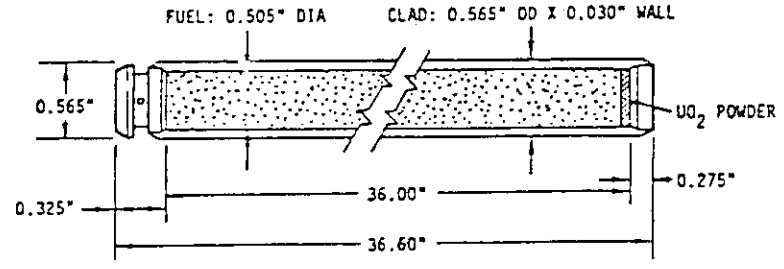

2. CLADDING: ZIRCALOY-2 TUBING WITH PLUGS SEAL WELDED AT BOTH ENDS.
3. TOTAL WEIGHT OF LOADED FUEL RODS: 1340 gms (AVERAGE)

FUEL LOADINGS

1. PuO_2 MIXED IN NATURAL UO_2 AND VIBRATIONALLY COMPACTED.
2. 1128 gms OF UO_2-PuO_2 MIX/ROD.
3. CHEMICAL COMPOSITION WT%: Pu/PuO_2 = 88.1 U/UO_2 = 88.0 Pu/MIX = 1.760.
4. PuO_2 IS 2.00 WT% OF TOTAL MIXTURE.
5. FUEL DENSITY - 9.54 gm/cc (~87% THEORETICAL DENSITY).
6. UO_2 POWDER AT THE END OF FUEL COLUMN.
7. THE ISOTOPIC DISTRIBUTION OF PLUTONIUM

8% (NOMINAL) ^{240}Pu ATOM PERCENT	
91.615	^{239}Pu
7.654	^{240}Pu
0.701	^{241}Pu
0.031	^{242}Pu

8. ANALYSIS DATE: JANUARY 1965
9. SEPARATIONS DATE: APRIL 1962
10. ^{241}Am CONTENT: NOT KNOWN

Fig. 3.C.9.3 UO_2-2 wt% PuO_2 (8% ^{240}Pu) fuel description.

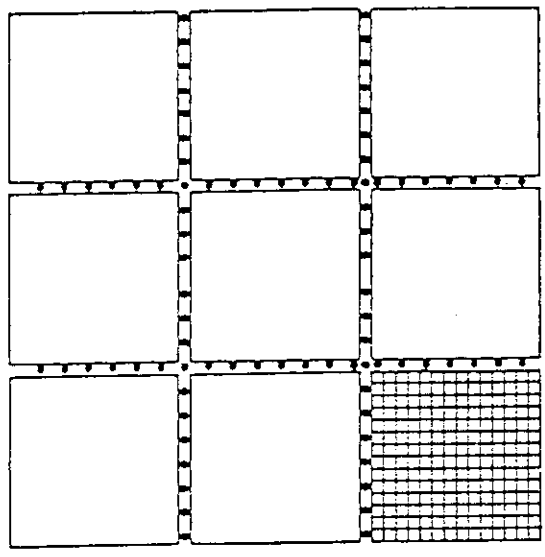

Fig. 3.C.10.1 An example of core loading patterns, nine arrays separated by one pin pitch with 84 B_4C pins.

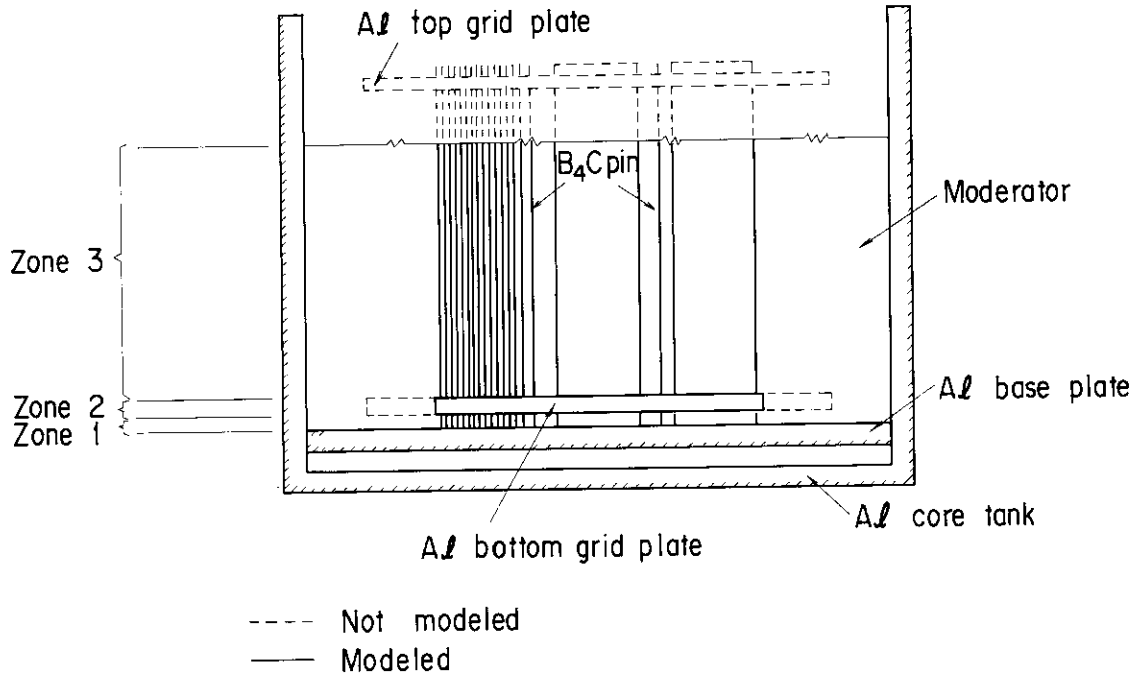

Fig. 3.C.10.2 KENO calculational model for Core I-IX.

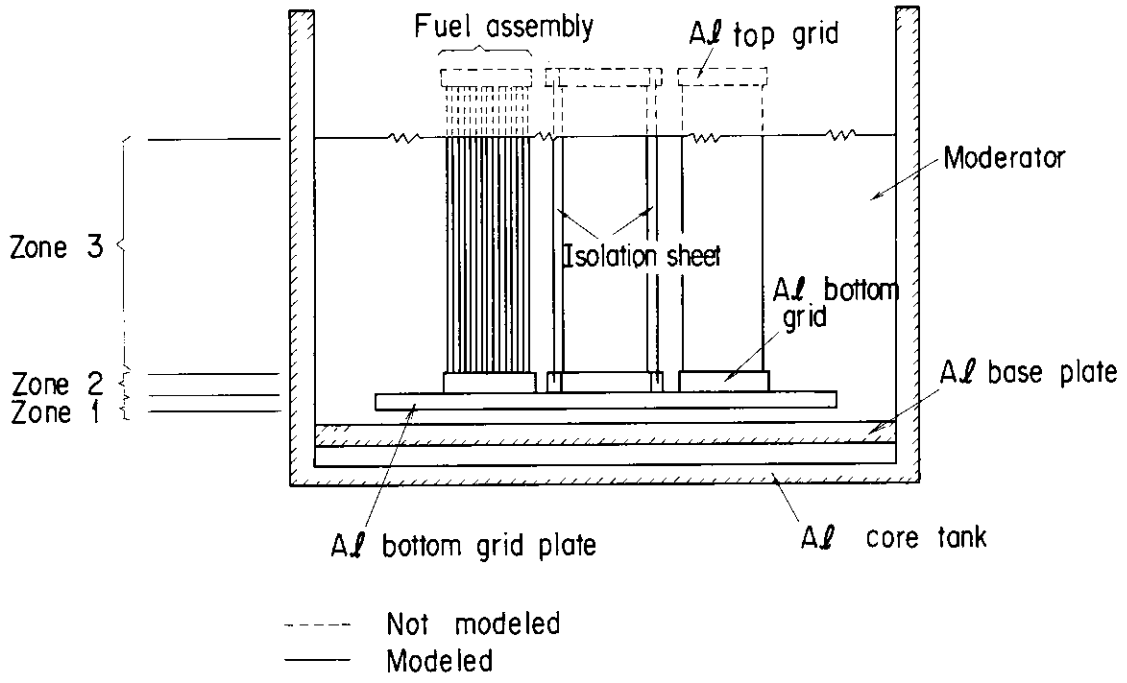

Fig. 3.C.10.3 KENO calculational model for Core X-XXI.

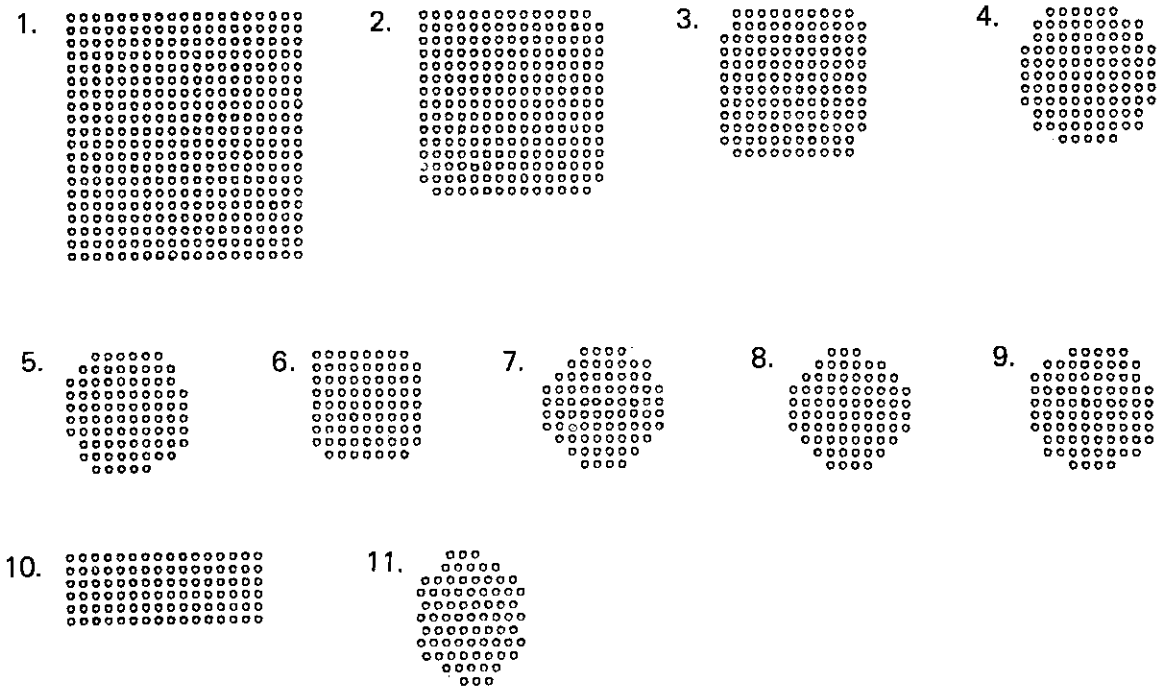

Fig. 3.C.11.1 Lattices of EBOR (Experimental Beryllium Oxide Reactor) fuel pins in water.

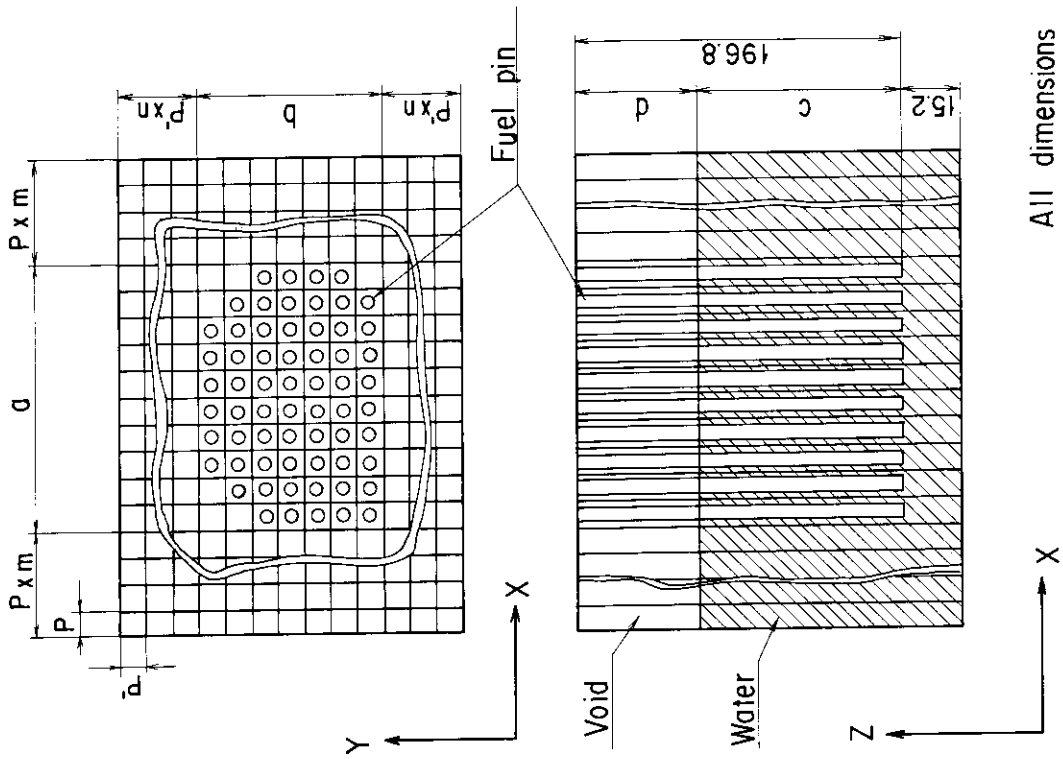

Fig. 3.C.11.3 Geometrical model of fuel pins in water.

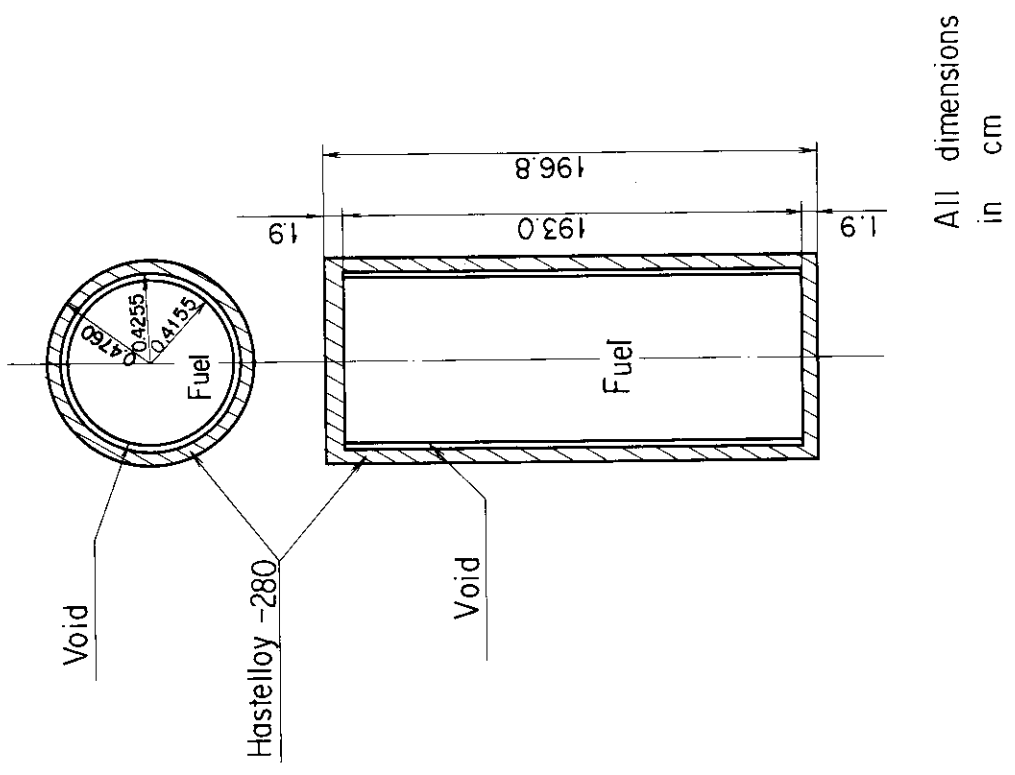

Fig. 3.C.11.2 Schema of the fuel pin model.

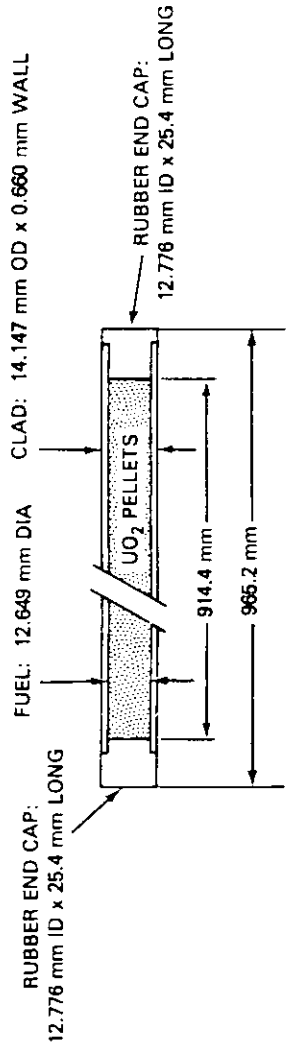

CLADDING: 6061 ALUMINUM TUBING

LOADING:

ENRICHMENT - 4.31 ± 0.01 WT% ^{235}U
FUEL DENSITY - 94.9 ± 0.55% OF THEORETICAL DENSITY
URANIUM ASSAY - 88.066 ± 0.281 WT% OF TOTAL FUEL COMPOSITION
UO_2 - 1203.38 ± 4.12 g/ROD

END CAP:

DENSITY - 1.321 g/cm^3 S-1.7 ± 0.2 WT%
COMPOSITION -C-58 ± 1 WT% O-22.1 WT% (BALANCE)
H-6.5 ± 0.3 WT% Si-0.3 ± 0.1 WT%
Ca-11.4 ± 1.8 WT%

Fig. 3.C.12.1 Schema of the fuel rod used in the experiment.

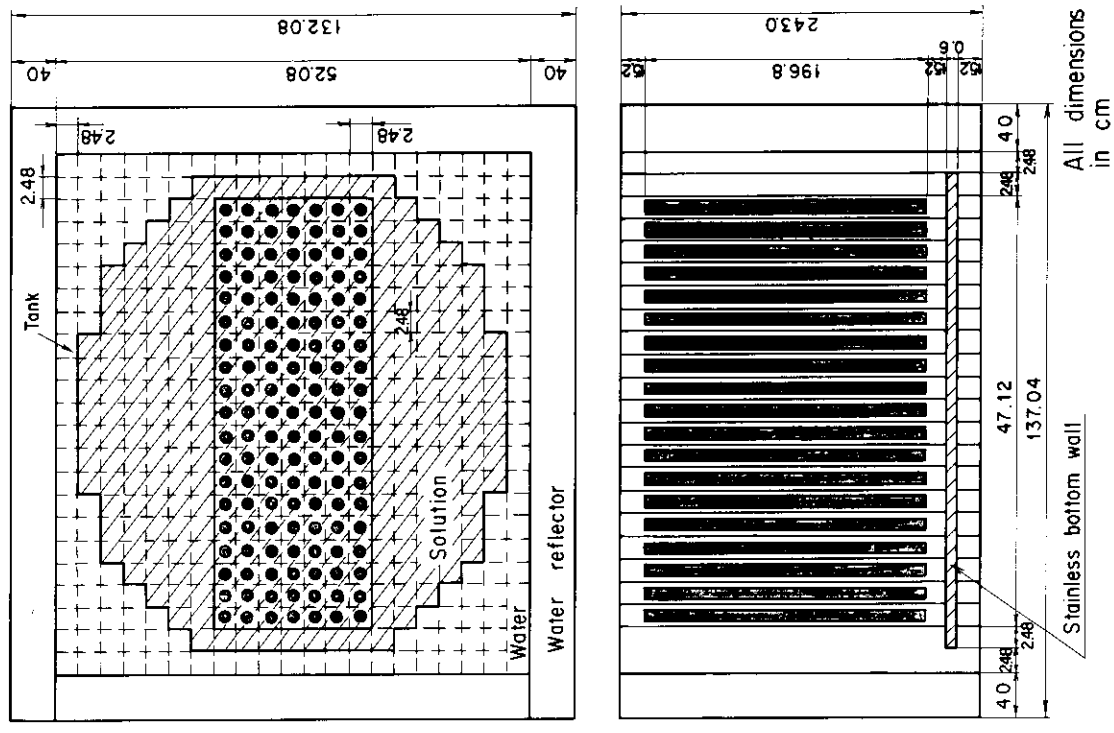

Fig. 3.C.11.4 Geometrical model of fuel pins in solution.

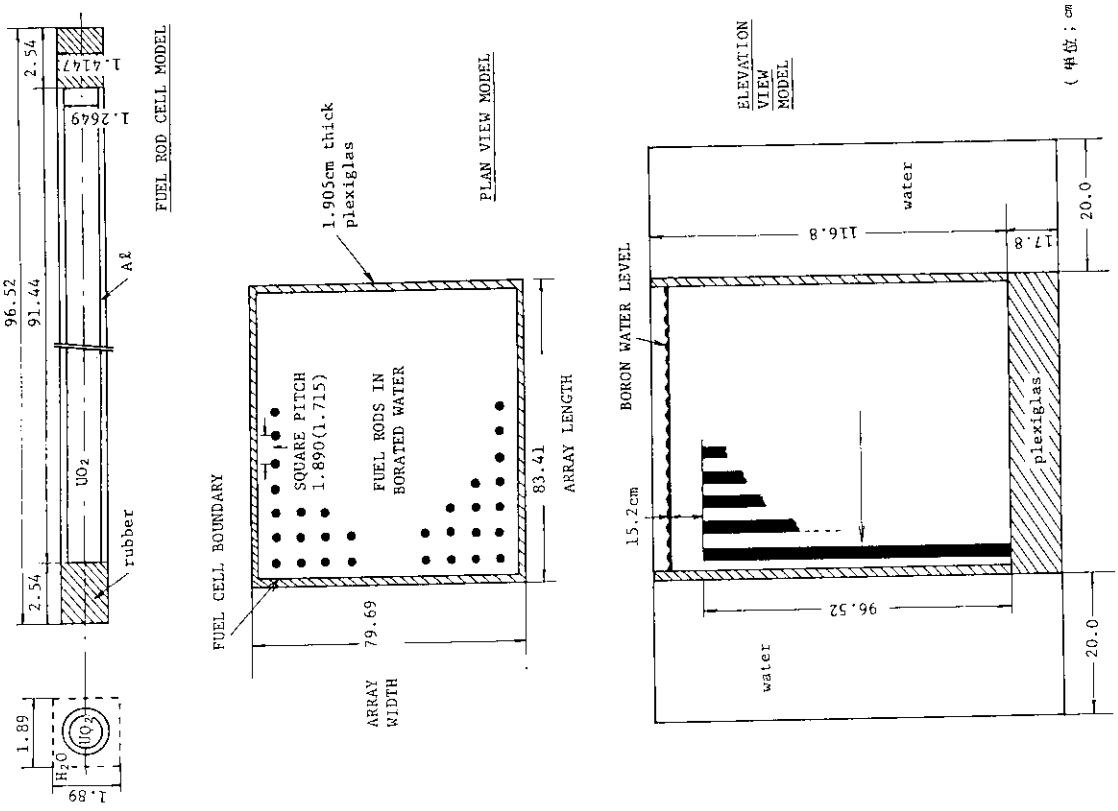

Fig. 3.C.12.3 Calculational model for UO_2 rod cluster fully immersed in borated water.

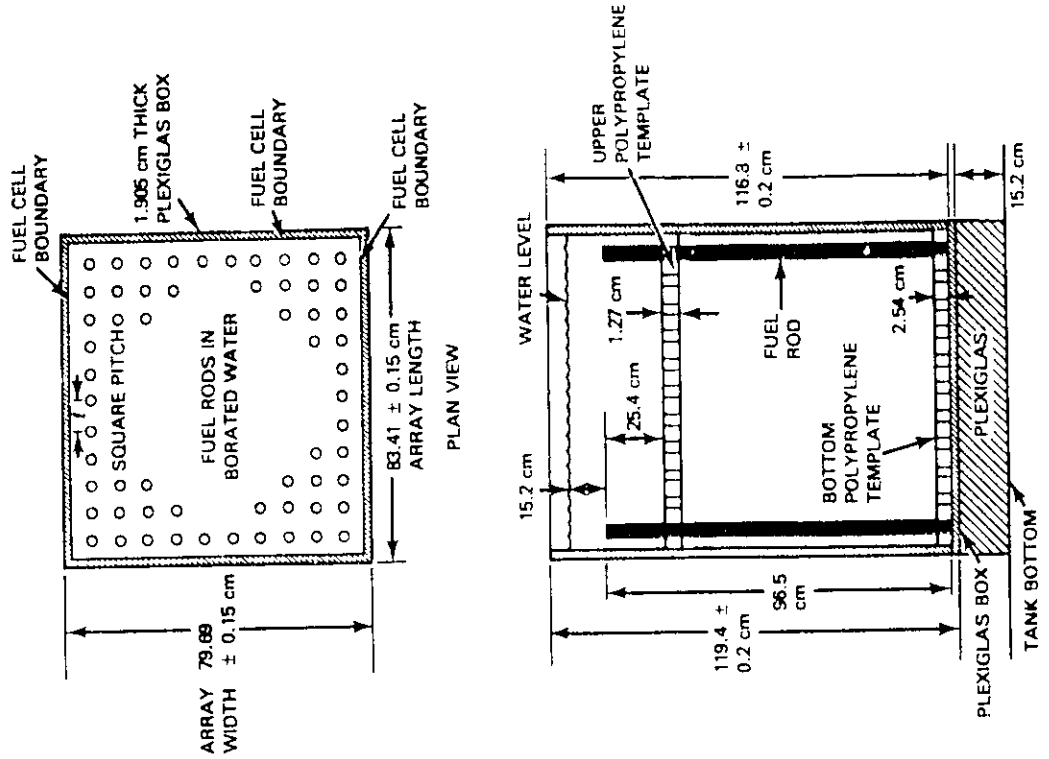

Fig. 3.C.12.2 Experimental arrangement of the UO_2 rod clusters immersed in borated water.

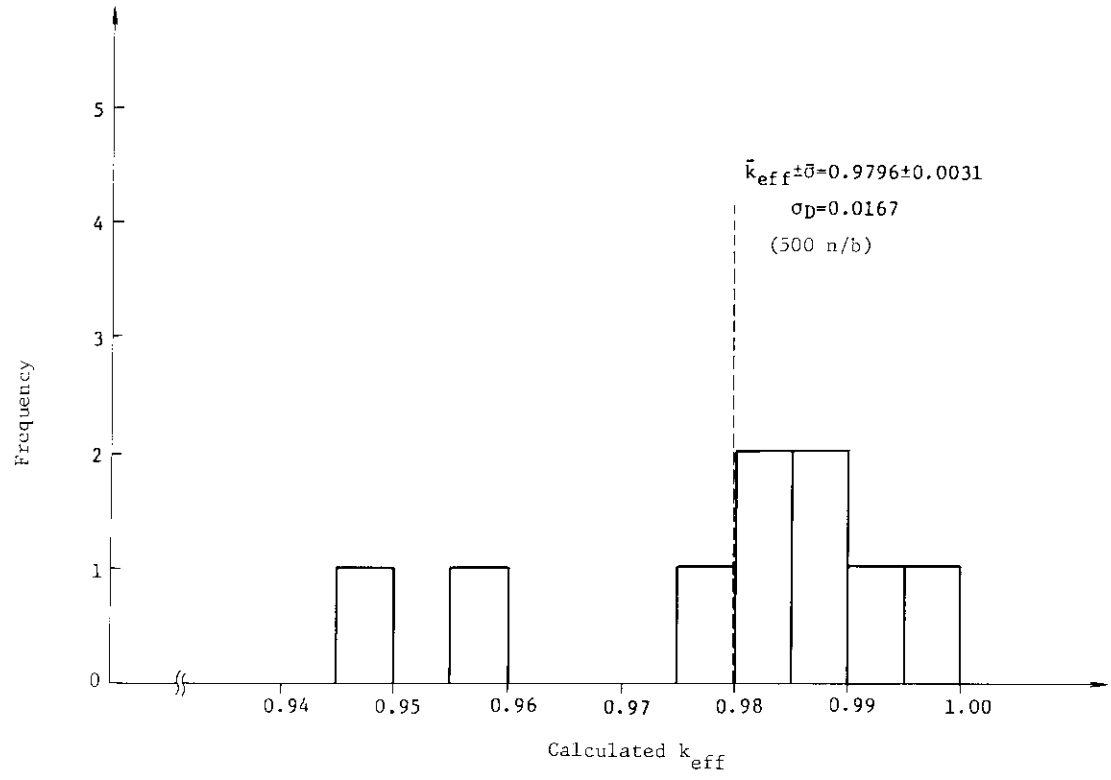

Fig. 3.C.12.4 Histogram of calculated k_{eff}'s for the UO_2 rod clusters fully immersed in borated water (1).

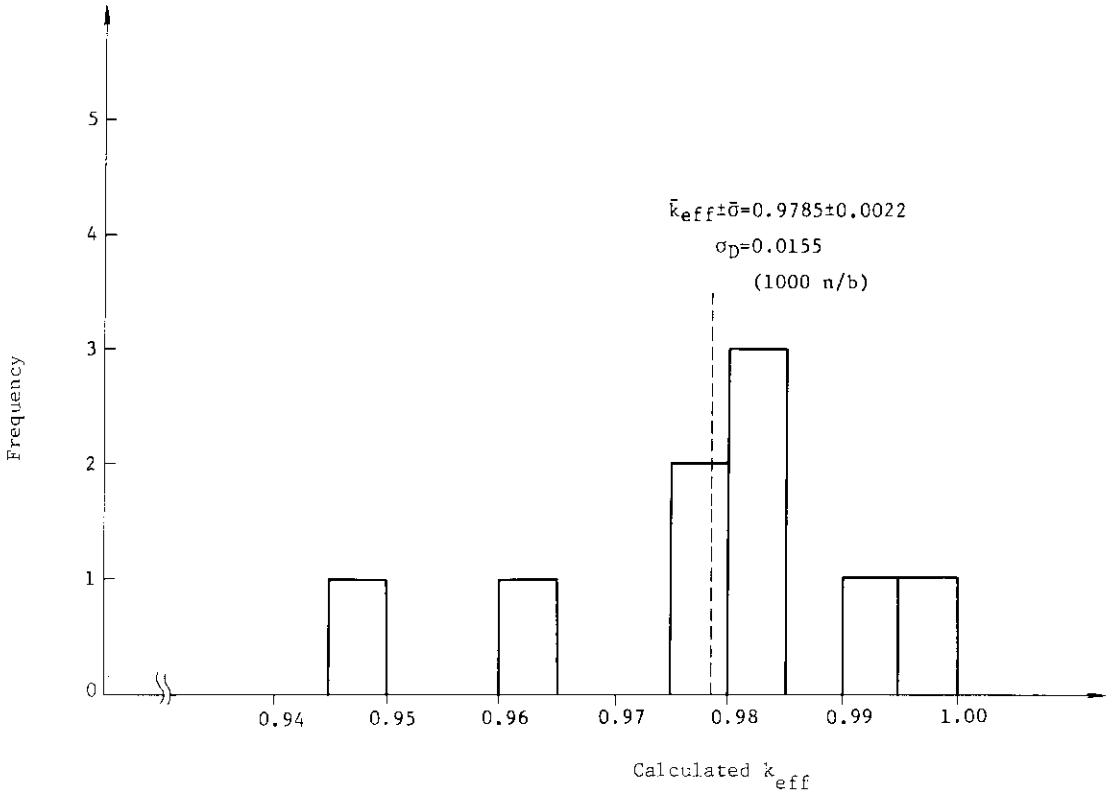

Fig. 3.C.12.5 Histogram of calculated k_{eff}'s for the UO_2 rod clusters fully immersed in borated water (2).

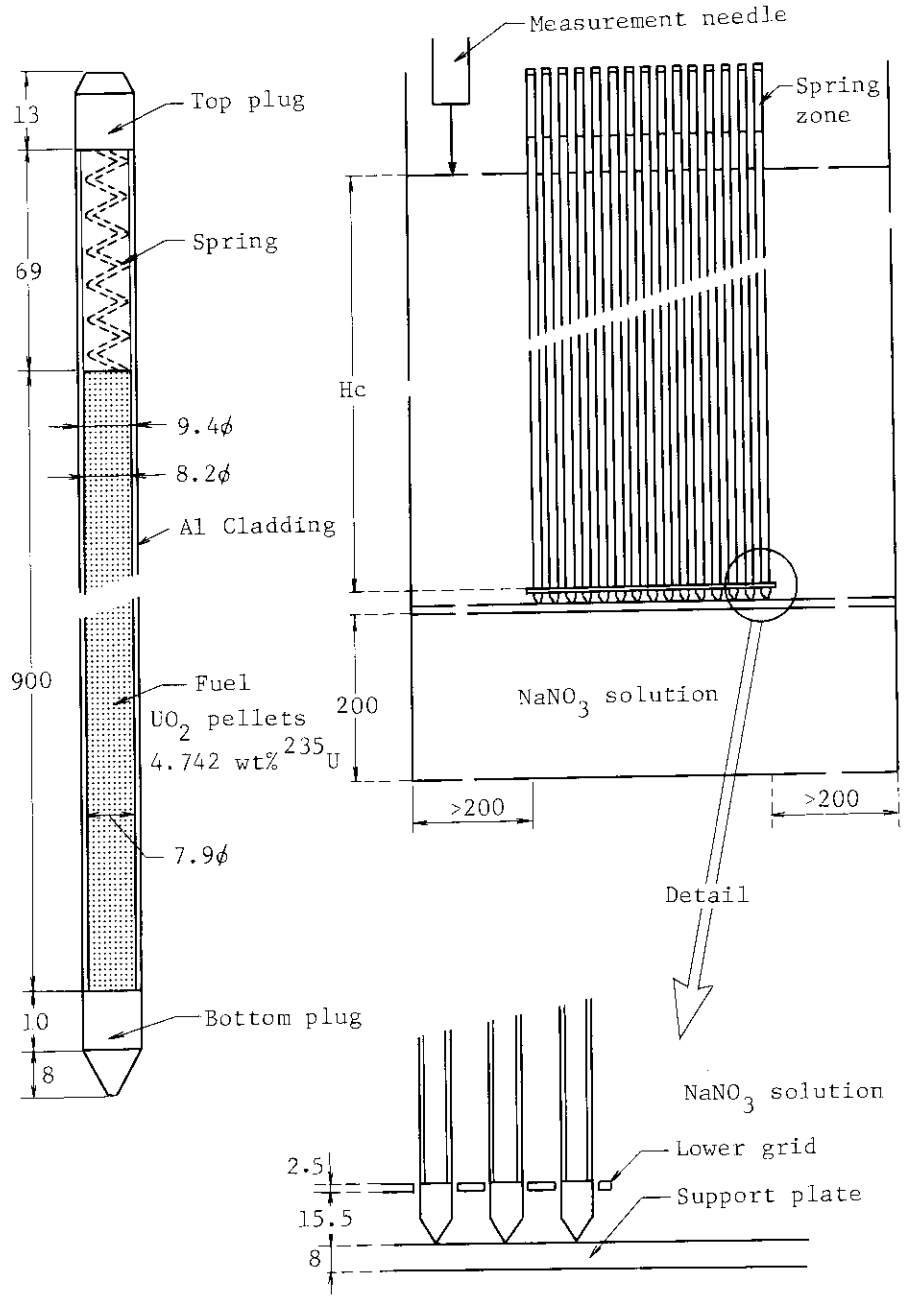

Fig. 3.C.13.1 Main dimensional figures of the fuel rods and the experimental basket (in millimeters).

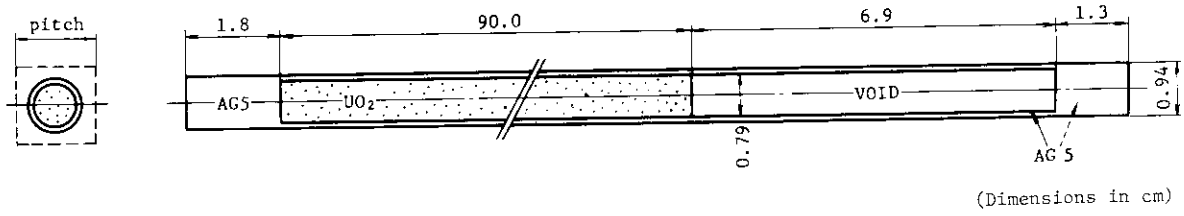

Fig. 3.C.13.2 Calculational model for a fuel rod.

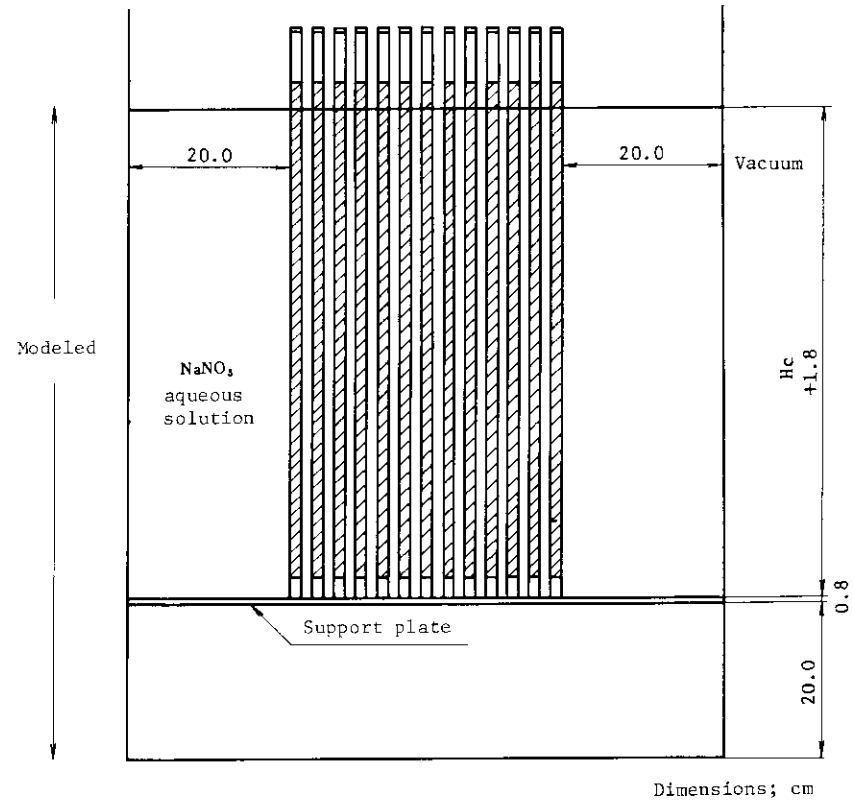

Fig. 3.C.13.3 Calculational model for a typical experimental system.

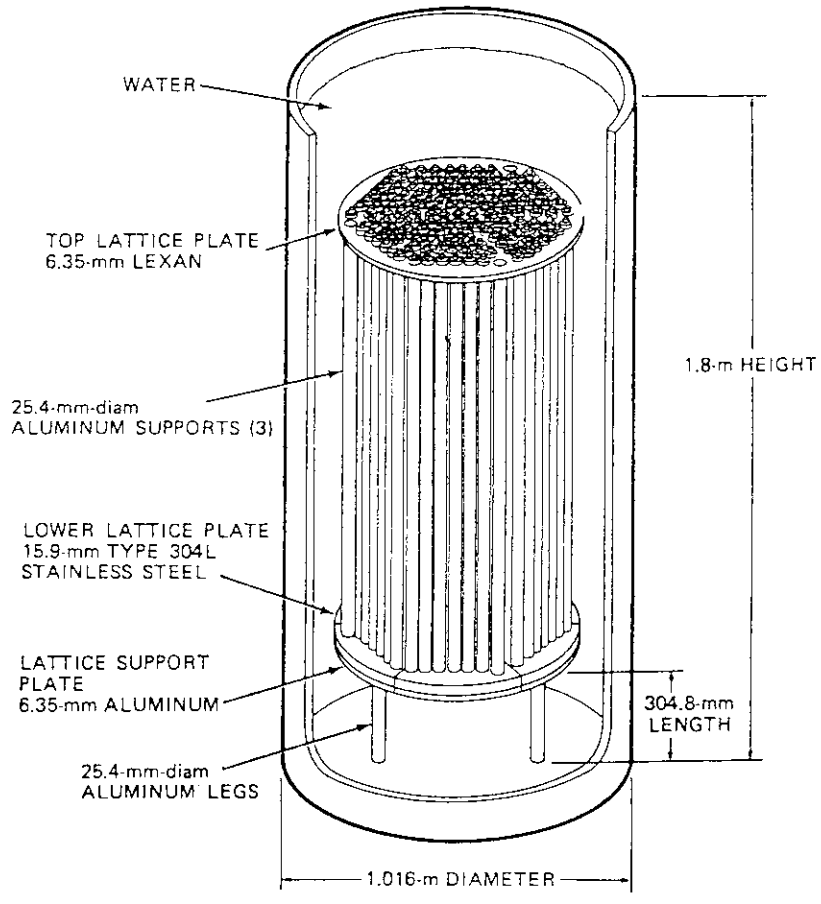

Fig. 3.C.14.1 Experimental arrangement of the triangular lattice in poisonous water tank.

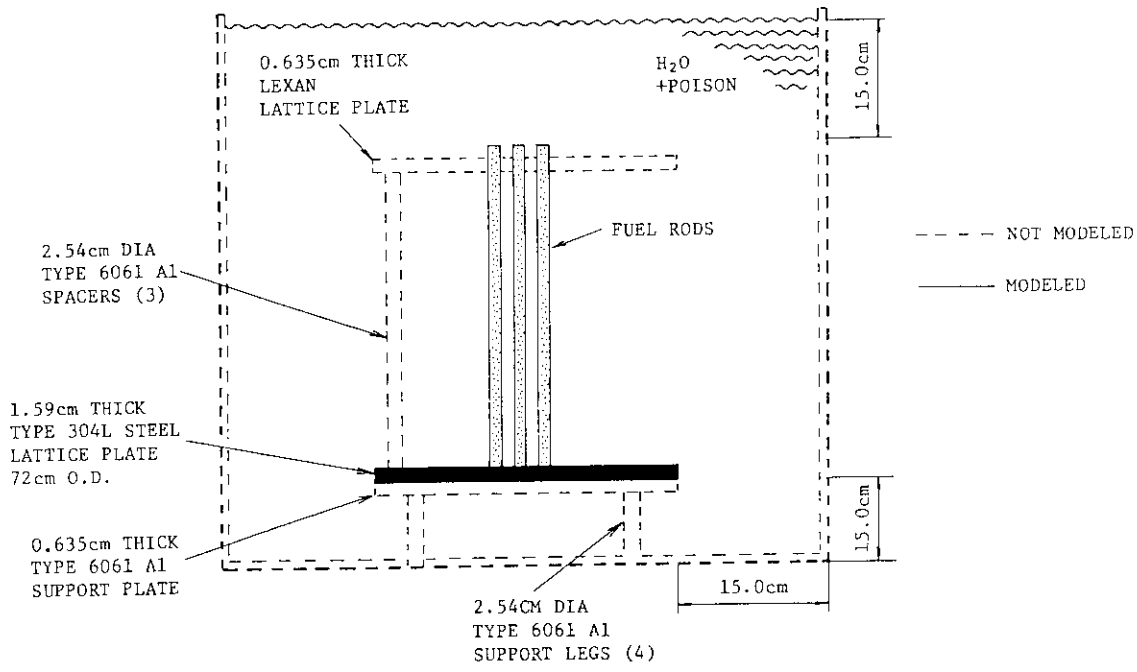

Fig. 3.C.14.2 Calculational model for UO_2 fuel rods, triangularly arranged in poisonous water tank.

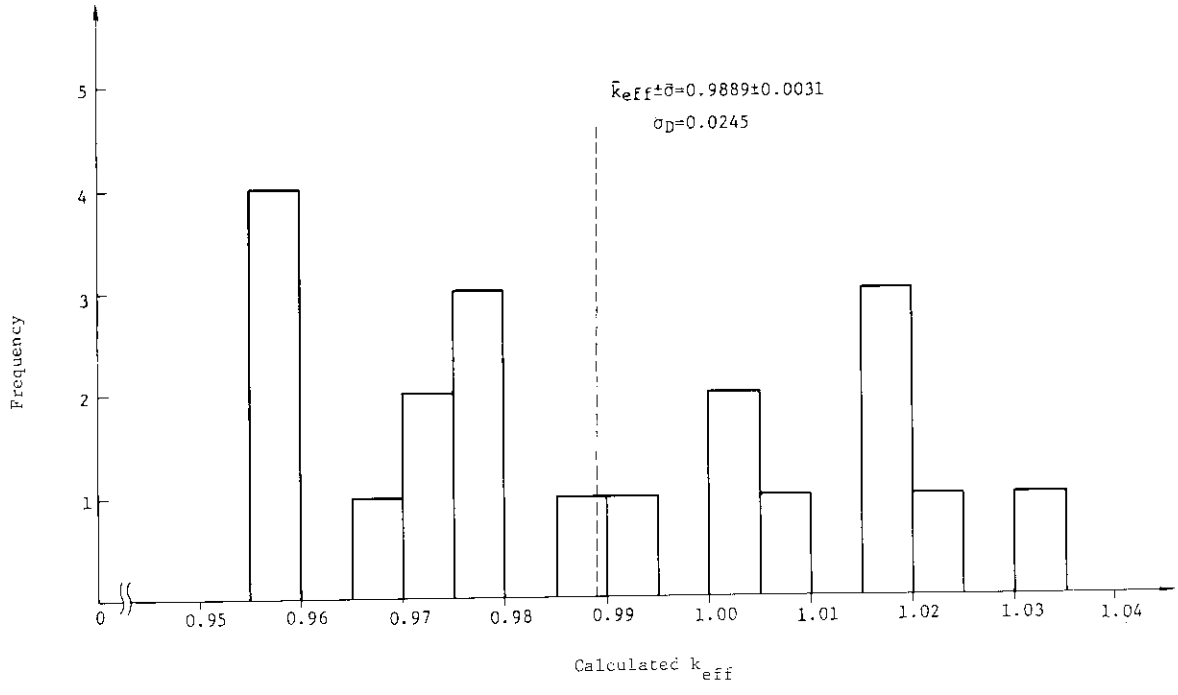

Fig. 3.C.14.3 Histogram of calculated k_{eff}'s for triangular lattice in poisonous water.

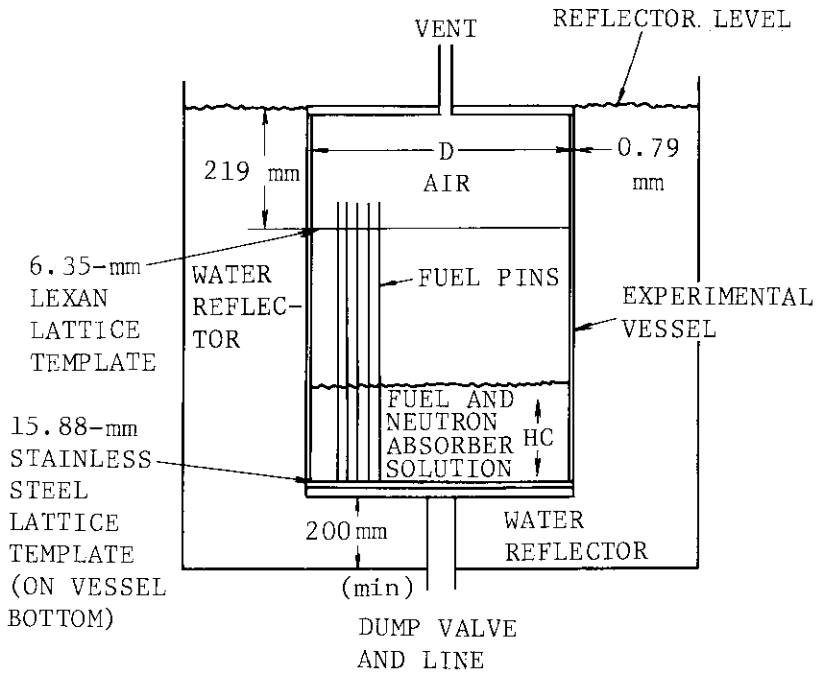

URANYL NITRATE COMPOSITION	
URANIUM CONCENTRATION (g/ℓ)	195.8
SPECIFIC GRAVITY	1.254
FREE ACID MOLARITY	1.52

DESCRIPTION OF EXPERIMENTAL VESSELS	
END THICKNESS (TOP AND BOTTOM) (mm)	9.5
EXPERIMENTAL VESSEL WALL THICKNESS (mm)	0.79
EXPERIMENTAL VESSEL HEIGHT (mm) (outside)	1067
WATER REFLECTOR o.d. (mm)	1016

INSIDE VESSEL DIAMETER, D (mm)	TRIANGULAR LATICE PITCH (mm)	NUMBER OF FUEL RODS
557.5	22.9	451
658.0	27.9	433
761.6	33.0	421

Fig. 3.C.15.1 Experimental arrangement for UO_2 rod clusters partially immersed in uranyl-nitrate solution.

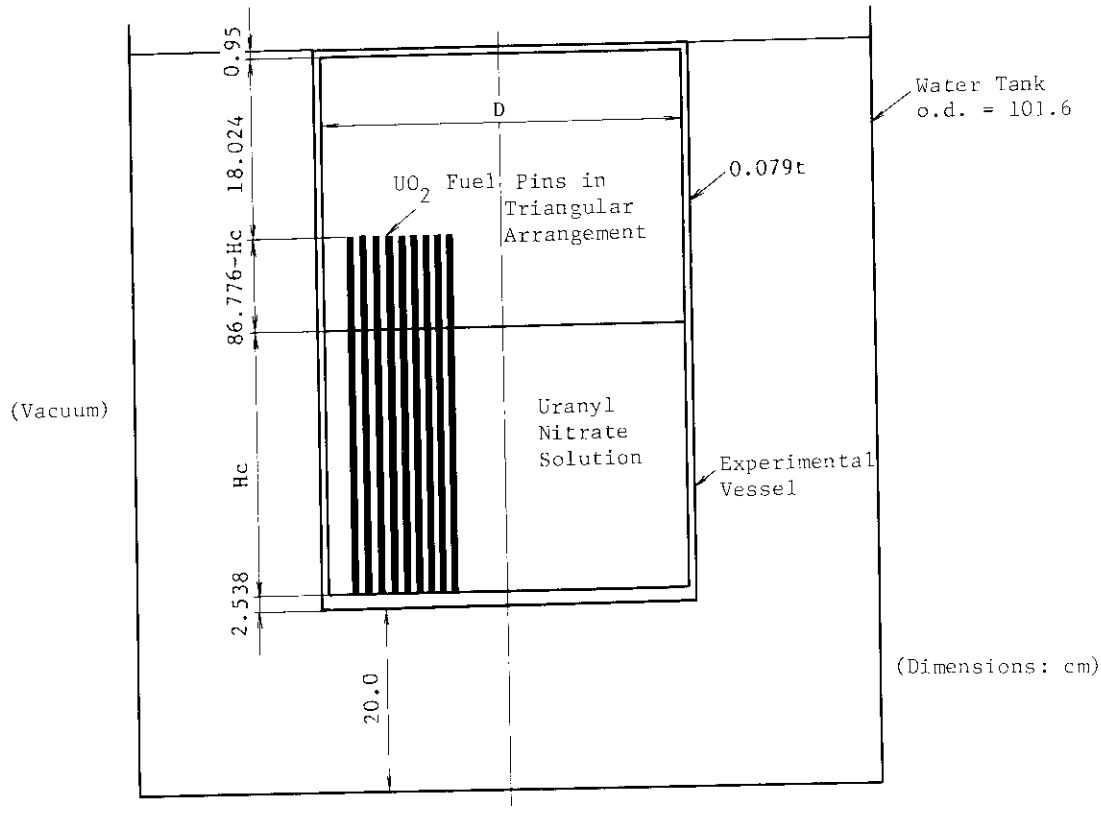

Fig. 3.C.15.2 Calculational model for UO_2 rod clusters partially immersed in uranyl-nitrate solution.

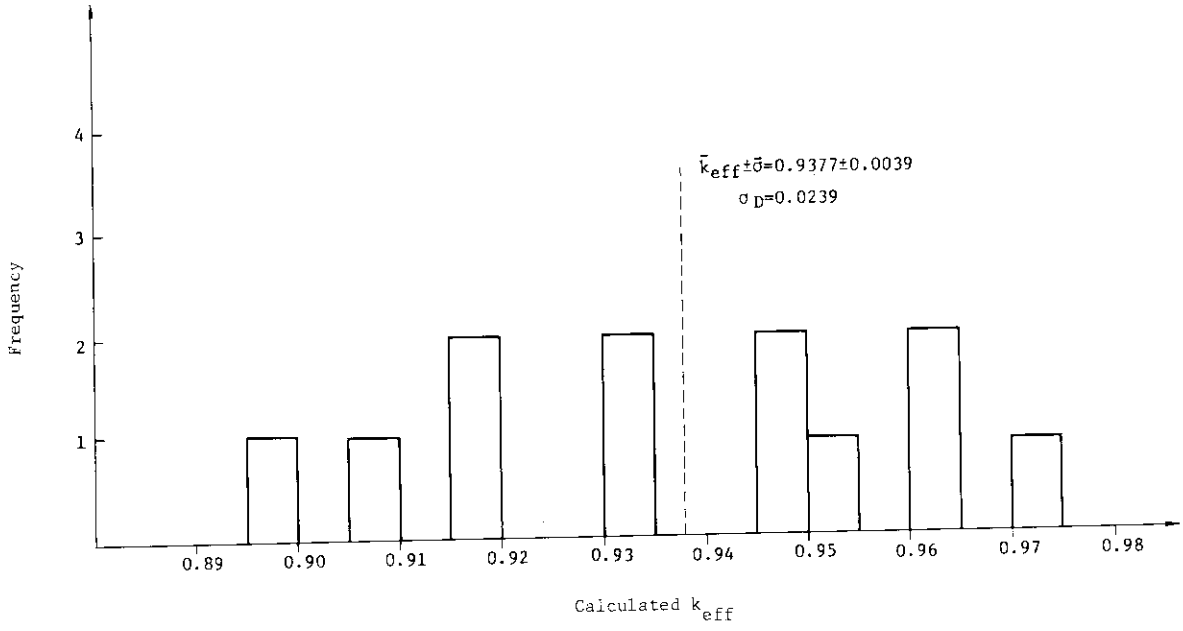

Fig. 3.C.15.3 Histogram of 12 calculated k_{eff}'s for rod clusters partially immersed in uranyl-nitrate solution.

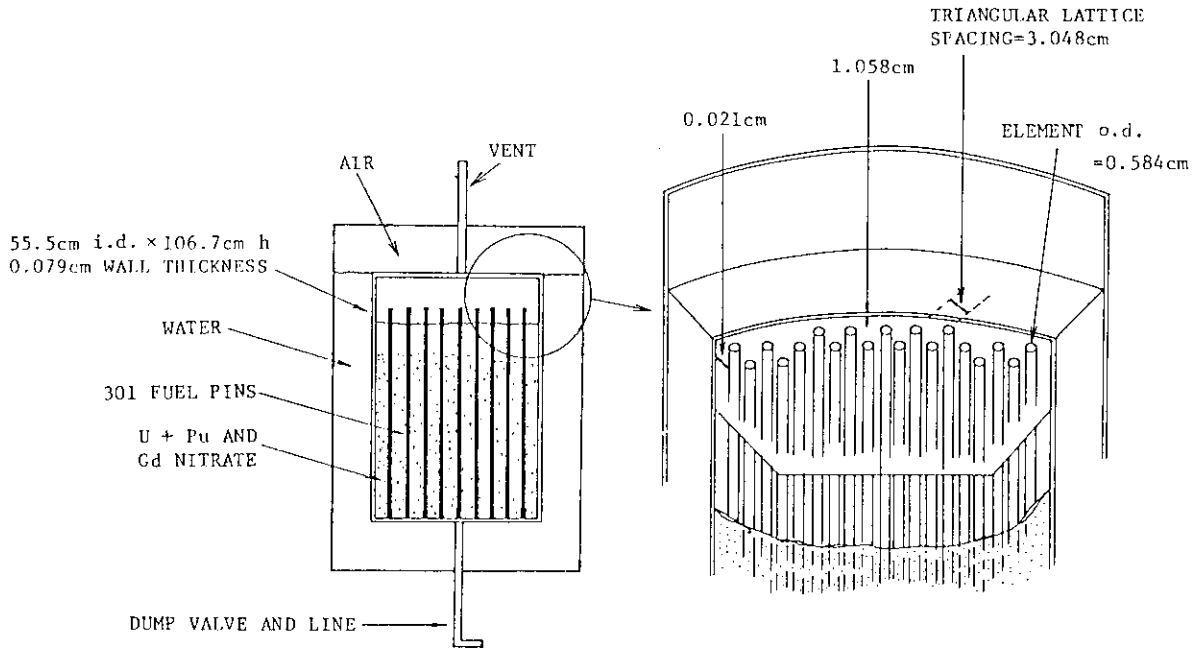

Fig. 3.C.16.1 Experimental arrangement for UO_2-PuO_2 fuel rods in fissile solution containing gadolinium and boron.

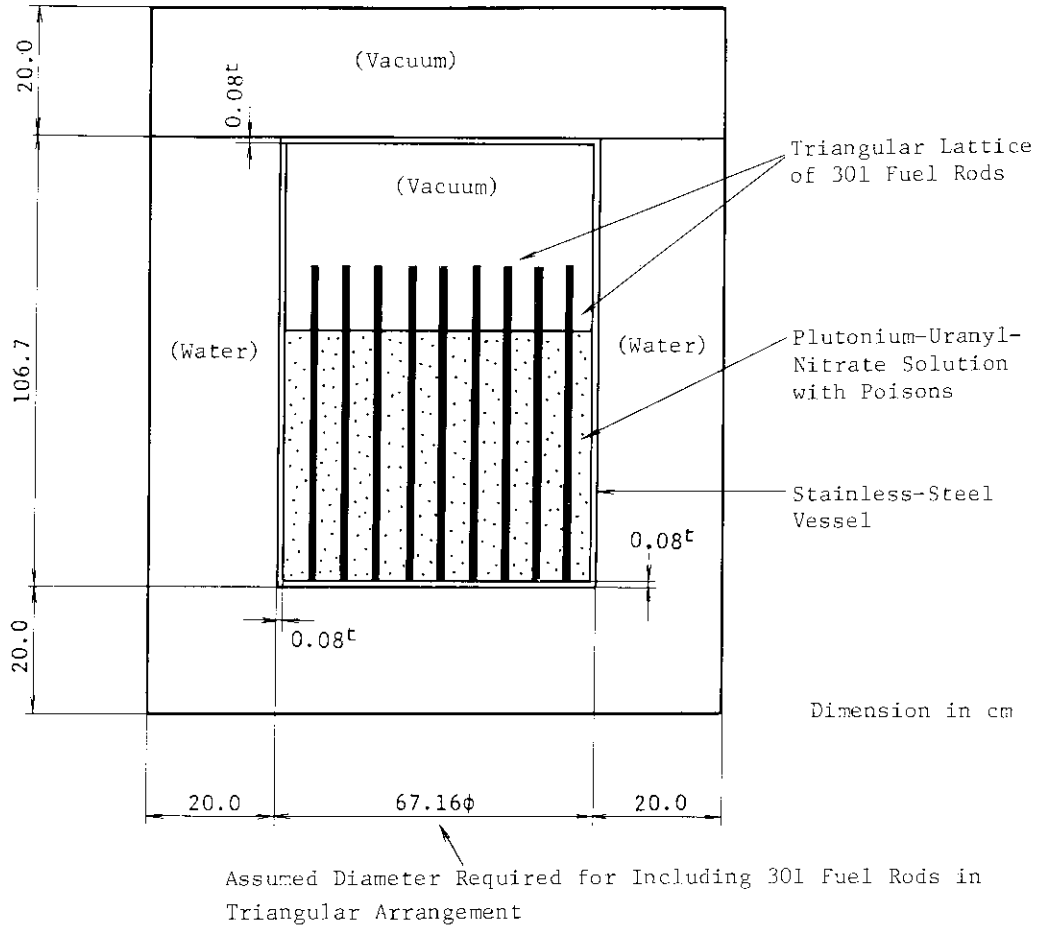

Fig. 3.C.16.2 Calculational model for PuO_2-UO_2 fuel rods in plutonium-uranyl-nitrate solution containing gadolinium and boron.

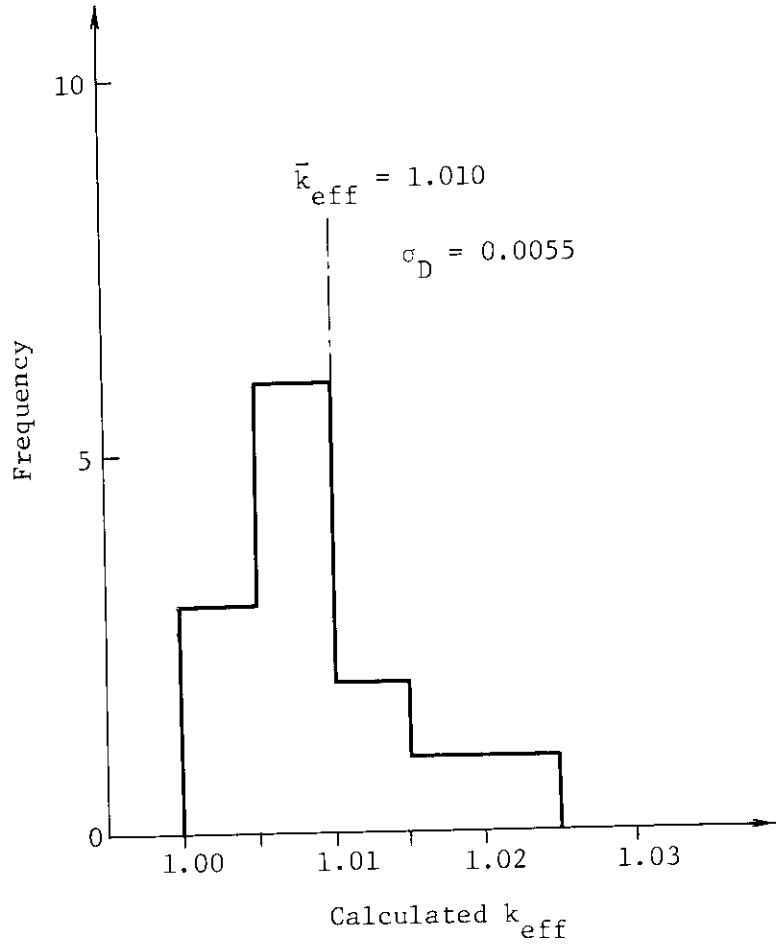

Fig. 3.C.16.3 Histogram of calculated k_{eff}'s for PuO_2-UO_2 fuel rods in plutonium-uranyl-nitrate solution containing gadolinium and boron.

4. Discussions and Interpretations

As explained in Chapter 3, calculated k_{eff}'s have a wide range of bias errors in comparison with statistical errors predicted by the KENO-IV Monte Carlo calculations. There might be some factors determining the trends of the bias errors. Let us try to make clear the effects of these factors, referring to the experimental data and the calculational results described in Chapter 3. In the following sections, they are quoted as the corresponding section number, for example, (**3.A.1**) if the "Pile of PuO_2-UO_2-Polystyrene Compacts with Various Poison Plate Materials" is cited in the discussion.

4.1 Effect of Reflecting Condition

In most of homogeneous multi-unit (interacting) experimental systems such as (**3.B.1**), (**3.B.2**), (**3.B.4**) and (**3.B.7**), where both reflected and unreflected conditions are studied in the same experiment, the calculated k_{eff}'s for the reflected arrays are discerned to be higher than those for the unreflected arrays. One can see this trend in **Figs. 3.B.1.2**, **3.B.1.3** and **3.B.2.3**, or in **Tables 3,B.4.1** and **3.B.7.1**. In the experiments (**3.B.2**) and (**3.B.7**), where the thickness of reflector is changed from case to case, the calculation predicts the higher k_{eff} value in the case of the thicker reflecting wall, as shown in **Figs. 4.1** and **4.2**. In these experimental systems most neutrons are considered to leak from fuel units. Consequently, interactions and reflections of the leaked neutrons are considered to play a dominant role in determining the reactivity in these experiments, since the calculated k_{eff}'s for other non-interacting systems such as homogeneous single-unit systems or heterogeneous systems don't have such a remarkable trend of bias errors. The KENO-IV Monte Carlo calculational method might have some problems in predicting the leaked neutron behavior, together with neutron interactions between units.

4.2 Effect of Moderating Condition

In under-moderated homogeneous single- or multi-unit systems, it is discerned that the lower the moderating ratio (H/(Pu or U), the higher the calculated k_{eff}'s. For example, **Fig. 3.A.6.11** shows the trend of the calculated k_{eff}'s with the variation of the H/Pu ratio of plutonium fuel of various shapes. To endorse this effect further, we can mention that the calculated k_{eff}'s for uranium metal arrays (**3.B.5**) and plutonium metal arrays (**3.B.6**) have averaged values of 1.012 and 0.999, respectively, as shown in **Figs. 3.B.5.2** and **3.B.6.5**, higher than those for plutonium or uranium solution unit arrays such as (**3.B.2**), (**3.B.3**), (**3.B.4**) and (**3.B.7**).

This trend in the calculated k_{eff}'s is also seen for heterogeneous systems. The calculated k_{eff}'s for UO_2 rod clusters in water at near-optimum moderation, such as in the system (**3.C.3**), have the average value of 0.990, as shown in **Figs. 3.C.3.6** and **3.C.3.7**, which is lower than that of 0.995 for UO_2 rod clusters in water at under-moderation, such as in the system (**3.C.5**).

On the other hand, in the case of over-moderating condition, the calculated k_{eff} bias seems to increase with increasing moderating ratio, as shown in **Fig. 4.3**. This trend is also discerned in homogeneous systems, for example, if **Fig. 3.A.6.11** is observed carefully.

Variation of the moderating condition affects the neutron energy dominating nuclear reactions of which cross section data do not have uniform errors in a wide range of neutron energy. Accordingly, the bias errors are considered to be introduced into the calculated k_{eff}'s with their particular trends and uncertainties from case to case, depending on the variation of moderating condition.

4.3 Effect of Soluble Neutron Absorber

Neutron absorber, such as boron or gadolinium, absorbes mainly low energy neutrons and makes neutron energy spectrum harden. Accordingly, its existance is considered to have the reverse effect on the calculated k_{eff}'s as compared with the effect of moderating material. There are some experiments, where neutron absorbers are used to simulate a spent fuel storage or dissolver. **Figures 4.4** and **4.5** show that the calculated k_{eff} bias changes with boron and gadolinium concentrations in the plutonium-uranyl nitrate solution used in the experimental system (**3.A.16**). It is seen from these figures that the KENO-IV calculation predicts higher k_{eff} value for lower concentration of the neutron absorber. The similar bias trend in the calculated k_{eff}'s is also seen in the experiment (**3.C.14**), as shown in **Fig. 4.6**, where boron, cadmium, gadolinium or their combination is resolved in the water moderator around the UO_2 rod clusters. In this figure, the Ft/At ratio (thermal neutron fissions versus thermal neutron absorptions, obtained by the KENO-IV calculation) is used instead of the neutron absorber concentration as an illustrative variable. The lower the neutron absorber concentration becomes, the softer the neutron spectrum and the smaller the Ft/At ratio becomes. Consequently, the reduction of the neutron absorber concentration in solution systems, considered to be at over-moderation, has the same effect as the increase of moderating ratio, introducing a positive trend in the calculated k_{eff}'s as discussed in the previous section.

On the other hand, a reverse trend is discerned in the calculated k_{eff} for the experiments (**3.C.8**) and (**3.C.10**), as shown in **Figs. 4.7** and **4.8**. In this case, neutrons are presumed to be at under-moderation. The reduction of the neutron absorber concentration results in the decrease of the calculated k_{eff} bias, as is also observed in the previous section.

4.4 Effect of Fuel Composition

Since numerical data of neutron cross sections of the fuel material play an important role in computing neutron multiplication factors, the error existing in the cross section data can be a direct cause to produce bias errors in the calculated k_{eff}'s.

Take the experiment (**3.A.2**) for an example, where the plutonium content in (Pu+U) mixed oxide fuel is varied with the H/Pu moderating ratio held approximately constant. The average value of the calculated k_{eff}'s for the reflected 30.0 wt% Pu content fuel listed in **Table 3.A.2.4**, is 1.0098, lower than 1.0128 for the reflected 7.89 wt% Pu content fuel in **Table 3.A.2.6**.

Furthermore, take the experiment (**3.A.13**) for another example, where the ^{240}Pu content in Pu is varied in plutonium-uranyl-nitrate solution with a water reflector. As shown in **Figs. 3.A.13.4** and **3.A.13.5**, the average value of calculated k_{eff}'s for the 5.6 wt% ^{240}Pu content fuel is 1.0012, higher than 0.9976 for the 23.0 wt% ^{240}Pu content fuel.

These trends of the calculated k_{eff} bias are successfully predicted by the following multiple regression equation.[67]

$$
\begin{aligned}
k_{eff,\exp} = {} & +0.000167-0.09471*(At/A-0.8446) \\
& +0.3795*(Pu/(Pu+U)-0.3613) \\
& -1.1453*((Pu/(Pu+U))^2-0.3117) \\
& +0.7926*(((Pu/(Pu+U))^3-0.3004) \\
& -0.09596*((fissile)/(Pu+U)-0.4606) \\
& +0.08482*((fissile)/(Pu+U))^2-0.3739),
\end{aligned}
$$

At/A : thermal neutron absorptions versus total neutron absorptions obtained by the KENO-IV calculation.

The above equation was induced from 243 cases of benchmark calculations on the homogeneous reflected single-unit systems selected from those in Subchapter 3.A.

Fuel compositions in nuclear fuel facilities cover so many varieties that a particular code system cannot predict neutron multiplication factors with sufficient accuracy for all these widely ranged fuel compositions. Therefore, it is considered to be advantageous for criticality safety evaluation to classify the experimental systems by indexing the representative fuel compositions and to estimate the critical values and their deviations calculated by the KENO-IV and MGCL code system according to the indexing. **Table 4.1** shows the results of the classification. In the case of homogeneous low enriched uranium system, for example, the critical k_{eff} value to be calculated by the KENO-IV and MGCL code system is 0.986, and the lower limit of the critical value is 0.965. Therefore, if k_{eff} value of a system to be evaluated is calculated by the KENO-IV and MGCL code system to be lower than 0.965, the system is concluded to be subcritical. These values listed in **Table 4.1** are obtained by processing statistically some 400 cases of benchmark calculations selected from those described in Chapter 3.

4.5 Effect of Distance Between Units

The calculated k_{eff}'s for the homogeneous multi-unit (interacting) systems (**3.B.6**), (**3.B.7**) and (**3.B.4**) are shown in **Figs. 4.9**, **4.10** and **4.11**, respectively, as a function of separation distance between units. The KENO-IV code tracks each neutron from birth to death. Since computing time restricts number of neutrons to be tracked, calculational difficulty increases rapidly with increasing the distance between units due to the lack of neutrons sufficient for the simulation of interaction between units.

Figures 4.9 and **4.10** show that the further the units of array separate each other, the lower the calculated k_{eff}'s become. In the related experimental systems (**3.B.6**) and (**3.B.7**), the neutron leakage from each unit is significant, and leaked neutrons contribute much to the system reactivity through reflection and interaction. Let us remove the reflectors surrounding the units from the calculational model. Calculated k_{eff}'s would be low enough, 0.75 on an average for the system (**3.B.6**) and 0.63 for the system (**3.B.7**). For such a system, with increasing the separation distance between units, the difficulty in computing k_{eff} by the KENO-IV code becomes remarkable.

On the other hand, no specific trend of the calculated k_{eff} is discerned in **Fig. 4.11** for the experiment (**3.B.4**), where two aluminum cylinders containing uranyl fluoride solution are positioned parallel in a water tank. The cylinders are some 100 cm high and 20-40 cm in the inner diameter, big enough to have most of neutrons kept in each unit. The contribution of leaked neutrons to the system reactivity is minor. The calculation for the assumed unreflected two parallel cylinders would give an averaged k_{eff} value of 0.93, rather close to the averaged calculated k_{eff} of 0.98 for the real system. Therefore, the calculational difficulties

of simulation of interaction don't produce serious error in k_{eff} calculation for this experiment.

It is possible that this calculational difficulty might be a cause for the calculated k_{eff} bias trend pointed out in the section 4.1.

Table 4.1 Validation results for reflected simple geometry systems with the (MGCL, KENO-IV) code system

Fuel	Index of Composition	Calculated k_{eff} at Critical	Calculated k_{eff} Estimated Lower Limit	Statistics Number of Samples	Statistics St. Deviation Distribution
Homo-geneous	Low-Enriched Uranium	0.986	0.965	40	0.008
	High-Enriched Uranium	0.985	0.954	68	0.013
	Plutonium	1.008	0.980	71	0.011
	Mixed Oxide (UO_2+PuO_2)	1.013	0.980	45	0.008
	Mix. Solution $UO_2(NO_3)_2$ $+Pu(NO_3)_4$	1.010	0.980	10	0.008
Hetero-geneous	Low-Enriched Uranium	0.995	0.978	88	0.007
	Plutonium	1.004	0.964	9	0.010
	Mixed Oxide (UO_2+PuO_2)	0.997	0.980	50	0.007

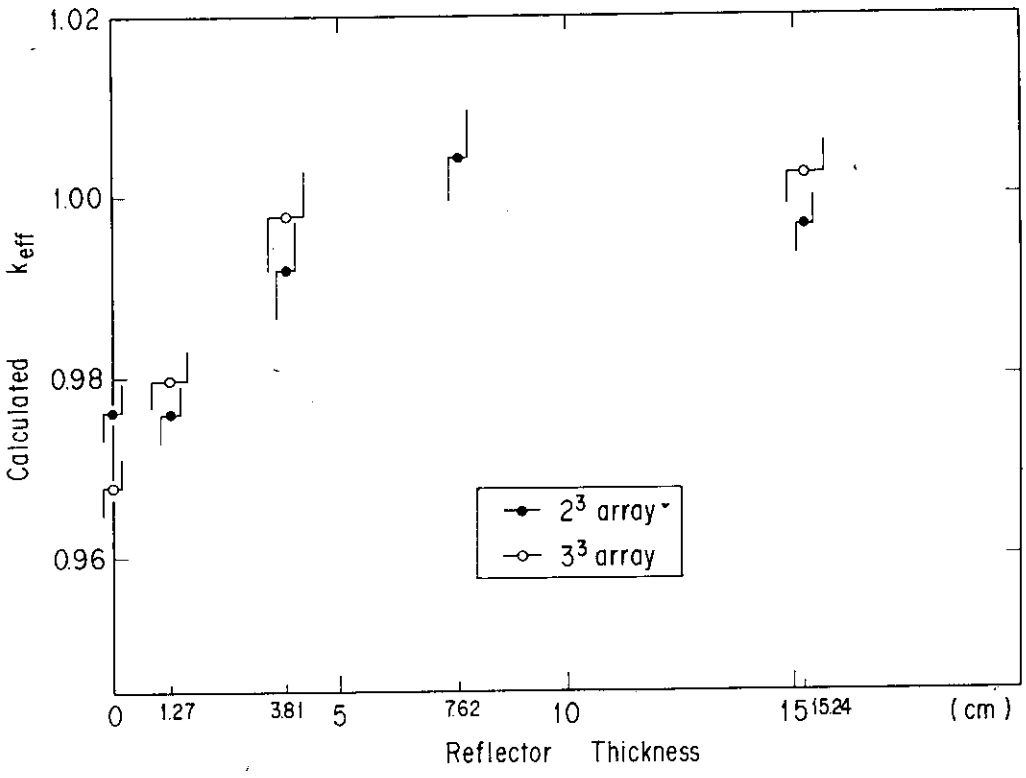

Fig. 4.2 Calculated k_{eff} as a function of relfector thickness surrounding the array of uranyl-nitrate solution cylinders.

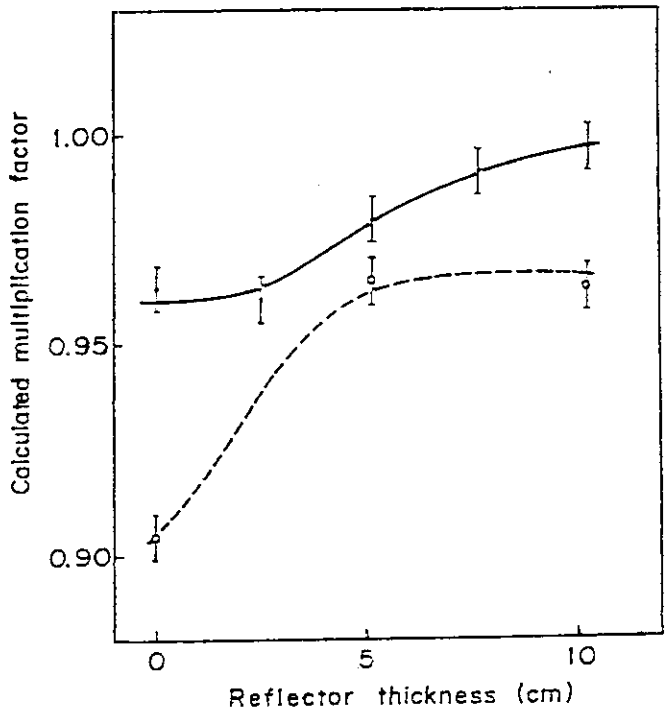

Fig. 4.1 Variation of calculated k_{eff} with reflector thickness. Closed circles indicate the change of k_{eff} with the top and side reflector thickness. Bottom reflector thickness is fixed to be 10.2 cm. Open circles indicate the change of k_{eff} with the bottom reflector thickness. There are no reflectors on the top and the side of the experimental apparatus.

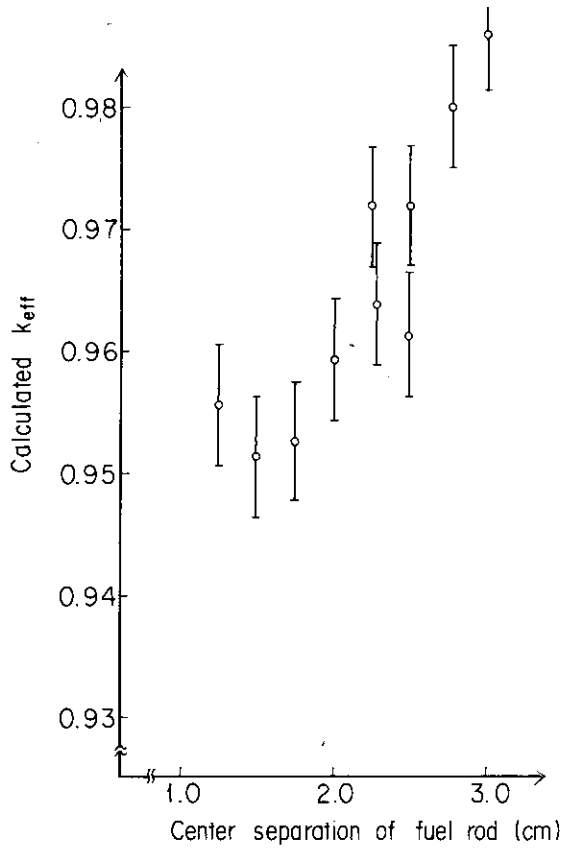

Fig. 4.3
Variation of k_{eff} with center separation of fuel rods in water in the experiment (3.C.11).

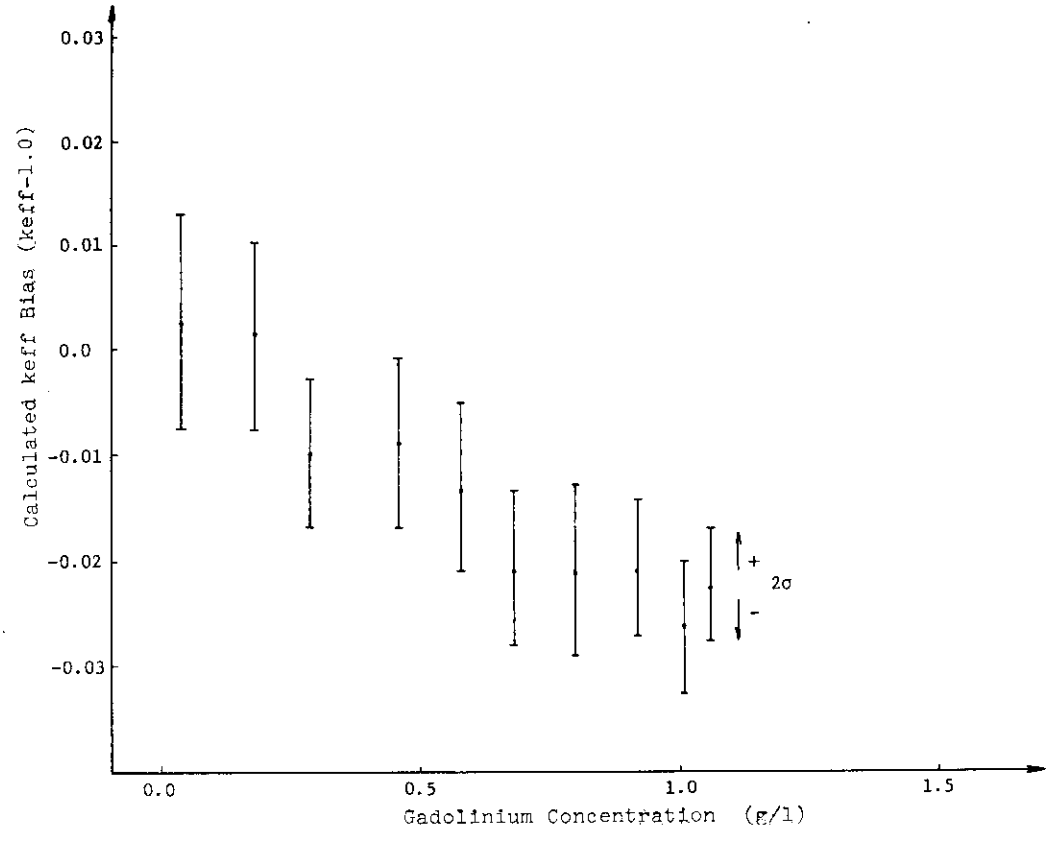

Fig. 4.4 Variation of calculated k_{eff} bias with gadolinium concentration in the experiment (3.A.16).

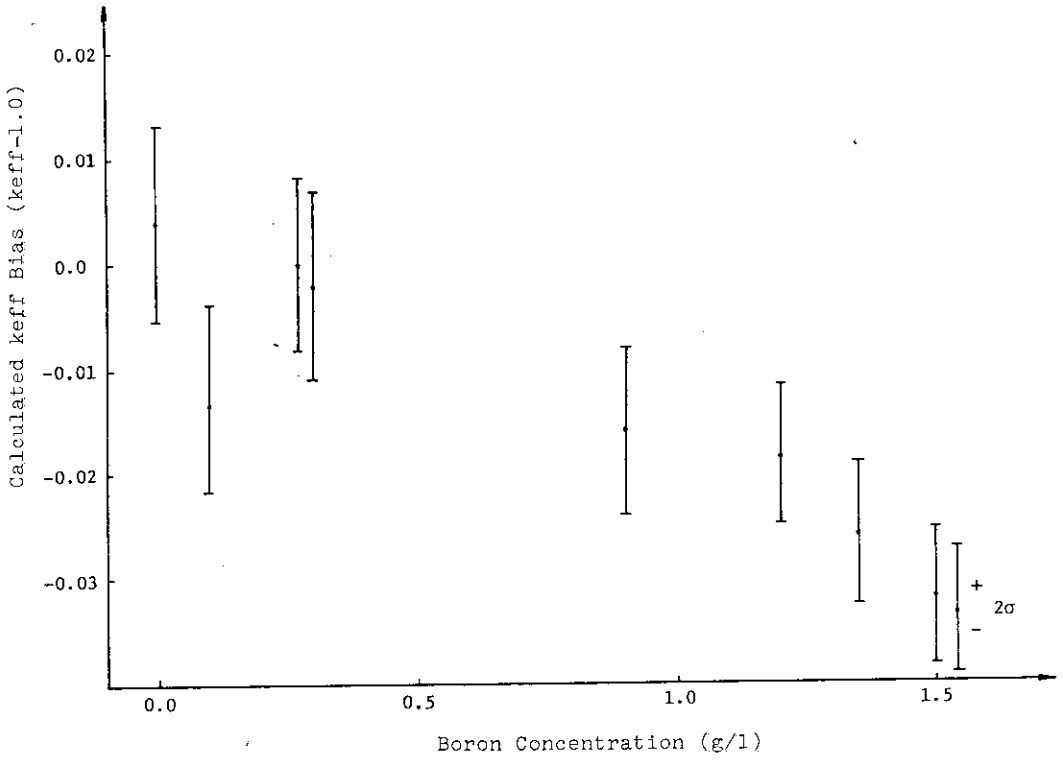

Fig. 4.5 Variation of calculated k_{eff} bias with boron concentration in the experiment (3.A.16).

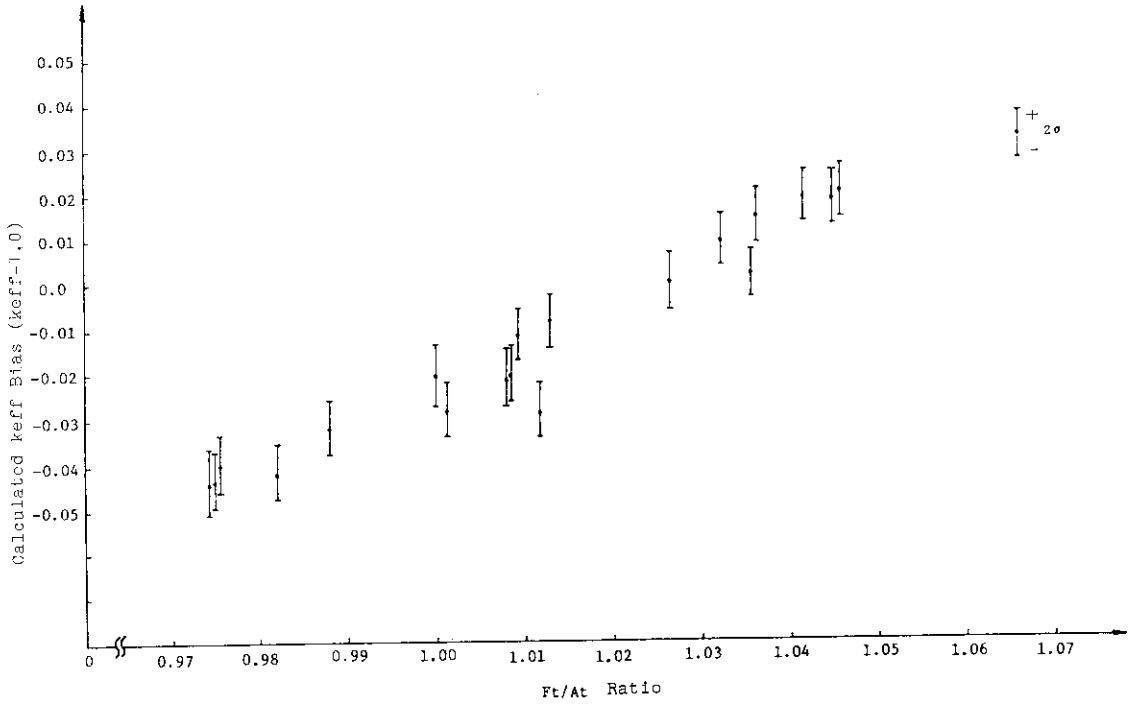

Fig. 4.6 Variation of calculated k_{eff} bias with Ft/At ratio in the experiment (3.C.14).

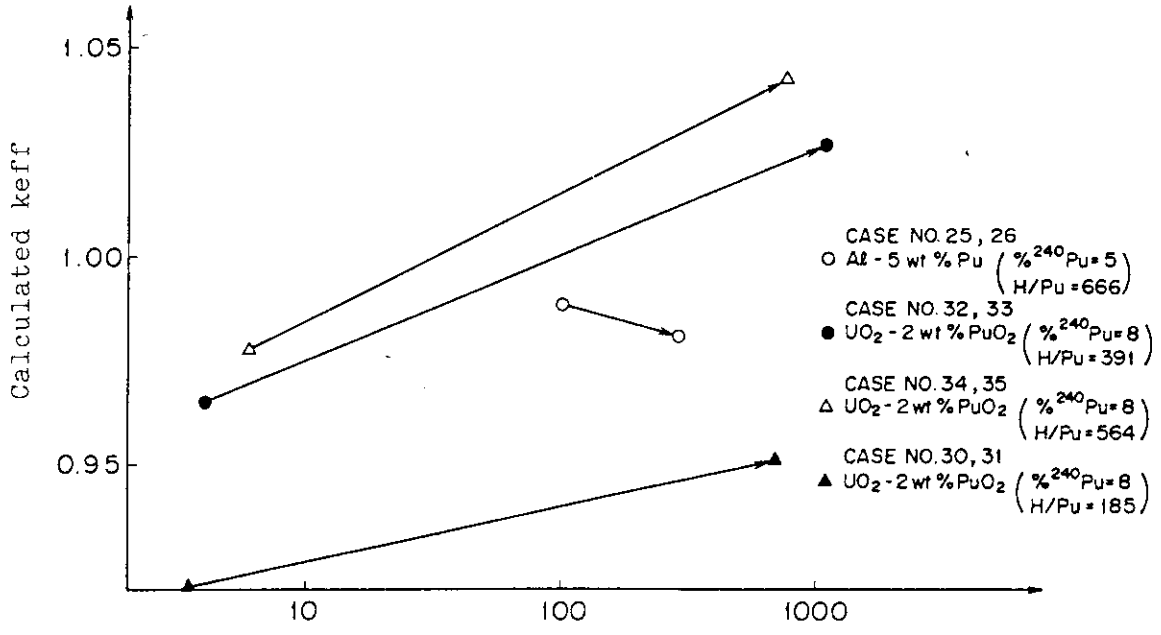

Fig. 4.7 Variation of calculated k_{eff} with boron concentration in the experiment (3.C.8).

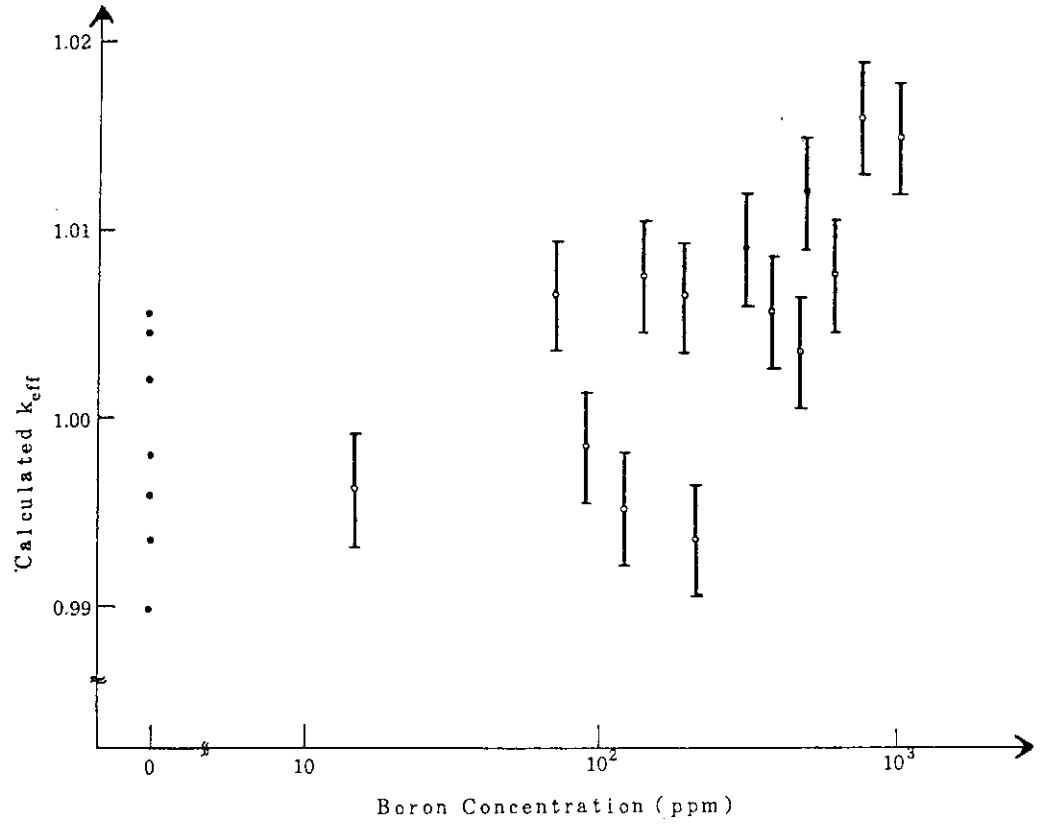

Fig. 4.8 Variation of calculated k_{eff} with boron concentration in the experiment (3.C.10).

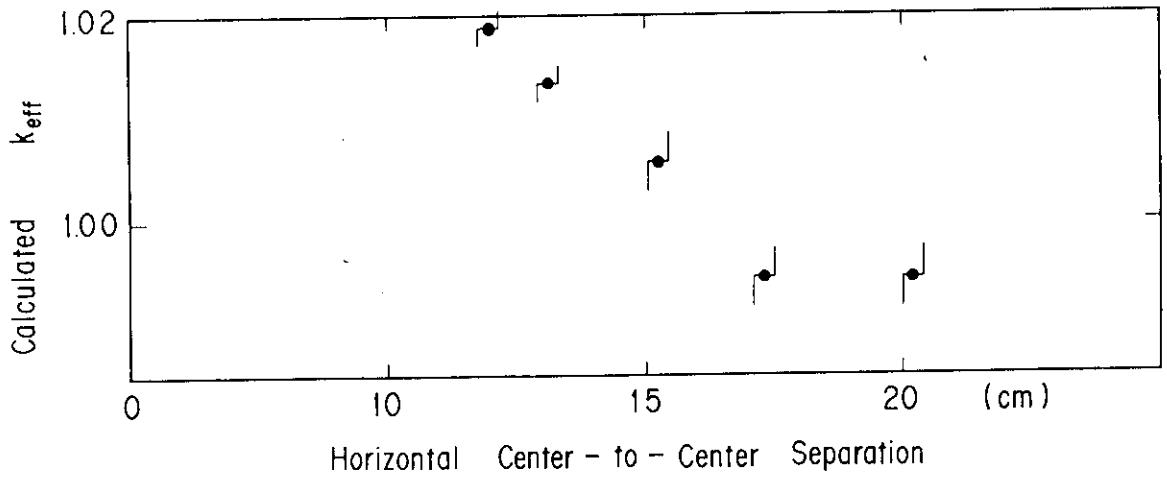

Fig. 4.9 Calculated k_{eff} as a function of center-to-center separation of plutonium metal cylinders in array disposition.
Array size : 4^3
Unit : 6 kg Pu billet
Moderator : None
Reflector : None

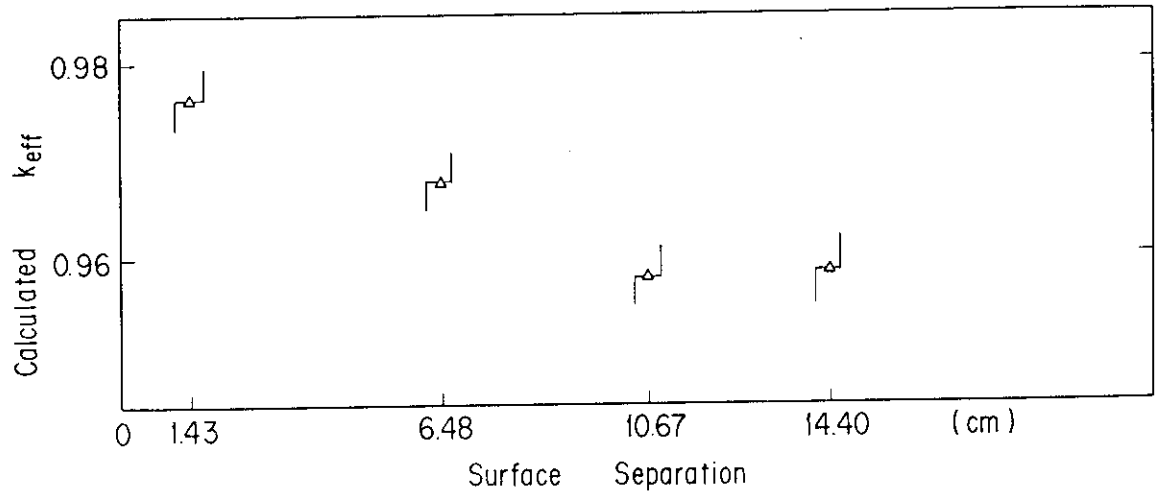

Fig. 4.10 Calculated k_{eff} as a function of surface separation of uranyl-nitrate solution cylinders in array disposition.
Array size : $2^3 - 5^3$
Unit : Uranyl-nitrate solution
Moderator : None
Reflector : None

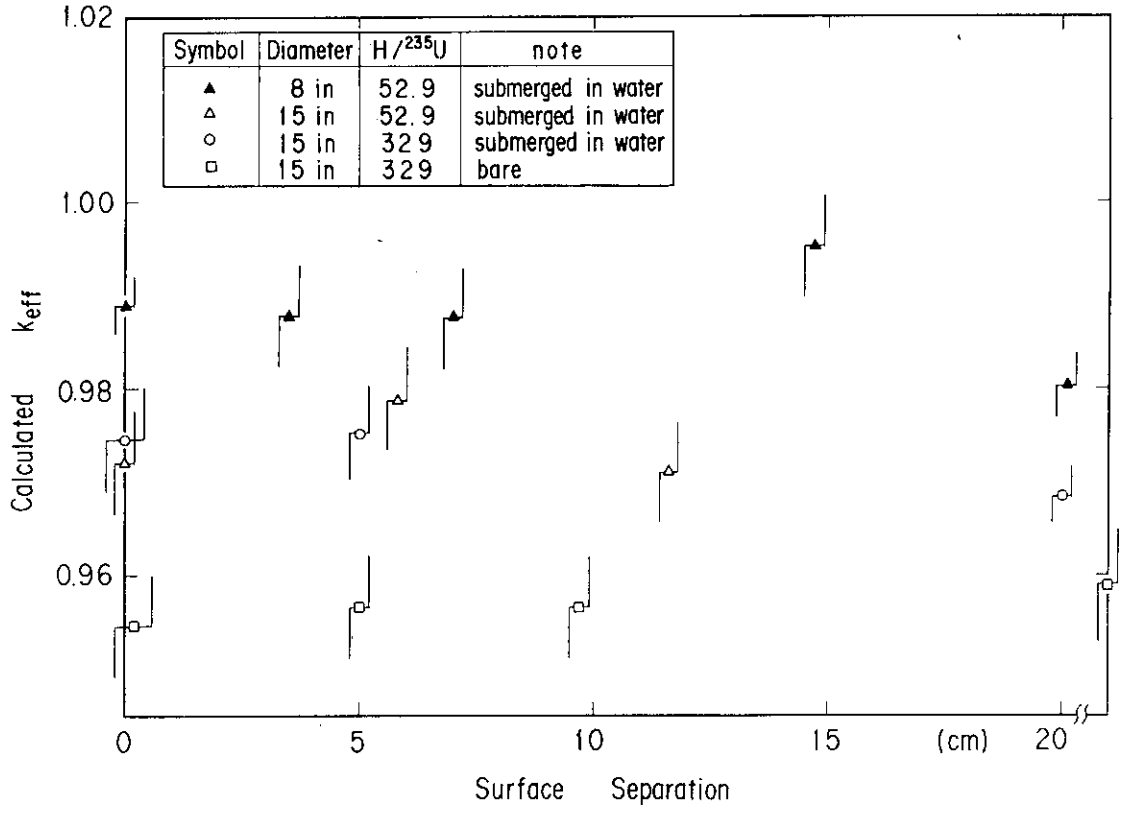

Fig. 4.11 Calculated k_{eff} v.s. surface separation of two aluminum cylinders containing uranyl-fluoride solution.

5. Conclusions

Brief descriptions have been presented on critical experiments and benchmark calculations by the aid of illustrative figures and tables. They render the presently available information on validation calculations concerning the JACS code system. Reported are 1394 cases in all, divided into 502 cases in 17 kinds of homogeneous single-unit systems, 331 cases in 8 kinds of homogeneous multi-unit systems and 561 cases in 16 kinds of heterogeneous systems.

Factors determining bias errors in the calculated k_{eff}'s are confirmed as follows:

1) reflecting conditions,
2) moderating conditions,
3) soluble neutron absorber,
4) fuel composition,
5) distance between units,

with their particular causes and effects.

As a result, in case of criticality analyses of nuclear fuel cycle facilities having these factors, it should be recommended that k_{eff}'s calculated by the JACS code system should be corrected for these bias errors.

Acknowledgment

The authers would like to thank Dr. T. Shimooke at the Department of Reactor Safety Research, JAERI, for useful suggestions. They also thank members of working group on evaluation of the KENO-IV code in Nuclear Code Committee of Japan who cooperated in the calculation and evaluation work.

5. Conclusions

Brief descriptions have been presented on critical experiments and benchmark calculations by the aid of illustrative figures and tables. They render the presently available information on validation calculations concerning the JACS code system. Reported are 1394 cases in all, divided into 502 cases in 17 kinds of homogeneous single-unit systems, 331 cases in 8 kinds of homogeneous multi-unit systems and 561 cases in 16 kinds of heterogeneous systems.

Factors determining bias errors in the calculated k_{eff}'s are confirmed as follows:

1) reflecting conditions,
2) moderating conditions,
3) soluble neutron absorber,
4) fuel composition,
5) distance between units,

with their particular causes and effects.

As a result, in case of criticality analyses of nuclear fuel cycle facilities having these factors, it should be recommended that k_{eff}'s calculated by the JACS code system should be corrected for these bias errors.

Acknowledgment

The authers would like to thank Dr. T. Shimooke at the Department of Reactor Safety Research, JAERI, for useful suggestions. They also thank members of working group on evaluation of the KENO-IV code in Nuclear Code Committee of Japan who cooperated in the calculation and evaluation work.

References

1) Katakura J., Naito Y. and Komuro Y. : Trans. Am. Nucl. Soc., **41**, 329 (1982).
2) Naito Y. et al. : "MGCL-Processor: A Computer Code System for Processing Multigroup Constants Library MGCL," JAERI-M 9396 (1981).
3) ENDF/B Summary Document BNL-NCS-17541 2nd ed. (1975).
4) Nakagawa T. ed. : "Summary of JENDL-2 General Purpose File," JAERI-M 84-103 (1984).
5) Bondarenko I.I. ed. : "Group Constants for Nuclear Reactor Calculations," Consultants Bureau, New York (1964).
6) Katsuragi S. et al. : "JAERI Fast Reactor Group Constants Systems Part I," JAERI 1195 (1970).
7) Wright R.Q. et al. : ORNL-TM-2679 (1969).
8) Macdougall J.D. : AEEW-M318 (1963).
9) Ozer O. : BNL-17134 (1974).
10) Petrie L.M. and Cross N.F. : ORNL-4938 (1975).
11) Naito Y. et al. : "MULTI-KENO: A Monte Carlo Code for Criticality Safety Analysis," JAERI-M 83-049 (1983).
12) Koyama K. et al. : "ANISN-JR: A One-Dimensional Discrete Ordinates Code for Neutron and Gamma-Ray Transport Calculations," JAERI-M 6954 (1977).
13) Phoades W.A. : CCC-276 (1977).
14) Fowler T.B. et al. : ORNL-TM 2496 (1970).
15) Bierman S.R., Durst B.M. and Clayton E.D. : BNWL-2129 (1976).
16) Komuro Y. et al. : "KENO-IV Code Benchmark Calculation (2) (A Pile of PuO_2-UO_2-Polystyrene Compact Fuel)," JAERI-M 9105 (1980) [in Japanese].
17) Bierman S.R. and Clayton E.D. : Nucl. Sci. Eng., **61**, 370 (1976).
18) Bierman S.R., Clayton E.D. and Hansen L.E. : Nucl. Sci. Eng., **50**, 115 (1973).
19) Lane R.C. and Perkins O.J.E. : AWRE O 32/68 (1986).
20) Richey C.R. et al. : Nucl. Sci. Eng., **23**, 150 (1965).
21) Bierman S.R. et al. : Nucl. Appl., **6**, 23 (1969).
22) Bierman S.R. and Clayton E.D. : Nucl. Technol., **11**, 185 (1971).
23) Rothe R.E. and Oh I. : Nucl. Technol., **41**, 207 (1978).
24) Nomura Y. et al. : "KENO-IV Code Benchmark Calculation (5) (Cylinders or a Tank Containing Uranyl Nitrate Solution)," JAERI-M 9108 (1980) [in Japanese].
25) Jenquin U.P. and Bierman S.R. : NUREG/CR-0210 (1978).
26) Nomura Y. et al. : "KENO-IV Code Benchmark Calculation (6) (Plutonium Fuel in Various Shape)," JAERI-M 9201 (1980) [in Japanese].
27) Johnson E.B. : Y-DR-129 (1970).
28) Nomura Y. et al. : "KENO-IV Code Benchmark Calculation (8) (Intersecting Cylinders of Aqueous Uranyl Fluoride Solutions)," JAERI-M 9085 (1980) [in Japanese].
29) Johnson E.B. and Cronin D.F. : Neutron Physics Division Annual Progress Report, ORNL-3714, p.31 (1964).
30) Johnson E.B. and Newlon C.E. : Neutron Physics Division Annual Progress Report, ORNL-4280, p.47 (1968).
31) Raffety S.J. and Mihalczo J.R. : Y-DR-14 (1969).
32) Lloyd R.C. et al. : Nucl. Sci. Eng., **25**, 165 (1966).
33) Colomb G., Mangin D. and Maubert L. : CEA-N-1898 (1973).
34) Lloyd R.C. and Clayton E.D. : Nucl. Sci. Eng., **60**, 143 (1976).
35) Tuck G. and Oh I. : NUREG/CR-0674 (1979).
36) Katakura J. et al. : "Benchmark Calculation with the Nuclear Criticality Safety Evaluation Code System JACS," JAERI-M 9859 (1981) [in Japanese].
37) Schmid L.C. : BNWL-1522-3 (1971).
38) Lloyd R.C. and Clayton E.D. : BNWL-B-482 (1976).
39) Thomas J.T. : Y-DR-128 (1974).
40) Katakura J. et al. : "KENO-IV Code Benchmark Calculation (3) (UF_6 Container Cylinder Critical Array)," JAERI-M 9025 (1980) [in Japanese].
41) Tuck G. and Clark H.E. : Nucl. Sci. Eng., **40**, 407 (1970).
42) Katakura J. et al. : "KENO-IV Code Benchmark Calculation (4) (Slab-Cylinder Critical Configuration of Uranium Nitrate Solution)," JAERI-M 9026 (1980) [in Japanese].

43) Callihan D. et al. : K-406 (1949).
44) Nomura Y. et al. : "Benchmark Calculations for Neutron-Interacting Systems by the Criticality Code-System JACS," JAERI-M 86-082 (1986) [in Japanese].
45) Thomas J.T. : ORNL-TM 868 (1964).
46) Morton III J.R. et al. : UCRL-50175 (1966).
47) Schuske C.L. and Paxton H.C. : Nucl. Technol., **30**, 101 (1975).
48) Magnuson D.W. : Y-DR-120 (1973).
49) Tsuruta H. et al. : "Critical Sizes of Light Water Moderated UO_2 and PuO_2-UO_2 Lattices," JAERI 1254 (1977).
50) Komuro Y. et al. : "KENO-IV Code Benchmark Calculation (10) (A Light Water Reactor Critical Assembly)," JAERI-M 9147 (1980) [in Japanese].
51) Manaranche J.C. et al. : Nucl. Sci. Eng., **71**, 154 (1979).
52) Bierman S.R., Clayton E.D. and Durst B.M. : PNL-2438 (1977).
53) Bierman S.R. et al. : NUREG/CR-0073 (1978).
54) Nomura Y. et al. : "KENO-IV Code Benchmark Calculation (9) (Three Clusters of UO_2 Rods Lattice)," JAERI-M 9168 (1980) [in Japanese].
55) Bierman S.R. et al. : NUREG/CR-0796 vol.1 (1979).
56) Bierman S.R. and Clayton E.D. : NUREG/CR-1547 (1980).
57) Bierman S.R., Durst B.M. and Clayton E.D. : NUREG/CR-0796 vol.2 (1981).
58) Bierman S.R. and Clayton E.D. : NUREG/CR-1784 (1981).
59) Nomura Y. et al. : "KENO-IV Code Benchmark Calculation (7) (Water Moderated Triangle Lattices of Plutonium Enriched Rods)," JAERI-M 9079 (1980) [in Japanese].
60) Smith R.I. and Konzek G.J. : EPRI NP-196 (1976).
61) Baldwin M.N. et al. : BAW-1484-7 (1979).
62) Johnson E.B. : ORNL-ENG 2 (1976).
63) Durst B.M., Bierman S.R. and Clayton E.D. : NUREG/CR-2709 (1982).
64) Manaranche J.C. et al. : Nucl. Technol., **50**, 148 (1980).
65) Lloyd R.C., Durst B.M. and Clayton E.D. : Nucl. Sci. Eng., **71**, 164 (1979).
66) Lloyd R.C. et al. : Nucl. Sci. Eng., **78**, 121 (1981).
67) Nomura Y. and Shimooke T. : Nucl. Technol., **65**, 340 (1984).